Structural studies of mercuric halide complexes.

JONES, Terry.

POND
SHEhUc-LD SI 1WB

6 W

7917084-01 Q

Structural Studies of Mercuric Halide Complexes.

Terry Jones.

A Thesis submitted to the Council for National Academic Awards

in partial fulfilment for the

Degree of Doctor of Philosophy

Sponsoring establishment: Sheffield City Polytechnic.

Collaborating establishment: Steetley Chemicals Ltd.,

Date: February, 1979.

Qft ?OLYTECHNIC

Acknowledgements

The author would like to thank his supervisors Drs. I.W. Nowell and M. Goldstein for their time, advice and interest shown during the course of this study.

I would also like to thank numerous members of the Science faculty at Sheffield City Polytechnic without whom this work could never have been completed; notably, Dr. N.A. Bell, Mrs. S.J. Sheldon and all Technician and Workshop staff.

Thanks and appreciation also to the collaborating establishment, Steetley Chemicals Ltd., especially Dr. P. Halewood, to Dr. T. Jenkins (Department of Physics, University College, Cardiff) and Dr. D.M. Adams (Department of Chemistry, University of Leicester) for the use of their Raman facilities, and Dr. M. Truter (Rothamsted Experimental Station, Harpenden) for the use of an Enraf-Nonius CAD-4 diffractometer.

Finally, I would like to thank the taxpayers of Britain, who, via the Science Research council, provided me with financial support for the past three years.

Contents

Abstract

Previous crystallographic and spectroscopic data compiled for complexes of the type $(L)HgX_2$ and $(L)_2HgX_2$ (where L= neutral unidentate ligand; X=Cl, Br or I) have been critically reviewed and indicate that gross assumptions, often invalid, have been made concerning the relationships between crystal structure and vibrational spectra.

In an attempt to provide a sound basis from which meaningful structure-spectra relationships could be drawn and also to improve our knowledge of the stereochemistry of mercuric halide complexes, the following crystal structures have been determined.

(1) $(PPh_3)HgCl_2$ (Br^a, I^a)

(2) (1,2,5-triphenylphosphole)$HgCl_2$ (Br^a)

(3) α-$(PBu^n_3)HgCl_2$

(4) $(PEt_3)HgCl_2$

(5) $(PMe_3)HgCl_2$ (Br^a)

(6) (2,4-dimethylpyridine)$HgBr_2$ (Cl^a)

(7) $(PEt_3)_2HgCl_2$

(8) $(PEtMe_2)_2HgBr_2$

(9) partial analysis of $(PBu^n_3)_2HgCl_2$

For the $(L)HgX_2$ complexes a variety of structures were observed ranging from discrete dimers (1 and 2), to a discrete tetramer (3) to varied extended structures (4,5 and 6). Discrete four-coordinate monomers, with varying degrees of distortion from a regular tetrahedral geometry, were observed for the $(L)_2HgX_2$ complexes (7,8 and 9).

The donor stength (which is related to both steric and electronic characteristics of the ligand) and the 'small size' of the donor ligand appear to favour extended $(L)HgX_2$ structures, whilst the same parameters explain the extreme distortion of the $(L)_2HgX_2$ monomers.

Examination of the solid-state vibrational spectra of the above complexes and their halo-derivatives have, in spite of problems caused by internal ligand mode interference, indicated certain structure/spectra relationships.

a - This equivalent halo complex is isostructural on the basis of single crystal X-ray photographs.

These relationships have been applied to a number of related complexes of unknown structure.

It was significant that the ν(HgX) modes found for $(L)_2HgX_2$ discrete monomers fell within the region associated with $\nu(HgX)_b$ modes observed for $(L)HgX_2$ associated structures. Consequently, it has been shown that low wavenumber ν(HgX) modes need not necessarily indicate the presence of Hg-X bridge bonds.

Finally, the 'ionic' structure of $(PEtMe_2)_3(HgCl_2)_2$, consisting of a continuous zig-zag chain of $[(PEtMe_2)_2HgCl]^+$ and $[PEtMe_2HgCl_3]^-$ ions is the first report of a structure of this stoicheiometry.

Abbreviations

Genera

TPP	—	1,2,5-tri phenylphosphole	Me	–	methy1
MPC	-	methyl pyrolidine-l-carbodithioate	Et	-	ethy 1
THD	-	trans-halogen bridged dimer	Prn	-	norma 1-propy1
0	-	cone angle	Pr‘	-	iso-propy1
0^*	-	Taft constant	Bun	-	normal-butyl
mL	-	entha1py of 1igat ion	Bu1	-	iso-buty1
ppm	-	parts per mi 11 ion	Ph	-	pheny1
M_r	-	relative molecular mass	Bz	-	benzy1
M	-	meta 1 atom	o-to 1y 1	-	ortho-to 1y 1
L	-	neutral uni dentate ligand	cy	-	eye 1ohexy1
X	-	halogen (C l, Br or 1)	tu	-	th iourea
R	-	a 1ky1- or ary1-	py	-	pyri dine
2,4-•Me2C^H^N	-	2,4-dimethy1pyridine	DMF	-	N,N-d imethy1formamide
2.6-Me2C^H^N	-	2,6-dimethylpyridine			
2.4.6-Me^C^H2N	-	2,4,6-trimethylpyridine			

Crystallographic

Å	-	Angstrom	(ooo)	number of electrons per unit cel l
Fo	-	observed structure factor	R	refinement factor
Fc	-	calculated structure factor	y(Mo-Ka)	absorption coefficient (using molybdenum Ka—X-rad iat ion)
D_m	-	measured density		
D_c	-	calculated density		
Z	-	number of molecules per unit cel l	I	- intensity, of a ref lection
w	-	weighting function		

Spectroscopic

s	strong	i.p.	in plane
m	medium	o.o.p.	out of plane
w	weak	n.m.r	nuclear magnetic resonance
sh	shoulder		
br	broad	Ra	Raman
v(HgL)	mercury-ligand stretching mode	IR	Infrared
		'j(Hg-P) -	Mercury-phosphorus coupling constant
vs(HgX) -	symmetric mercury-halogen stretching mode	g	gerade
$v_{as}(HgX_3)$ -	antisymmetric mercury-halogen stretching mode	u	ungerade
6(HgX)	mercury-halogen bending mode	t	terminal
		b	bridge

Contents

Since the early nineteen-sixties, as a result of the advent of modern Fourier transform spectrophotometers and laser Raman spectrophotometers, the far-infrared region of the electromagnetic spectrum C<500 cm *) has become accessible to the structural chemist on a routine basis. This low frequency region is of particular interest to the inorganic and coordination chemist for this is where metal - ligand modes may be observed.* Knowledge of the number, and wavenumber positions of these metal - ligand modes is potentially capable of yielding considerable information as to the structure of the compound under investigation.

In order fully to utilize these vibrational data it is first necessary to establish a basis from which to interpret the information. The most satisfactory method of forming this basis is to examine crystallographical ly characterised compounds and to correlate the results of both crystallographic and spectroscopic techniques. Unfortunately this approach has not always been followed and consequently spectroscopic data have often been misinterpreted.

A class of compounds which have received considerable attention since the instrumental improvements in the spectroscopic techniques are the simple and complex halometal lates, and metal halide addition complexes found with neutral ligands.* Structural inferences have been made for many of these complexes without the necessary crystallographic basis. The mercuric halide addition complexes and halomercurate(I I) complexes[34] provide a prime example of the misuse of vibrational spectroscopic data. It is the mercuric halide complexes with neutral unidentate ligands (L) which are the subject of the present work. At least eight different stoicheiometries are known to exist:-

a) (L)HgX2 b) (L)2HgX2 c) (L M H g X ^

d) (L)2(HgX2)3 e) (L)3(HgX2)2 f) (L)6HgX2

g) (L)4HgX2 h) (L)3HgX2

The first two of these stoicheiometries have received most spectroscopic and crystallographic attention and the major part of this work is concerned with these types.

Previous spectroscopic data reported for these complexes[2-33] are generally inadequate, for, in many cases, the important low frequency region of the spectrum (<200 cm '), where one might expect to gain information concerning long range mercury-halogen interactions, which are common in halo-complexes of mercury(II) , has not been recorded. Existing crystallographic information for these complexes is very sparse, and so unsystematic, that structure/spectra correlation is very difficult.

It is one of the foremost aims of this work, therefore, to provide a firm crystallographic basis for these complexes from which meaningful structure/spectra correlations can be made. Further, it is attempted to establish 'group frequency' regions in the spectrum where one might expect to locate modes associated with mercury-halogen stretching due to mercury-halogen bonds of a particular type.

It is well known that mercuric halide complexes in the solid state have the ability to increase their coordination numbers beyond that due to the isolated monomeric unit,[35] this usually being facilitated via halogen-bridges. It is of structural interest to understand the criteria required for bridging and the resulting solid state structures which are formed. Questions which arise are, for example:

(a) What role does the halogen play?

(b) What is the effect of varying the donor atom?

(c) How important is the steric nature of the ligand(s)?

A second but no less important aim of this project therefore is to go some way towards answering these questions and thereby improving our present knowledge of the stereochemistry of mercuric halide complexes.

1.2. VIBRATIONAL SPECTROSCOPY AS A STRUCTURAL TOOL

Use of both IR and Raman spectroscopic techniques in the far IR region of the spectrum ($\lesssim$500 cm^{-1}) can indicate the presence of metal - ligand vibrations.[1] The number, activities, symmetries and wavenumber positions of the modes of vibration of a particular compound are characteristic of that compound's structure.

Using group theory one may predict the theoretical number, activities and symmetries of the modes expected for a structure of particular symmetry. If predicted and experimentally observed data correspond, then in principle, the structure used to predict the vibrational modes is the correct one. There are two methods which have generally been employed for this purpose.

(i) Point group analysis[36] - where the molecular symmetry (point group) is used to predict information concerning internal (molecular) modes of vibration. (Extensions of this method include two procedures for treating one or two-dimensional polymeric structures i.e. line group analysis, where one considers symmetry elements of a chain polymer, and plane group analysis, where the symmetry of a sheet polymer is considered).

(ii) Factor group analysis[37,120] - where one considers the symmetry properties of the primitive unit cell (factor group) of a crystalline substance to gain information concerning both internal and external (translational and rotational) lattice modes. These considerations involve knowledge of the symmetry of the molecule (point group), the symmetry associated with the position of the molecules in the unit cell (site group) and also the possible influence which molecules in the unit cell may have upon one another (correlation effects).

In principle these techniques are very useful; however, in practice, because of difficulties which arise while interpreting vibrational data, their full potential is often not realized. Difficulties arise mainly because results derived from the group theory approach give no information about

the intensities and wavenumber positions of the predicted vibrational modes.

The predictive methods employed in this work vary, but are those which allow the most simple spectral interpretation. Details of individual analyses maybe found in Appendix. 4.

1.3. A SURVEY OF THE STEREOCHEMISTRY OF MERCURIC HALIDE COMPLEXES IN THE SOLID STATE

1.3.1. Introduction

The sterochemistry of mercury(II) compounds is probably the most diverse and complicated of all metal complexes. These complications arise mainly in the solid state. The problem is one of deciding whether or not the atoms which surround mercury may be said to be in contact or not.[35]

For an isolated molecule there is no problem, each chemical bond represents one contact. In the solid state however, if the molecules contain ligands which have electronegative donor atoms (e.g. the halogens, oxygen or sulphur), these molecules can pack together in such a manner as to give rise to further long-range (bridging) interactions. These further mercury-ligand distances do not follow the additivity rule of the atomic radii, but are less than the sum of the van der Waals' radii. Even when a number of atoms of the same element surround mercury a range of different mercury-ligand atom distances may be found. These observations have prompted Grdenic[35] to propose:-

"All atoms surrounding mercury at a distance less than the sum of the van der Waals1 radii,

$$D(Hg - L) - R(Hg) + R(L) \qquad \text{EquationI}$$

are in contact and are considered to belong to the mercury coordination sphere". Grdenic has also observed that the coordination behaviour of mercury(II) can be classified in terms of a characteristic coordination number (m), in the system HgL_n where the Hg - L bonds are relatively short and an actual or effective coordination number (n) which includes

ligands for which Equation I holds true. In subsequent discussion we shall use Equation I loosely to describe the requirements necessary for a mercury/ligand long range interaction. (N.B. The sum of the van der Waals' radii of mercury and the halogens are,[35] 3.30-3.53, 3.45-3.68, and 3.65-3.88 Å for Hg-Cl, Hg-Br and Hg-I, respectively.)

The mercuric halide complexes give rise to a wide and varied range of structures containing halogen-bridges. There are two main classes of such compound, viz. the halomercurate(II) complexes and the addition complexes formed between the mercuric halides and unidentate ligands. In the next two sections an attempt will be made to give a general indication as to the diversity of halogen-bridged structures found, as well as providing a detailed structural review of systems relevant to the present work.

1.3.2. Halomercurate(II) complexes

Polymeric structures are often formed as a result of mercury-halogen bridging. A very common coordination arrangement observed for these polymers finds mercury in a distorted octahedral environment with an effective coordination number of six (n=6) and a characteristic coordination number of two (m=2). The structure of the K_2HgCl_4, H_2O complex[38] contains distorted $[HgCl_6]$ octahedra which share opposite edges; there are two short apical Hg-Cl bonds and two pairs of longer equatorial contacts (Figure 1.1) which give rise to a continuous two-dimensional chain.

The $NaHgCl_3,2H_2O$ complex[39] has a structure which consists of two chains, similar to that found in the previous structure, linked together via a third edge of the $[HgCl_6]$ octahedra (Figure 1.2). A similarly arranged chloromercurate(II) skeleton has been observed for NH_4HgCl_3,H_2O,[40] but with a different cation environment to the Na salt.

An infinite two-dimensional sheet structure, in which $[HgCl_6]$ octahedra share all four equatorial chlorine atoms, and contain two colinear Hg-Cl bonds, is found for α-NH_4HgCl_3[41] (Figure 1.3). The corresponding Rb

FIG.1.1 THE STRUCTURE OF $K_2HgCl_4.H_2O$

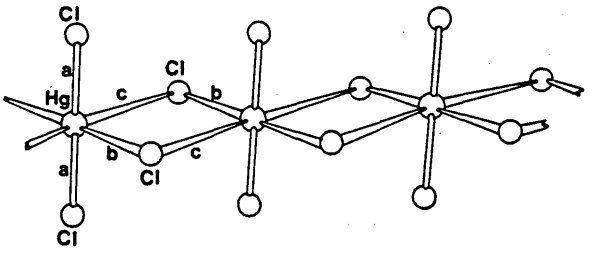

Distances (Å)	Angle (°)
a = 2.38	a^a = 169.96
b = 2.80	
c = 3.25	

FIG.1.2 THE STRUCTURE OF $Na[HgCl_3].2H_2O$

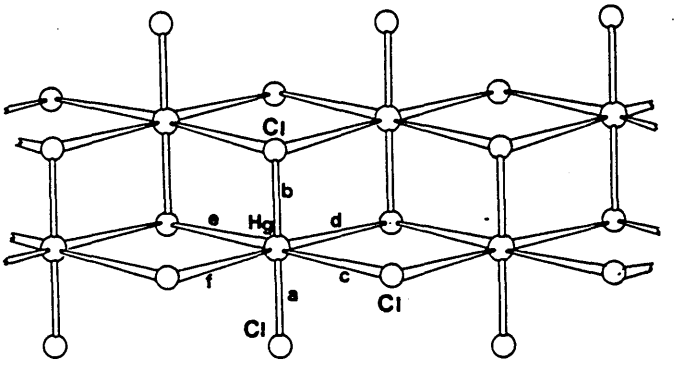

Distances (Å)	Angle (°)
a = 2.35	a^b = 180
b = 2.40	
c = 2.81	
d = 3.27	
e = 2.81	
f = 3.27	

FIG.1.3 THE STRUCTURE OF α-$NH_4[HgCl_3]$

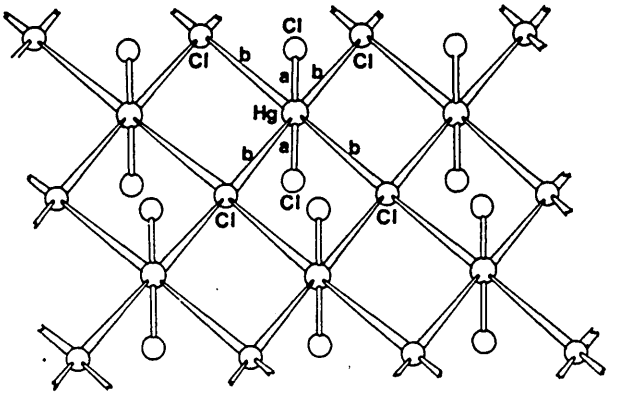

Distances (Å)	Angle (°)
a = 2.34	a^a = 180
b = 2.96	

FIG.1.4 THE STRUCTURE OF SOME TRIHALOMERCURATE ANIONS

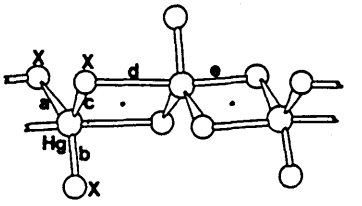

$[SMe_3]HgCl_3$		$[SMe_3]HgI_3$		α-$[NEt_4]HgCl_3$	
Distances (Å)	Angles°	Distances (Å)	Angles°	Distances (Å)	Angles°
a = 2.45	a^b=120.2	a = 2.72	a^b = 124	a=2.43	a^b=118.3
b = 2.40	a^c=115.6	b = 2.69	a^c = 113	b=2.44	a^c=122.9
c = 2.42	b^c=124.2	c = 2.73	b^c = 123	c=2.43	b^c=118.9
d = 3.05		d = 3.69		d=3.05	
e = 3.04		e = 3.52		e=3.02	

FIG.1.6 THE STRUCTURE OF $[NMe_4][HgBr_3]$

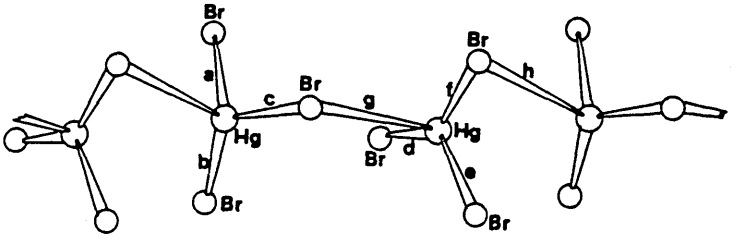

Distances (Å)	Angles (°)
a = 2.53	a^b = 121.8
b = 2.48	a^c = 119.1
c = 2.56	b^c = 114.4
d = 2.55	d^e = 125.3
e = 2.49	d^f = 116.9
f = 2.52	e^f = 113.3
g = 2.92	
h = 2.94	

FIG.1.5 $[S_4N_3]HgCl_3$

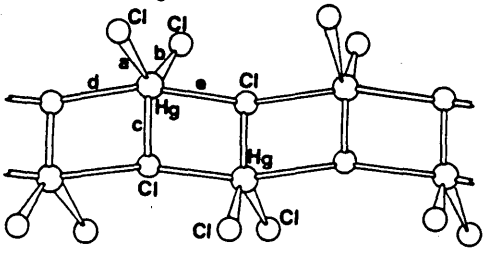

Distances (Å)	Angles (°)
a = 2.49	a^b = 112.9
b = 2.35	a^c = 108.4
c = 2.43	b^c = 138.4
d = 3.02	d^e = 165.4
e = 3.20	

Table 1.1

Bond parameters for some $[Hg_2X_6]^{2-}$ species.*

Compound	Terminal bonds a,b/Å	Bridge bonds c,d/Å	Terminal angle β/°	Bridge angle α/°
$[NEt_4]_2[Hg_2Br_6]$ [50]	2.521, 2.500	2.721, 2.749	122.3	89
$[Ph_3AsO{---}H{---}OAsPh_3][Hg_2Br_6]$ [51]	2.51 , 2.52	2.75 , 2.76	127	87
$[Hg(3,2,3\text{-}N_5)Br]_2[Hg_2Br_6]$ [52]	2.49, 2.51	2.65, 2.86	124.4	89.3
$[S_3C_2N_2Et_4][Hg_2I_6]$ [53]	2.701, 2.582	2.897, 2.950	118.5	86.4
$[S_3C_2N_2Et_4][Hg_2I_6]$ [53]	2.697, 2.669	2.880, 3.044	126.7	86.4
$[(Cu_2Au)(Bu_2dtc)_6][Hg_2Br_6]$ [54]	2.522, 2.513	2.731, 2.717	122.3	89.1

* All these $[Hg_2X_6]^{2-}$ species contain a centre of symmetry

Fig.1.7 The structures of some $[Hg_2X_6]^{2-}$ species

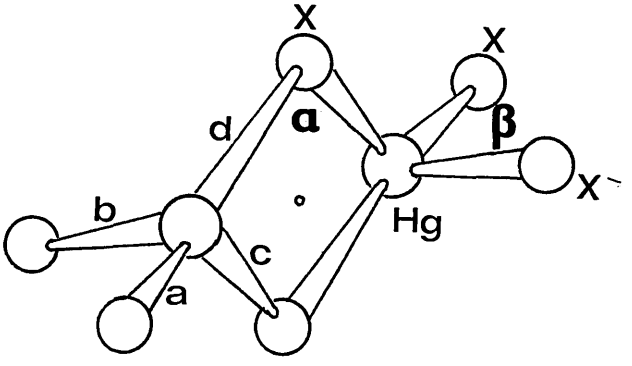

analogue, $RbHgCl_3$ has been reported to be isostructural from X-ray powder pattern studies.[42]

Distorted octahedral geometries based on digonal characteristic coordination have also been found for the solid state extended structures of $HgCl_2$,[35] $HgBr_2$[43] and the metastable yellow form of HgI_2.[44]

Different polymeric arrangements have been found for the complexes $[SMe_3][HgX_3]$ (X=Cl[45] or I[46]) and α-$[NEt_4][HgCl_3]$,[47] each contain columns of planar $[HgX_3]^-$ units held together by relatively weak apical contacts giving rise to continuous chain structures (Figure I.4) in which mercury lies in a distorted trigonal bipyramidal environment. A similar coordination polyhedron, but totally different packing arrangement of $[HgCl_3]^-$ units, is found for $[S_4N_3][HgCl_3]$[48] (Figure I.5).

Yet another polymeric arrangement is found for $[NMe_4][HgBr_3]$,[49] in which a continuous chain of non-planar $[HgBr_3]^-$ ions share a bromine atom with the mercury of an adjacent anion (Figure I.6). Mercury lies in a very distorted tetrahedral environment.

Quite recently a number of hexahalodimercury(II) anions $[Hg_2X_6]^{2-}$, in which mercury lies in a distorted tetrahedral environment (Figure I.7), have been reported. Table I.1 contains relevant bond parameters for these complexes.[50-54]

Before concluding this section on halomercurate(II) complexes it should be noted that unassociated structures containing discrete $[HgX_4]^{2-}$ tetrahedra have been observed for $[SMe_3]_2[HgI_4]$[55] and $[NMe_4]_2[HgX_4]$ (where X=Cl or Br)[56] (Figure I.8).

I.3.3. Addition complexes

Considering the vast number and varying stoicheiometry of the complexes formed between the mercuric halides and neutral unidentate ligands, little sound structural data are available. The majority of previous data, concerned with the 1:1 and 2:1 systems, indicate a tendency for mercury-halogen associated structures to be formed. A comprehensive survey of each of these

Table 1.2

Bond parameters for some discrete dimeric (DHgX^ structures

Compound	d(Hg-X)/A		d(Hg-L)/A (d)	Angles/®	
	Terminal (a)	Bridge <b,c)		Terminal (3)	Bridge (a)
(Ph3PSe)HgCl?57	2.33	2.78, 2.60	2.53	136.3	91.7
(MPC)HgCl258	2.37	2.78, 2.57	2.42	131.9	92.7
(1-methylcytosine)HgCl2[59*]	2.32	2.75, 2.72	2.17	148.0	95.4
(cyclopentadienylide)Hg12^^	2.68	2.98, 2.94	2.30	131.5	86.2

There is also a weak interaction between the oxygen of 1-methylcytosine and mercury; Hg-0=2.84 A (sum of the van der Waals* radii of mercury and oxygen = 3.0 A).

FIG. 1.9 The structure of some (L)HgX2 complexes

Cl

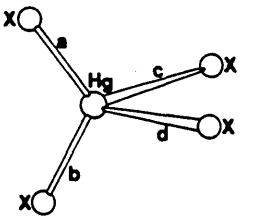

$[NMe_3]_2[HgBr_4]$

Distances (Å)	Angles (°)
a = 2.59	The angles range from;
b = 2.59	a^d = 108.0
c = 2.59	b^d = 113.7
d = 2.59	

N.B. The corresponding chloro complex is isomorphous

$[SMe_3]_2[HgI_4]$

Distances (Å)	Angles (°)
a = 2.80	The angles range from;
b = 2.73	a^b = 105.2
c = 2.69	b^c = 119.8
d = 2.68	

FIG.1.10 (2,4,6-TRIMETHYLPYRIDINE) $HgCl_2$

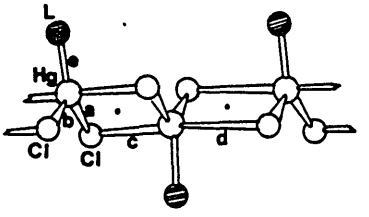

DISTANCES (Å)	ANGLES (°)
a = 2.56	a^b = 110.1
b = 2.54	a^e = 122.5
c = 2.96	b^e = 128.4
d = 2.95	
e = 2.18	

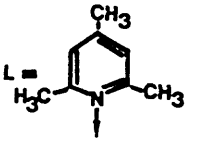

FIG.1.11 THE STRUCTURE OF GUANOSINE $HgCl_2$

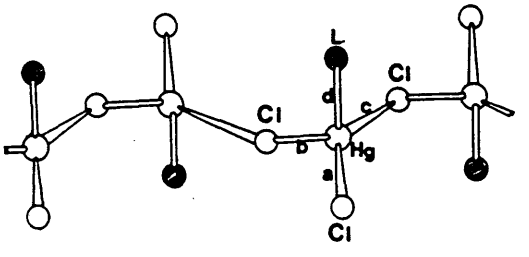

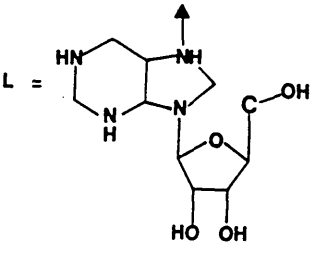

Distances (Å)	Angles (°)
a = 2.34	a^d = 155.5
b = 2.66	b^c = 107.9
c = 2.76	
d = 2.16	

systems will be given.

(L)HgX_2 complexes. Many vibrational spectroscopic data reported for the (L)HgX_2 system suggest the presence of discrete dimeric halogen-bridged structures (Figure I.9) in which mercury lies in a tetrahedral environment and the ligands are mutually trans to one another. However, at the outset of this project only (Ph_3PSe)$HgCl_2$[57] and (MPC)$HgCl_2$[58] were known to have this structure, which, together with the recently reported structures of (1-methylcytosine)$HgCl_2$[59] and (cyclopentadienylide)HgI_2,[50] makes only four occasions when it has justifiably been cited.

Table I.2 contains relevant bond parameters for all four complexes. It should be noted that the mercury atom always lies in a very distorted tetrahedral environment and that each halogen-bridged four-membered ring is asymmetric.

Although the complex ($AsEt_3$)HgI_2[61] has also been reported as having a discrete dimeric structure the evidence presented is not conclusive; no bond parameters were quoted.

The (2,4,6-trimethylpyridine)$HgCl_2$ complex[62] gives rise to a more associated structure. Thus '$NHgCl_2$' units are packed one upon another and joined via two long range Hg - Cl contacts resulting in a polymeric chain in which mercury lies at the centre of a distorted trigonal bipyramid (Figure I.10).

The (guanosine - N^7)$HgCl_2$ complex[63] gives rise to another type of chain-like arrangement (Figure I.11). There are two short bonds to a chlorine and to a nitrogen atom of the ligand, and two longer bonds to chlorine atoms completing an irregular four-coordinate environment about mercury resulting in an infinite $[- Cl - Hg - Cl - Hg -]_n$ zig-zag chain.

The sulphur-donor complex (C_4H_8S)$HgCl_2$[64] has been described as a substitution complex rather than an addition complex and consists of a zig-zag ribbon of alternating $[C_4H_8SHgCl]^+$ and Cl^- ions (Figure I.12).

It has been found that oxygen and sulphur atoms may compete with the

FIG.1.12 (TETRAHYDROTHIOPHENE) $HgCl_2$

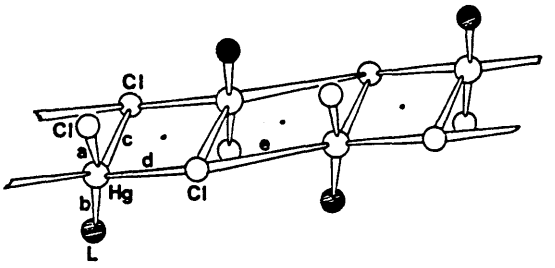

DISTANCES (Å)	ANGLE (°)
a = 2.30	a^b = 142.8
b = 2.40	
c = 2.62	L = 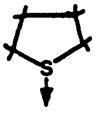
d = 2.83	
e = 3.07	

FIG.1.13 (DEHYDRODITHIZONE) $HgCl_2$

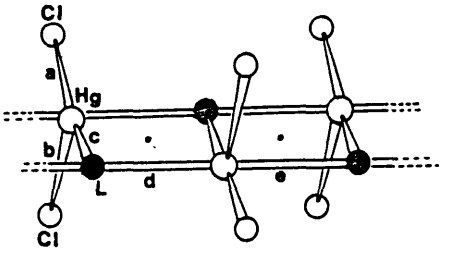

DISTANCES (Å)	ANGLES (°)
a = 2.35	a^b = 111.5
b = 2.56	a^c = 151.8
c = 2.40	b^c = 96.2
d = 3.24	d^e = 162.1
e = 3.24	

L = 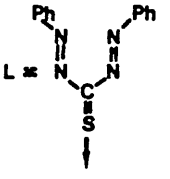

FIG.1.14 THE STRUCTURE OF (TRIPHENYLARSINEOXIDE) $HgCl_2$

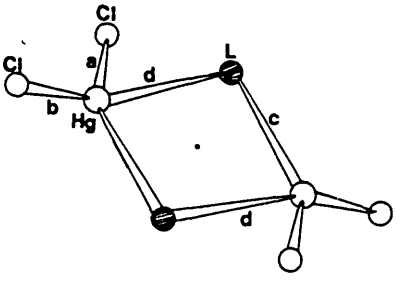

Distances (Å)	Angles (°)
a = 2.32	a^b = 144.8
b = 2.32	c^d = 97.6
c = 2.46	c^d = 82.4
d = 2.48	

L = $Ph_3As{=}O\longrightarrow$

halogen to become the bridge atom. The (dehydrodithizone)$HgCl_2$ complex[65] has a polymeric chain structure containing sulphur-bridges.

Approximately trigonal planar '$SHgCl_2$' units are joined via two long range mercury/sulphur contacts completing a trigonal bipyramidal polyhedron about mercury and giving a continuous structure (Figure 1.13).

'Mercury-oxygen' bridging has also been reported. For example $(Ph_3AsO)HgCl_2$ consists of discrete oxygen-bridged dimeric molecules (Figure 1.14) in which mercury lies in a very distorted tetrahedral environment,[66] whereas (cyclononanone)$HgCl_2$ consists of a continuous chain of cyclonanone molecules and virtually undistorted $HgCl_2$ units held together by oxygen-bridges (Figure 1.15).[67]

In (pyridine-N-oxide)$HgCl_2$[68] and (quinoline-N-oxide)$HgCl_2$[69] both oxygen and chlorine bridges are observed. The structures of both complexes are similar and are shown in Figure 1.16 together with relevant bond parameters. The oxygen-bridges appear to be of comparable strength in both complexes. The Cl-Hg-Cl angle in (pyridine-N-oxide)$HgCl_2$ (163.1°) and (quinoline-N-oxide)$HgCl_2$ (171°) both approach linearity which suggests weak Hg-O interaction. Both complexes may be described as having 'net like' structures in which mercury lies in a very distorted octahedral environment.

The three complexes (tetrahydrofuran)$HgBr_2$,[70] (coumarin)$HgCl_2$[71] and (azoxyanisole)$HgCl_2$[69] all exhibit the 'prefered' distorted octahedral effective coordination behaviour (Figure 1.17). There are two short mercury-halogen bonds within an almost undistorted HgX_2 unit (X-Hg-X angles are ca. 170°), an apparently weak Hg-O bond and three further long range mercury-halogen contacts at ca. 3 Å.

A slight modification of the previous structure has been observed for $(Ph_2SO)HgCl_2$[72] and (3,5-dibromopyridine-N-oxide)$HgCl_2$[73] (Figure 1.18). Again, the $HgCl_2$ units are only slightly distorted by Hg-O interactions. However, only two long range mercury-chlorine contacts are present here, the third contact being seemingly hindered by the position of the donor ligand in

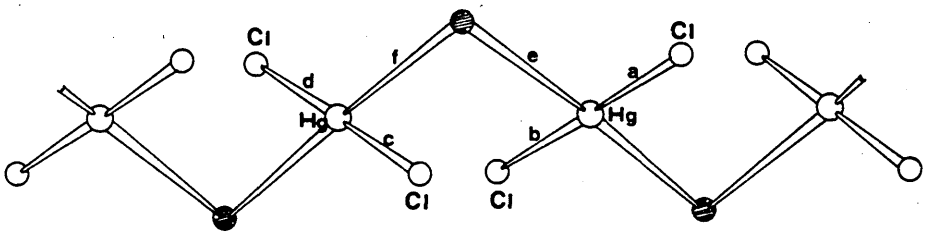

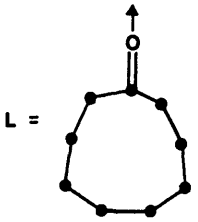

Distances (Å)	Angles (°)
a = 2.28	a^b = 177.2
b = 2.28	c^d = 177.5
c = 2.26	e^f = 84.1
d = 2.28	
e = 2.91	
f = 2.76	

FIG.1.16 THE STRUCTURE OF SOME (L)$HgCl_2$ COMPLEXES

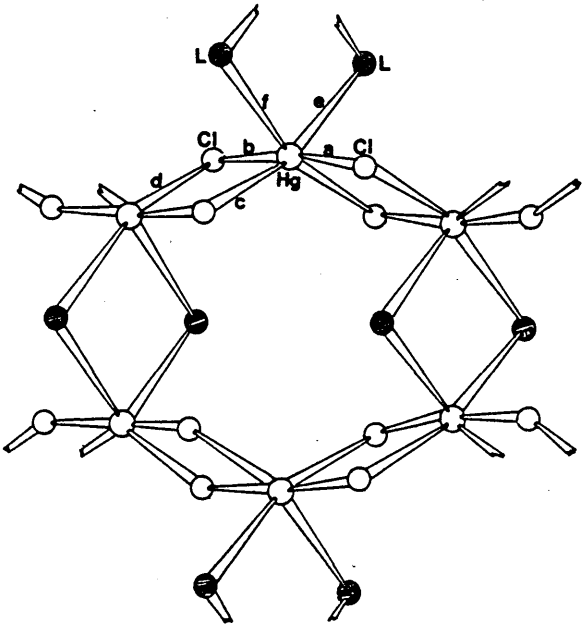

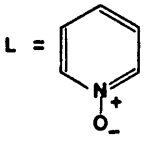

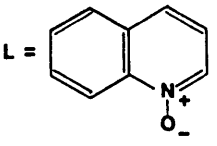

L = Pyridine-N-oxide

Distances (Å)	Angle (°)
a = 2.32	a^b = 163.1
b = 2.34	
e = 3.18	
d = 3.32	
e = 2.60	
f = 2.59	

L = Quinoline-N-oxide

Distances (Å)	Angle (°)
a = 2.30	a^b = 174
b = 2.30	
e = 3.12	
d = 3.35	
e = 2.56	
f = 2.61	

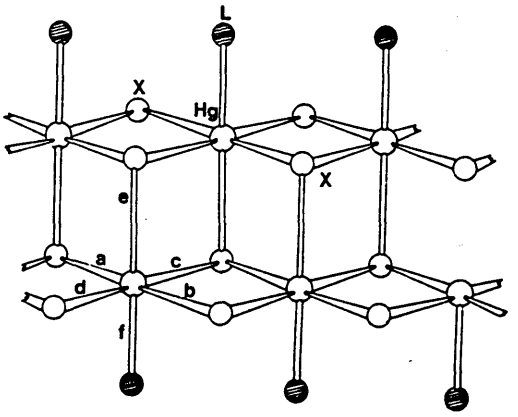

L = Coumarin , X = Cl		L = Azoxyanisole , X = Cl		L=Tetrahydrofuran , X = Br	
a = 2.33 Å		a = 2.28 Å		a = 2.48 Å	
b = 2.33 "	a^b	b = 2.29 "	a^b	b = 2.47 "	a^b
c = 2.94 "	= 171°	c = 3.10 "	= 175°	c = 3.15 "	= 174.6°
d = 3.18 "		d = 3.15 "		d = 3.27 "	
e = 3.34 "		e = 3.18 "		e = 3.47 "	
f = 2.38 "		f = 2.60 "		f = 2.67 "	

FIG.1.18 THE STRUCTURES OF SOME $(L)HgCl_2$ COMPLEXES

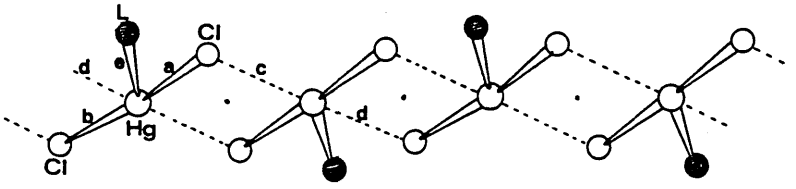

L=Diphenylsulphoxide

Distances (Å)

a = 2.29
b = 2.29
c = 3.28
d = 3.23
e = 2.58

Angles (°)

a^b = 172.4
b^e = 94.3
b^d = 82.5
a^d = 94.7

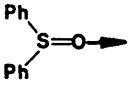

L = 3,5-Dibromopyridine-N-oxide

Distances (Å)

a = 2.29
b = 2.31
c = 3.21
d = 3.12
e = 2.51

Angle (°)

a^b = 173.5

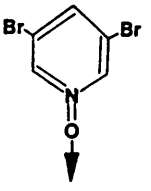

FIG.1.20 THE STRUCTURE OF $(THIOUREA)_2 HgI_2$

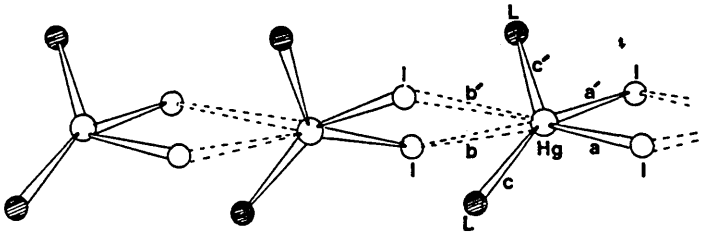

Distances (Å)	Angles (°)
a,a' = 2.84	a^a' = 102
b,b' = 3.86	a^c = 121
c,c' = 2.46	a^c' = 95
	a'^c = 95
	a'^c' = 121
	c^c' = 124

L = 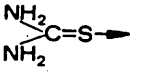

each case.

(UgHgXg complexes. Monomeric $(L)_2HgX_2$ tetrahedra have been observed on a number of occasions for this system (Figure 1.19). Table 1.3 contains relevant bond parameters to describe each structure. It can readily be seen that mercury lies in a very distorted tetrahedral environment in each of these structures.

Associated structures have also been reported for complexes of this stoicheiometry. In the case of $(thiourea)_2HgX_2$ (X=Cl, Br or I) there is a variation in the mode of association depending on X. The iodo compound[79] consists of distorted ^Hg^' tetrahedra linked together via weak Hg-I contacts forming a loosely bound chain (Figure 1.20). The bromo complex[80] has a similar structure but the tetrahedra show greater association resulting in a more tightly bound chain in which mercury lies in an effective distorted octahedral environment (Figure 1.21).

The complex (thiourea^HgCI^[81] has a structure which may best be described as ionic containing trigonal planar ^HgCI*' cations and Cl anions. There is further contact (3.2 Å) between the cations (Figure 1.22). An apparently similar structure has been reported[82] for (penicillamine^HgCl H_2O. The two Hg-S distances are about 2.34 Å, whilst the shortest Hg-Cl distance is 2.85 A. The S-Hg-S angle is 171.6°.

The complex (thiosemicarbazide^HgCI^[83] has a similar chain like arrangement to those found for (thiourea)2HgX_2 (X=Br or I) (Figure 1.21). Very distorted ^HgC^' units, with S-Hg-S angles of 160.7° and Hg-Cl bond lengths of ca. 2.8 Å, are held together via longer Hg-Cl contacts which complete a distorted octahedral environment about mercury.

The complexes (Py^HgC^#[84] (methanol^HgCI^[85] ancl (phenoxathiin^HgCI^[86] each have the 'prefered' distorted octahedral arrangement based on digonal characteristic coordination. Each structure contains perfectly linear HgC^ units with very weak mercury-donor atom interactions. These four coordinate units are held together via two long Hg-Cl contacts of ca. 3 Å which complete

Table 1.3

Bond parameters for some discrete monomeric $(L)_2HgX_2$ tetrahedra

Compound	d(Hg-X)/Å	d(Hg-L)/Å	∝ /°	β /°
$(PPh_3)_2HgI_2$ [74]	2.733, 2.763	2.574, 2.574	110.43	108.95
(O-ethylthiocarbamate)$_2HgCl_2$ [75]	2.62 , 2.58	2.45 , 2.43	96.2	129.9
(1,4-thioxan)$_2HgCl_2$ [76]	2.43 , 2.52	2.54 , 2.59	114.0	115.0
$(Ph_3AsO)_2HgCl_2$ [77]	2.33 , 2.32	2.32 , 2.37	146.6	92.5
(6-mercaptopurine)$_2HgCl_2$ [78]	2.622, 2.622	2.460, 2.460	Not reported	139.8

Fig 1.19 The structures of some $(L)_2HgX_2$ complexes

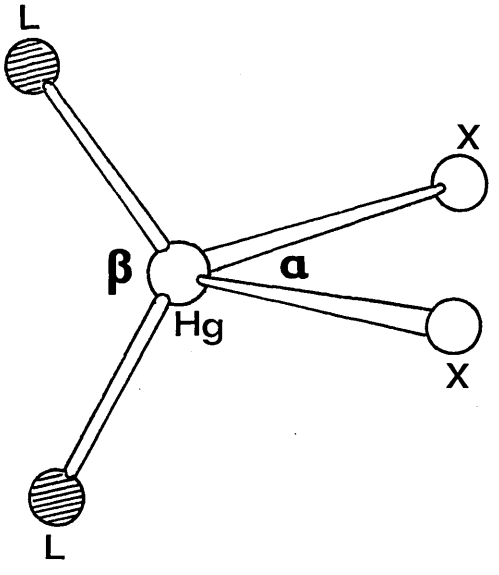

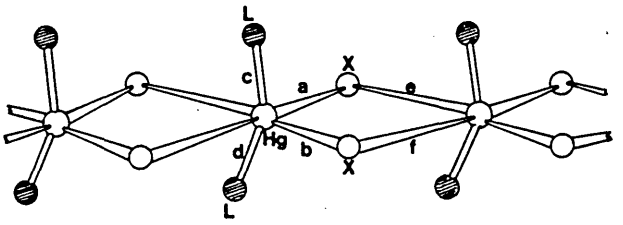

L = Thiourea X= Br

L = Thiosemicarbazide X=Cl

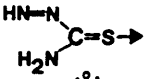

Distances (Å)	Angles (°)
a = 2.81	a^b = 84
b = 3.00	c^d = 145
c = 2.42	
d = 2.42	
e = 3.32	
f = 3.41	

Distances (Å)	Angles (°)
a = 2.82	a^b = 96.6
b = 2.82	c^d = 160.7
c = 2.42	
d = 2.42	
e = 3.25	
f = 3.25	

FIG.1.22 THE STRUCTURE OF $(THIOUREA)_2HgCl_2$

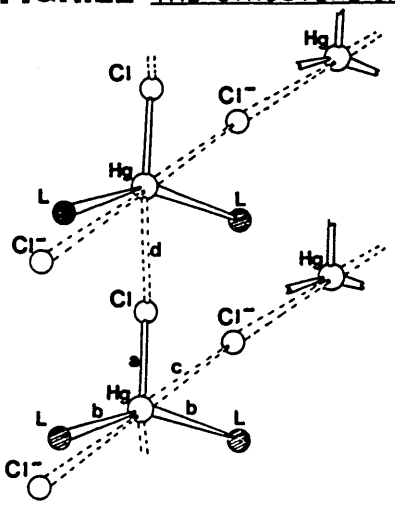

Distances (Å)

a = 2.57
b = 2.42
c = 3.22
d = 3.34

Angles (°)

b^b = 138.6
a^b = 110.8

FIG.1.23 THE STRUCTURE OF SOME $(L)_2HgCl_2$ COMPLEXES

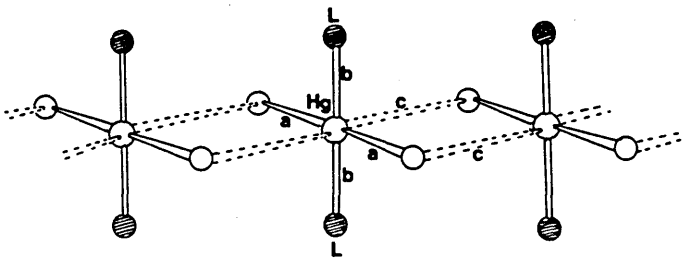

L=Phenoxathiin

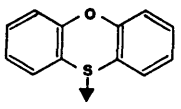

Distances (Å)	Angle (°)
a = 2.34	a^a = 180
b = 2.60	
c = 3.25	

L = Pyridine

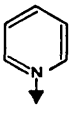

Distances (Å)	Angle (°)
a = 2.33	a^a = 180
b = 3.12	
c = 3.08	

L = Methanol

CH_3OH

Distances (Å)	Angle (°)
a = 2.31	a^a = 180
b = 2.82	
c = 3.07	

FIG.1.24 THE STRUCTURE OF (cis-4-CHLOROPHENYL -THIAN-1-OXIDE)$_2$ $HgCl_2$

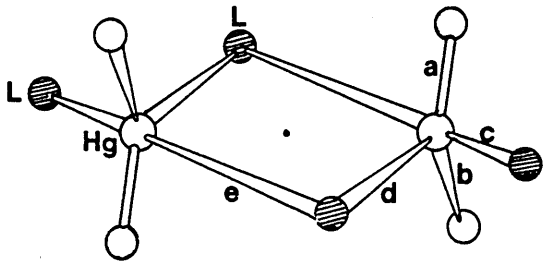

Distances (Å)	Angle (°)
a = 2.28	a^b = 164.0
b = 2.30	
c = 2.70	
d = 2.48	
e = 2.97	

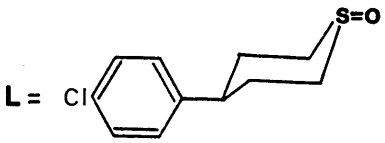

the distorted octahedral environment resulting in a continuous chain (Figure I.23).

Distorted octahedral coordination has also been found for the unique oxygen-bridged dimeric structure of (cis-4-p-chlorophenyltrian-1-oxide^$HgCl_2$ (Figure I.24)

1.3.4. Factors affecting the stereochemistry of mercuric halide complexes in the solid state

There have been some attempts to rationalize the factors influencing the coordination behaviour of mercury (II) in the solid state. Approximately one-third of the structures, presented in the previous section, form two relatively strong digonal bonds, which suggests a tendency towards digonal characteristic coordination. This phenomenon has been explained by Orgel[88] and Nyholm in terms of a relatively small 5d*— ■5d 6s separation. The dz and s orbitals can be mixed together to give two new orbitals. If two electrons from the dz^2 orbital of Hg^{2+} are put into the ds hybrid orbital, strong electronegativity will develop along the +z and -z axes which favours linear two coordination.

's'

Small d^{10} - d^9s separation is conducive to greater mixing.

Characteristic coordination numbers other than two are just as common. Iodo complexes of mercury (II) in particular have a tendency to take up higher characteristic coordination numbers than their chloro or bromo equivalents.[35] Unfortunately no equivalent theory has been put forward to explain these

observations and it can only be deduced that the small $d^{10} \longrightarrow d^9 s$ separation is not an over-riding consideration. However, Grdenic[35] has made the empirical observation that the electronegativity of the ligands attached to mercury (II) is a major factor influencing the resultant coordination number. A critical value of electronegativity $\chi(L)$ is 2.5. Generally when $\chi(L) > 2.5$ digonal characteristic coordination is prefered, whereas when $\chi(L) < 2.5$ tetrahedral characteristic coordination is prefered. At the time this observation was made (1965), there were a number of violations of this rule which Grdenic explained in terms of crystal packing and steric requirements. Certainly the results of some recent reliable spectroscopic studies[90,91] on the complexes $[NR_4]_2HgX_4$ and $[NR_4]HgX_3$ (R= alkyl; X=Cl, Br or I) indicate steric requirements are very important. For the tetrahalomercurate(II) species, when $[NR_4]^+$ is a large cation the $[HgX_4]^{2-}$ ions exist as discrete tetrahedral units where m=n=4.[91] This is true even for the $[HgCl_4]^{2-}$ anions where $\chi(Cl) = 3.5$. It is found for the trihalomercurate(II) salts that small cations are conducive to extended structures of the type $[HgX_3]_n^{n-}$ (where n is an integer), whereas larger cations give rise to discrete dimeric units of the type $[Hg_2X_6]^{2-}$.[91] We should perhaps up-date Grdenic's rationale for the factors influencing Hg(II) coordination therefore, by including steric requirements as just as significant a parameter as electronegativity.

As already indicated in Section 1.3.2, for addition complexes there is the possibility of long-range interaction via any of the coordinating groups. Consequently in this situation the electronegativity of the donor atom of the organic ligand also becomes important in determining the resultant solid-state structure.

1.4. A SURVEY OF MERCURY(II) - HALOGEN STRETCHING MODES

1.4.1. Halomercurate(II) complexes

The vibrational spectra of halomercurate(II) complexes, to some extent corroborate the wide range of structures shown. The data presented

in Table I.4 consist of what are felt to be the more reliable spectroscopic studies, i.e. those based on sound crystallographic evidence. (N.B. only stretching modes are presented as in the main only these have been reported). These data are by no means comprehensive but will serve as general indicators of specific mercury-halogen coordination behaviour.

It should be realized that the notation $\nu(HgX)_t$ used in Table I.4 does not refer to a specific type of terminal mercury-halogen stretching mode but rather refers to stretching of what is the shortest Hg-X bond e.g. the terminal Hg-X bond in a discrete $[Hg_2X_6]^{2-}$ dimer, and even then [as there are a number of $(HgX)_t$ modes in such species] the nature of the vibration is not specified.

As one might expect the highest observed wavenumber positions for mercury-halogen stretching modes are found for the mercuric halides themselves.[92-94] Further, there is a trend whereby the highest observed mercury-halogen modes decrease in wavenumber in a diminishing sequence for structures containing X-Hg-X units, to $[HgX_3]^-$ units, to $[HgX_4]^{2-}$ units, respectively. This observation is not surprising when one considers the effects of increasing coordination upon the original HgX_2 unit. Therefore some indication of the characteristic coordination about mercury can be obtained by study of the higher wavenumber region of the mercury-halogen vibrational spectrum. Further information with respect to the way in which individual units pack together (or not) to give extended (or monomeric) structures is contained in the lower wavenumber regions of the spectrum where $\nu(HgX)_b$ modes occur.

Unfortunately, low wavenumber data available for mercury-halogen bridge stretching modes are rather limited. Only for the dimeric systems such as those presented in Table I.4 have valid assignments been made. For example, $\nu(HgBr)_b$ modes have been assigned at 128 and 125 cm^{-1} in the IR spectrum of the $[Hg_2Br_6]^{2-}$ species contained in $[NEt_4]_2[Hg_2Br_6]$. The chloro and iodo complexes show analogous spectra.

Modes arising from weaker bridge interaction, i.e. from contact approach-

Vibrational spectroscopic data for some mercuric halide compounds

| | | |

Table 1.4, continued

Table 1.4, continued

Table 1.4, continued

ing the sum of the van der Waals' radii of mercury and the halogen, have only been assigned on a few occasions. The reasons for this are two-fold. Firstly, there is a problem of definition. The difficulty in defining a mercury-halogen bridge bond (Section 1.3.1) again manifests itself when trying to explain what is a mercury-halogen bridge mode. It will be remembered that a wide range of mercury-halogen bridge distances are observed so we may similarly expect to find a wide wavenumber range within which $\nu(HgX)_b$ modes will lie. For the lower wavenumber bands arising from mercury-halogen vibrations, a problem of interpretation arises as to whether or not to call these bands $\nu(Hg\text{-}X)_b$ modes, where there is still considered to be some bonding interaction, or to call them external lattice modes where there is no longer any bonding interaction. Unfortunately there is no clear change over point from one to the other and it appears from the literature that definition is left to the spectroscopist's discretion, apparently on a structure-to-structure basis. Consider for instance some of the associated structures presented in Table 1.4. Mercury-halogen bridge stretching modes, or more correctly in-plane or out-of-plane deformations, have been assigned for α-$[NH_4][HgCl_3]$ at 92 cm^{-1} (IR), and for $K_2[HgCl_4],H_2O$ at 168 and 125 cm^{-1} (IR). However, no such $\nu(HgX)_b$ modes have been assigned for the complexes α-$[NEt_4][HgCl_3]$, $[SMe_3][HgCl_3]$, $[NMe_4][HgBr_3]$ and $[SMe_3][HgI_3]$. All these complexes, in both groups, are known to contain bridge bonds as defined by Equation 1 (Section 1.3.1). Barr and Goldstein state[95] that bridge interactions present in the latter group of structures are "so weak as to have little or no influence on the vibrational spectrum." Presumably the modes of vibration arising from these 'bridge' interactions are interpreted as external lattice modes. External lattice modes have not been assigned for these complexes, probably as a result of the complexity of the lower wavenumber regions of the spectra. The complex nature of the lower reaches of the vibrational spectra is the second reason for the lack of low wavenumber mercury-halogen bridge stretching mode data.

In this region one may expect to observe various types of bending modes and also begin to observe other external lattice modes. Consequently one may envisage considerable band overlap which would make assignment very difficult.

In conclusion, therefore, it may be stated that at the present time vibrational data can give some information about the characteristic coordination about mercury, but information concerning bridging interactions is restricted as a result of limitations to spectral interpretation at very low wavenumbers.

1.4.2. Addition complexes

The present work is concerned with the addition complexes of 1:1 and 2:1 stoicheiometries formed between unidentate ligands and mercuric halides. The vibrational data given in Section 1.4.1 for halomercurate(II) complexes are fairly reliable, having been based on sound crystallographic knowledge. Unfortunately the same cannot be said for the data reported for addition complexes. This may be attributed to three reasons:

a) misinterpretation of crystallographic data;

b) neglect of relevant crystallographic data;

c) inadequate vibrational spectroscopic studies (especially true of earlier work).

Furthermore,Raman data have often not been reported and even the IR studies have terminated at ca. 200 cm thus not covering the complete far-IR region. A fairly comprehensive survey of existing spectroscopic data for the $(L)HgX_2$ and $(L)_2HgX_2$ complexes will now be presented.

$(L)HgX_2$ complexes. Previous data, and those data published whilst this work has been in progress, are presented in Table 1.5. Authors infer from the majority of these data that complexes of the 1:1 stoicheiometry exhibit discrete dimeric structures in which mercury lies in a tetrahedral environment with the donor ligands mutually trans to one another. (In subsequent discussion this structure shall be donoted by the abbreviation trans halogen - bridged dimer, THD).

Using the point group approach one may predict the following stretching modes for a molecule of this symmetry (C_{2h}):-

$\nu(HgL)_t$, $\nu(HgX)_t$, $2 \times \nu(HgX)_b$ IR-active

$\nu(HgL)_t$, $\nu(HgX)_t$, $2 \times \nu(HgX)_b$ Ra-active

The evidence for the inferences made in Table I.5 have, in many cases, been based on the assignment of a single $\nu(HgX)_t$ IR-active mode. For example, the considerable work on N-donor complexes,[2,10,19] some work on P(As)-donor complexes,[5,6] 'pyridine-N-oxide type' complexes[11] and R_2S(Se, Te) complexes.[14]

Clearly this situation is not satisfactory because halogen-bridge interactions have been inferred without actually observing $\nu(HgX)_b$ modes. It is also interesting to note the surprisingly wide wavenumber ranges within which $\nu(HgX)_t$ modes for a dimer have been assigned for complexes of reportedly similar structure, i.e. 273-349, 179-253 and 123-160 cm^{-1} for chloro, bromo and iodo complexes respectively.

There have been studies where the THD structure has been inferred in which $\nu(HgX)_b$ modes have been assigned, notably some P(As)-donor complexes,[4, 5,7,80,90,95] N-donor complexes,[10,19] and S-donor complexes.[14,16] Generally the basis for these assignments is poor; they are usually no more than guesses. Furthermore, the wavenumber positions of the assigned bands cover surprisingly wide ranges when one considers their supposedly similar origin, viz. 83-230, 61-195, and 34-137 cm^{-1} for chloro, bromo and iodo complexes respectively. Point group analysis predicts two sets of $\nu(HgX)_b$ modes, each set consisting one IR-active and one Ra-active mode. On the few occasions where modes from both sets have been assigned there appears to be some controversy as to their relative wavenumber positions. For example, we find for $(PBu^n_3)HgX_2$[90] and $(PPh_3)HgX_2$[8] (X=Cl, Br or I) a relatively small wavenumber separation is given, whereas for $(PCy_3)HgX_2$,[6] $(AsPh_3)HgX_2$,[5] $(SbPh_2Me)HgX_2$[9] and $(PPh_3)HgX_2$[7] (X=Cl, Br or I) a relatively large wavenumber separation is proposed.

Only the studies of $(Ph_3PSe)HgX_2$,[96] (dehydrodithizone)HgX_2[104] (X=Cl, Br or I) and $(Ph_3AsO)HgCl_2$[27] have been based on known crystal structures. Only in the first of these cases did the author study the Raman as well as the IR spectra and then, even with the crystallographic knowledge, it was concluded that complete assignment of ν(HgX) modes was not possible.[96]

Other studies, notably on $(R_2SO)HgCl_2$,[101] complexes of the type (pyridine-N-oxide)HgX_2,[102] and $(R_2S)HgCl_2$[103] have been interpreted bearing in mind related crystal structures. Generally however, relevant crystallographic data, which indicates a variety of structures for the 1:1 system, has been ignored.[2,10,14,19] The majority of vibrational spectroscopic data presented in Table 1.5 has been interpreted using the partial crystallographic analysis of $(AsEt_3)HgI_2$[61] as a basis.

The reliability of $\nu(HgL)_t$ assignments is questionable. There appears to be a general uncertainty as to their wavenumber position as indicated by the wide wavenumber ranges within which they have been assigned viz. $\nu(HgN)_t$ at 104-420,[10,30,96] $\nu(HgP)_t$ at 110-364,[4,7,97] $\nu(Hg\text{-}O)_t$ at 95-414,[11, 13,30,101,102] and $\nu(HgS)_t$ at 209-347 cm^{-1}.[14,16,103]

$(L)_2HgX_2$ complexes. Although there appears to be better use of available crystallographic data for these compounds, the vibrational data used to make structural inference are generally incomplete (Table 1.6). Only the reports on $(Py)_2HgX_2$,[98] $(PR_3)_2HgX_2$,[90] $[(NMe_2)HCS]_2HgX_2$[100] and $[(EtNH)_2CS]_2HgX_2$[16] (X=Cl, Br or I ; $R_3=Bu^n_3$ or $EtMe_2$) have contained both IR and Ra data covering all the far-IR region (<500 cm^{-1}).

The $(Py)_2HgCl_2$ complex, known to have a polymeric structure with mercury in a distorted octahedral environment, has been studied by various workers.[2,5,8,98] The most recent and most thorough of these studies is that by Barr and Goldstein,[98] which indicates that the previously reported data[2,18] are erroneous due to decomposition during experiments:

$$(Py)_2HgCl_2 \longrightarrow (Py)HgCl_2 + Py$$

As the spectral interpretation of several substituted pyridine complexes[2] has been based on erroneous results for $(Py)_2HgCl_2$, such assignments must be in question. The assignment of Barr and Goldstein[98] is very interesting because although the structure of $(py)_2HgCl_2$ contains short Hg-Cl distances of 2.34 Å, no ν(HgCl) modes are observed above ca. 200 cm^{-1} (Table I.5). The 3.25 Å bridging interactions in this structure are said to have considerable influence on the vibrational spectra. All modes are described as $\nu(HgCl)_b$ of the $[(Py)_2HgCl_2]_n$ chain, with motion of both short and long Hg-Cl bonds contributing to all these modes.

The discrete tetrahedral monomer is known to be a common structure for this system (Section I.3.3, Table I.3). Table I.6 indicates the numerous occasions for which vibrational spectra have been used to infer this type of structure. It is surprising to note the very wide wavenumber ranges over which the ν(HgX) modes have been assigned, viz. 200-335, 128-235 and 105-200 cm^{-1} for the IR-active modes of chloro, bromo and iodo complexes respectively. Another surprising observation (Table I.6) is that complexes of very similar ν(HgX) spectra have been inferred to have totally different structures. For example, $[(MeNH)_2CS]_2HgBr_2$, which has ν(HgBr) at 145 cm^{-1}, is said to have a distorted octahedral polymeric structure whereas $[(Me_2N)_2CS]_2HgBr_2$ which has ν(HgBr) at 152 cm^{-1} is said to have a tetrahedral monomeric structure.[16]

Reports of other structural types inferred from vibrational data include studies of $(PMe_3)_2HgX_2$ (X=Cl, Br or I),[4] where ionic structures containing linear $[P\text{-}Hg\text{-}P]^{2+}$ and $2X^-$ ions are suggested, and of $(PEtMe_2)_2HgX_2$ (X=Cl, Br or I),[90] where polymeric structures are tentatively proposed in which there are linear [P-Hg-P] units surrounded by four halogens at longer distances in an equatorial plane. Although solution-phase studies employing measurements of conductivity and ^{31}P n.m.r. spectra have been cited in

support of these proposals, there is no sound crystallographic basis.[4,90]

Assignments of v(HgL) modes indicate a general uncertainty as to their wavenumber positions. For example, v(HgN) at 123-415,[3,10,18,19,98] v(HgS) at 192-327,[16,23,25,26,99,100] and v(HgP) at 104-337 cm^{-1}.[4,6,7] Certainly, the problem of assignment of v(HgP) modes may be attributed to their generally low intensities.[106] Finally, mention is made of (ethylene-thiourea^HgCI^[22,23] for which there is some controversy as to whether the ligand is bidentate, bonding via N- and S-,[22] or unidentate, bonding via S-.[23] The spectroscopic evidence presented in either case is not entirely sound.

1-5- THE SCOPE OF THE PRESENT WORK

In an attempt to rationalize the coordination behaviour of mercury(||) in the (L)HgX_2 system and also to provide a sound crystal lographic basis from which meaningful structure/spectra correlations may be made, the crysta structures of the complexes (PR^JHgC^ (PR^PMe^, PE+^, PBu^, PPh^ and TPP) and the complex (2,4-Me2C^H^NJHgEl^ were determined. Wherever possible preliminary single-crystal X-ray studies have been used to indicate whether or not equivalent halo complexes are isostructural.

Structure/spectra relationships have been further investigated by examination of the vibrational spectra of some (L)HgX_2 complexes (L=Ph^PS, C4H8S, MPC, 2,4,6-trimethylpyridine, coumarin, quino line-N-oxide and Pf^SO) of known crystal structure.

The structure/spectra correlations observed from the above work have been applied to a number of other (L)HgX_2 complexes of unknown structure where (L) is a N- or P- donor ligand.

A similar approach has been adopted for study of $(L)_2HgX_2$ compounds. Rationalisation of the coordination behaviour of mercury(||) in this system and provision of a firm basis for structure/spectra correlation has been attempted by determination of the crystal structures of (PEt^^HgC^ and

$(PEtMe_2)_2HgBr_2$, and the partial crystallographic analysis of $(PBu^n_3)_2HgCl_2$.

The vibrational spectra of a number of other $(PR_3)_2HgX_2$ complexes have been studied and have been interpreted in the light of the above work.

Table 1.5.

Vibrational spectroscopic data for the $(L)HgX_2$ system.

Compound	Ref.	Assignment $\nu(HgL)_t$	Assignment $\nu(HgX)_t$	Assignment $\nu(HgX)_b$	Structural inference
$(L)HgCl_2$ complexes					
L=,					
Py	2		349,289		THD
Py	96		293,(306) (290)	209,154,124 163;(162)	NI
2-MePic	2		285	218	THD
2-MePic	96		285,(284)		NI
3-MePic	2		336		THD
4-MePic	2		319		THD
4-MePic	96	125	320,273 (268)		NI
2,4-Me_2Lut	2		285		THD
2,6-Me_2Lut	2		336	219	THD
3-CNPy	2		328,289		THD
4-CNPy	2		312		THD
$C_5H_{11}N$	19		300	208	THD
Pr^n-NH_2	10	390-370	315	ca. 230	THD
Pr^i-NH_2	10	390	315	ca. 230	THD
Bu^n-NH_2	10		330-310	ca. 230	THD
Bu^i-NH_2	10	395-365	317	ca. 215	THD
p-toluidine	3		275		THD
Isoquinoline	28		320	208	THD
3,5-dimethyl-isoxazole	30	151(?)	279	218	THD

N.B. 1. Wavenumber values contained in parentheses denote Ra active bands.

2. Wavenumber values separated by semi-colon arise from different sets of $\nu(HgX)_b$ mode.

THD - is an abbreviation which denotes a halogen-bridged dimeric structure in which donor ligands (L) are trans to one another and mercury lies in a tetrahedral environment.

NI - no inference.

? - denotes an assignment or structural proposal which the author feels is tentative.

Pic = picoline = methylpyridine. Lut = lutidine = dimethylpyridine.

CNPy = cyanopyridine. Py = pyridine.

Table 1.5, continued

Compound	Ref.	Assignment $\nu(HgL)_t$	Assignment $\nu(HgX)_t$	Assignment $\nu(HgX)_b$	Structural inference
$(L)HgCl_2$ complexes, continued.					
L=,					
PMe_3	4	364,(362)	304,(295)	(177)	THD
$P(p\text{-}C_6H_4NMe_2)Me_2$	5		307		THD
PBu^n_3	90		297,(298)	153,(177);105,(148)	THD
PBu^t_3	97	(123)	270,(266)	175,169,(162)	THD
PCy_3	6		283,273		THD
PPh_3	5		289		THD
PPh_3	7	152	287	180;97,83	THD
PPh_3	8		288	190,179;150	THD
P(o-tolyl)$_3$	7	(138)	276,(264)	179,(181)	THD
$PPhMe_2$	5		305		THD
$PEtMe_2$	90		307,(301)	195,(200);108,(105)	extended structure like $(PMe_3)HgCl_2$*
$AsEt_3$	5		285		THD
$AsPh_3$	5		290		THD
$AsPh_3$	27	138	288	[184] [138]	THD
$AsPh_3$	8		291	[202,183] [139]	THD
$SbPh_2Me$	9		260	[202] [88]	THD
Me_2SO	101	392,(394)	359,312 (309)		CBC
Et_2SO	101	401,(400)	350,306 (353),(289)		CBC

* - the structure of $(PMe_3)HgCl_2$ determined in this work (Section 2) has already appeared in J.C.S. CHEMM. COMM., 1039, 1976.

CBC - denotes a chlorine-bridged structure containing slightly distorted $HgCl_2$ units.

Table 1.5, continued

Compound	Ref.	Assignment ν (HgL)$_t$	ν (HgX)$_t$	ν (HgX)$_b$	Structural Inference
(L)$HgCl_2$ complexes, continued. L=,					
Pr^n_2SO	101	(414)	343,289 (290)		CBC
Bu^n_2SO	101	403,(400)	348,304 (298)		CBC
Bu^i_2SO	101	390	354,306 (305)		CBC
Ph_2SO	101	398	360,311 (362),(308)		CBC
Ph_3AsO	27		353-323, 278		OBD
PyO	11	340	315		THD
PyO	12		335,310		OBD
PyO	13	278	340,315	278	THD
PyO	102	163	314,338 (282)	163,139	LHD
PyO	96		340,319,285 (340),(288)	162,(168)	NI
2-MePyO	11	339	292	224	THD
2-MePyO	13		340	292	THD
2-MePyO	102	(144)	340,(286)	(144),(120)	LHD
3-MePyO	11	353,344, 317	306		THD
3-MePyO	13	288	342	288	THD
3-MePyO	102	(155)	344,(298)	(155),(120)	LHD
4-MePyO	11	345	296		THD
4-MePyO	13		342	290	THD
4-MePyO	102	(192)	346,(290)	(192),(119)	LHD
4-CNPyO	11	346	295		THD
2,6-Me_2PyO	11	355,330	310,305	205	THD

OBD - denotes an oxygen-bridged dimer.

LHD - denotes a halogen-bridged dimer containing linear $HgCl_2$ units, with the likelihood of further Hg---Cl interaction.

Table 1.5, continued

Compound	Ref.	Assignment ν (HgL)$_t$	ν (HgX)$_t$	ν (HgX)$_b$	Structural Inference
(L)$HgCl_2$ complexes, continued. L=,					
Acridine-N-oxide	31		340		NI
isoxazole	30	310-330	278	215	THD
Et_2S	103	306,288	339,306 288		NI
Et_2S	14	308	371,340	160	THD
Pr^n_2S	103	272,253	352,272 253		NI
Pr^n_2S	14	295	353,340	161,137	THD
Pr^i_2S	103	262,248	262,248		NI
Bu^n_2S	14	298	370,351	136	THD
Bu^t_2S	103	313,300	360,313 300		NI
Bu^i_2S	14	313	360	ca. 165	THD
Bu^tMeS	103	259	259		NI
Bu^s_2S	14	235-275	353	142(?)	THD
C_4H_8S	103	305	305		$[C_4H_8HgCl]^+$ and Cl^- known
2,1,3-benzothiadiazole*	15		346		THD
$(NH_2)_2CS$	16	254	282	192	THD
$(NMe_2)_2CS$	16	209	268	223	THD
(NEtH)(NH_2)CS	16	271	297	208	THD
$(NMeH)_2CS$	16	246	302	206	THD
$(NEtH)_2CS$	16	347,(312)	305,(301)	187,(198)	THD
dehydrodithizone	104	255	322,312 202		S-bridged polymer known
thiomorpholin-3-thione	29		305	212	THD

* benzothiadiazole = 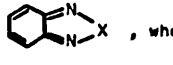 , when X=S

Table 1.5, continued

Compound	Ref.	Assignment $\nu(HgL)_t$	Assignment $\nu(HgX)_t$	Assignment $\nu(HgX)_b$	Structural Inference
(L)$HgCl_2$ complexes, continued. L=,					
2,1,3-benzoselenoadiazole*	15		305		THD
Ph_3PSe	96		297,293 (294),(299)	200,180 (208),(183)	THD known
Et_2Se	14	190	305,288	160	THD
$(NH_2)CSe$	17	183	276	200	THD
Et_2Te	14		330,320 293	140-165	THD
Bu^n_2Te	5		299		THD
(L)$HgBr_2$ complexes L=,					
2-MePy	2		222		THD
2-MePy	96		201,153 (196),(161)		NI
3-MePy	2		225		THD
3-MePy	96	110 (?) (111)	230,182 (229),(180)		NI
4-MePy	2		228		THD
4-MePy	96	124	230,180 (229),(175)		NI
$2,4\text{-}Me_2Py$	2		200		THD
$2,6\text{-}Me_2Py$	2		246		THD
2-CNPy	2		225		THD
3-CNPy	2		240		THD
$C_5H_{11}N$	19		218		THD
$Pr^n_3NH_2$	10	385	ca. 235		THD
$Pr^i_3NH_2$	10	390	ca. 230		THD
$Bu^n_3NH_2$	10	420	ca. 230		THD
$Bu^i_3NH_2$	10	360-390	ca. 230		THD

* benzoselenoadiazole = 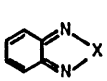 , when X = Se

Table 1.5, continued

Compound	Ref.	Assignment $\nu(HgL)_t$	Assignment $\nu(HgX)_t$	Assignment $\nu(HgX)_b$	Structural Inference
(L)$HgBr_2$ complexes, continued. L=,					
Isoquinoline	28		226		THD
3,5-dimethyl-Isoxazole	30	149(?)	237	140	THD
PMe_3	4	(353)	(167)		THD
$P(p\text{-}C_6H_4NMe_2)Me_2$	5		214		THD
PBu^n_3	90		188,(185)	168,(169);101,(149)	THD
PBu^t_3	97	(116)	178,(174)	134	THD
PCy_3	6		(180)	(141);(44)	THD
PPh_3	7	127	198,189	129,111;66,60	THD
$P(o\text{-}tolyl)_3$	97		189,(180)	132,(132)	THD
$PEtMe_2$	90		160,(168)		C_{21} Monomer
$AsPh_3$	27	112(?)	196	126,110;61	THD
$SbPh_2Me$	9		186	148;63	THD
PyO	11	326	247		THD
PyO	13		246		THD
PyO	102	(138)	247,(191)	(138),(100)	LHD
2-MePyO	11	350,322	239		THD
2-MePyO	13		240		THD
2-MePyO	102	(142)	239,(188)	(142),(105)	LHD
3-MePyO	11	312	250		THD
3-MePyO	13		250		THD
3-MePyO	102	(136)	250,(195)	(136),(106)	LHD
4-MePyO	11	349,335	244		THD
4-MePyO	13		242		THD
4-MePyO	102	(190)	251,(181)	(190),(106)	LHD
4-CNPyO	11		243		THD
$2,6\text{-}Me_2PyO$	11	332,310	252		THD

Table 1.5, continued

Compound	Ref.	Assignment $\nu(HgL)_t$	Assignment $\nu(HgX)_t$	Assignment $\nu(HgX)_b$	Structural Inference
(L)$HgBr_2$ complexes, continued. L=,					
quinoline-N-oxide	31		258		NI
isoxazole	30	310-330	212	140	THD
Et_2S	14	275(?)	250,188	158	THD
Pr^n_2S	14	294	250	195	THD
Bu^n_2S	14	295	250,240	ca. 125	THD
Bu^i_2S	14	295	253,208	138	THD
Bu^s_2S	14		248,240	155	THD
$(NH_2)_2CS$	16	252	194	144	THD
$(NMe_2)_2CS$	16	217	179	154	THD
$(NEtH)(NH_2)CS$	16	278	192	130	THD
$(NMeH)_2CS$	16	249	196	146	THD
$(NEtH)_2CS$	16	339,(340)	214,(208)	118,(113)	THD
dehydrodithizone	104	260	232,168		S-bridged polymer
thiomorpholin-3-thione	29		215	148	THD
Ph_3PSe	96		206,174 (203),(172)	136,(145)	NI
Et_2Se	14	203	258,213	135,125	THD
Et_2Te	14	110,98	203,190	123	THD
(L)HgI_2 complexes L=,					
2-MePy	96		172 (166),(135)		NI
3-MePy	96	104 (?) (105)	187,145,135 (185),(142), (132)		NI
4-MePy	96		185,131 (182),(136)		NI

Table 1.5, continued

Compound	Ref.	Assignment $\nu(HgL)_t$	Assignment $\nu(HgX)_t$	Assignment $\nu(HgX)_b$	Structural Inference
(L)HgI_2 complexes, continued. L=,					
PMe_3	4	(342)	123		THD
PBu^n_3	90		150,(149)	128,(129);75,(116)	THD
PBu^t_3	97	110	140,(138)		THD
PCy_3	6		(154)	(137),(104);(34)	THD
PPh_3	7	135	156	110,86;50	THD
P(o-tolyl)$_3$	97	(122)	143,(140)		THD
$PEtMe_2$	90		130,(123)		C_{2v} Monomer
PyO	102	(98)	195,(143)	(98),(80)	LHD
2-MePyO	102	(95)	193,(142)	(95),(73)	LHD
3-MePyO	102	(97)	200,(147)	(97),(73)	LHD
4-MePyO	102	(175)	197,(139)	(175),(98)	LHD
$(NH_2)_2CS$	16	235	148	106	THD
$(NMe_2)_2CS$	16	216	146	90	THD
$(NEtH)(NH_2)CS$	16	270	150	92	THD
$(NMeH)_2CS$	16	256	144	104	THD
dehydrodithizone	104	252	156		S-bridged polymer
Ph_3PSe	96		175,151 (171),(150)	115,(119)	NI
Et_2Se	14		160	107	THD

Table 1.6.

Vibrational spectroscopic data for the $(L)_2HgX_2$ system.

Compound	Ref.	Assignment ν(HgL)	Assignment ν(HgX)	Structural inference
$(L)_2HgCl_2$ complexes				
L=,				
2-MePic	2		287	DPO
3-MePic	2		336,304,275	DPO
4-MePic	2		320,275	DPO
2,4-Me_2Lut	2		287,261	DPO
2-CNPy	2		295	DPO
4-CNPy	2		320	DPO
3-CNPy	105		328,287	NI
Py	5	No bands observed above 200 cm^{-1} in IR		known DPO
Py	2		292	DPO
Py	98	123,(122)	168,(204) 159,(162)	DPO
Py	18	<200	292	DPO
Pr^n-NH_2	10	380	315	TM
Pr^i-NH_2	10	385	335-320	TM
Bu^n-NH_2	10		335	TM
Bu^i-NH_2	10	390	312	TM
$C_5H_{11}N$	19	ca.320(?)	300	TM or DPO
β-naphthylamine	20	375	325	TM

N.B. Wavenumber values contained in parentheses denote Ra-active bands.

? - denotes an assignment or structural proposal which the author feels is tentative.

DPO - is an abbreviation used to denote a polymeric arrangement of almost linear X-Hg-X units, within which mercury lies in a distorted octahedral environment.

TM - is an abbreviation to denote a discrete monomeric arrangement in which mercury lies in a tetrahedral environment.

NI - no inference

Table 1.6, continued

Compound	Ref.	Assignment ν(HgL)	Assignment ν(HgX)	Structural inference
$(L)_2HgCl_2$ complexes, continued.				
L=,				
$C_6H_5NH_2$	3	370	297	TM
quinoline	28		270	DPO
isoquinoline	28		298,278	DPO
3,5-diphenylisoxazole	33	150	310	TM
o-toluidine	3	410	315	TM
m-toluidine	3	415	290	TM
m-chlorotoluidine	3	402	300	TM
ethylenethiourea	22	275	380	DPO
PMe_3	4	(335)		linear [P-Hg-P] and 2Cl-
PBu^n_3	90		205,(215)	TM
$PEtMe_2$	90		176,(233)	NI
PCy_3	6	(134)	200,(208),(187)	TM
PPh_3	7	137,108	232,221	TM
$(NH_2)_2CS$	99	251,236		known $[S_2HgCl]^*$
$(NMeH)_2CS$	16	250	205	DPO
$(NMe_2)_2CS$	16	198	220,234	NI
$(NHEt)_2CS$	16	276,252	220 (218) 186 (181)	NI
$(NMe_2)HCS$	100	313,(327),(308)	245,(240) 226,(227)	TM(?)
$(NHPh)(NH_2)CS$	25	277	327-331	TM(?)
$(NHPh)_2CS$	25	261		TM(?)
ethylenethiourea	23	218	218	TM
pyrollidine-2-thione	26		254	TM
$(NH_2)_2CSe$	17	204,200,176	204,200,176	NI
tzSe*	32	152	228,205	TM
tzO*	32	176	230	TM

* tzSe = Se=C-NH-CH_2-CH_2-S , tzO = O=C-NH-CH_2-CH_2-S

Table 1.6, continued

Compound	Ref.	Assignment ν(HgL)	Assignment ν(HgX)	Structural Inference
$(L)_2HgBr_2$ complexes				
L=,				
2-MePy	2		223	DPO
3-MePy	2		230,215	DPO
4-MePy	2		228	DPO
$2,4\text{-Me}_2\text{Py}$	2		205	DPO
4-CNPy	2		240	DPO
Py	2		215	DPO
Py	98	145,(144) 115,(113)	217,(220) 182,(184)	TM
Py	18	<200	215	DPO
$Pr^n\text{-}NH_2$	10	ca.370	ca.235	TM
$Pr^i\text{-}NH_2$	10	375		TM
$Bu^n\text{-}NH_2$	10	410	ca.230	TM
$Bu^i\text{-}NH_2$	10	395	ca.230	TM
$C_5H_{11}N$	19	ca.320(?)	220	DPO
β-naphthylamine	20	370	230	DPO
$C_6H_5NH_2$	3	365,345		TM
Isoquinoline	28		213	DPO
3,5-diphenylisoxazole	33	148	247,231	TM
o-toluidine	3	400		TM
m-toluidine	3	415		TM
p-toluidine	3	396		TM
PMe_3	4	(337)		linear $[P\text{-}Hg\text{-}P]^{2+}$ and $2Cl^-$
$PEtMe_2$	90		118,(119)	Bridged structure with linear P-Hg-P
PBu^n_3	90		128,(136)	TM
PCy_3	6	(132)	(144),(132)	TM
PPh_3	7	132,104	153	TM
$(NMeH)_2CS$	16	246	(145)	DPO
$(NMe_2)_2CS$	16	198	(152)	TM
$(NEtH)_2CS$	16	268,254	158,(165)	TM

Table 1.6, continued

Compound	Ref.	Assignment ν(HgL)	Assignment ν(HgX)	Structural Inference
$(L)_2HgBr_2$ complexes, continued.				
L=,				
$(NH_2)_2CS$	99	252,228		NI
ethylenethiourea	23	215,208	<200	TM
$(NH_2)_2CSe$	17	189,172,148	189,172,148	$[L_2HgBr]^{2+} + 2Br^-$
tzSe	32	152	190	TM
tzO	32	176	190	TM
$(L)_2HgI_2$ complexes				
L=,				
Py	98	147,124,(124) 140	176,(176) 147,(142) 140	TM
$Pr^n\text{-}NH_2$	10		<200	TM
$Pr^i\text{-}NH_2$	10	385	<200	TM
$Bu^n\text{-}NH_2$	10		<200	TM
$Bu^i\text{-}NH_2$	10	ca.375	<200	TM
PMe_3	4	(331)		linear $[P\text{-}Hg\text{-}P]^{2+}$ and $2Cl^-$
$PEtMe_2$	90		96,(94)	Bridged structure with linear P-Hg-P
PBu^n_3	90		105,(119),(107)	TM
PCy_3	6	(132),(128)	(103)	TM
PPh_3	7	133,98	127	TM
$AsPh_3$	27		147,142,133	TM
$(NMeH)_2CS$	16	278,235	136	TM
$(NMe_2)_2CS$	16	192	127	TM
$(NEtH)_2CS$	16	242,201	146,(147) 124,(129)	TM
$(NMe_2)HCS$	100	305,(311)	(167),(127)	TM(?)
ethylenethiourea	23		< 200	TM
$(NH_2)_2CSe$	17	155,126,112	155,126,112	NI

Chapter 2

Crystallographic studies of some $(L)HgX_2$ complexes.

Contents

2.1. CRYSTALLOGRAPHIC METHODS

The general methods of structure solution and refinement used in this work are very similar for all the structures studied,[107] and therefore a general description of the crystallographic approach used will be outlined. Note is given to special considerations required for individual structures as they are discussed.

Space group determination. Space groups were determined by examination of oscillation, Weissenberg and precession photographs. Initially crystal systems were determined by examination for axial symmetry, then location of systematic absences allowed space group assignment. In instances where photographs could not uniquely define the space group, e.g. differentiation between P1 and $P\bar{1}$ and also between Cc and C2/c, the final determination was carried out during structure solution and refinement.

Diffraction data. All data collected in this work, unless otherwise stated have been collected using Mo-K_α radiation, λ=0.71069 Å, with a Stoe Stadi 2 two-circle diffractometer using the background, ω-scan, background technique. In all cases Lorentz and polarisation corrections have been made and also where possible absorption corrections have been applied (Appendix I). Structure factors have been corrected for the real and imaginary components of anomalous dispersion.[109]

Structure solution and refinement. The initial solution for each structure involved use of standard Patterson syntheses to locate the mercury atoms, followed by succesive Fourier synthesis to locate remaining non-hydrogen atoms. The structures were refined by full-matrix least squares methods with all non-carbon atoms given anisotropic thermal parameters of the form:-

$$\exp\,[\,-2\pi^2\,(U_{11}h^2a^{*2} + U_{22}k^2b^{*2} + U_{33}l^2c^{*2} + 2U_{12}hka^*b^* + 2U_{13}hla^*c^* + 2U_{23}klb^*c^*)]$$

Carbon atoms and atoms of comparable atomic number were given isotropic

temperature factors. Scattering factors used were those for neutral atoms.[108,109]

The weighting schemes,[110] used were of the form:-

$w = k/[\sigma^2 |F_o| + abs\ (g)|F_o|^2]$.

Wherever necessary inter-layer scale factors have been applied. Computation was carried out on an IBM 370/135 computer using the 'SHELX' X-ray computing package.[110]

2.2. CRYSTALLOGRAPHIC STUDIES OF SOME (L)HgX_2 COMPLEXES (WHERE L= A NEUTRAL UNIDENTATE LIGAND AND X = Cl, Br or I)

2.2.1. Introduction

For the small number of existing crystallographic studies reported for this 1:1 system one observes a range of solid state structures. Usually, these structures reflect varying degrees of long range mercury-halogen interaction.[57-73] Unfortunately one is not able to draw any conclusions as to the relationships between structure and chemical formula. This may be attributed to the nature of the complexes studied with regard to the diverse range of ligands they contain. Factors which may well influence solid state structures include:

a) the nature of the donor atom (N,P,S, etc.);

b) the electronic effect of the substituents attached to the donor atom;

c) the steric effect of the substituents attached to the donor atom;

d) the nature of the halogen atoms.

The importance of each of these properties can only be determined by a systematic crystallographic study of the (L)HgX_2 system.

The small number of crystallographic studies together with the limited understanding of the criteria which determine the solid state structures of (L)HgX_2 complexes are, in part at least, responsible for the poor quality of many of the vibrational spectroscopic reports for this system. Consequently, the vibrational spectroscopist may also benefit from such a systematic

crystallographic study.

The present work has been designed to examine the factors influencing the solid state structures of $(L)HgX_2$ complexes. Initial studies include a crystallographic investigation of the complexes formed between HgX_2 and the widely used tertiary phosphines, PPh_3, PEt_3 and PMe_3. This study allows one to monitor the electronic and steric effects of the substituents attached to phosphorus and also provides a firm basis from which structure/spectra correlations may be made.

The peculiarity of 1,2,5-triphenylphosphole (TPP) with regards its electronic and steric properties as a potential ligand and also the simplicity of the vibrational spectra of the $(TPP)HgX_2$ (X=Cl or Br) complexes has prompted the crystallographic examination of the latter compounds.

The vibrational spectra of the $(PBu^n_3)HgX_2$ (X=Cl, Br or I) complexes could not be satisfactorily explained in terms of the other structural data presented in this work. Therefore crystallographic examination of these complexes were undertaken.

Crystallographic studies of (2,4-dimethylpyridine)HgX_2 (X=Cl or Br) and $(AsPh_3)HgCl_2$ were undertaken in order to investigate in a preliminary way the effect of different donor atoms upon the solid state structure. At the same time these studies also provided further definitive structural data for structure/spectra correlation.

2.2.2. Crystallographic examination of the $(PPh_3)HgX_2$ (X=Cl, Br or I) complexes.

The crystal structure of the chloro complex has been determined.

Crystal Data

$C_{18}H_{15}PHgCl_2$; M_r=533.78, Monoclinic,

a=12.304(8), b=11.356(7), c=13.444(10) Å

α=90.00, β=92.50(5), γ=90.00°

D_m=1.92 g cm^{-3}(by flotation using $CHCl_3/CHBr_3$), D_c=1.89 g cm^{-3},

Z=4, $F_{(000)}$=1007.82, μ(Mo-K_α)=82.33 cm^{-1}.

Systematic absences:

hol reflections are absent for (h+l) = 2n+1

oko reflections are absent for k = 2n+1

These absences uniquely assign the crystals to the non-standard space group $P2_1/n$.

Data Collection and Structure Refinement. A colourless crystal, approximate dimensions 0.37 x 0.47 x 0.20 mm, was mounted about b. Eleven layers, hOl → hlOl, were collected; 1635 reflections were recorded with $2\theta < 50°$ of which 1616 had $I/\sigma(I) \geq 3.0$ and were used for refinement. Unit weights were used.

An attempt was made to apply an absorption correction, but no improvement was observed either for the R value or in the errors associated with the atomic and thermal parameters. This may reflect the difficulty encountered in accurately defining the shape of what was an irregularly shaped crystal.

The three phenyl rings of the triphenylphosphine ligand were refined as idealized regular hexagons, with C-C distances of 1.395 Å. The structure was refined by full matrix least squares methods, finally with all non-carbon atoms anisotropic. The function minimised was $\Sigma(|F_o| - |F_c|)^2$. The final R value, given by

$$R = \frac{\Sigma \; ||F_o| - |F_c||}{\Sigma \; |F_o|}$$

settled at 0.083.

Final atomic and thermal parameters are given in Table A2.1 (Appendix 2). Calculated and observed structure factors are contained in Appendix 3 (Table A3.1). A complete set of bond distances and bond angles may be found in Table 2.1.

Description of Structure. The structure consists of discrete chlorine-bridged dimers (Figure 2.1) in which mercury lies in a distorted tetrahedral environment with angles about mercury ranging from 85.4(3) to 128.7(4)°. The PPh_3 ligands are arranged mutually trans to one another. At the centre of the planar four-membered ring there is a centre of symmetry; there are no further elements of point symmetry in the molecule and the molecule belongs to the C_i point group. The Hg-Cl bridge distances are almost equal at 2.62(1) and 2.66(1) Å. This situation is in contrast to the bridge distances found for other dimeric structures (Table 2.2) where the four membered ring is asymmetric. The Hg-Cl(2')-Hg' bridge angle, the P-Hg-Cl(1) terminal angle and the Hg-Cl(1) terminal bond found in the present study are comparable to the equivalent bond parameters found for the other known dimeric systems (Table 2.2).

The molecular packing diagram (Figure 2.2) shows how the dimeric molecules are arranged with respect to one another, with two dimers per unit cell. As one can see there is no further Hg-Cl interaction beyond the dimer stage. The closest inter-dimer distance is between C(25') and C(34") at 3.77 Å. The geometry of the complexed ligand can be compared with that of the free ligand.[111] The average P-C distance (1.80 Å) found here is close to that observed for the free PPh_3 ligand (1.828 Å). The coordination polyhedron around phosphorus is affected on complexation; there appears to be less distortion of the C-P-C angles from regular tetrahedral for the complexed ligand (av. 108°) as compared to the free ligand (av. 103.0°). This is not surprising when one realises that the lone pair, which probably

causes contraction of the C-P-C angles in the free ligand, is drawn away from the P-C bonds as a result of bonding to mercury. The C-P-Hg angles are also close to the regular tetrahedral value (Table 2.1).

The three phenyl rings within the complexed ligand are planar, as they are in PPh_3, all deviations from planarity for PPh_3 being less than 0.01 Å (Appendix 6). The configuration of the rings in the complexed ligand is very similar to that found for free PPh_3; the angles between the mean planes are given in Table 2.1.

The corresponding bromo and iodo complexes have been studied by single-crystal X-ray photographic techniques, which indicate that both compounds are isomorphous and are probably isostructural (Table 2.9).

Fig.2.1 The molecular structure of $PPh_3 \cdot HgCl_2$

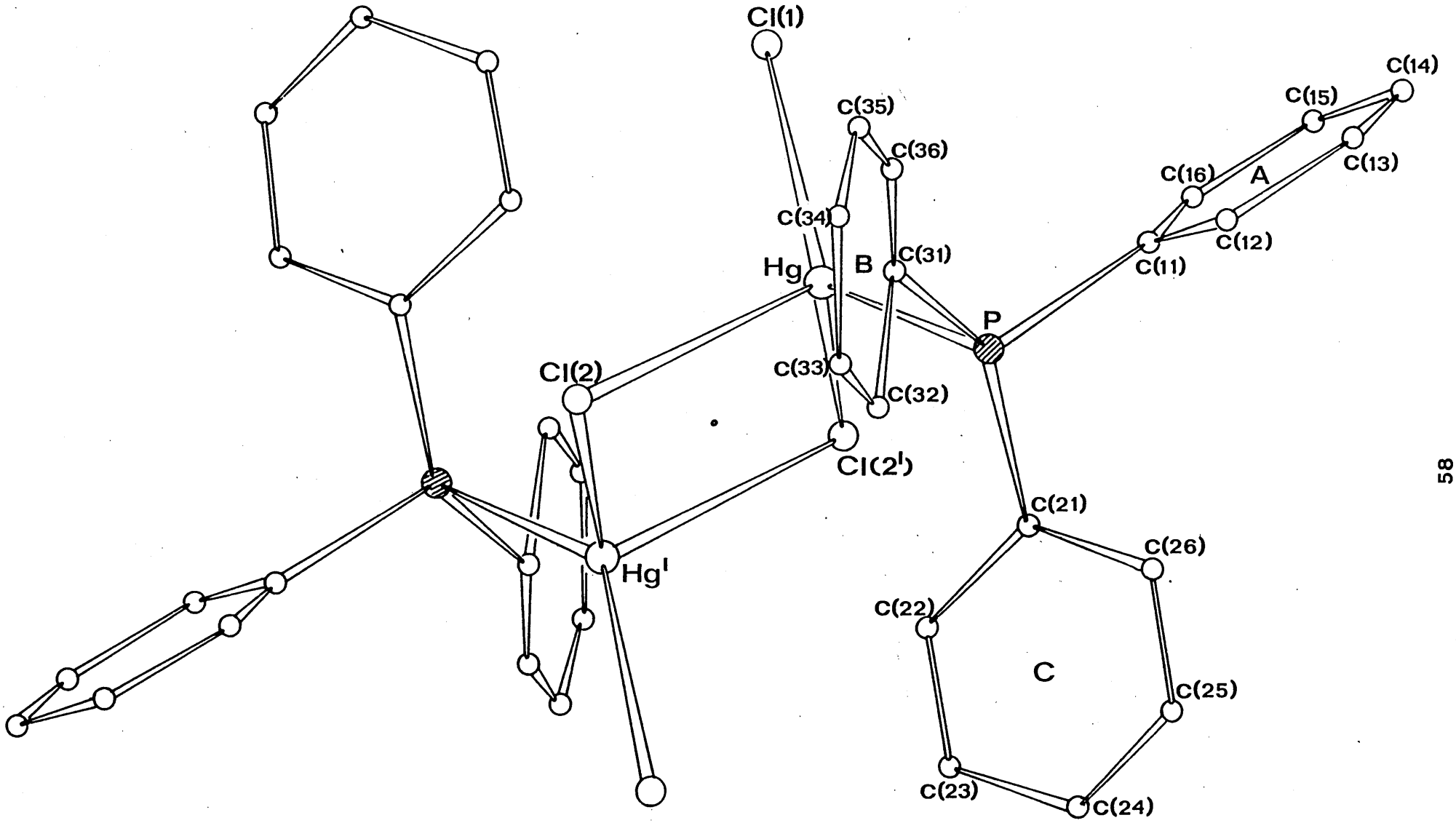

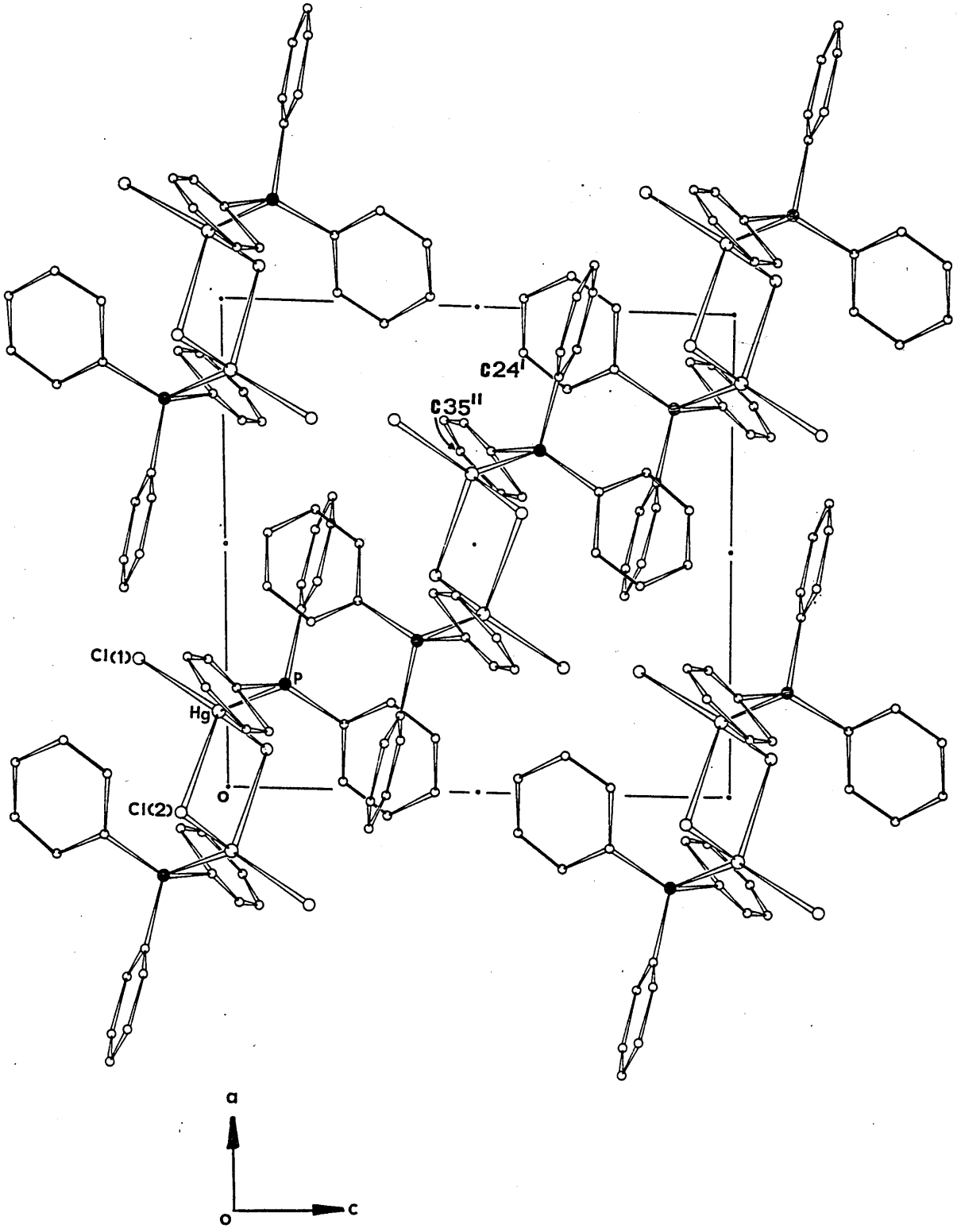
C24I
C35II
Cl(1)
P
Hg
O
Cl(2)
a
o
c

Table 2.1.

Bond distances and angles for $(PPh_3)HgCl_2$ with standard deviations in parentheses.

Distances/Å		Angles/°	
Hg-Cl(1)	= 2.370(10)	Cl(1)-Hg-Cl(2)	= 104.7(3)
Hg-Cl(2)	= 2.658(8)	Cl(1)-Hg-Cl(2')	= 103.8(3)
Hg-Cl(2')	= 2.623(8)	Cl(1)-Hg-P	= 128.7(4)
Hg-P	= 2.406(7)	Cl(2)-Hg-Cl(2')	= 85.4(3)
Hg-Hg'	= 3.881(3)	Cl(2)-Hg-P	= 114.3(3)
		Cl(2')-Hg-P	= 111.1(4)
P-C(11)	= 1.86(2)		
P-C(21)	= 1.75(2)	Hg-Cl(2')-Hg'	= 94.6(3)
P-C(31)	= 1.80(2)		
		C(11)-P-C(21)	= 109(1)
		C(11)-P-C(31)	= 106(1)
		C(11)-P-Hg	= 110(1)
		C(21)-P-C(31)	= 109(1)
		C(21)-P-Hg	= 114(1)
		C(31)-P-Hg	= 109(1)

Angles between mean planes for :-

Mean Planes[a]	Free ligand[111]	Complexed ligand
A-B	84.0°	84.4°
B-C	78.1°	80.1°
C-A	76.5°	75.4°

a - mean planes equations may be found in Appendix 6.

Table 2.2.

A comparison of the structure of $(PPh_3)HgCl_2$ — with other dimeric systems.

	Distances/Å			Angles/°	
Compound	$d(Hg\text{-}Cl)_t$	$d(Hg\text{-}Cl)_b$	$d(Hg\text{-}L)_t$	$(L\text{-}Hg\text{-}Cl)_t$	$(Hg\text{-}Cl\text{-}Hg)_b$
$(Ph_3PSe)HgCl_2$ [52]	2.33	2.78,2.60	2.53	136.3	91.7
$(MPC)HgCl_2$ [53]	2.37	2.78,2.57	2.42	131.9	92.7
$(PPh_3)HgCl_2$	2.37	2.66,2.62	2.41	128.7	94.6

2.2.3. Crystallographic examination of the (1,2,5-triphenylphosphole)HgX_2 (X=Cl or Br) complexes.

The crystal structure of (TPP)$HgCl_2$ has been determined

Crystal Data

$C_{22}H_{17}PHgCl_2$; M_r=583.84, Triclinic,

a=11.854(10), b=10.041(10), c=9.443(9) Å

α=84.16(5), β=103.38(5), γ=114.29(5)°.

D_m=1.97 g cm^{-3} (by flotation using $CHCl_3/CHBr_3$ mixture), D_c=1.95 g cm^{-3},

Z=2, $F_{(000)}$= 555.91, μ(Mo-K_α)=77.56 cm^{-1}.

Systematic absences:

None.

The crystals belonged to either of the triclinic space groups P1 or $P\bar{1}$. Subsequent structure solution unambiguously distinguished the space group as $P\bar{1}$ (C_i^1, No.2).[112]

Data Collection and Structure Refinement. A yellow crystal, approximate dimensions 0.16 x 0.08 x 0.08 mm, was mounted about b. Eleven layers, h0l ⟶ h10l, were collected; 2932 reflections were recorded with 2θ <50° of which 1272 had $I/\sigma(I) \geq 4.0$ and were used for refinement. Interlayer scaling was used and an absorption correction was applied.

The final weighting scheme used was:-

$$w = 1.4848 / (\sigma^2 |F_o| + 0.002649 |F_o|^2)$$

Full matrix refinement with anisotropic temperature factors for the non-carbon atoms gave R_w=0.074. The R_w factor is given by:

$$R_w = \frac{\Sigma ||F_o| - |F_c|| \times \sqrt{w}}{\Sigma |F_o| \times \sqrt{w}}$$

where w = weighting function. R= 0.070.

Atomic and thermal parameters are given in Table A2.2 (Appendix 2). Calculated and observed structure factors are contained in Appendix 3 (Table A3.2). A complete set of bond distances and angles maybe found in Table 2.3.

Description of Structure. The structure of $(TPP)HgCl_2$ (Figure 2.3) is very similar to that found for $(PPh_3)HgCl_2$ in that it consists of discrete chlorine-bridged dimers in which mercury lies in a distorted tetrahedral environment with the angles about mercury ranging from 86.5(4) to 127.8(5)°, and with the TPP ligands arranged mutually trans to one another. Again the dimer belongs to the C_i point group. The Hg-Cl(2)-Hg' bridge angle of 93.5(4)°, the P-Hg-Cl(1) terminal angle of 127.8(5)°, the terminal Hg-Cl(1) bond of 2.40(1) Å and the Hg-P bond of 2.44(1) Å are all very similar to the equivalent parameters found for the $(PPh_3)HgCl_2$ complex (Section 2.2.2). Again, there is no further Hg-Cl interaction beyond the dimer stage. There is, however, a subtle difference between the two structures, for in the present case the Hg-Cl bridge distances are of distinctly different length at 2.54(1) and 2.75(1) Å. This situation is similar to the bridge distances found for other dimer species[52,53] (Table 2.2). The closest inter-dimer contact is between C(20) and C(21') at a distance of 3.35 Å.

In comparison of the geometry of the complexed and free[113] TPP ligand (Table 2.3), it is noted that accuracy of atom positions is greater for the free ligand. This may be explained by the presence of the heavy mercury atom, for the complexed ligand, which dominates the diffraction data within the 2θ range recorded.

The P-C distances in the present case are not significantly different from one another, which is also the case for the free ligand.[113] The average P-C distance (1.83 Å) compares favourably with those found for free TPP[113] (1.822 Å), the free PPh_3 ligand[111] (1.828 Å) and the $(PPh_3)HgCl_2$ complex (Section 2.2.2). The coordination about phosphorus is distorted tetrahedral, the angle between C(1)-P-C(4), within the phosphole ring, not surprisingly, has the largest deviation from regular tetrahedral at 93(1)°. The coordination around phosphorus in the free ligand has been described as "essentially tetrahedral"; however comparison between C(1)-P-C(4) angles cannot be made

because neither this angle nor atomic coordinates were reported. A similar C-P-C angle of 93.9(9)°, within the phosphole ring, has been observed for 5-(p-bromobenzyl)-5-phenyl-dibenzophosphonium bromide.[117] The carbon-carbon distances within the phosphole ring for free and complexed ligand are not significantly different from one another (Table 2.3). As found for the free ligand, the heterocyclic ring is almost planar (Table 2.3), the degree of distortion from planarity being slightly greater in the present case. The phenyl ring C attached directly to phosphorus and both phenyl rings, A and B, attached to the phosphole ring (Figure 2.3) have been refined as regular hexagons and as such are planar. The angles between the mean plane of the phosphole ring and those of the three phenyl rings are 25.6, 52.5 and 87.4° for rings A, B and C, respectively. Unfortunately, these parameters have not been reported for the free ligand and so cannot be compared with the present results. It is difficult to understand why the angles between the planes of the phosphole ring and ring A (25.6°), and ring B (52.5°) differ; there is no indication of any steric interference.

Preliminary single-crystal X-ray photographs indicate that (TPP)$HgBr_2$ is isomorphous and probably isostructural with the chloro analogue (Table 2.9). The equivalent iodo complex could not be prepared by similar methods.

Table 2.3.

Comparison of the phosphole rings within the free and complexed 1,2,5-triphenylphosphole ligands.

Parameter	Complexed ligand/Å	Free ligand[113]/Å
av. P-C distance	1.83	1.822
C(1)-C(2)	1.35(6)	1.35(1)
C(2)-C(3)	1.56(5)	1.44(1)
C(3)-C(4)	1.33(3)	1.35(1)
P deviation from mean plane*	0.048	0.0370
C(1) " " " "	-0.053	-0.0051
C(2) " " " "	0.031	-0.0335
C(3) " " " "	0.019	0.0705
C(4) " " " "	-0.045	-0.0689

* - The equation for the mean plane of the phosphole ring maybe found in Appendix 6.

Fig. 2.3 The molecular structure of $TPP,HgCl_2$

N.B.

$c20 - c21' = 3.35\ \mathring{A}$

c20; X, Y, Z
c21'; $\bar{X}-1$, $\bar{Y}$, $\bar{Z}$

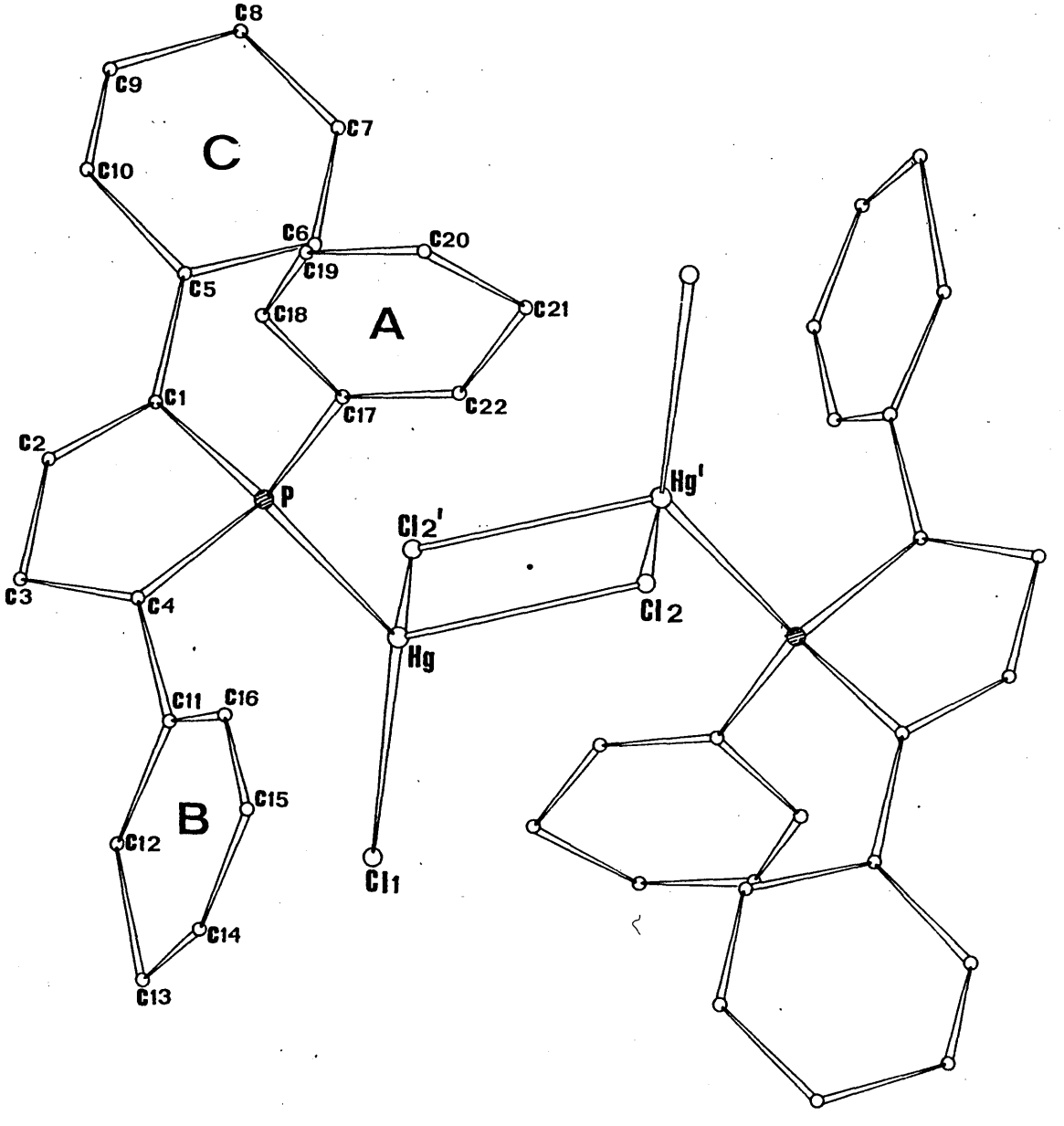

Table 2.4.

Bond distances and angles for $(TPP)HgCl_2$ with standard deviations in parentheses.

(a) Distances/Å :-

Hg-Cl(1)	= 2.40(1)	P-C(1)	= 1.88(4)
Hg-Cl(2)	= 2.54(1)	P-C(4)	= 1.81(4)
Hg-Cl(2')	= 2.75(1)	P-C(5)	= 1.81(2)
Hg-P	= 2.44(1)	C(1)-C(2)	= 1.35(6)
Hg-Hg'	= 3.855(4)	C(2)-C(3)	= 1.56(5)
		C(3)-C(4)	= 1.33(6)

(b) Angles/° :-

Cl(1)-Hg-Cl(2)	= 107.4(5)	Hg-P-C(1)	= 114(1)
Cl(1)-Hg-Cl(2')	= 95.4(5)	Hg-P-C(4)	= 106(1)
Cl(1)-Hg-P	= 127.8(5)	Hg-P-C(5)	= 119(1)
Cl(2)-Hg-Cl(2')	= 86.5(4)	C(1)-P-C(4)	= 93(2)
Cl(2)-Hg-P	= 118.4(4)	C(1)-P-C(5)	= 110(1)
Cl(2')-Hg-P	= 110.3(4)	C(4)-P-C(5)	= 112(2)
Hg-Cl(2)-Hg'	= 93.5(4)	P-C(1)-C(2)	= 105(3)
		C(1)-C(2)-C(3)	= 119(4)
		C(2)-C(3)-C(4)	= 110(4)
		C(3)-C(4)-P	= 113(3)

N.B. The phenyl rings in the TPP ligand have been refined as regular hexagons with C-C distances of 1.395 Å.

2.2.4. Crystallographic examination of (PEt^HgCI^•

The crystal structure of CPEt^JHgC^ has been determined.

Crystal Data

C&H|jjPHgC1₂ ; Mr=389.65, Monoclinic,

a=7.454(8), b=II.543(10), c=I3.673(12) A

a=90.00, 8=105.94(5), y=90.00°.

Dm=2.3I g cm ^ (by flotation using CHCI^/CHBr-j mixture), Dc=2.29 g cm

Z=4, F,(ooo)=719.83, u(Mo-K a)=I36.33 cm" 1

Systematic absences:

oko reflections are absent for k = 2n + 1

hoi " " M " I = 2n + 1

These absences uniquely define the crystals as belonging to the space group P2₁/c (No.14).* 12

Data Collection and Structure Refinement. A colourless crystal, approximate dimensions 0.33 x 0.17 x 0.23 mm, was mounted about a. Nine layers, okl—»fc8kl, were collected; 1467 reflections were recorded with $2\theta < 45^{\circ}$ of which 1240 had I/cr(I) ^4.0 and were used for refinement. Unit weights and interlayer scaling were used, and no absorption correction was appli ed.

Difficulty was encountered on trying to locate the ethyl carbon atoms of the PEt^ ligand. This phenomenon has been observed on other occasions[114,115] for other heavy metal-halide triethylphosphine complexes and has been attributed to disorder[114] or considerable vibration of the ethyl groups at room temperature.[115] Similar phenomena, together with the fact that diffraction data in the 20 range measured are dominated by information concerning chlorine, phosphorus and in particular mercury, may be the cause in the present case. Whichever the reason the high temperature factors and high errors on positional parameters reflect the uncertainty in the exact positions of the ethyl carbon atoms with the result that P-C and C-C bond lengths have high

errors associated with them.

Full-matrix refinement with anisotropic temperature factors for all non-carbon atoms gave $\underline{R}$ = 0.087. The final atomic and thermal parameters are contained is Table A2.3 (Appendix 2). Calculated and observed structure factors are contained in Appendix 3 (Table A3.3). A full set of bond distances and angles may be found in Table 2.5.

Description of Structure. This structure may be described as a chlorine-bridged polymer (Figure 2.4), in which discrete dimeric species cannot be distinguished. Mercury lies in a distorted trigonal bipyramidal environment with two relatively short Hg-Cl bonds at 2.42(1) and 2.56(1) Å and a short Hg-P bond at 2.35(1) Å lying in equatorial positions and two longer apical Hg-Cl contacts at 3.04(1) and 3.21(1) Å. The P, Hg, Cl(1) and Cl(2) atoms are not coplanar, the deviations from the mean plane (Appendix 6) being ca. 0.6, 0.9, 0.7 and 1.0 Å respectively. The angles within the '$PHgCl_2$' unit range from 98.7(3)° for Cl(2)-Hg-Cl(1), to 145.4(4)° for the P-Hg-Cl(2) angle. The angle between the two longer apical contacts, Cl(1')-Hg-Cl(2') is close to linearity at 170.8(3)°. The Hg-Cl(1)-Hg' and Hg'-Cl(2)-Hg bridge angles are 93.2(3) and 91.1(3)° respectively.

There are centres of symmetry at the centres of each planar four-membered ring formed by the polymer. As no other symmetry is present the chain belongs to the C_i line group. There are two of these chains per unit cell arranged as shown in Figure 2.5, running parallel to the $\underline{a}$ - axis.

Similar chain-like arrangements have been observed for a number of chloromercurate(II) complexes[45-47] and for[62] (2,4,6-trimethylpyridine)$HgCl_2$ (Sections 1.3.2 and 1.3.3); however, the coordination polyhedron about mercury in these structures is closer to regular trigonal bipyramidal.

As already mentioned there are high errors associated with the positional and thermal parameters of the carbon atoms contained in the PEt_3 ligand. These errors are of the order reported for some other ethyl carbon atoms contained

in other PEt_3 complexes of heavy metals.[114,115] Little can be said about the ethyl groups, but it does appear that bond lengths within the sets of both P-C and C-C bonds are significantly different from one another.

Different conformational arrangements of β-carbon atoms of ethyl groups in PEt_3 are known to exist, e.g. the expected 'propellor' arrangement in which β-carbon atoms are skew (1), skew (1), skew (1) with respect to the mercury atom[116] (Figure 2.6a) and also the skew (1),anti, skew (2) conformation[114,115] (Figure 2.6b). In $(PEt_3)HgCl_2$ there is yet another conformational arrangement i.e. skew (1), anti, skew (1). Rationalization of the factors influencing conformational preference is difficult. The energy differences between the three conformations are probably only very small ca. 20 kJ mol^{-1} (by comparison with analogous conformers of butane), and the conformer adopted is probably dependent upon only very subtle variations in electronic and steric environment of the complexed PEt_3 ligand.

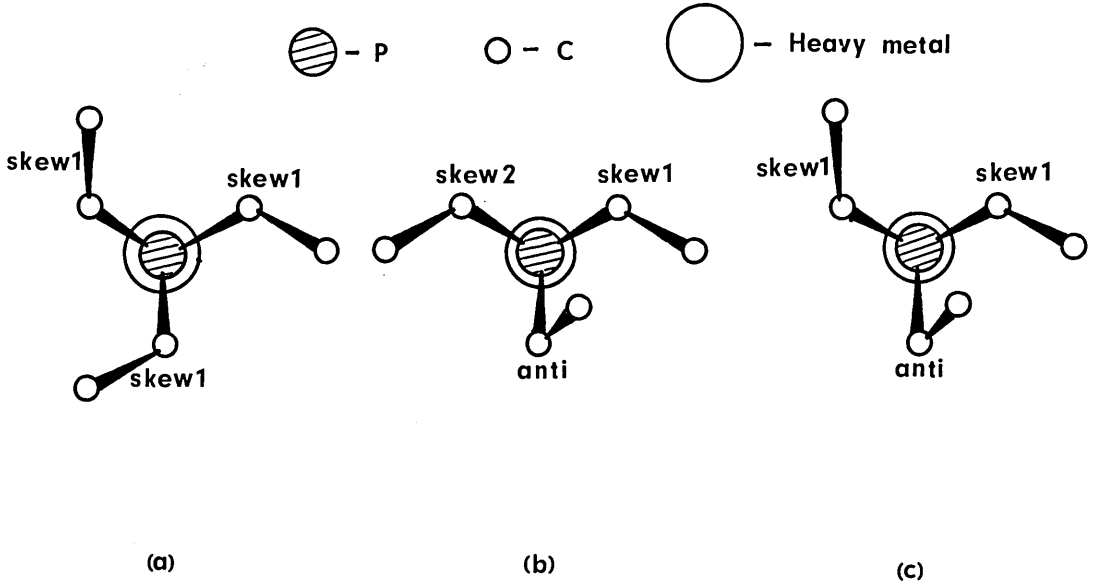
- P
- C
- Heavy metal
skew1
skew1
skew1
skew2
skew1
anti
skew1
skew1
anti

(a) (b) (c)

Fig. 2.4 The molecular structure of $(PEt_3)HgCl_2$

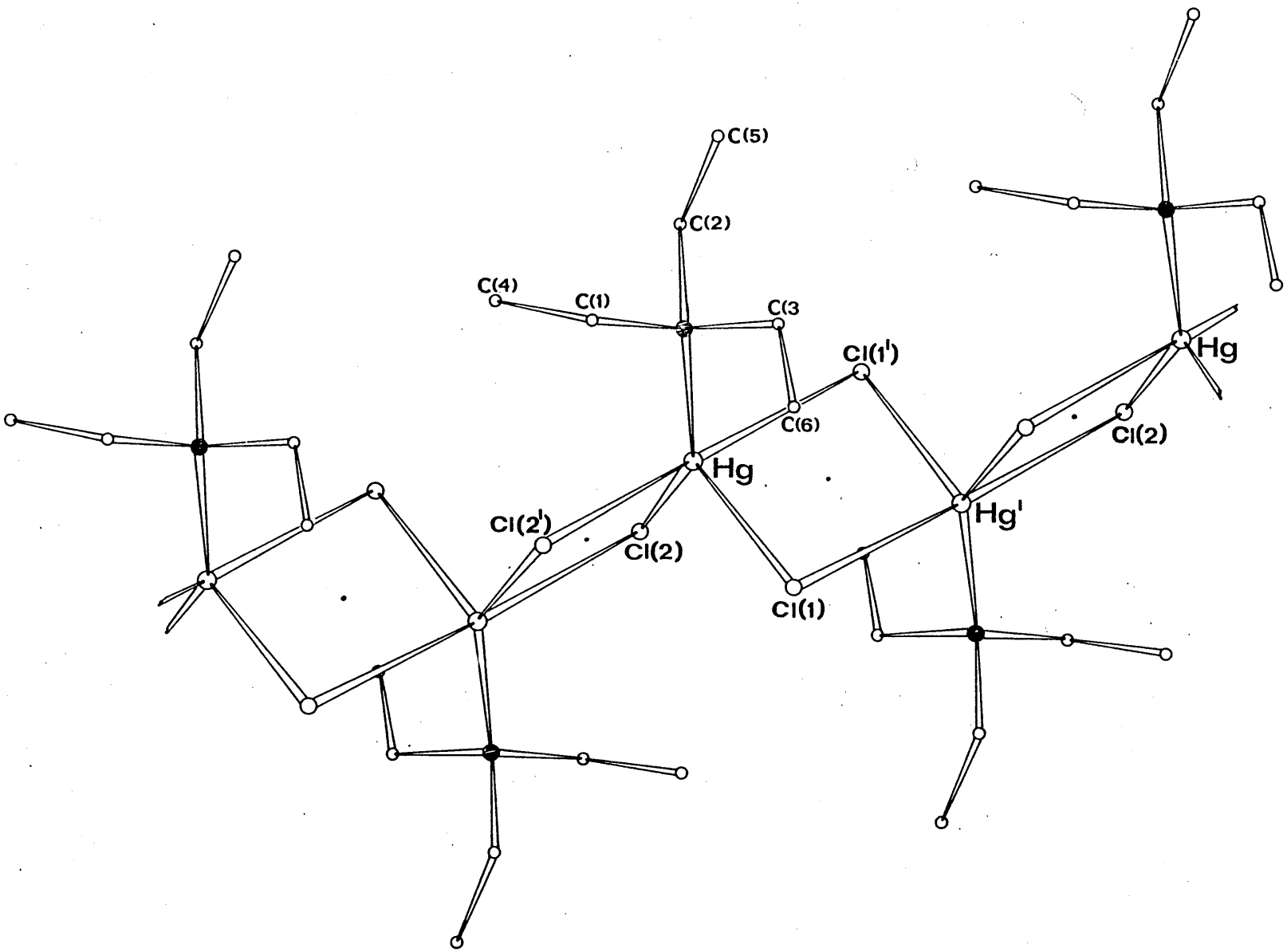

Fig. 2.5 The Crystal structure[a] of $(PEt_3)HgCl_2$ – viewed along the b-axis

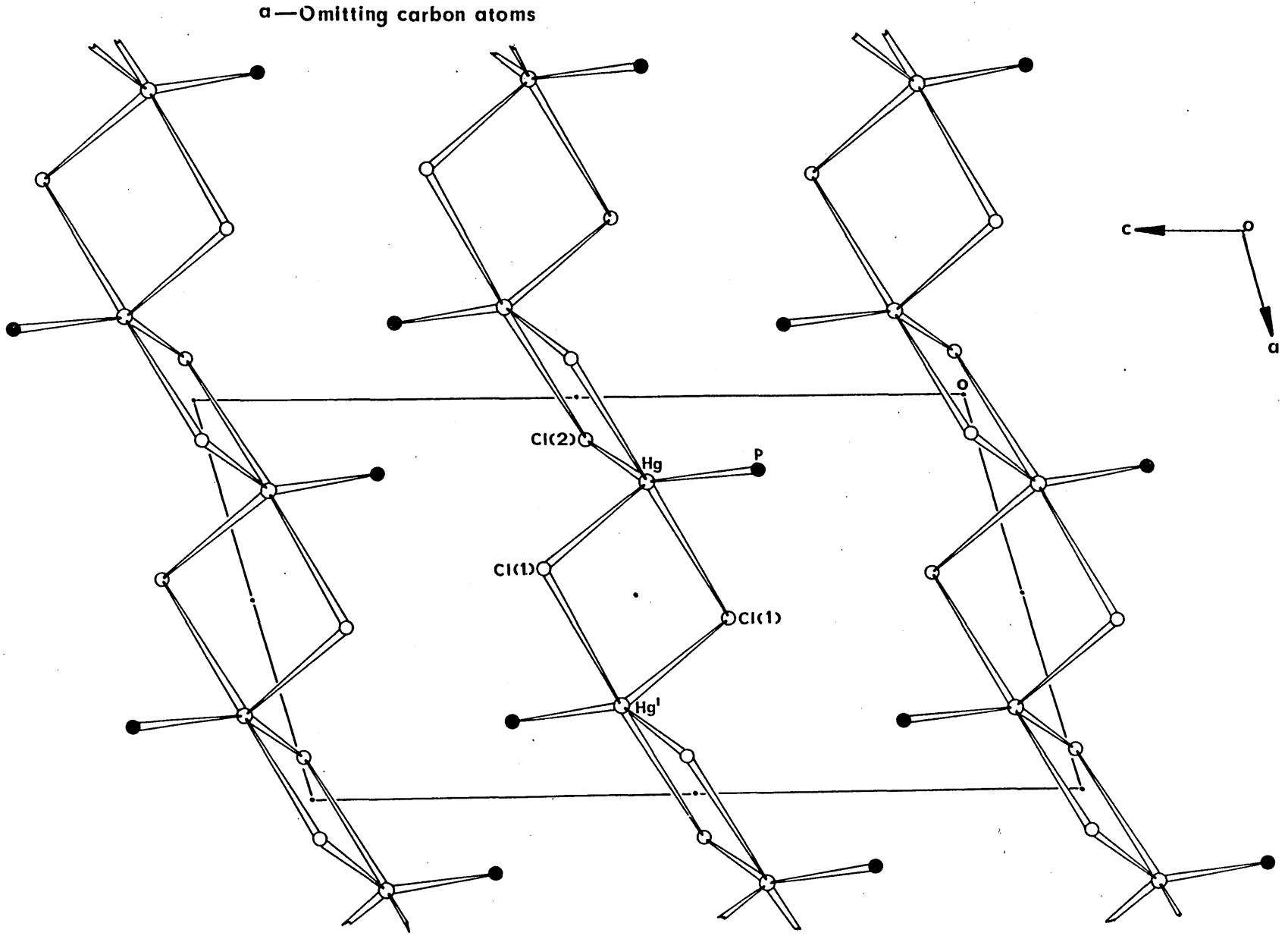

Table 2.5.

Bond distances and bond angles for $(PEt_3)HgCl_2$ with standard deviations in parentheses.

(a) Distances/Å:-

Hg-Cl(1)	= 2.56(1)	P-C(1)	= 1.74(5)
Hg-Cl(1')	= 3.04(1)	P-C(2)	= 2.04(9)
Hg-Cl(2)	= 2.42(1)	P-C(3)	= 1.73(7)
Hg-Cl(2')	= 3.21(1)		
Hg-P	= 2.35(1)	C(1)-C(4)	= 1.67(7)
Hg-Hg'	= 4.057(2)	C(2)-C(5)	= 1.59(9)
		C(3)-C(6)	= 1.40(7)

(b) Angles/°:-

Cl(1)-Hg-Cl(1')	= 86.8(3)	C(1)-P-C(2)	= 101(3)
Cl(1)-Hg-Cl(2)	= 98.7(3)	C(1)-P-C(3)	= 106(3)
Cl(1)-Hg-Cl(2')	= 86.7(3)	C(1)-P-Hg	= 115(2)
Cl(1)-Hg-P	= 115.6(3)	C(2)-P-C(3)	= 120(4)
Cl(1')-Hg-Cl(2)	= 98.8(3)	C(2)-P-Hg	= 104(3)
Cl(1')-Hg-Cl(2')	= 170.8(3)	C(3)-P-Hg	= 111(2)
Cl(1')-Hg-P	= 85.2(3)		
Cl(2)-Hg-Cl(2')	= 88.9(3)	P-C(1)-C(4)	= 118(3)
Cl(2)-Hg-P	= 145.4(3)	P-C(2)-C(5)	= 106(5)
Cl(2')-Hg-P	= 91.6(4)	P-C(3)-C(6)	= 122.(5)
Hg-Cl(1)-Hg'	= 93.2(3)		
Hg-Cl(2)-Hg'	= 91.1(3)		

2.2.5. Crystallographic examination of the $(PMe_3)HgX_2$ (X=Cl, Br or I) complexes.

The crystal structure of the chloro complex has been determined.

Crystal Data

$C_3H_9PHgCl_2$; M_r=347.56, Triclinic,

a=6.408(6), b=8.894(9), c=7.270(9) Å;

α=89.13(5), β=92.00(5), γ=95.83(5)°.

D_m=2.79 g cm^{-3} (by flotation using $CHCl_3/CHBr_3$ mixture), D_c=2.80 g cm^{-3},

Z=2, $F_{(000)}$=311.91, $\mu(Mo\text{-}K_\alpha)$=187.11 cm^{-1}.

Systematic absences:-

None.

The crystals belonged to either of the triclinic space groups P1 or $P\bar{1}$. Subsequent structure solution unambiguously distinguished the space group as $P\bar{1}$ (C_i^1, No. 2).[112]

Data Collection and Structure Refinement. A colourless crystal, approximate dimensions 0.15 x 0.12 x 0.27 mm, was mounted about c. Eleven layers, hk0 → hk10, were collected; 1732 reflections were recorded with $2\theta < 60°$ of which 1674 had $I/\sigma(I) \geq 3.0$ and were used for refinement. Unit weights and interlayer scaling have been used, and an absorption correction has been applied (Appendix 1).

Full-matrix refinement with anisotropic temperature factors for all non-carbon atoms gave R = 0.057. The final atomic and thermal parameters are given in Table A2.4 (Appendix 2). Calculated and observed structure factors are contained in Appendix 3 (Table A3.4). A complete set of bond distances and angles may be found in Table 2.6.

Description of Structure. The structure may best be described as 'ionic', containing $[Cl\text{-}Hg\text{-}PMe_3]^+$ and Cl^- ions alternately arranged in a zig-zag chain (Figure 2.7).

The $[Cl\text{-}Hg\text{-}PMe_3]^+$ cation is almost linear with a Cl-Hg-P angle of

162.1(1)°. The Hg-Cl(2) and Hg-P bond lengths are 2.355(4) and 2.365(3) Å, respectively. The effective coordination number of mercury is five as a result of three further Hg---Cl contacts at 2.782(4), 2.941(4) and 3.489(4) Å between Hg and Cl(1), Cl(1') and Cl(1'') respectively. The 'ionic' description is preferred in the present case because of the almost linear Cl(2)-Hg-P angle and the considerable distance from the Cl(2)-Hg-P species to the next 'chloride ion'.

This chain-like arrangement is different to that found for $(PEt_3)HgCl_2$ in that bridge interaction occurrs via only one of the chlorine atoms of the 'Cl_2HgPMe_3' unit. There are centres of symmetry located at the centres of both four-membered rings formed by the 'ionic' chain. The atoms making up the chain are virtually coplanar, with no atom deviating from the mean plane by more than 0.14 Å (Appendix 6).

A very similar structure has been observed [64] for $(C_4H_8S)HgCl_2$ (Section 1.3.3), but in this case the Cl-Hg-S angle (142.8°) is further from linearity and Hg---Cl contacts are proportionally shorter at 2.62, 2.83 and 3.07 Å. The geometry of the complexed PMe_3 ligand is similar to that observed in $(PMe_3)PtCl_2$ [118] and is close to an ideal tetrahedral arrangement.

Preliminary single-crystal X-ray photographs indicate that in comparison with the chloride the equivalent $(PMe_3)HgBr_2$ complex is isomorphous and probably isostructural, whereas the iodo complex is not isomorphous and probably not isostructural (Table 2.9).

Fig. 2.7 The molecular structure of $(PMe_3)HgCl_2$

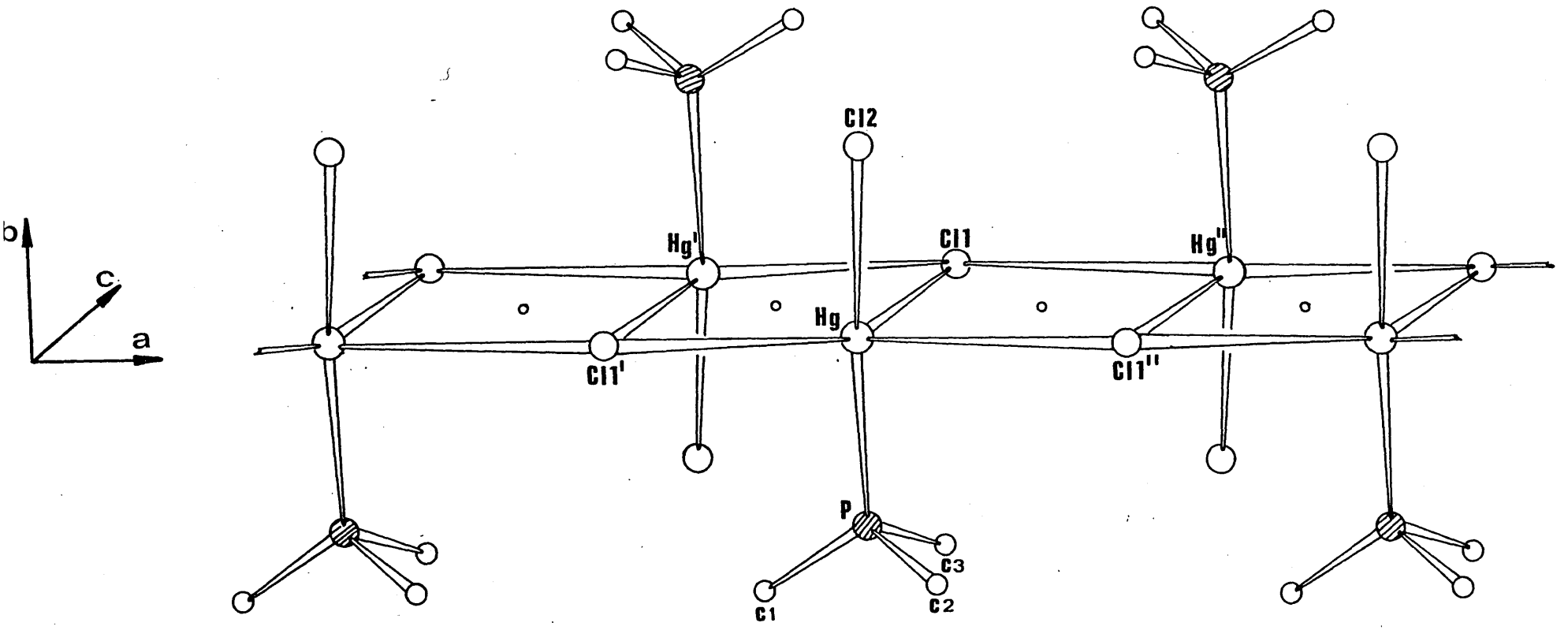

Table 2.6.

Bond distances and anqles for (PMe^)$HgCJ_2$.

with standard deviations in parentheses.

(a) Distances/Å:-

Hg-Cl(l)	=2.782(4)	P-C(l)	l.82(2)
Hg-Cl (.|»).	= 2.941(4)	P-C(2)	l.80(2)
Hg-Cl(IM)	= 3.489(4)	P-C(3)	l.83(2)
Hg-Cl(2)	= 2.355(4)		
Hg-P	= 2.365(3)		
Hg-Hg»	= 3.884(2)		
Hg-Hg”	= 4.826(2)		

(b) Angles/°

Cl(l)-Hg-Cl(l1)	= 94.6(1)	C(l)-P-Hg	lll.4(7)
Cl (l)-Hg-Cl(l'')	= 79.6(1)	C(l)-P-C(2)	= 104.6(9)
Cl(l)-Hg-Cl(2)	= 98.2(1)	C(l)-P-C(3)	= 107.7(9)
Cl(l)-Hg-P	= 98.2(1)	C(2)-P-Hg	lll.0(7)
Cl(lT)-Hg-Cl(l11)	= 170.6(1)	C(2)-P-C(3)	= 108.2(9)
Cl (l')-Hg-Cl(2)	= 90.6(1)	C(3)-P-Hg	l13.5(7)
Cl(l')-Hg-P	= 95.2(1)		
Cl (l M)-Hg-Cl (2)	= 97.6(1)		
Cl (l'1)-Hg-P	= 78.4(1)		
Cl(2)-Hg-P	= 162.1(l)		

2.2.6. Crystallographic examination of the $(PBu^n_3)HgX_2$ (X=Cl, Br or I) complexes.

Vibrational spectroscopic studies (Section 3.3.1e) have shown there to be two isomeric forms of $(PBu^n_3)HgCl_2$. The crystal structure of one of these forms has been determined and is hereinafter referred to as the α-form.

Crystal Data

$C_{12}H_{27}PHgCl_2$; M_r=473.75, Monoclinic,

a=13.698(12), b=25.475(17), c=10.621(9) Å;

α=90.00, β=100.75(5), γ=90.00 .

D_m=1.70 g cm^{-3} (by flotation using CCl_4/CHI_3 mixture), D_c=1.73 g cm^{-3},

Z=8(with two independent molecules), $F_{(000)}$=1823.65, μ(Mo-K_α)=84.79 cm^{-1}.

Systematic absences:-

hol reflections are absent for (h+l) = 2n + 1

oko " " " " k = 2n + 1

These absences uniquely assign the crystals to the non-standard space group $P2_1/n$.

Data Collection and Structure Refinement. A colourless crystal, approximate dimensions 0.42 x 0.23 x 0.13 mm, was mounted about b. Eleven layers, h0l → h10l, were collected; 4380 reflections were recorded with $2\theta < 60^\circ$ of which 1464 had $I/\sigma(I) \geq 4.0$ and were used for refinement. Unit weights were used, and no absorption correction was applied.

The temperature factors observed for all atoms suggests considerable vibrational movement of the molecules within the unit cell. These thermal parameters would appear to reflect both the low melting point ca.80°C of the solid and also the very long intermolecular distances within the unit cell (Figure 2.9), suggesting quite low lattice energy holding the molecules in the crystal together. The high degree of freedom of the molecules in the unit cell was further brought to light when preliminary data collection at

low temperature (ca. 100K)* showed considerable volume contraction of the unit cell (ca. 6.3% contraction).

Density measurement showed there were eight 'monomers' per unit cell; consequently there are two independent molecules present. Full-matrix refinement, with anisotropic temperature factors for all non-carbon atoms gave R = 0.083. Final atomic and thermal parameters may be found in Table A2.5 (Appendix 2). Calculated and observed structure factors are contained in Table A3.5 (Appendix 3). Bond distances and angles are given in Table 2.7.

Description of structure. This structure consists of discrete tetrameric units (Figure 2.8). Within each tetramer, mercury is both four- and five-coordinate. Hg(1) and Hg(2) are 3.793(4) Å apart, and two chlorine atoms, Cl(3) and Cl(2), are arranged so as to give rise to an unsymmetric chlorine-bridged dimer, the Hg-Cl bridge distances having values of 2.63(2), 2.71(2), 2.67(2) and 2.90(2) Å. Two of these unsymmetric dimers are related via a centre of symmetry and are joined by relatively long contacts of 3.38(3) Å between Hg(2)-Cl(4') and Hg(2')-Cl(4); the Hg(2)-Hg(2') distance is 4.142(6) Å. There is no other symmetry associated with the tetrameric unit and consequently there is C_i point symmetry.

The coordination polyhedron about the terminal Hg(1) atom is very distorted tetrahedron with the Cl(2)-Hg(1)-Cl(3) angle at 92.6(7)° and the P(1)-Hg(1)-Cl(1) angle at 147.8(7)°. Because of the additional interaction with Cl(4), the Hg(2) atom is situated in a distorted trigonal bipyramidal environment. The angles within the equatorial plane range from 98.6(7)° for Cl(4)-Hg(2)-Cl(2) to 150.6(7)° for P(2)-Hg(2)-Cl(4), these four atoms lying approximately in one plane deviations in Å from the mean plane are:- Hg(2), 0.159; Cl(2), -0.027; Cl(4), -0.065; P(2), -0.068. The angle, Cl(3)-Hg(2)-Cl(4'), between the two apical bonds is close to linearity at 177(1)°.

* - Carried out at Rothamsted Experimental Station. The low temperature cell is:-

a=13.4723(93)	b=24.9602(94)	c=10.3914(36) Å;
α=90.00	β=102.44(4)	γ=90.00°

The bridge angles within the asymmetric dimer portions of the tetramer are close to 90°, as observed for discrete centrosymmetric dimer species, viz. Hg(1)-Cl(3)-Hg(2) = 86.6(7)° and Hg(1)-Cl(2)-Hg(2) = 89.8(6) Å. The Hg(2)-Cl(4)-Hg(2') bridge angle is 92.1(7)°.

The way in which tetramers pack together is shown in Figure 2.9. There is no further Hg-Cl interaction beyond the tetramer stage, the next shortest Hg-Cl distance being ca. 7.2 Å.

Preliminary single-crystal X-ray photographs indicate, even though full space group determination has not been performed, that the bromo and iodo complexes are isomorphous and probably isostructural with one another (Table 2.9). There appears to be no relationship, however, between the single-crystal X-ray photographs of these halo analogues and those of the chloro complex. Vibrational spectroscopic data on the other hand do suggest similar molecular structures for all three complexes (Section 3.3.1e).

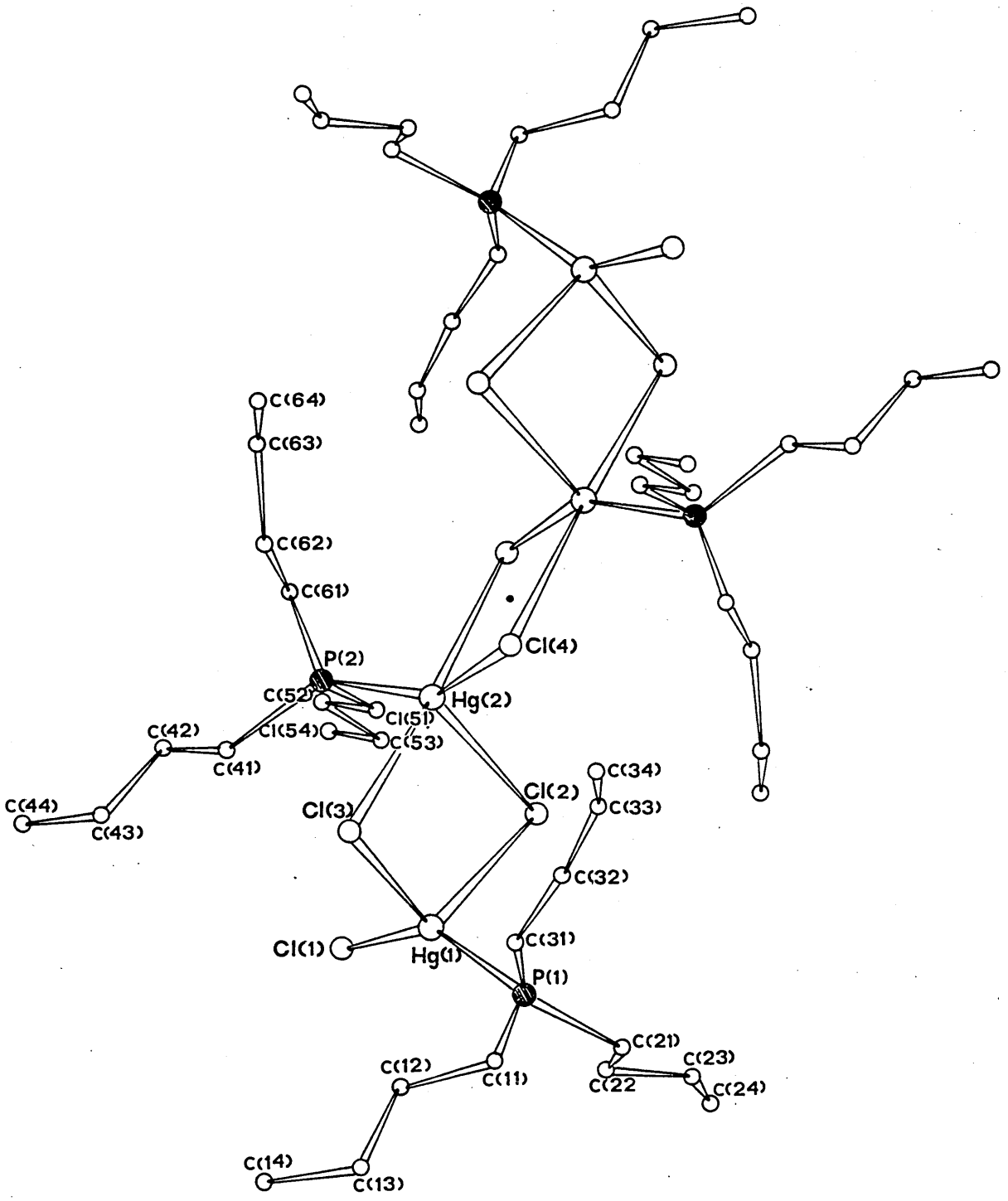
C(64)
C(63)
C(62)
C(61)
P(2)
C(52)
C(42)
C(41)
C(44)
C(43)
Cl(54)
Cl(51)
C(53)
Hg(2)
Cl(4)
Cl(3)
Cl(2)
C(34)
C(33)
C(32)
Cl(1)
Hg(1)
C(31)
P(1)
C(21)
C(12)
C(11)
C(23)
C(22)
C(24)
C(14)
C(13)

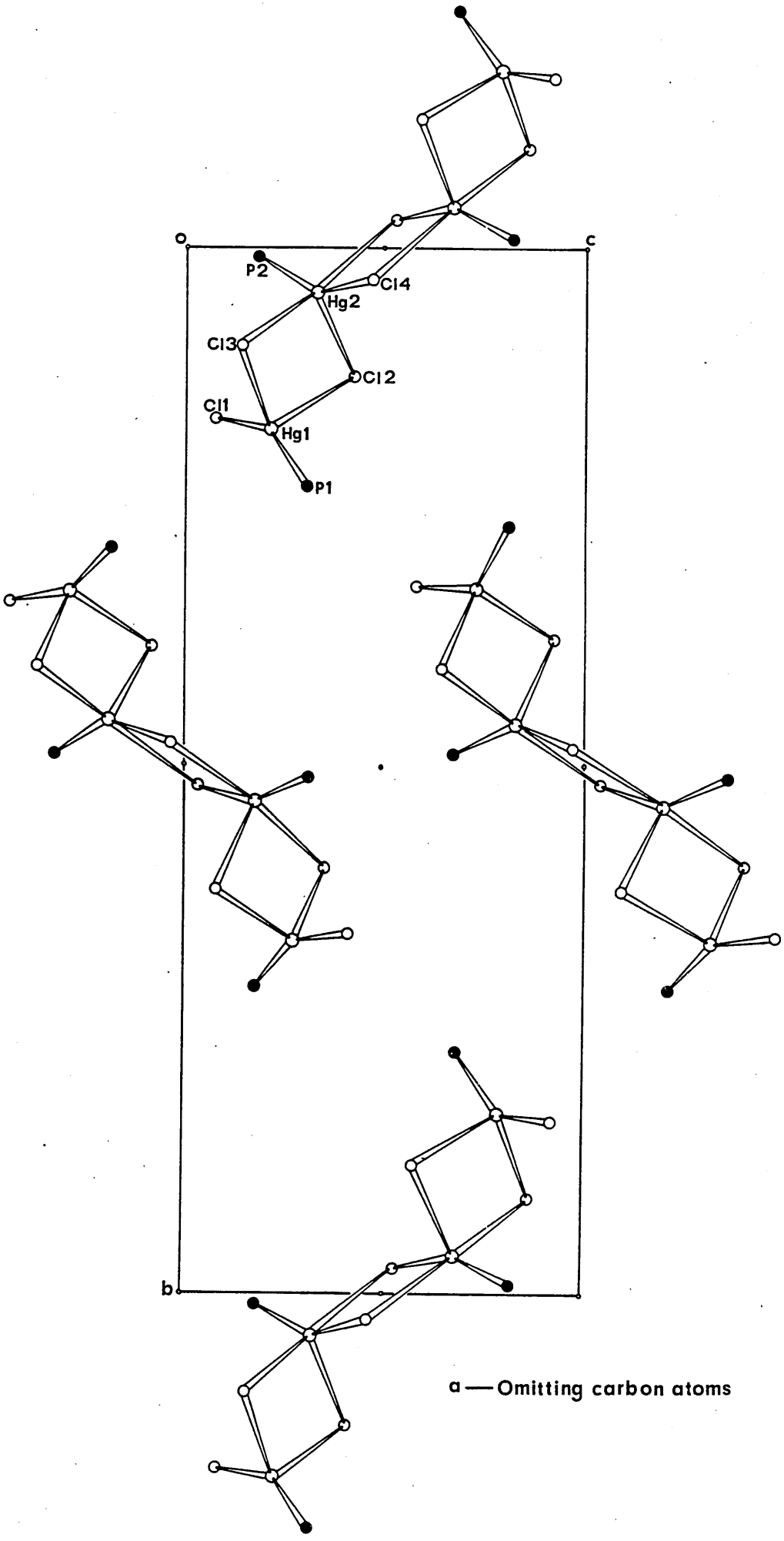

a — Omitting carbon atoms

Table 2.7.

Bond distances and anqles for a-(PBui]HjgCJ^
with standard deviations in parentheses.

(a) Pi stances/Å

Hg(l)-Cl(1)	= 2.27(3)	P(l)-Cdl)	= 1.77(18)
Hg(1)-C1(2)	= 2.71(2)	P(l)-C(2!)	= 2.02(16)
Hg(1)-Cl(3)	= 2.63(2)	P(1)—C(31)	= 1.79(15)
Hg(1)—P(1)	= 2.35(2)	P(2)—C(41)	= 1.86(8)
Hg(2)-C1(2)	= 2.67(2)	P(2)-C(5l)	= 1.77(11)
Hg(2)-Cl(3)	= 2.90(2)	P(2)-C(6l)	= 1.90(8)
Hg(2)-C1(4)	= 2.28(3)		
Hg(2)-Cl(4')	= 3.38(3)	Average C-C	
Hg(2)-P(2)	= 2.34(3)	distance	1.54
Hg(2)-Hg(2')	= 4.142(6)		
Hg(2)-Hg(l)	= 3.792(4)		

(b) Anales/°

C1(1)“Hg(1)-Cl(2)	= 98.4(7)
Cl(1)-Hg(l)-Cl(3)	= 102.4(7)
Cl(1)-Hg(1)-P(l)	= 147.8(7)
Cl(2)-Hg(1)-Cl(3)	= 92.6(6)
Cl(3)-Hg(l)-P(l)	= 102.1(7)
Cl(2)–Hg(2)–C1(3)	= 87.8(6)
Cl(2)—Hg(2)–C1(4)	= 98.6(7)
Cl(2)-Hg(2)-Cl(41)	= 90.9(7)
Cl(2)-Hg(2)-P(l)	= 101.1(7)
Cl(2)-Hg(2)-P(2)	= 107.7(6)
Cl(3)-Hg(2)-C1(4)	= 95.1(7)
Cl(3)-Hg(2)-Cl(4f)	= 177 (1)
Cl(3)-Hg(2)-P(2)	= 98.7(7)
Cl(4)—Hg(2)—C1(41)	= 87.9(7)
Cl(4)-Hg(2)-P(2)	= 150.6(7)
Cl(4')-Hg(2)-P(2)	= 79.1(7)
HgC1)-C1(2)-Hg(2)	= 89.8(6)
Hg(1)-C1(3)-Hg(2)	= 86.6(7)

Average tetrahedral angles
about phosphorus atoms 0
= 109 .

2.2.7. Crystallographic examination of (2,4-dimethylpyridine)HgX_2 (X=Cl or Br) complexes.

The crystal structure of (2,4-dimethylpyridine)$HgBr_2$ has been determined.

Crystal Data

$C_7H_9NHgBr_2$; M_r=467.55, Monoclinic,

a=12.750(11), b=10.804(11), c=7.780(8) Å;

α=90.00, β=94.00(5), γ=90.00°.

D_m=2.91 g cm^{-3} (by flotation using $CHBr_3/CHI_3$ mixture), D_c=2.90 g cm^{-3},

Z=4, $F_{(000)}$=831.82, μ(Mo-K_α)=211.63 cm^{-1}.

Systematic absences:-

hkl reflections are absent for (h+k) = 2n + 1

h0l " " " " l = 2n + 1

These absences suggest the crystals belong to space group C2/c or Cc. Subsequent structure solution and point symmetry considerations, unambiguously distinguished the space group as Cc(C_s^4, No. 9).[112]

Data Collection and Structure Refinement. A colourless crystal, approximate dimensions 0.17 x 0.18 x 0.28 mm, was mounted about c. Eight layers, hk0 → hk7, were collected; 927 reflections were recorded with $2\theta < 50°$ of which 684 had $I/\sigma(I) \geq 2.0$ and were used for refinement. Inter-layer scaling was used and no absorption correction was applied.

The weighting scheme used was:-

$$w = 0.5262/(\sigma^2|F_o| + 0.002649|F_o|^2)$$

Only the y-coordinate of the mercury atom could be found from the Patterson synthesis, the x- and z- coordinates remaining unassigned. In this space group there is no unique origin point on the glide plane c, so the x- and z- coordinates were assigned at x=0.00 and z=0.25. For this space group if one atom is located at (0.00, y, 0.25) another atom will be located at ($\bar{0}$.00, $\bar{y}$, $\bar{0}$.25). It is obvious that these two atoms are related by a centre

of symmetry even though the space group is non-centrosymmetric. Consequently when the phase angles, deduced on the basis of the Hg position, were used to phase the subsequent difference Fourier synthesis the electron density map showed peaks for both the true structure and that of a 'ghost' structure which was related by a pseudo-mirror plane. At this stage it was not possible to determine which molecule was genuine. This problem was overcome by refining the mercury atom plus one of the four 'possible' bromine atoms one at a time and computing further difference Fourier syntheses on a trial and error basis. The correct bromine positions were reflected by the disappearance of the ghost structure, brought about by the introduction of adequate asymmetry into the phase angles. The nitrogen atom and carbon atoms of the heterocycle were readily found from subsequent Fourier syntheses. The errors associated with the positional parameters for the lighter nitrogen and carbon atoms, which also manifest themselves in the errors associated with N-C and C-C bond distances, may again be attributed to the presence of the very large mercury and bromine atoms.

Full-matrix refinement with anisotropic temperature factors for the non-carbon atoms gave R_w=0.054.* Final atomic and thermal parameters may be found in Table A2.6 (Appendix 2). Calculated and observed structure factors are given in Table A3.6 (Appendix 3). Bond distances and angles may be found in Table 2.8.

Description of Structure. The structure is essentially polymeric (Figure 2.10). Mercury is five-coordinate lying in an extremely distorted trigonal bipyramidal environment. There are three relatively short bonds in the equatorial plane between Hg-Br(1), Hg-Br(2) and Hg-N at 2.621(3), 2.486(4) and 2.21(4) Å, respectively, separated by angles ranging from 106(1)° for Br(1)-Hg-N to 129(1)° for Br(2)-Hg-N. The degree of planarity of the '$NHgBr_2$' unit is indicated by the deviations of Hg, 0.15; Br(1), -0.04; Br(2), -0.06; and N, -0.06 Å from the calculated mean plane (Appendix 6).

* - R = 0.053

The coordination polyhedron about Hg is completed via two long-range interactions of 2.911(3) to Br(1') and 3.548(4) Å to Br(2''), the angle between these two apical bonds being 164.9(2)°. The resulting bromine-bridged polymer is different to that found[64] for (2,4,6-trimethylpyridine)$HgCl_2$ in that there are no centres of symmetry within the four-membered rings formed by the mercury and bromine atoms of the bridges. The chain therefore belongs to the C_1 line group.

As far as it is possible to tell, taking into account the high errors associated with N-C and C-C bond distances, comparison with other complexes of methyl substituted pyridines [64,119] indicates that the dimensions of the heterocyclic ring are normal. The N-C distances, av. = 1.34 Å, and C-C distances, av. = 1.40 Å, of the conjugated ring are, as one would expect, significantly shorter than the C-C single bonds (av. = 1.51 Å) of the methyl groups attached to the ring. All angles about and within the heterocyclic ring are close to 120°.

The atoms contained in the heterocyclic ring are essentially coplanar, the maximum deviation of any atom from the mean plane being 0.04 Å for (Appendix 6). As one may note (Figure 2.9) the mean plane of the heterocyclic ring is slightly twisted (22.5°) from the mean plane of the '$NHgBr_2$' unit, a similar situation to that found[64] for (2,4,6-trimethylpyridine)$HgCl_2$ (the angle between the planes being 30.9°).

Single-crystal photographs indicate that the analogous chloro complex is isostructural with its bromo counterpart (Table 2.9).

Fig. 2.10 The molecular structure of (2,4—dimethylpyridine)$HgBr_2$

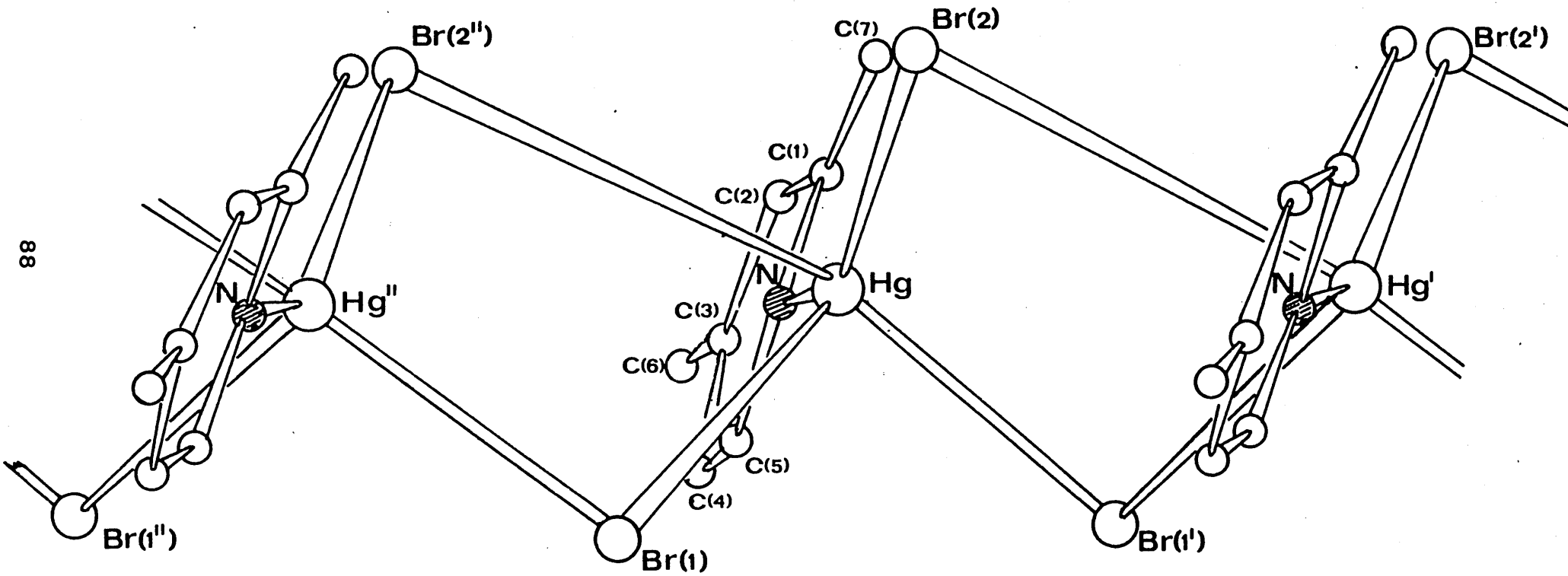

Table 2.8.

Bond distances and angles for (2,4-dimethylpyridine)$HgBr_2$ with standard deviations in parentheses.

(a) Distances/Å:-

Hg-Br(1)	= 2.621(3)	N-C(1)	= 1.30(5)
Hg-Br(1')	= 2.911(3)	C(1)-C(2)	= 1.37(5)
Hg-Br(2)	= 2.486(4)	C(2)-C(3)	= 1.33(5)
Hg-Br(2')	= 3.548(4)	C(3)-C(4)	= 1.49(5)
Hg-N	= 2.21(2)	C(4)-C(5)	= 1.40(5)
Hg-Hg'	= 3.972(1)	C(5)-N	= 1.38(5)
		C(1)-C(7)	= 1.54(5)
		C(3)-C(6)	= 1.47(6)

(b) Angles/°:-

		N-C(1)-C(2)	= 125(3)
Br(1)-Hg- Br(1')	= 92.4(2)	C(1)-C(2)-C(3)	= 123(4)
Br(1)-Hg-Br(2)	= 122.2(2)	C(2)-C(3)-C(4)	= 115(3)
Br(1)-Hg-Br(2'')	= 83.5(2)	C(3)-C(4)-C(5)	= 118(3)
Br(1)-Hg-N	= 106(1)	C(4)-C(5)-N	= 123(3)
Br(1')-Hg-Br(2)	= 100.8(2)	C(2)-C(1)-C(7)	= 121(3)
Br(1')-Hg-Br(2'')	= 164.9(2)	C(7)-C(1)-N	= 114(3)
Br(1')-Hg-N	= 90(1)	C(2)-C(3)-C(6)	= 126(4)
Br(2)-Hg-Br(2'')	= 93.6(2)	C(6)-C(3)-C(4)	= 119(3)
Br(2)-Hg-N	= 129(1)	C(1)-N-C(5)	= 117(3)
Br(2'')-Hg-N	= 77(1)	C(1)-N-Hg	= 128(3)
		C(5)-N-Hg	= 115(2)
Hg-Br(2)-Hg'	= 80.3(2)		
Hg-Br(1')-Hg'	= 91.6(2)		

2.2.8. Crystallographic examination of the $(AsPh_3)HgCl_2$ complex.

Preliminary crystallographic investigation of the $(AsPh_3)HgCl_2$ complex has shown it to be isostructural with $(PPh_3)HgCl_2$. Unit cell dimensions and relevant bond parameters are listed below, using the same notation as in Figure 2.1.

a=12.263(13), b=11.511(10), c=13.520(14) Å;

α=90.00, β=93.85(5), γ=90.00°.

Bonds within the dimer (Å)		Angles within the dimer (°)	
Hg(1)-Cl(2)	= 2.64	Cl(3)-Hg(1)-As(1)	= 128.4
Hg(1)-Cl(2')	= 2.59	Cl(2')-Hg(1)-Cl(2)	= 86.3
Hg(1)-Cl(3)	= 2.36	Hg(1)-Cl(2')-Hg(1')	= 93.7
Hg(1)-As(1)	= 2.50		

This geometry is virtually identical to that of the $(PPh_3)HgCl_2$ complex suggesting very similar donor atom-mercury interaction and very similar packing requirements.

2.2.9. Single-crystal photographic studies of some $(L)HgX_2$ complexes.

Whenever possible single-crystal photographic studies have been undertaken to indicate whether or not the analogous halo complexes of those compounds which have received full crystallographic analysis are isostructural and /or isomorphous. Unit cell dimensions have been used to indicate isomorphism and comparison of the relative intensities of diffraction patterns have been used to indicate whether or not compounds are isostructural. The dimensions of real cells and an indication of the isostructural nature of these complexes are given in Table 2.9.

Table 2.9.

Comparative crystallographic studies of some $(L)HgX_2$ complexes

(standard deviations associated with positional parameters are in parentheses)

Compound	a/Å	b/Å	c/Å	α/°	β/°	γ/°	Space Group
$(PPh_3)HgCl_2$ [a]	12.304(8)	11.356(7)	13.444(10)	90.00	92.50(5)	90.00	$P2_1/n$
$(PPh_3)HgI_2$	13.613	11.225	13.436	90.00	91.00	90.00	$P2_1/n$
$(PPh_3)HgBr_2$ [b]	18.749	10.962	9.317	90.00	90.42	90.00	$P2_1/c$
$(TPP)HgCl_2$ [a]	11.854(10)	10.041(10)	9.443(9)	84.16(5)	103.88(5)	114.29(5)	$P\bar{1}$
$(TPP)HgBr_2$	11.793	10.285	9.413	84.99	102.30	114.19	P1 or $P\bar{1}$
$(PMe_3)HgCl_2$ [a]	6.408(6)	8.894(9)	7.270(9)	89.13(5)	92.00(5)	95.83(5)	$P\bar{1}$
$(PMe_3)HgBr_2$	6.594	9.133	7.347	89.28	92.39	95.28	P1 or $P\bar{1}$
$(PMe_3)HgI_2$	15.431	14.072	9.435	90.00	90.00	90.00	$P2_12_12_1$
α-$(PBu^n_3)HgCl_2$ [a]	13.698(12)	25.475(17)	10.621(9)	90.00	100.75(5)	90.00	$P2_1/n$
$(PBu^n_3)HgBr_2$	16.33	28.23	24.40	90.00	111.55	90.00	
$(PBu^n_3)HgI_2$	16.63	28.57	23.99	90.00	113.00	90.00	
$(2,4\text{-}Me_2C_4H_3N)HgBr_2$ [a]	12.750(11)	10.804(11)	7.780(8)	90.00	94.00(5)	90.00	Cc
$(2,4\text{-}Me_2C_4H_3N)HgCl_2$	12.361	10.934	7.504	90.00	95.33	90.00	Cc or C2/c

a - Denotes compound having undergone full crystallographic analysis. Compounds thought to be isostructural on the basis of diffraction patterns are indicated by brackets in the last column.

b - Conversion of the standard unit cell ($P2_1/c$) of $(PPh_3)HgBr_2$ to the equivalent non-standard unit cell ($P2_1/$ indicates that it is isomorphous and probably isostructural with the chloro and iodo compounds.

2.3. DISCUSSION OF THE FACTORS INFLUENCING THE STRUCTURES OF $(L)HgX_2$ COMPLEXES IN THE SOLID STATE.

2.3.1. Tertiary phosphine complexes

With regards $(TPP)HgCl_2$ and the four $(PR_3)HgCl_2$ complexes studied in this work, no two have identical structures. The structures observed are summarized in Table 2.10.

Apart from the gross differences in structural appearance there are other more subtle differences, concerned with the mercury coordination sphere, which need to be explained as follows:

(a) Why does the Cl_s-Hg-P* angle vary so greatly within the series?

(b) Why is one of the Hg-Cl bonds substantially longer than in $HgCl_2$ and why does its length vary so widely?

(c) Why is there a variation in the extent of bridging interaction within the series?

In order to rationalize the factors which influence coordination behaviour and final structural arrangement, it is possible to consider the probable reaction pathway from reactants, $HgCl_2 + PR_3$ in solution, through to products, $[(PR_3)HgCl_2]_n$ in the solid state, as occuring in three stages:

a) Initial Hg-P interaction in solution:

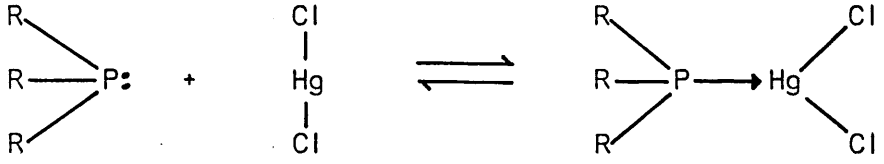

b) Formation of the most stable solution state species:

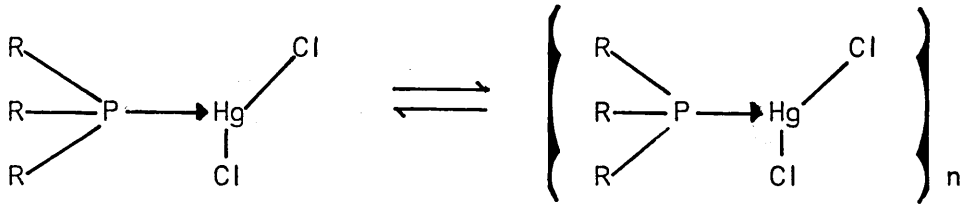

$n \geq 1$

* the subscript s denotes shortest, and refers to the shortest Hg-Cl distance within a structure.

Table 2.10.

Summary of the structures of some (tertiary phosphine)$HgCl_2$ complexes.

Complex	Structure	Cl_s-Hg-P* / °	d(Hg-P)$_t$ /Å	d(Hg-Cl)$_s$* /Å	d(Hg-Cl)$_b$ /Å	Coordination polyhedron about mercury
$(TPP)HgCl_2$	asymmetric dimer	127.8(5)	2.44(1)	2.40	2.54,2.75	distorted tetrahedron
$(PPh_3)HgCl_2$	symmetric dimer	128.7(4)	2.406(7)	2.37	2.62,2.66	"
$(PBu^n_3)HgCl_2$	tetramer	147.8(7)	2.35(2)	2.27	2.63,2.71 2.67,2.90	a. "
		150.6(7)	2.34(3)	2.28	3.38	b. distorted trigonal bipyramidal
$(PEt_3)HgCl_2$	polymeric chain	145.4(3)	2.35(1)	2.42	2.56,3.04 3.21	"
$(PMe_3)HgCl_2$	'ionic'	162.1(1)	2.365(3)	2.355	2.78,2.94 3.49	distorted square pyramidal

* - the subscript $_s$ denotes shortest, and refers to the shortest Hg-Cl distance within a structure.

c) Solid state structures:

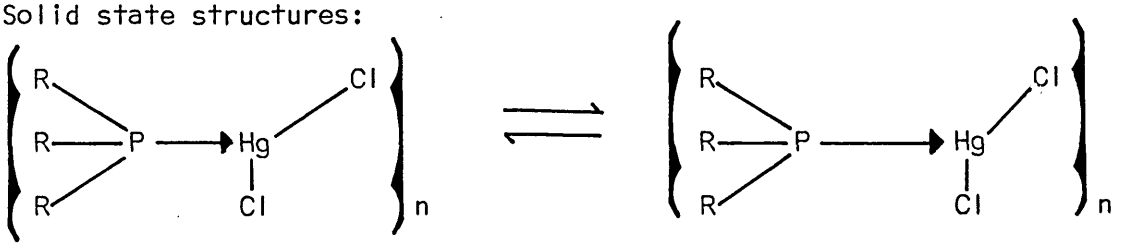

$n \geq 1$ $\qquad\qquad$ $n \geq 2$

solution $\qquad\qquad$ solid

An appreciation of the driving forces within each individual step may help to explain the resulting solid state structures.

(a) Initial Hg-P interaction in solution.

The extent of initial Hg-P interaction will be dependent upon the donor properties of the PR_3 ligand, which, in turn is dependent upon the nature of the R-substituents joined to the phosphorus atom.

Donor properties of PR_3 ligands may be related to the following parameters:-

(i) Taft constants $(\Sigma\sigma^*)$[121] - which are purely electronic in origin arising from the inductive effects of the R-substituents.

(ii) Basicity values (pk_a's)[121] - experimentally determined values of the extent of interaction between PR_3 and a proton in aqueous solution.

(iii) Cone angle (θ)[122] - a steric parameter, which is a measure of the degree of congestion around the bonding face of phosphorus (for fuller description see Appendix 7).

Henderson and Streuli[121] have measured the pka values of a range of $PPh_{3-n}R_n$ ligands. Figure 2.11 shows the results they obtained plotted against Taft constants. This curve indicates the importance of electronic effects in this reaction, however, the deviations from the curve found for the trialkylphosphine series has been explained in terms of steric effects.[121]

Tolman,[122] in a recent review brought together quite a convincing array of structural, spectroscopic and equilibria data some of which could be correlated with cone angle (θ), and some of which could more readily be

FiG. 2.11

Plot of pKq of PR-, _l_iqands in water versus Taft constants Ea^{*} I21

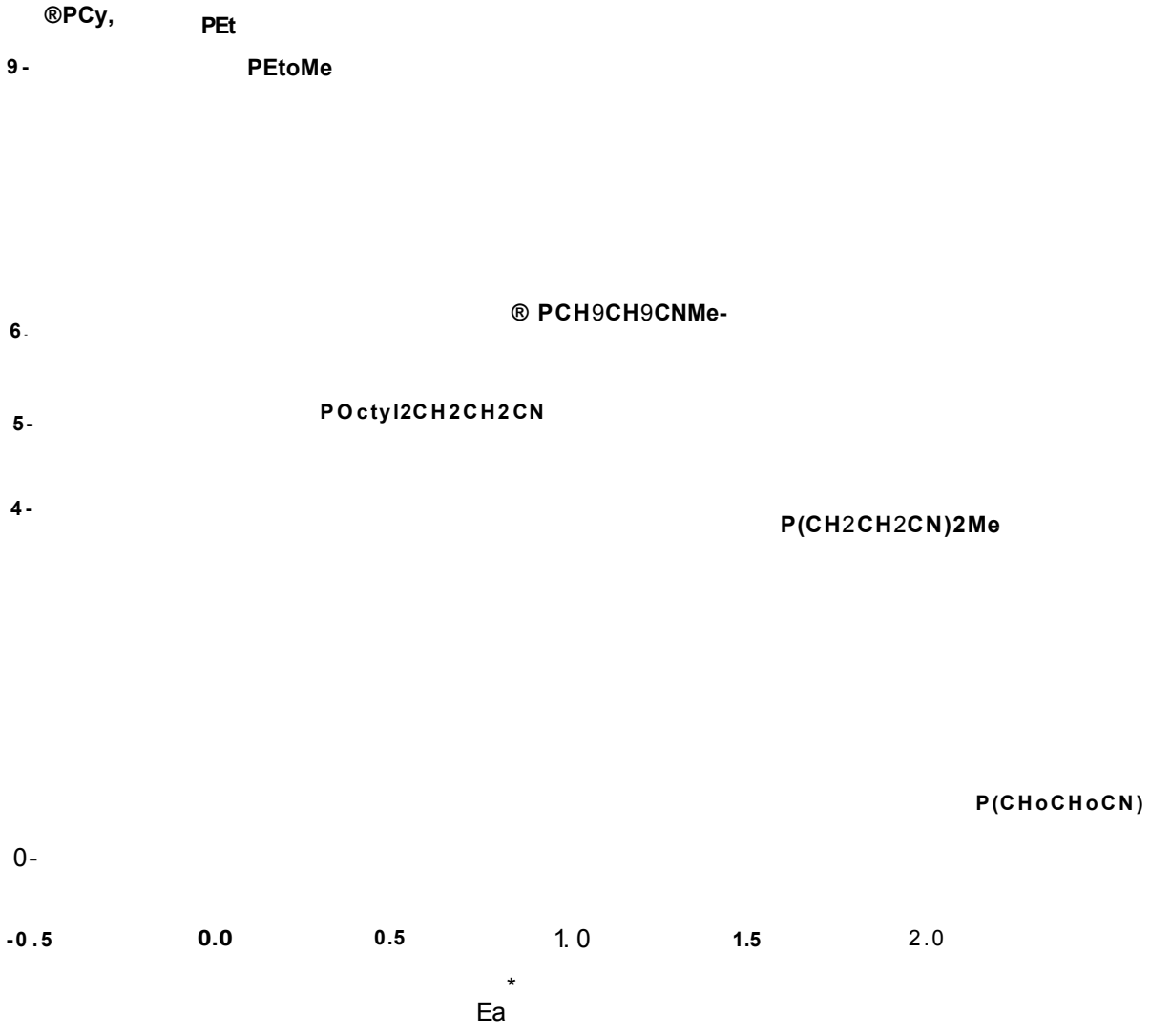

explained in terms of electronic parameters. Tolman[122] stressed that electronic and steric effects are intimately related and it is difficult to make a clear separation between the two.

An example of this inter-relation between steric and electronic parameters has been reported by Mann,[123] who measured ^{31}P chemical shifts for a range of tertiary phosphines and found it was not possible satisfactorily to explain the chemical shift values obtained, solely in terms of the electronegativities of the R-substituents joined to phosphorus. It was concluded that C-P-C angles were also a dominant factor. Therefore as a result of steric effects the electronic environment about phosphorus can be drastically altered.

For the present series of PR_3 ligands the order of donor strengths predicted by each parameter are:-

(i) Basicity values (pk_a)

$PEt_3(8.69) \sim PMe_3(8.65) \sim PBu^n_3(8.64) > PPh_3(2.73)$, TPP*

(ii) Taft constants ($\Sigma\sigma^*$)

$PBu^n_3(-0.39) \sim PEt_3(-0.30) > PMe_3(0.00) > PPh_3(+1.80)$, TPP*

(iii) Cone angles (θ)

$PMe_3(118^\circ) > PBu^n_3(132^\circ) > PEt_3(132^\circ) > PPh_3(145^\circ) >$ TPP(162°)*

The reactions between three of the above PR_3 ligands, PBu^n_3, PPh_3 and TPP, and mercuric chloride have been studied thermodynamically by Gallagher et al.[124] who reported their enthalpies of ligation (ΔH_L). Although this term also includes the enthalpy of dimerization (or further association) the authors state that " the enthalpy of dimerization is only very small, almost certainly 10 kJ (g-atom Hg)$^{-1}$." This is only ca. 10% of the total ΔH_L term. Therefore ΔH_L should be a good guide as to the extent of initial Hg-P interaction.

* Taft and pk_a values are not available for TPP, however the cone angle (θ) has been determined in the present work.

The ΔH_L values ($kJ(g\text{-atom } Hg)^{-1}$) obtained for the present series of PR_3 ligands indicate the following order of donor strength:-

$$PBu^n_3(123) > PPh_3(75) > TPP(67)$$

In addition to these PR_3 ligands, the ΔH_L values for a range of $PPh_{3-n}R_n$ ligands were also determined. Gallagher *et al.*[124] indicate for this series that there is a correlation between ΔH_L and Taft constants (the electronic effects of the substituents) (Figure 2.12). Unfortunately the reactions between $HgCl_2$ and the smaller PEt_3 and PMe_3 ligands were not examined. In view of the observations that the experimentally determined pk_a and ^{31}P chemical shift values for PMe_3 and PEt_3 appear to be dependent upon the steric as well as the electronic nature of these phosphines, at this stage it is difficult to predict unequivocally the likely extent of their initial interaction with $HgCl_2$.

All parameters (Taft constants, pk_a values and cone angles) do suggest, however, that PEt_3 and PBu^n_3 will exhibit a similar degree of Hg-P interaction and that interaction with PMe_3 will be of the same order if not larger. Additionally these three phosphines will exhibit a far greater initial Hg-P interaction than will PPh_3 or TPP.

(b) Formation of the most stable solution-phase species.

This the second step of the proposed reaction pathway is very important because information concerning the structure of the most stable solution-phase species might shed light both on the effects of initial Hg-P interaction and on the effect of these species upon one another during crystallization.

Unfortunately, the solubilities of the present series of complexes in suitable solvents, with the exception of $(PBu^n_3)HgX_2$ (X=Cl, Br or I), were too low to enable solution-phase study (e.g. relative molecular mass determination, ^{31}P n.m.r or vibrational spectroscopy) to be undertaken.

Literature data for other $(PR_3)HgX_2$ complexes in solution are also sparse, probably for similar reasons as above, but the limited data available

FIG. 2.12

Correlation between AHt and £a

(6H |OUU) r>i/ HV

are given in Table 2.11.

Molecular mass determinations suggest,[6,61,90,128,*] at least for trialkylphosphine complexes, that the most stable species in solution is dimeric. Gallagher et al.,[124] however, have reported that if one of the substituents joined to the PR_3 ligand is a phenyl group, the resultant $(PPh_{3-n}R_n)HgX_2$ complex will be monomeric in solution. [It should be noted, however, that in the present work the $(PPh_3)HgCl_2$ complex was insufficiently soluble in benzene to allow molecular mass determination even though Gallagher et al. have stated that this complex is monomeric in benzene. It can only be assumed that this determination was carried out at extremely low concentrations].

Much of the ^{31}P n.m.r data presented in Table 2.11, mostly attributable to Shah[127] and to Grim et al.,[125] have been interpreted on the assumption that dimers are present in solution. However, only for $(PBu^n_3)HgX_2$,[90,*] $(PPr^n_3)HgX_2$* (X=Cl, Br or I), and $(PPhBu^n_2)HgI_2$[125] has this definitely been confirmed by molecular mass determinations.

It is interesting to note that J(Hg-P) values obtained for the complexes known to be dimeric in solution are of the same order as those J(Hg-P) values reported by Shah[127] and Grim et al.[125] Although these comparisons add evidence to support the assumption of Grim et al.[125] and Shah[127] that the compounds they studied are dimeric in solution, one must remember that there is no information regarding the order of J(Hg-P) values characteristic of $(PR_3)HgX_2$ monomers or higher polymers in the literature with which to compare.

It should be noted that for some $(PR_3)HgI_2$ complexes, two structurally different species in equilibrium in solution have been indicated e.g. $(PBu^n_3)HgI_2$[90,125] and $(PPhEt_2)HgI_2$.[125]

Although dimers and monomers have been shown to exist in solution there is no detailed knowledge as to their structure. The only indication of the

* Present work (Section 3.3.3)

Table 2.11.

Solution-phase data for $(PR_3)HgX_2$ complexes.

Compound	Structure	Solvent	^{31}P n.m.r chemical shift ppm	Other determinations	Ref.
$(L)HgCl_2$ complexes					
L=					
PBu^n_3 (α-form)	dimeric	benzene		M_r, IR	*
Bu^n_3 (β-form)	dimeric	CD_2Cl_2	7412	M_r, IR, Ra	90
PBu^n_3?	dimeric	benzene		M_r	124
PBu^n_3?	Assumed dimeric	benzene	7446		125
PBu^n_3?	Assumed dimeric		7480		126
$P(C_6H_{12})_3$	dimeric	benzene		M_r	6
$P(Octyl)_3$	Assumed dimeric		7380		126
$PPhPr^n_2$	Monomeric	benzene		M_r	124
$PPhBu^n_2$	Monomeric	benzene		M_r	124
PPh_3	Monomeric	benzene			124
$PPhBu^n_2$	Assumed dimeric	CH_2Cl_2	7514		125
$PPhEt_2$	Assumed dimeric	CH_2Cl_2	n.o.		125
$PPh_2(C_6H_4C_8H_{17}$-p)	Assumed dimeric	CH_2Cl_2	7506		127
$P(C_6H_4SiMe_3$-p$)_3$	Assumed dimeric	CH_2Cl_2	7546		127
$P(C_6H_4CMe_3$-p$)_3$	Assumed dimeric	CH_2Cl_2	6559		127
PPr^n_3	dimeric	benzene	7389	M_r, IR	*
$(L)HgBr_2$ complexes					
L=					
PBu^n_3	dimeric	benzene		M_r, IR	*
PBu^n_3	dimeric	CH_2Cl_2	6628	M_r, IR, Ra	90
PBu^n_3	trimeric-tetrameric	benzene		M_r	124
PBu^n_3	Assumed dimeric	CH_2Cl_2	6624		125
PBu^n_3	Assumed dimeric		6680		126
$P(Octyl)_3$	Assumed dimeric		6620		126
$PPhBu^n_2$	Assumed dimeric	CH_2Cl_2	6658		125
PPh_2Bu^n	Assumed dimeric	CH_2Cl_2	6553		125
PPh_3	Monomeric	benzene		M_r	124
$PPhEt_2$	Assumed dimeric	CH_2Cl_2	6627		125
$PPhEt_2$	dimeric	benzene		M_r	128

Table 2.11, continued.

Compound	Structure	Solvent	^{31}P n.m.r chemical shift ppm	Other determinations	Ref.
(L)$HgBr_2$ complexes, continued					
L=					
$PPhEt_2$	1.2-1.6 association	Acetone		M_r	128
$PEt_2(C_6H_4CF_3)$	dimeric	benzene		M_r	128
$PEt_2(C_6H_4CF_3)$	1.4-1.7 association	Acetone		M_r	128
PPr^n_3	dimeric	benzene	6611	IR, M_r	*
PPr^n_3	1.5-1.85 association	boiling Acetone		M_r	128
$PPh_2(C_6H_4C_8H_{17}$-p)	Assumed dimeric	CH_2Cl_2	6427		127
$PPh_2(C_6H_4C_6H_{13}$-p)	Assumed dimeric	CH_2Cl_2	6491		127
$P(C_6H_4SiMe_3$-p$)_3$	Assumed dimeric	CH_2Cl_2	6391		127
$P(C_6H_4CMe_3$-p$)_3$	Assumed dimeric	CH_2Cl_2	6559		127
(L)HgI_2 complexes					
L=					
PBu^n_3	dimeric	benzene		M_r, IR	*
PBu^n_3	dimeric	CH_2Cl_2	5088	M_r, IR, Ra	90
PBu^n_3	dimeric	benzene		M_r	124
PBu^n_3	dimeric	CH_2Cl_2	5120,4358	M_r	125
PBu^n_3	Assumed dimeric		5440		126
$PPhMe_2$	Monomeric	benzene		M_r	124
PPh_2Bu^n	Monomeric	benzene		M_r	124
$PPBu^n_2$	dimeric	CH_2Cl_2	5020,4250	M_r	125
PPr^n_3 (α-form)	dimeric	benzene	5071	M_r, IR	*
PPr^n_3 (α-form)	dimeric	benzene		M_r	61
PPr^n_3 (β-form)	dimeric	benzene	5053	M_r, IR	*
PPr^n_3((β-form)	dimeric	benzene		M_r	61
$P(Octyl)_3$	Assumed dimeric		5380		126
$P(n\text{-amyl})_3$	1.2-1.3 association	Acetone		M_r	61
$P(C_6H_4CMe_3$-p$)_3$	Assumed dimeric	CH_2Cl_2	4907		127

* - Present work (Section 3.3.3)

nature of these species has been determined by some vibrational spectroscopic studies on the dimeric $(PBu^n_3)HgX_2$ (X=Cl, Br or I) complexes in benzene carried out in the present work. By comparison of the solution phase IR spectrum of $(PBu^n_3)HgCl_2$ with a range of solid state vibrational spectra of compounds for which crystallographic data also exist (Section 3.3.1), it is proposed that $(PBu^n_3)HgCl_2$ exists as a trans chlorine-bridged dimer with a short Hg-Cl_t bond of ca. 2.3 Å and with Hg-Cl_b bonds of ca. 2.7 Å or greater.

Obviously further work is required to gain further structural information for these compounds in solution but for the purpose of subsequent discussion it seems reasonable to assume, at least for trialkylphosphine complexes studied in this work viz. $(PR_3)HgCl_2$ (PR_3=PMe_3, PEt_3 or PBu^n_3), that trans chlorine-bridged dimers are the most stable solution phase species. Even though $(PPh_3)HgCl_2$ has been shown to be monomeric in benzene,[124] as previously mentioned, this determination must have been carried out in extremely dilute solutions. Therefore it is also assumed, for the purpose of subsequent discussion, that the $(PPh_3)HgCl_2$ and $(TPP)HgCl_2$ complexes, which are dimeric in the solid state, are also dimeric in solution at higher concentrations just prior to crystallization.

(c) Solid-state species.

Information concerning the last step in the proposed reaction pathway is provided in the form of the crystallographic data summarized in Table 2.10. which show that discrete dimeric structures exist for $(TPP)HgCl_2$ and $(PPh_3)HgCl_2$, whereas more associated structures are found for $(PR_3)HgCl_2$ (PR_3=PMe_3, PEt_3 or PBu^n_3).

We may now attempt to explain the present series of solid state structures, in terms of the above proposed reaction pathway, paying special attention to:-

(a) the variation in Cl_s-Hg-P angles

(b) the length of the one Hg-Cl bond which is substantially longer than in $HgCl_2$

(c) the variation in the extent of Hg-Cl association.

Why does the Cl_s-Hg-P angle vary so greatly within the series?

There are two effects which may possibly explain the variation in Cl_s-Hg-P angle.

a) The initial Hg-P interaction, whereby the PR_3 ligand may be attempting to replace a chlorine atom of the $HgCl_2$ unit to achieve ultimately a linear Cl_s-Hg-P arrangement.

b) Solid-state effects, caused by 'inter-dimer' interaction in a manner such that increase in Cl_s-Hg-P angle is dependent upon the mode and extent of association .

It is suggested that it is the initial Hg-P interaction which is the dominant factor influencing the Cl_s-Hg-P angle. The evidence to support this suggestion is outlined below:-

(i) Consideration of the large P-Hg-P angles and large Hg-X bond lengths in the structures of monomeric $(PEt_3)_2HgCl_2$ (P-Hg-P = ca.158°, Hg-Cl = ca.2.7 Å) and monomeric $(PEtMe_2)_2HgBr_2$ (P-Hg-P = ca.150°, Hg-Br = ca.2.8 Å) (Section 4.2) indicate that although Hg(II) is four coordinate, it is as if mercury is 'attempting' to retain the 'preferred' digonal coordination environment (lost on complexation) by elimination of the halogen atoms. These observations indicate that mercury has a preference for phosphorus, in PEt_3 and $PEtMe_2$ at least, with respect to chlorine or bromine. The large P-Hg-P angles and long Hg-X bonds can in no way be attributed to solid state association, but must be due to initial Hg-P interaction. Further evidence suggests (Section 4.2) that P-Hg-P angles and Hg-X bond lengths are dependent on the individual donor strengths of PR_3 ligands.

Vibrational spectroscopic evidence supporting the existence of linear $[P\text{-}Hg\text{-}P]^{2+}$ cations has been reported on two separate occasions for $(PMe_3)_2HgX_2$ (X=Cl, Br or I)[4] and $[(PMe_3)_2Hg]X_2$ ($X^-=NO_3$ or BF_4).[106] These observations again indicate the preference of mercury(II) to achieve the linear coordination

arrangement with the relatively strong PMe_3 donor ligand.

Therefore, one may envisage a similar situation for the present 1:1 complexes, whereby a PR_3 ligand may 'compete' with one of the chlorine atoms of $HgCl_2$ in an attempt to achieve a linear P-Hg-Cl arrangement; the donor strength of the phosphine determines its success in displacing the chlorine atom.

Indeed, Pearson[129] has also indicated that PR_3 ligands are 'softer' donors than Cl^-, so that one might expect the 'soft' acid, Hg(II), to prefer the 'soft' PR_3 ligands.

(ii) Consider the discrete dimers $(TPP)HgCl_2$ and $(PPh_3)HgCl_2$ and the discrete tetramer α-$(PBu^n_3)HgCl_2$, in terms of their P, Hg and Cl 'skeletons'. The immediate environments of the Cl_s-Hg-P terminal segments are very similar for all three structures and there is no possibility of further dimer or tetramer interaction which could influence the coordination about mercury. However, it is immediately apparent that the Cl_s-Hg-P angles are quite different between tetramer and dimers (Table 2.10). The Cl_s-Hg-P angle for the tetramer is ca. 150° whereas for the two dimers it is ca. 128°. The larger angle found for the PBu^n_3 compound can be explained quite well in terms of a stronger initial Hg-P interaction with PBu^n_3 as compared with PPh_3 and TPP. This stronger interaction is indicated by:

(i) ΔH_L (kJ(g-atom Hg)$^{-1}$);

PBu^n_3(123) > PPh_3(75) > TPP(67)

(ii) pK_a;

PBu^n_3(8.64) > PPh_3(2.73), TPP*

(iii) Cone angle (°);

PBu^n_3(132) > PPh_3(145) > TPP(162),

and reflected by Hg-P_t bond lengths (Å):

PBu^n_3[2.35(2)] > PPh_3[2.406(7)] > TPP[2.44(1)].

* - The pK_a value of TPP is not available.

(iii) Evidence to support the limited effect of long range interactions, of ca. 3.2 Å and above, upon Cl_s-Hg-P may be found if the central Cl_s-Hg-P angle of the α-$(PBu^n_3)HgCl_2$ tetramer is considered. The length of the Hg-Cl 'inter-dimer' contact in this compound is 3.38 Å. The difference between terminal, 150.6(7)°, and central, 147.8(7)°, Cl_s-Hg-P angles is only just significant. Therefore the effects of 'inter-dimer' interaction upon Cl_s-Hg-P angles for $(PMe_3)HgCl_2$ ('inter-dimer' contact of 3.49 Å) and $(PEt_3)HgCl_2$ ('inter-dimer' contact of 3.21 Å) are likely also to be small.

If it is accepted that Cl_s-Hg-P angle reflects the strength of the initial Hg-P interaction, then the donor strengths of the phosphines studied fall into the order:

$$PMe_3 > PBu^n_3 \sim PEt_3 > PPh_3 > TPP$$

This order would not seem unreasonable in view of the orders of donor strength predicted previously, and suggests that the steric nature of PMe_3 in some way promotes its binding ability to mercury above that expected from purely electronic considerations (Taft values). In fact there is a correlation between cone angle (θ) for the PR_3 studied here, and the Cl_s-Hg-P angles in the structures of the $(PR_3)HgCl_2$ complexes they form (Figure 2.13a).

What constitutes this "apparent steric effect" is difficult to assess. Is the "effect" solely a steric one, explicable in terms of the PMe_3 ligand being able to get 'closer-in' to the mercury and thus interact more strongly than other ligands? Alternatively, could it be a combination of steric and electronic effects, such as observed by Mann[123] during his ^{31}P n.m.r determinations, whereby as a result of changes in C-P-C angles, the electronic situation about phosphorus is drastically altered? Certainly, C-P-C angles and cone angles are intimately related. e.g. the C-P-C angles for PMe_3[130] and PPh_3[111] are 98.9° and 103°, respectively, whereas their cone angles[122] are 118° and 145°, respectively. Contraction of C-P-C obviously causes a similar effect upon the angle of the 'cone' and therefore it may be that in

the present series of PR_3 ligands that differences in C-P-C angles (which as shown by the ^{31}P chemical shift data have important electronic consequences) are the important parameters and cone angles merely reflect these C-P-C angles. Whether it is a purely steric effect, or a steric plus electronic effect which influences the donor properties of PR_3 ligands in the present situation can only be clarified by further experiment.

Returning to the correlation between cone angle and Cl_s-Hg-P angle (Figure 2.13a). It should be emphasized that even if it is a steric parameter which effects Cl_s-Hg-P angles the almost linear relationship shown in Figure 2.13a cannot be extended because of limitations on cone angles (cone angles reported by Tolman[122] range from 87° for PH_3 itself, to 212° for P(mesityl)$_3$ and structural limits imposed by the $(PR_3)HgCl_2$ compounds. On the basis of the curve shown in Figure 2.13a, at a cone angle of ca.110°, the maximum limit of Cl_s-Hg-P angle (180°) would be reached. Consequently, in this lower cone angle region the formation of a plateau may be envisaged (Figure 2.13b). Similarly, at the high cone angle end of the curve (Figure 2.12a) it is difficult to imagine a Cl_s-Hg-P angle diminishing further than ca. 90°, and so in the region of cone angle ca. 160-170° a tailing off in the curve may be envisaged (Figure 2.12b). It appears that this 'tailing-off' effect is already beginning to occur for the TPP ligand.

Why is one of the Hg-Cl bonds substantially longer than in $HgCl_2$ and why does its length vary so widely?

The one common feature in all five structures is the presence of a short Hg-Cl bond of ca. 2.3 Å, a value which is close to that found for $HgCl_2$ itself (the Hg-Cl bond lengths in solid $HgCl_2$ are each 2.25 Å[35]). Also, for each structure one Hg-Cl bond is longer and the extent of elongation varies from compound to compound. It is the length of this Hg-Cl bond (which is also the shortest Hg-Cl bridge bond) which is examined in this section. Again the cause of these variations in Hg-Cl distance may be attributed to :-

Fig. 2.13a

A plot of Cl_s-Hg-P angle against cone angle for some $(PR_3)HgCl_2$ complexes.

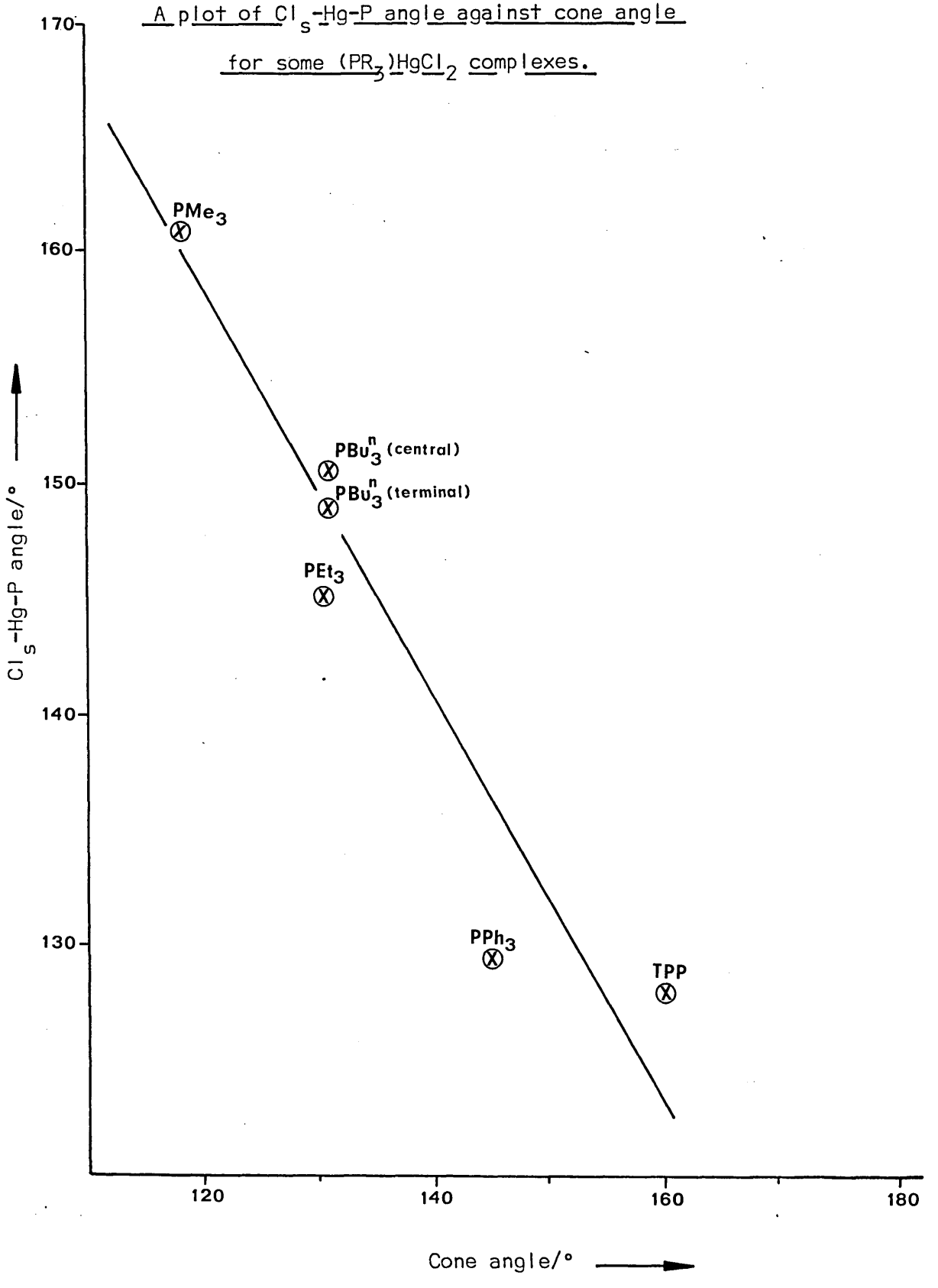

Fig. 2.13b Envisaged plot of Cl_s-Hg-P angle against cone angle, over the complete cone angle range.

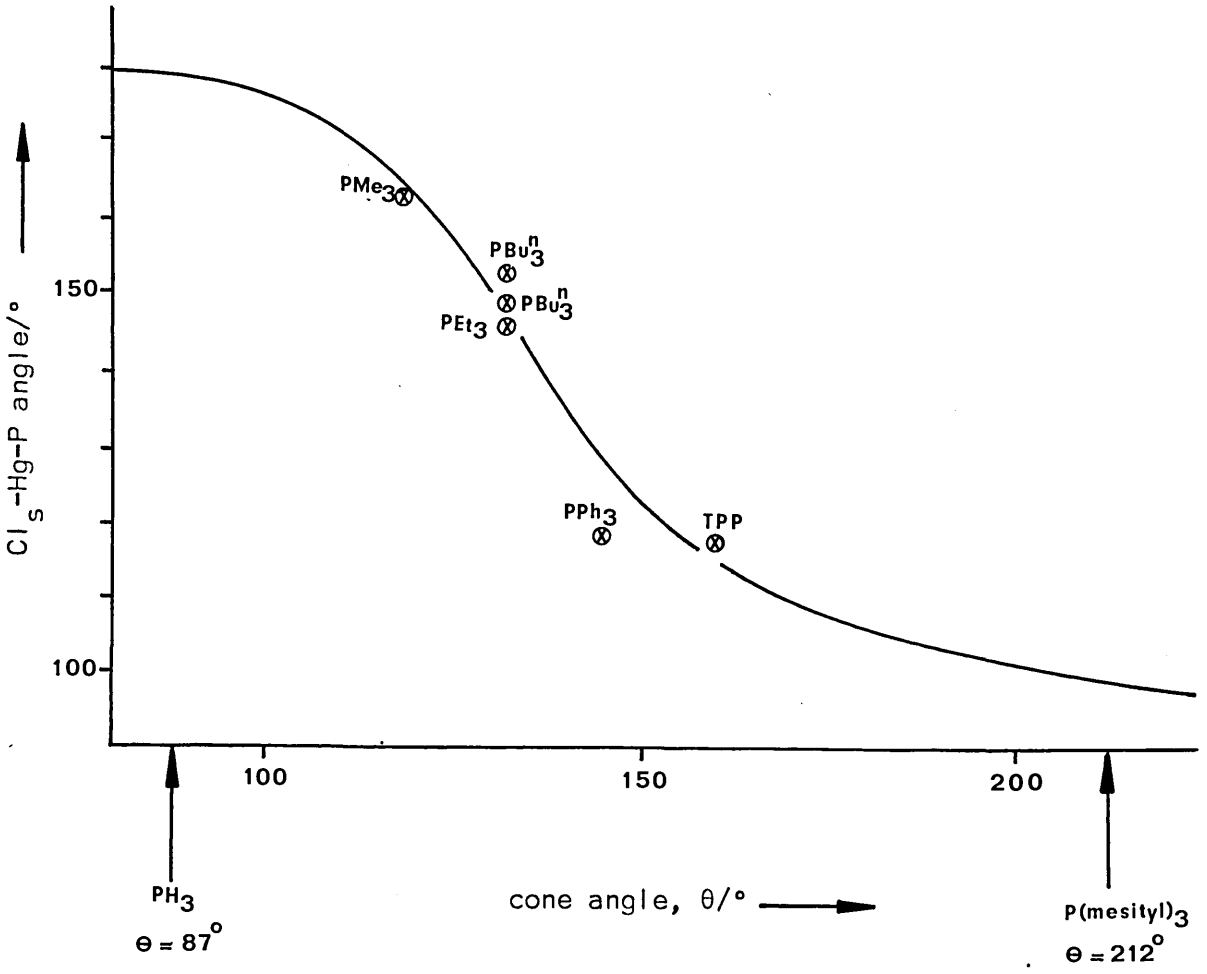

a) extent of initial Hg-P interaction.

b) extent of Hg-Cl bridging.

If one regards the reaction between HgCl2 and PR^ as approaching a 'subsitiution' reaction in which the PR^ ligand is trying to displace one of the chlorine atoms of HgCl2, the length of the Hg-Cl bond in question may have been expected to be directly related to the donor strength of PR^ as indeed Cls-Hg-P angle appears to be. However, this is not the case, thus suggesting Hg-Cl bridging also plays a role in the present case. If on the otherhand one identifies what is the most 'tightly* bound four-membered ring in each of the five structures, as indicated by the Hg-Cl^ distances in (i) there is a correlation (Figure 2.14).

(i)

Compound	Hg—Cl^ distances/A	Sum of Hg-Cl^ distance/A
$(PPh_3)HgCl_2$	2.62,2.66	5.28
$(TPP)HgCl_2$	2.54,2.75	5.29
(PEt3)HgCl2	2.56,3.04	5.60
(PMe3)HgCl2	2.78,2.94	5.72
ot-(PBu$_3^n$)HgCl?	2.63,2.67 2.71,2.90	5.46*

In effect, what this correlation means is that the resultant bridging capacity of the chlorine atom in the bridge, given by the sum of the two Hg—Cl^ distances within the four-membered ring, is dependent upon the extent to which the PR3 ligand 'displaces' that chlorine atom, and also upon the way in which that chlorine atom is allowed to interact to form the four-membered ring.

Therefore the length of the shortest of these Hg-Clb bonds, which is under consideration here may be explained in terms of two effects viz.the degree of 'displacement' of the chlorine atom due to Hg-P interaction and the extent to which this chlorine atom participates in further Hg-Cl interaction,

this is an average value of two Hg—Cl^ bonds in the unsymmetric four-membered rinq.

Fig. 2.14

Relationship between cone angle and the sum of the two shortest Hg-Cl bridge bonds.

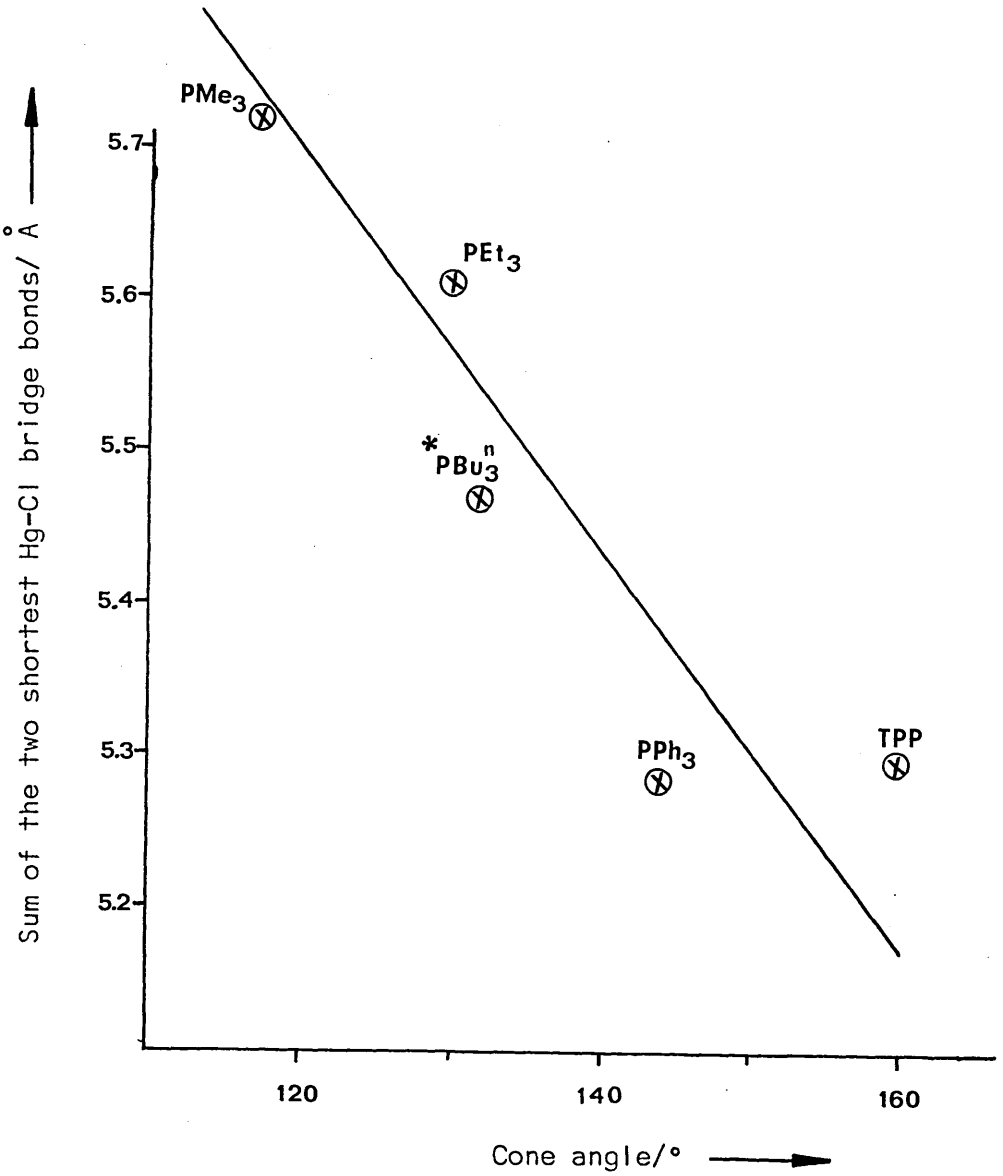

* - the average value of two bonds in the unsymmetric four-membered ring, has been plotted.

Why is there a variation in the extent of bridging interaction within a series?

To answer this question one should consider the final step in the proposed reaction pathway i.e. the manner in which the most stable solution state species pack together to produce the solid state structure. Obviously the precise structures of solution-phase species are extremely important in this discussion but little is known about them and so, as previously mentioned, dimers are assumed to be the most stable solution-phase species. However, two very important parameters may still be discussed:-

a) the overall steric bulk of the PR_3 ligand;

b) the magnitude of the Cl_s-Hg-P angle (assuming they are similar in solution to those observed in the solid).

It is easy to see for the two dimeric species containing the very bulky (PPh_3) and (TPP) ligands why association beyond the dimer stage does not occur in the solid. The sheer bulk of the ligand molecules, not helped by their relative dispostions as a result of the Cl_s-Hg-P angles of ca. 128°, prevents further interaction between Cl and Hg.

For $(PMe_3)HgCl_2$ where there is strong initial Hg-P interaction, probably giving rise to a large Cl_s-Hg-P angle in solution and the steric bulk of the PMe_3 ligand is very small, further interaction appears to be allowed. The mode of interaction is such that it is the Hg-Cl bridge bonds of the 'original dimer' which take part in further association.

For the PEt_3 and PBu^n_3 complexes in which the initial Hg-P interaction is probably similar, the Cl_s-Hg-P angles in solution are most likely close to the solid state values (ca. 145°). The extent of further association would therefore be dependent upon the relative steric bulk of the ligands. The $(PEt_3)HgCl_2$ complex has a continuous polymeric structure, which could be described as a continuous chain of dimers linked end-to-end via their 'terminal Hg-Cl bonds'. The mode of further association in this structure differs from that found for $(PMe_3)HgCl_2$. This may be attributed to a combina-

tion of the larger steric bulk of PEt_3 and perhaps a lower Cl_s-Hg-P angle in solution.

The $(PBu^n_3)HgCl_2$ complex exists as a tetramer in the solid state, whereas vibrational spectroscopic studies, as already mentioned, suggest that the most stable solution phase species is a dimer. The way in which these dimers pack together results in two stereochemically different Hg atoms being observed, one of which is in a distorted tetrahedral environment, cf. $(PPh_3)HgCl_2$, and the other which is in a distroted trigonal bipyramidal environment, cf. $(PEt_3)HgCl_2$. The Cl_s-Hg-P angle of the dimer in solution, is probably close to the solid state values (ca. 148°). This angle and the steric bulk of PBu^n_3 seem to be of such a magnitude as to allow further Hg-Cl interaction, through terminal Hg-Cl bonds of the dimer, as in $(PEt_3)HgCl_2$, but only to the tetramer stage.

Discussion has been restricted to the $(PR_3)HgCl_2$ complexes because these are the ones which have been subject to full crystallographic analysis in the present study. However, preliminary single crystal X-ray photographic studies (Section 2.2) and vibrational spectroscopic studies (Section 3.3.1) suggest that, in general, similar behaviour is shown by the bromo analogues i.e. $(TPP)HgBr_2$, $(PMe_3)HgBr_2$, $(PEt_3)HgBr_2$ and $(PBu^n_3)HgBr_2$ all appear to be isostructural with the respective chloro complexes. Similar studies on iodo complexes sometimes show them to be isostructural with their halo analogues, e.g. $(PPh_3)HgI_2$. However, on other occasions different structures seem likely, e.g. $(PMe_3)HgI_2$. Obviously then, the influence of the halogen atom on the solid-state structure should not be ignored. Unfortunately sufficient information concerning the nature of this influence is unavailable at present and so no further inferences can be drawn.

2.3.2. $(L)HgX_2$ complexes (L=N- or As-donor ligand).

Preliminary crystallographic analysis of the $(AsPh_3)HgCl_2$ complex indicates that it is isostructural with $(PPh_3)HgCl_2$, the geometry of the

mercury-chlorine-donor atom skeletons being virtually identical. This indicates similar mercury-ligand interactions and similar crystal packing requirements. The interaction between nitrogen and mercury in (2,4-dimethylpyridine)$HgBr_2$ is very similar to that found in (2,4,6-trimethylpyridine)$HgCl_2$.[62] In each case mercury is surrounded by two short mercury-halogen bonds and one mercury-nitrogen bond in a trigonal planar arrangement with the X_s-Hg-N angles of 129° (X=Br) or 128° (X=Cl), and the ratio of the two short Hg-X bonds at 0.95 (X=Br) and 0.97 (Cl), respectively. There is no information concerning these complexes in solution but considering the solid state structures it seems likely that '$NHgX_2$' units exist as trigonal monomers in solution and pack together in a manner dependent upon the steric properties of the N-donor ligand. The packing of the '$NHgX_2$' units in both structures is similar, in that two further long range mercury-halogen interactions arise completing distorted trigonal bipyramidal environments. However, as previously mentioned, the packing arrangements are subtly different from one another (Figure 2.10 and Figure 1.10).

In (guanosine-N^7)$HgCl_2$[63] (Figure 1.11) the interaction between nitrogen and mercury appears to be much stronger than in the complexes of the substituted pyridines, as suggested by the large Cl_s-Hg-N angle of 155.5° and the length of the second shortest Hg-Cl bond (2.659 Å). The solid-state packing arrangement is totally different to those found for the other N-donor complexes, consisting of infinite $[-Cl-Hg-Cl-Hg-]_n$ zig-zag chains in which mercury lies in an irregular four-coordinate environment (Figure 2.14). These differences in the solid-state structure of (guanosine-N^7)$HgCl_2$ may be attributed to a combination of electronic and steric properties of the guanosine-N^7 ligand and packing requirements of the solution phase species.

2.3.3. General Summary.

With regard to all the crystallographic data now available for the (L)HgX_2 system, one may now observe the following trend emerging.

There are two distinct forms of interaction between ligands and mercuric halides:

a) For oxygen donor complexes. - Here there appear to be relatively weak donor-acceptor interactions, causing little distortion of the HgX_2 units, i.e. both angular and bond length distortion are small.

b) For group VB and VIB (non-oxygen) donor complexes. - Here there is stronger interaction causing distortion of the HgX_2 unit in terms of angular distortion of the X-Hg-X unit and increase in length of one of the Hg-X bonds. There appears to be a variation in the extent of these stronger interactions within this class of donor atom depending on the electronic and steric nature of the substituents attached.

These observations comply with the 'hard-soft' formalism of Pearson[129] and the Class A and Class B formalism of Ahrland *et al.*,[131] whereby O-donors are 'hard' donors (Class A), P-, As-, S-donors are 'soft' donors (Class B), and nitrogen-donors are classed as 'borderline' donors.[129] The thermodynamic data of Farhanghi and Graddon,[132] in the form of values for ΔH_L of ligation for a number of O-, S-, N-, and As-donor ligands with the mercuric halides, add further support to the distinction between mercury-oxygen interaction and the varying strengths of interaction observed for the 'soft' (Class B) donors and 'borderline' donors.

Substituent effects cannot be discussed in general because of the different number of substituents which may be attached to each donor atom. Thus for a tertiary phosphine there are three substituents whereas for dialkyl sulphides there is only the possibility of two substituents. These individual properties obviously cause differences in electronic and steric properties of phosphorus and sulphur donor ligands, even when substituents are similar. Nevertheless, one may still note, even from the small number of crystallographic data presented (Section 1.3.3) that the properties of the substituents joined to the donor atoms are of paramount importance in determining solid state structure, as indeed has been shown for the $(PR_3)HgCl_2$ complexes.

Because of the lack of crystallographic data available for the bromo and iodo systems at the present time, it is not possible to make any reliable suggestions as to the effects of changing the halogen atom on the solid state structure of $(L)HgX_2$ complexes. However, judging from the $(PR_3)HgX_2$ complexes studied in the present work, the effect should not be ignored, especially on passing from bromo to iodo complexes cf. $[SMe_3]HgX_3$ (X=Cl or I) (Section 1.3.2).

Chapter 3.

Spectroscopic studies of some $(L)HgX_2$ complexes.

Contents

3.1. DIAGRAMMATIC SUMMARY OF SOME (L)HgX2 COMPLEXES

Below are summarized the structures of the (PR-^HgC^ complexes determined in this work together with some other (1:1) structures. This summary is presented to assist the reader in the subsequent spectroscopic discussion.

(PPh-,)HqC l^

,2.41

(TPP)HQCI2

2 40

2 44

Similar structures have been observed for the (MPOHgC^^ and (Ph^PSe)HgCl^ complexes

(PEt^)HqCl2

2.5

2.35

a-(PBu^)HqCU

2.67

2.28

2.27

2.63

$(PMe_3)HgCl_2$

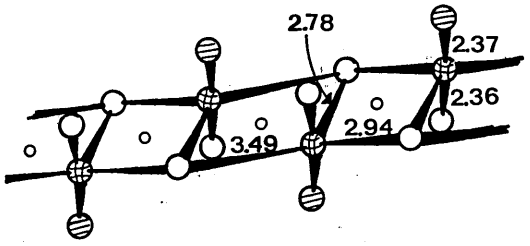

A similar arrangement has been observed for $(C_4H_8S)HgCl_2$[64]

(2,4,6-trimethylpyridine)$HgCl_2$

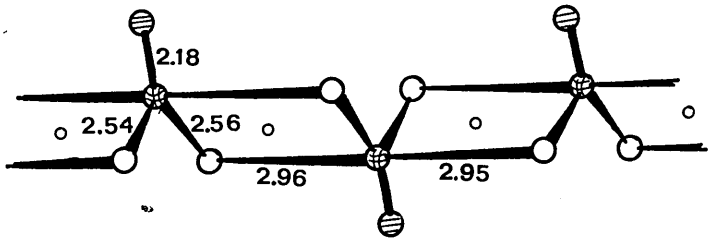

(2,4-dimethylpyridine)$HgBr_2$

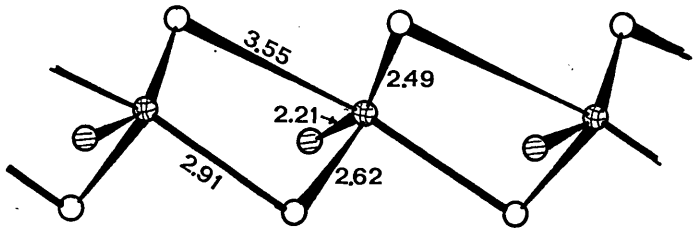

KEY

⊕ = Hg ○ = halogen ⊖ = ligand

3.2. BASIS FOR VIBRATIONAL ASSIGNMENTS FOR $(PR_3)HgX_2$ COMPLEXES

3.2.1. Mercury-halogen stretching modes.

The crystallographic data presented in Section 2.2 indicate a range of crystal structures for $(PR_3)HgX_2$ (X=Cl, Br or I) complexes. At one extreme there is $(PPh_3)HgCl_2$ which exists simply as a discrete dimeric unit, while at the other there are extended structures such as those found for $(PMe_3)HgCl_2$ and $(PEt_3)HgCl_2$. As a result of the varying structures shown by these compounds, substantial differences are expected, and indeed are found, in the vibrational spectra. In order satisfactorily to interpret the spectra it was found necessary to treat each structural type separately. The criteria employed when making vibrational assignments for each of these structural types is outlined below.

Symmetric dimers (equal bridge bond lengths). Consider the simplest structure, that of a dimeric molecule of C_{2h} symmetry, such as that found for $[(PPh_3)HgX_2]_2$ (in fact only approximately C_{2h}, actually C_i). Point group analysis (taking PPh_3 as point mass) predicts the following optically active $\nu(HgX)$ modes:-[7]

$$\Gamma\ \nu\ (HgX)_t = A_g(Ra) + B_u(IR)$$

$$\Gamma\ \nu\ (HgX)_b = A_g(Ra) + B_g(Ra) + A_u(IR) + B_u(IR)$$

This means one would expect to find one mode associated with terminal mercury-halogen stretching and two stretching modes associated with the mercury-halogen bridge bonds in each of the IR and Raman spectra. The approximate form of motion of each of these modes has been derived using character-tables and by comparison with the normal modes of vibration for M_2X_6 systems (D_{2h}) indicated by Nakamoto,[134] (Figure 3.1a). By comparison with other halogen-bridged dimeric systems[135,136] one would expect the stretching modes associated with terminal bonds to occur at substantially higher wavenumber values than those due to bridge bonds.

The conventional methods of locating $\nu(MX)$ modes are the 'halogen-mass

Figure 3.1a.

ν(HgX) modes for a C_{2h} dimer.

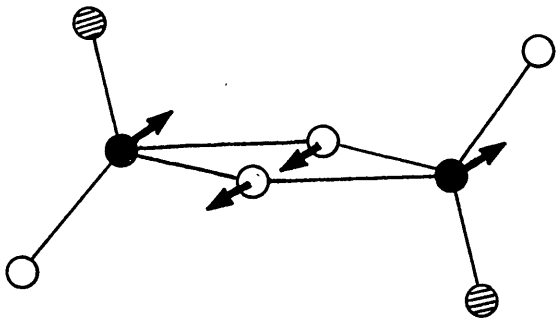

ν(HgX)b

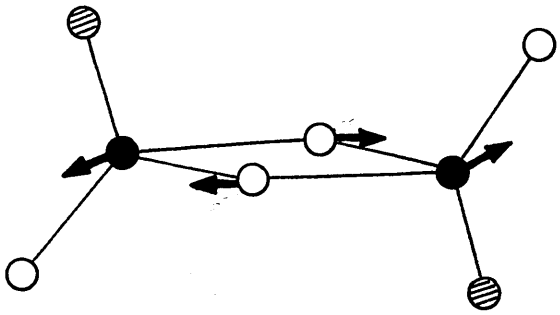

ν(HgX)b

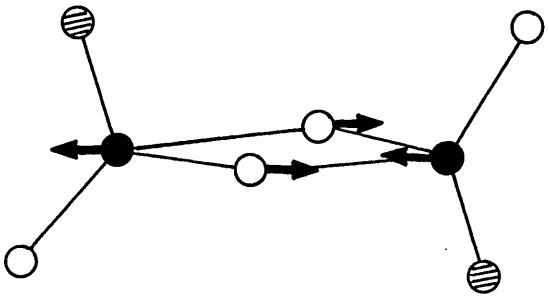

ν(HgX)b

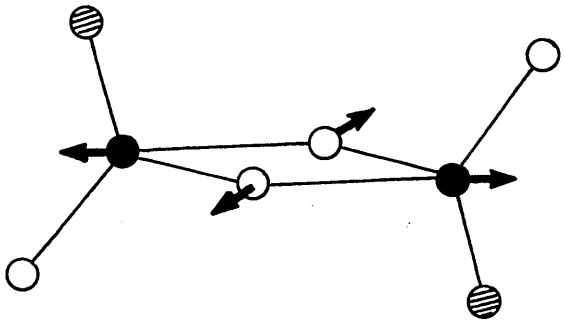

ν(HgX)b

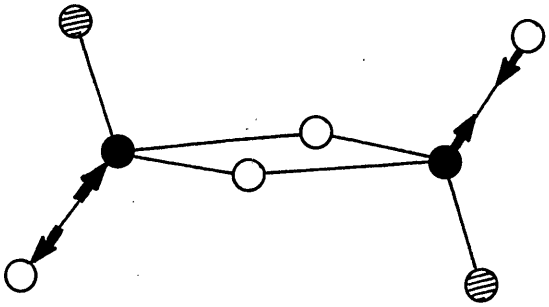

ν_{as}(HgX)†

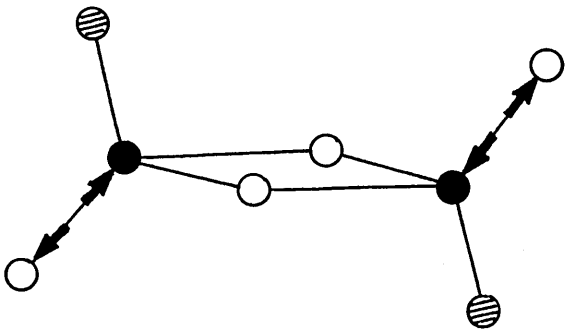

ν_{s}(HgX)†

dependence method' coupled with subtraction of the free ligand spectrum from that of the 'metal complex' spectrum. There is a problem whilst using these methods as they are based upon the premise that chloro-, bromo- and iodo-complexes are isomorphous and isostructural. This, as has been found in the present work (Chapter 2), is not always the case for $(PR_3)HgX_2$. Nevertheless, wherever possible, taking due care, these methods may be employed.

As already indicated (Section 1.4.2), previous vibrational assignments for $(PR_3)HgX_2$ complexes, which are generally inferred to have dimeric C_{2h} structures, are far from reliable due to lack of consistency and lack of a firm crystallographic basis. The crystallographic data presented in Section 2.2 have shown that only in the case of $(PPh_3)HgX_2$ (X=Cl, Br or I) has the proposal for a dimeric structure based on the vibrational spectra been confirmed. The assignments made to justify these proposals however, are not entirely consistent. For example, consider the work of Deacon *et al.*[7] and Adams *et al.*[8] The infrared spectra reported by both sets of workers appear to be totally consistent. There is agreement as to the assignment of the $\nu(HgCl)_t$ mode and also one of the $\nu(HgCl)_b$ modes, which by comparison with related dimeric systems, Al_2Cl_6,[135] I_2Cl_6[136] and Au_2Cl_6,[136] are probably correct. However, there is disagreement as to the assignment of the second $\nu(HgCl)_b$ mode. Deacon *et al.*[7] prefer to assign the lower wavenumber bonds at 97, 83 cm^{-1} to this mode, whereas Adams *et al.*[8] prefer to assign a higher wavenumber band at 150 cm^{-1}. Barr[96] reports a similar problem of assignment and uncertainty of wavenumber position of the second $\nu(HgX)_b$ modes in the dimeric complexes $[(Ph_3PSe)HgX_2]_2$ (X=Cl, Br or I).

Clearly there is ambiguity with regard to which region of the spectrum the second $\nu(HgCl)_b$ mode occurs. It was considered useful therefore to make a further comparison of the present system with related planar four-membered ring systems.

Baran[137] has studied a number of such systems and has derived some

simple approximate equations which relate the two IR-active ν(M-X) modes to the angles between the bridge bonds in a four-membered ring [M<X>X>M]. The bridge angle M—X—M, denoted by ϕ, is related to the two IR-active modes (arbitrarily denoted ν_s and ν_a) by the equation:-

$$\text{Cos } \phi = \frac{[(\nu_s/\nu_a)^2 - 1]}{[(\nu_s/\nu_a)^2 + 1]} \qquad (1)$$

(see Appendix 5 for derivation)

Baran has tested this equation by calculating for a wide range of planar four-membered ring systems using reliable far-IR data, and comparing the results with values of derived from definitive structural studies.

Careful scrutiny of Baran's original paper shows that the agreement between the values of ϕ obtained crystallographically and those calculated from equation (1) is better for structures where the relative atomic masses of M and X are widely separated. This is not entirely surprising when one considers that Baran's formula has been derived on the basis of a stationary M atom. Unlike the case where there is a large difference in atomic masses between X and M, and thus the heavier M atom is virtually unperturbed during ring vibrations and can be approximated to a stationary M atom, one would expect a considerable kinematic effect of motion of X upon M during ring vibrations if the relative atomic masses of X and M were close to one another. Consequently equation (1) is less likely to be of use in the latter situation. For the present problem one may envisage the formula being more applicable to chloro-, than to bromo-, than to iodo-structures. Table 3.1 contains some related ring systems (i.e. those containing a planar symmetric four-membered ring in which there is considerable difference in the relative atomic masses of X and M) together with relevant structural data which show a reasonable correspondence between ϕ_{obs} and ϕ_{calc}, therefore giving some justification for the use of equation (1).

For the purpose of the present problem, determination of the relative

Table 3.1.

Comparison of ϕ_{obs} and ϕ_{calc} for some four-membered ring systems.

Compound	Structural Information		$\phi_{obs}/^{\circ}$	$\phi_{calc}/^{\circ}$	$\nu(HgX)_b$ modes/cm^{-1}
	bridge distances/Å	Source			
Au_2Cl_6 [136]	2x3.33(2),2x2.34(2)	X-Ray	94(2)	90.9	310 305
I_2Cl_6 [136]	4x2.70	"	96	100.7	205 176
Ga_2Cl_6 [140]		N.C.A*1	86	86.5	305 287
$[NEt_4][Hg_2Br_6]$ [96]	4x2.75	X-Ray	91(2)	92.3	128 123*2

*1 - N.C.A. denotes normal coordinate analysis.

*2 - denotes present assignment.

Table 3.2.

Assignment of mercury-chlorine stretching modes in $(PR_3)HgCl_2$ using a simple point group approximation.

Complex	$\nu_{as}(HgCl)_t/cm^{-1}$	$\nu(HgCl)_b/cm^{-1}$	$\nu(HgCl)_b/cm^{-1}$
$(PPh_3)HgCl_2$	297	188	183
$(TPP)HgCl_2$	283	219	156
$(PEt_3)HgCl_2$	286	198	117,105,90
$(PMe_3)HgCl_2$	300	141	124,113

wavenumber positions of the two IR-active V(HgX)^ modes in dimeric structures such as [(PPh^HgX^ 2, equation (I) may be rearranged to the form:

$$v_s/v_0 = \left(\cos\phi + \frac{1}{(1 - \cos\phi)}\right)$$

Therefore, knowing the actual (P> angle, the ratio v_s/v_a can be calculated. It follows that for a <J>=90°, vs/va = I and the two IR-active v(HgX)^ modes should be coincident. In the present case the structure of [(PPh^)HgCl has $(j)_{obs}$ = 94.6 which affords a v_s/v_a ratio of 1.08. Therefore the v(HgCl).$_b$ modes are expected to appear reasonably close together. Other evidence in favour of a relatively small wavenumber separation between the two bridge modes is found from the consideration of the vibrational data available for the closely related $[Cd^X^]^{2-}$ system for which relatively small wavenumber separation between the v(CdX)b modes has been reported.[138]

Although this discussion has been confined to the IR-active v(HgX)b modes a similar wavenumber order may be envisaged for their Raman-active counterparts, as indeed has been observed in other related systems, e.g. [Cd2X5] 2“ (X=Br or I) 138 and [Pt2CIg] 2“ . 139

It is these criteria which have been borne in mind when making vibrational assignments for a symmetric dimeric system such as for [(PPh^)HgX2I$_2$ (X=CI, Br or I).

Asymmetric dimers (unequal bridge bond lengths). Consideration of the vibrational spectra of the dimeric (TPP)HgX2 (X=Cl or Br) complexes, showed it was not possible to make assignments based on the above arguments. This was attributed to the asymmetric nature of the four-membered ring, in the present case (see Section 3.1). It was therefore attempted to show, using a similar approach to that of Baran,*3^ that when the planar four-membered ring becomes asymmetric, due to extension or contraction of either of the bridge bonds, the wavenumber positions of the ^(MX)^ modes will separate, this separation being directly dependent upon the degree of

asymmetry (for derivation see Appendix 5).

To test whether the assumptions made in the derivation of this relationship are valid, and also to test whether there is a correlation between $\nu(MX)_b$ mode separation and asymmetry, it would be sensible to consult the literature concerning related series of compounds for which sufficient crystallographic and spectroscopic results are available. Unfortunately, such data are sadly lacking for halogen-bridged metal complexes. However, similar phenomena of increased asymmetry causing separation of symmetric and asymmetric modes have been observed in other branches of coordination chemistry. For example, Nakamoto[134] has reported that the wavenumber positions of the $\nu_a(COO)$ and $\nu_s(COO)$ modes of the carboxylate ion separate as a result of the asymmetry of the $O\diagup C\diagdown O$ unit brought about by its varying denticity. Also the $\nu_a(NO_2)$ and $\nu_s(NO_2)$ modes of the $-NO_2$ ion show varied degrees of separation related to whether or not metal-ligand bonding is via oxygen (where there is asymmetry of the $-NO_2$ unit giving a relatively large separation), or via nitrogen, (where there are equal bond lengths in the $-NO_2$ unit giving a relatively small wavenumber separation).

Extended structures. The vibrational spectra of the complex $(PEt_3)HgCl_2$ and $(PMe_3)HgCl_2$ could similarly be interpreted on the basis of the above argument concerning the effects of an asymmetric ring on the vibrational spectrum. Neglecting the longer range interactions of 3.03 Å for $(PEt_3)HgCl_2$ and 3.49 Å for $(PMe_3)HgCl_2$ each structure approximates to a series of asymmetric dimers (Section 3.1). Table 3.2 shows the assignments of the three IR-active modes for four complexes studied in this work based on a simple point group treatment. One may note the effects of asymmetry on the spectra and also the correlation between bond length and $\nu(HgCl)_b$ wavenumber position.

In spite of the way in which the results on $(PEt_3)HgCl_2$ and $(PMe_3)HgCl_2$ fit into the above argument (when treated as 'discrete dimeric structures'),

it was considered more correct in view of the crystallographic data (Section 3.1) not to ignore the longer range interactions and to make vibrational assignments treating these structures as polymeric chain and 'ionic' chain respectively.

Tetramer. The vibrational spectra of α-$(PBu^n_3)HgCl_2$ are very complicated, reflecting the nature of the tetrameric structure, and it was not possible to relate these spectra to those previously described for dimers and extended structures.

A simple point group analysis for a C_i tetramer has therefore been adopted.

3.2.2. Mercury-phosphorus stretching modes.

Whichever treatment (polymeric chain, dimeric unit or 'ionic' structure) is used to predict the number of ν(HgP) modes in the $(PR_3)HgX_2$ complexes the same result is obtained, i.e. one ν_{as}(HgP) mode (IR-active) and one ν_s(HgP) mode (Ra-active), assuming no solid state effects. Again, there appears to be some controversy in the literature as to the wavenumber position of these ν(HgP) modes. Most workers[6,7,97] prefer to assign bands in the region 120-150 cm^{-1} to these modes. However, Schmidbaur et al.[4], in their work on $(PMe_3)HgX_2$ (X=Cl, Br or I), assign bands at ca. 360 cm^{-1} as arising from ν(HgP). Alyea et al.[97], in their paper concerned with $(PR_3)HgX_2$ (R=Bu^t or o-tolyl; X=Cl, Br or I), state that they believe the assignments of Schmidbaur et al.[4] to be erroneous because of their high wavenumber position at ca. 360 cm^{-1} compared with values of ca. 130 cm^{-1} in their own work.

Contrary to this view a case may be presented in favour of both sets of assignments. An important factor which Alyea et al.[97] have not taken into account is the coordination environment about mercury which, as has been shown (Section 2.2) varies from one structure to another.

Firstly consider the work of Alyea et al.[97], in which Hg-P bonds are probably in an approximately tetrahedral environment. As a result of the

metal isotope studies of Nakamoto[134] on tetrahedral $(PR^{\wedge})_2NiX_2$ complexes, which are the most reliable v(M-P) data available to date, v(Ni-P) modes are known to occur at ca^. 190 cm ' for tetrahedra lly coordinated nickel. It would thus seem reasonable, considering the higher mass of mercury to expect v(Hg-P) modes due to tetrahedra lly coordinated Hg-*P bonds to appear at wave-number values <190 cm *. This would explain theV(HgP) assignments made by Alyea e+ aj_.[97] and also those of Deacon et al.[7]

As already mentioned, Schmidbaur[4] assigns v(HgP) modes at ca_. 360 cm^{-1} for $(PMe^{\wedge})HgCl_2$ (X=CI, Br or I). Goggin et aj_.[106] have studied a number of ionic structures containing [X-Hg-PMe^I + species and observed bands at ca_.360 cm ' which were assigned toV(HgP) modes, thus substantiating Schmidbaur's assignments.

To understand why there is this large variation in wavenumber position for v(HgP) modes it must be remembered that the geometry of the tX-Hg-PMe^I species in $(PMe^{\wedge})HgX_2$ (X=CI or Br) approaches linearity (XHgP angle of ca. 160 °) which is probably also true for the tX-Hg-PMe^]+ species studied by Goggin et £]_.[106] Therefore, one may envisage a similar correlation arising between wavenumber and coordination geometry as is found for mercury-halogen stretching modes (Section 1.4.1). Allen et a_l_.,[141] and Nakamoto[134] (using metal isotope techniques) have reported similar wavenumber differences between v(Ni P) modes for tetrahedral and planar (PR-^NiC^ complexes.

Another vital point which Alyea et a_.[97] did not take into consideration whilst commenting upon the high wavenumber position of V(HgP) modes for the $[X\text{-}Hg\text{-}PMe^{\wedge}]^+$ species (X=CI, Br or I)[4] was the positive charge on the cation. It has been shown on numerous occasions' that the wavenumber position of v(ML) modes for species of the type $ML^{\wedge}+$ (x= 4 or 6 and n=l,2,3 etc.) are dependent on the value of n; the higher the value of n, and thus positive charge the higher the wavenumber of the v(ML) mode. For example, v_a(FeCl) for Fe(I l)Cl_2(diarsine) occurs at 349 cm ' (IR),* whereas v_a(FeCl) for

$[Fe(III)Cl_2(diarsine)]^+$ occurs at 373 cm^{-1} (IR).[1]

It should be mentioned that the mass of the PR_3 group obviously changes from PMe_3 through to PPh_3, and this itself might be expected to cause a shift to higher wavenumber on decreasing mass of phosphine. However, Allen and Wilkinson,[141] who studied a range of $(PR_3)_2NiX_2$ complexes (R= alkyl or aryl; X=Cl, Br or I), reported approximately constant ν(NiP) wavenumber positions irrespective of the mass of the phosphine.

Finally it should be mentioned that the intensity of modes associated with Hg-P stretching are reported often to be quite low, and that there may be fluctuation in intensity going from one halo analogue to another. This would obviously hinder location and assignment of ν(HgP) modes.

On the few occasions where assignment of ν(HgP) modes have been attempted in the present work, they have been made in the light of the above arguments.

3.3. SOLID STATE VIBRATIONAL SPECTRA OF SOME TERTIARY PHOSPHINE COMPLEXES.

3.3.1. Complexes of known structure.

(a) $(TPP)HgX_2$ (X=Cl or Br). The structure of the chloro complex has been determined (Section 3.1). The molecules crystallize in a triclinic system, space group $P\bar{1}$, one molecule per unit cell, in the form of discrete dimeric units. The four-membered ring system has a centre of symmetry, but its bridge bonds are of unequal length (2.54 and 2.75 Å). The TPP ligands are mutually trans about approximately tetrahedrally coordinated mercury atoms. The dimeric molecules belong to the C_i point group. Preliminary photographs indicate that the bromo analogue is isomorphous and most probably isostructural with its chloro counterpart. The iodo complex could not be prepared. The total number of modes of the primitive unit cell may predicted by factor group analysis (Appendix 4):-

$$\Gamma_{Total} = 12A_g(Ra) + 12A_u(IR)$$

the modes due to ν(HgX) are:-

$$\Gamma\ \nu(HgX)_t = A_g(Ra) + A_u(IR)$$

$$\Gamma\ \nu(HgX)_b = 2A_g(Ra) + 2A_u(IR)$$

while those due to ν(HgP) are:-

$$\Gamma\ \nu(HgP) = A_g(Ra) + A_u(IR)$$

Because there is only one dimer per unit cell, which lies on a centre of symmetry, the results of this factor group analysis for internal modes are the same as predicted using point group analysis.

The vibrational spectra are shown in Figures 3.1a and 3.1b. Table 3.3 contains the wavenumber positions and vibrational assignments. The IR spectra of both the chloro and bromo analogues each show three very prominent halogen mass-dependent bands. Internal modes due to the TPP ligand are easily eliminated due to their constant position in both complexes. It is unlikely that these modes are ν(HgP) due to their relatively high wavenumber position. Bearing in mind that one $\nu(HgX)_t$ A_u mode is predicted in each IR spectrum, the highest wavenumber band in each case (283 and 195 cm^{-1} for chloro and bromo complexes respectively) are thus assigned. The two remaining halogen mass-dependent bands in each spectrum, at 219 and 156 cm^{-1} for the chloro-compound, and 151 and 117 for the bromo-compound, are assigned to the two $\nu(HgX)_b$ A_u modes. The separation of the two bridge modes (63 cm^{-1} for the chloro complex and 34 cm^{-1} for the bromo complex), is attributed to the asymmetric nature of the four-membered ring (Section 3.2.1). The Raman spectra of these complexes are more difficult to interpret due to strong bands arising from internal modes of the ligand. However, three halogen mass-dependent bands (at 278(*), 204, 168(*) cm^{-1} for the chloro complex and 198/194, 154 and 124 cm^{-1} for the bromo complex) may be assigned in each case, as the $\nu(HgX)_t$ and the two $\nu(HgX)_b$ modes, respectively.

* - denotes a band which has some contribution from an internal mode of the ligand.

Figure 3.1a.

Far infrared spectra (ca.30K) of $(TPP)HgX_2$ (X=Cl or Br) (cm^{-1})

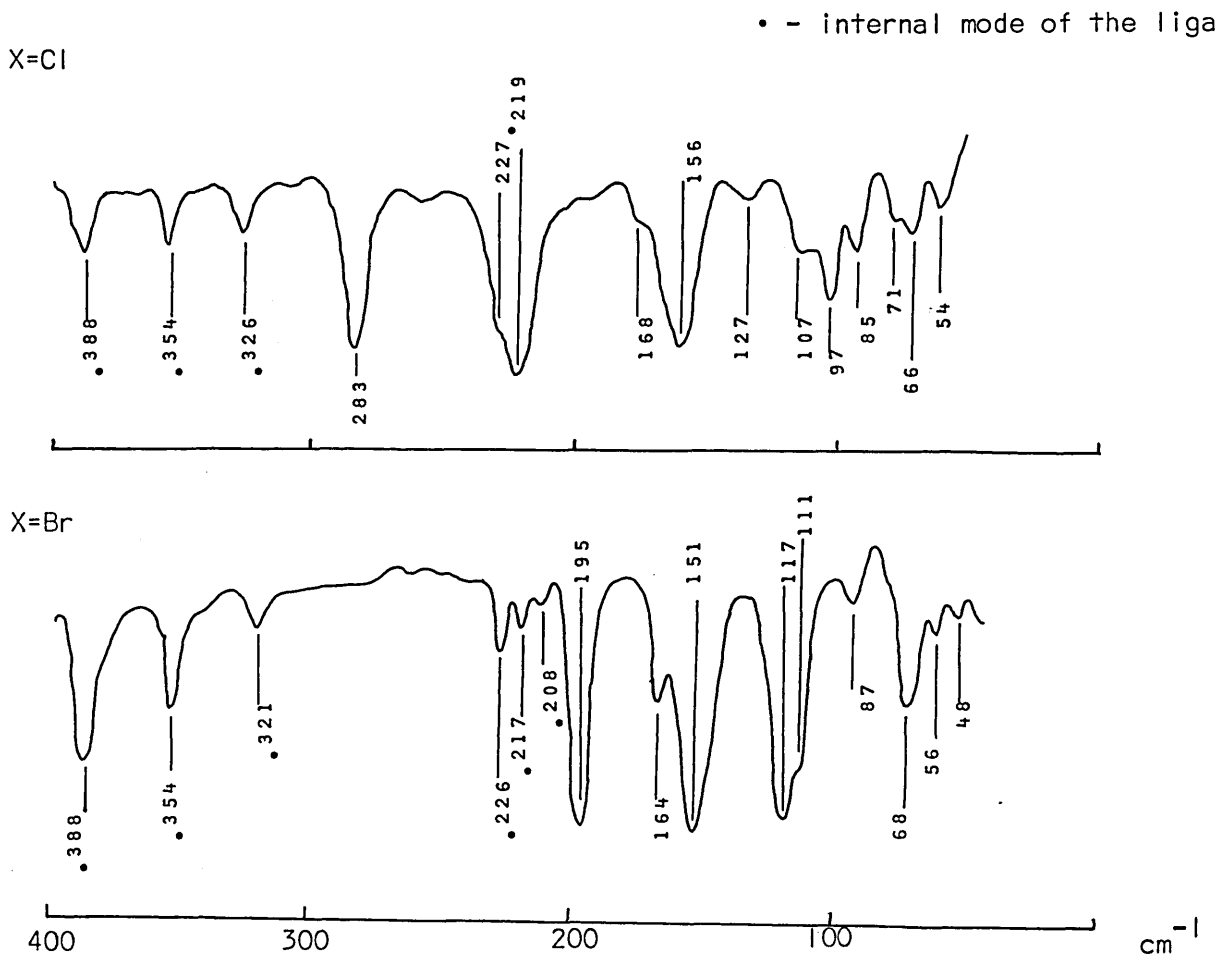

Figure 3.1b.

Raman spectra (RT) of $(TPP)HgX_2$ (X=Cl or Br) (cm^{-1})

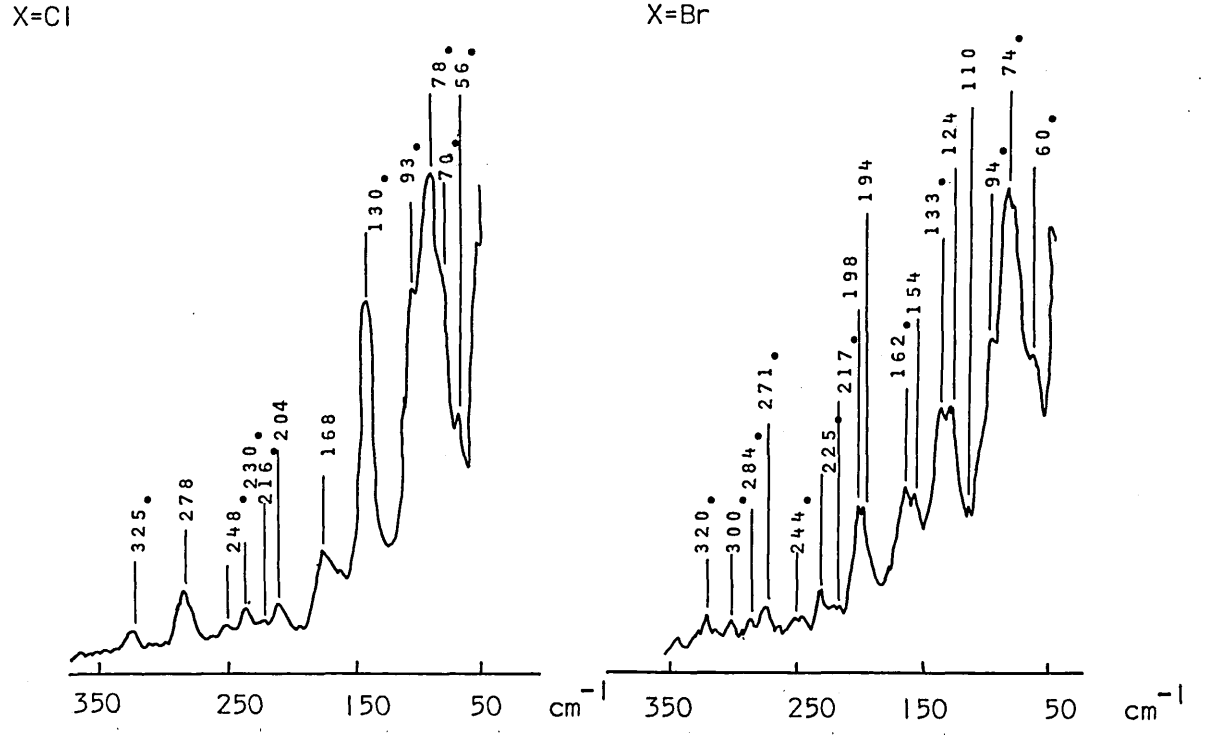

Table 3.3.

Vibrational assignments[a] for $(TPP)HgX_2$ (X=Cl or Br)

Cl		Br		
IR[b]	Ra[c]	IR[b]	Ra[c]	Assignments
283s		195s		$\nu_{as}(HgX)_t$ A_u
	278m[d]		198m 194m	$\nu_s(HgX)_t$ A_g
219s		151s		$\nu(HgX)_b$ A_u
	204mw		154m	$\nu(HgX)_b$ A_g
156s		117s		$\nu(HgX)_b$ A_u
	168m[d]		124s	$\nu(HgX)_b$ A_g
168sh		164mw		$\nu_{as}(HgP)$ A_u (tentative)
				$\nu_s(HgP)$ A_g
127w		111sh	110w	Bending and lattice[e] modes
107sh		87w		
97m		68m		
85mw		56w		
71w		48w		
66mw				
54w				

a - Omitting internal modes of the ligand

b - recorded at room temperature

c - recorded at ca. 30K

d - denotes a band which has some contribution from an internal mode of the ligand

e - bending and lattice modes in the Ra spectra are 'masked' by internal modes of the ligand

The shoulder at 168 cm^{-1} and the medium-weak resolved shoulder at 164 cm^{-1} in the chloro and bromo complexes respectively are tentatively assigned as ν(HgP). This is the region where ν(HgP) modes associated with 'tetrahedrally' coordinated Hg-P bonds are expected to occur (Section 3.2.2).

(b) $(PPh_3)HgX_2$ (X=Cl, Br or I). The crystal structure of the chloro complex has been determined (Section 3.1). The structure consists of discrete dimers; the four-membered ring has a centre of symmetry and bridge bonds are of almost equal length (2.62 and 2.66 Å). The PPh_3 ligands are mutually trans and mercury lies in a distorted tetrahedral environment. Two of these molecules crystallize in a monoclinic system, space group $P2_1/n$ ($\equiv P2_1/c$). The symmetry of the isolated molecules is very close to C_{2h} (actually C_i).

Preliminary photographs indicate that the bromo and iodo complexes are isomorphous and probably isostructural with the chloride.

The positions of the bands observed in the room temperature far-infrared spectra of all three complexes recorded here are in agreement with those reported by previous workers,[5,7,8] but some assignments made in the present work are different. Because low temperature far-infrared spectra, and for the first time room temperature Raman spectra, have been recorded in the present work a more detailed assignment has been attempted which takes into account correlation effects.

Using a simple point group treatment (assuming C_{2h} symmetry and taking PPh_3 as a point mass) one may predict the internal modes of vibration (3N-6) of the dimer:-

$$\Gamma_{int} = 6A_g(Ra) + 3B_g(Ra) + 3A_u(IR) + 6B_u(IR)$$

Internal modes associated with ν(HgP) and ν(HgX) are:-

$$\Gamma\ \nu(HgP) = A_g(Ra + B_u(IR)$$

$$\Gamma\ \nu(HgCl)_t = A_g(Ra) + B_u(IR)$$

$$\Gamma\ \nu(HgX)_b = A_g(Ra) + B_g(Ra) + A_u(IR) + B_u(IR)$$

Allowing for correlation effects and lattice modes the total number of vibrational modes for the primitive cell are:- (Appendix 4)

$$\Gamma_{Total} = 12A_g(Ra) + 12B_g(Ra) + 12A_u(IR) + 12B_u(IR)$$

The number of internal modes of the dimers are:-

$$\Gamma_{int} = 9A_g(Ra) + 9B_g(Ra) + 9A_u(IR) + 9B_u(IR)$$

Internal modes associated with ν(HgP) and ν(HgX) are:-

$$\Gamma\nu(HgP) = A_g(Ra) + B_g(Ra) + A_u(IR) + B_u(IR)$$

$$\Gamma\nu(HgX) = A_g(Ra) + B_g(Ra) + A_u(IR) + B_u(IR)$$

$$\Gamma\nu(HgX)_b = 2A_g(Ra) + 2B_g(Ra) + 2A_u(IR) + 2B_u(IR)$$

The correlation diagram (Table 3.4a) indicates how the internal modes of the crystal are derived from the internal modes of the isolated molecule. Each Raman- or infrared-active internal mode of the molecule splits into two components in the crystal, one IR-active (arising from out-of-phase coupling) and the other Ra-active (arising from in-phase coupling).

Thus two $\nu(HgX)_t$ and four $\nu(HgX)_b$ modes active in IR and Ra spectra are predicted.* The vibrational spectra are shown in Figures 3.2a and 3.2b, and Table 3.4b contains wavenumber positions and vibrational assignments. The assignments made are based upon the criteria presented in Section 3.2.1. Equation (1) is expected to be more applicable for the present series of $(PPh_3)HgX_2$ complexes, in the sequence chloro, bromo and iodo, respectively.

The effect of correlation coupling is expected to be relatively weak, and indeed is often not observed. The internal modes due to the PPh_3 ligand have been eliminated from the vibrational spectra of all three complexes using conventional methods. The band at 291 cm^{-1} (IR) and the bands at 288 (IR) and 286 (Ra) cm^{-1} for the chloro complex can quite definitely be assigned $\nu_{as}(HgCl)_t$ and $\nu_s(HgCl)_t$ respectively. These assignments are essentially

* - mutually exclusive

Table 3.4a

Correlation diagram for point and factor group symmetry for $[(PPh_3)HgX_2]_2$ (X=Cl or I)

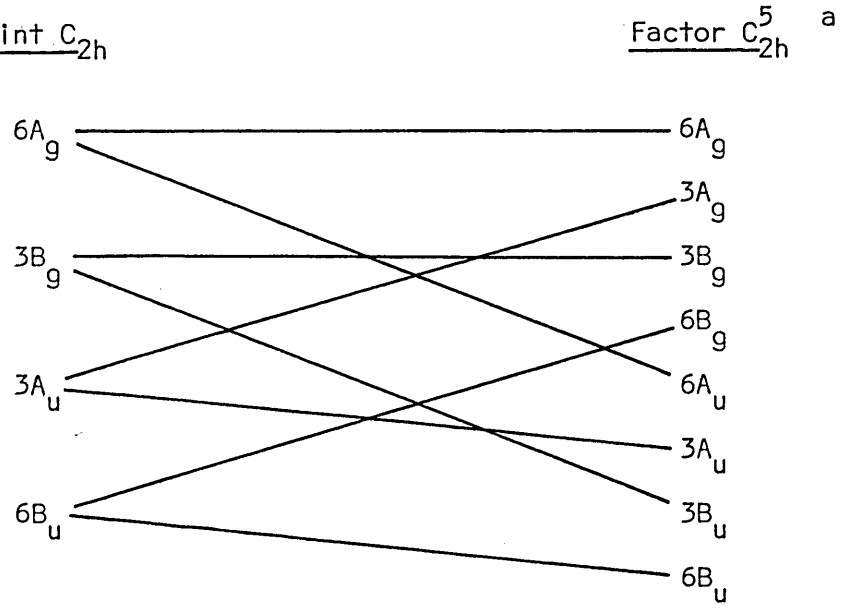

a - only internal modes are included.

Figure 3.2a.

Far infrared spectra (ca. 30K) of $(PPh_3)HgX_2$ (X=Cl, Br or I) (cm^{-1})

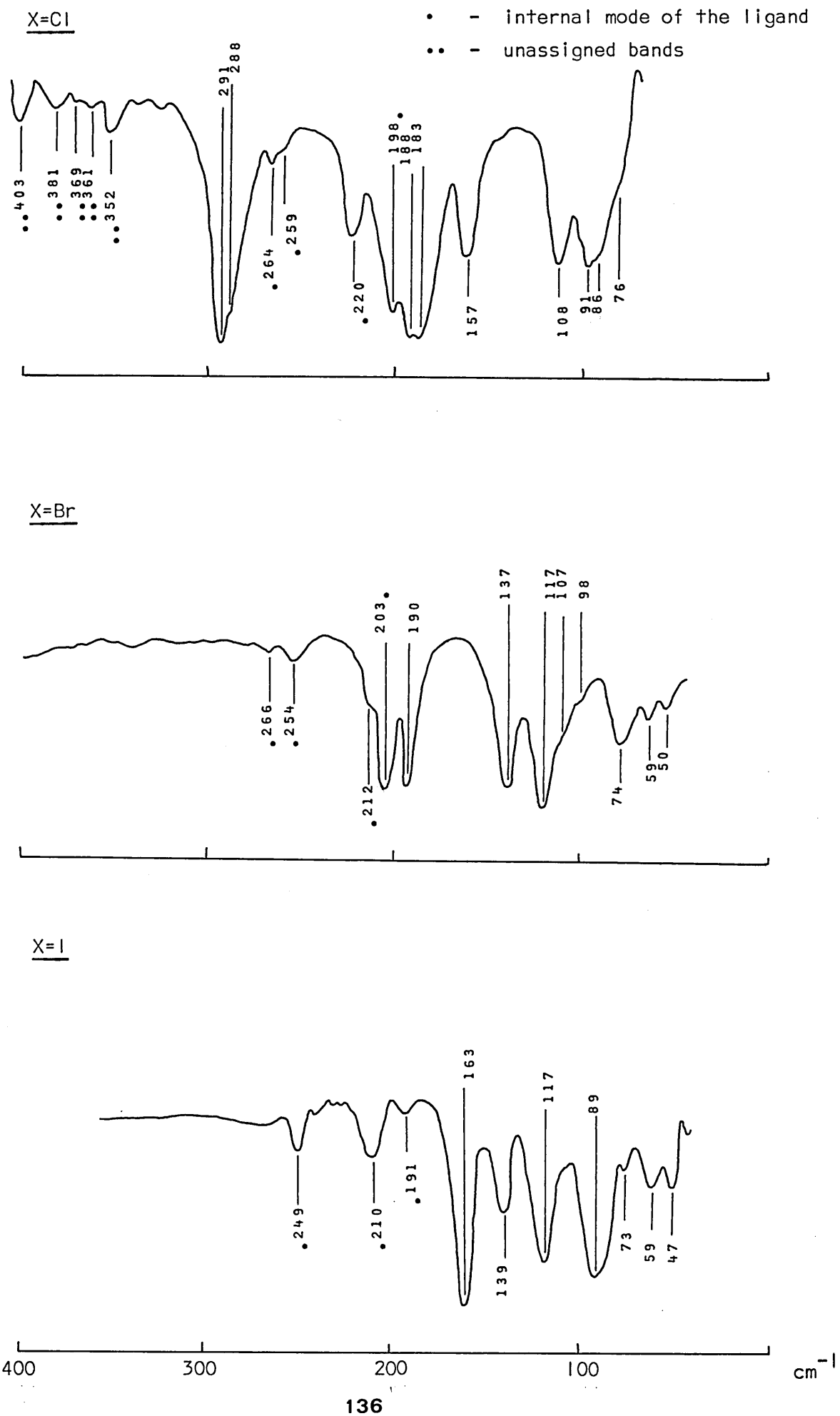

Raman spectra (RT) of $(PPh_3)HgX_2$ (X=Cl, Br or I) (cm^{-1})

• - internal mode of the ligand

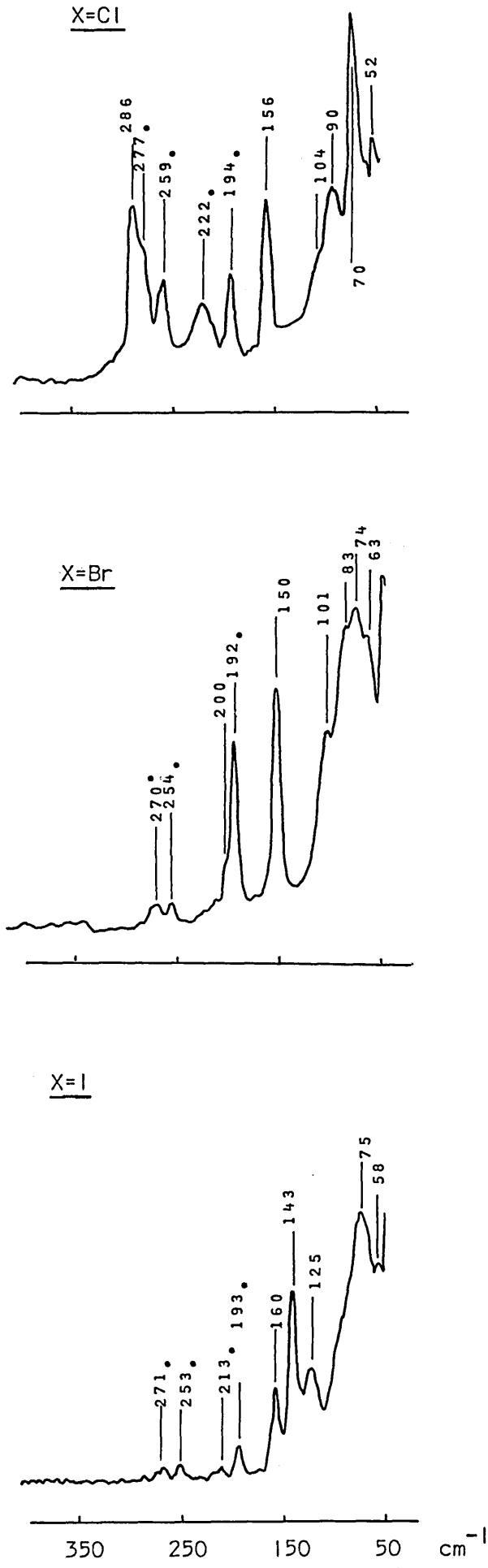

Table 3.4b

Vibrational assignments[a] for $(PPh_3)HgX_2$ (X=Cl, Br or I)

Cl		Br		I		Assignments	
IR[b]	Ra[c]	IR[b]	Ra[c]	IR[b]	Ra[c]	IR	Ra
291s		203s[a]	200sh	163s	160m	$\nu_{as}(HgX)_t$ B_u	$\nu_{as}(HgX)_t$ B_g
288sh	286s	190s	192s[a]	139m	143s	$\nu_s(HgX)_t$ A_u	$\nu_s(HgX)_t$ A_g
188s		137s		117s		$\nu(HgX)_b$ A_u	$\nu(HgX)_b$ A_g
			150s		125ms	$\nu(HgX)_b$ B_u	$\nu(HgX)_b$ B_g
183s		117s		89s		$\nu(HgX)_b$ B_u	$\nu(HgX)_b$ B_g
						$\nu(HgX)_b$ A_u	$\nu(HgX)_b$ A_g
157m		137s		139m		$?\nu_{as}(HgP)$ B_u	$?\nu_{as}(HgP)$ B_g
	156s		150s		143a	$?\ \nu_s(HgP)$ A_u	$?\ \nu_s(HgP)$ A_g
108m	104sh	107sh	101sh	73vw	75s		
91m	90s	98sh	84sh	59w	58s		
86sh	70s	74m	74s	47w		Bending and lattice modes etc.	
76sh	52m	59w	63sh				
		50w					

a - omitting internal modes of the ligand

b - recorded at ca. 30K

c - recorded at room temperature

in agreement with previous work.[5,7,8] The bands at 188 (IR) and 183 cm^{-1} (IR) are assigned to each of the individual IR-active $\nu(HgCl)_b$ modes (which originate from the two $\nu(HgCl)_b$ modes of the isolated molecule), the small wavenumber separation between these modes being consistent with an almost symmetric four-membered ring. These assignments, in detail, are at variance with those of previous workers[7,8] (Section 1.4.2, Table 1.5). Unfortunately it was not possible to locate $\nu(HgCl)_b$ modes in the corresponding Raman spectrum because of 'masking' by the internal modes of the ligand. The medium intense band at 157 (IR) and the strong band 156 (Ra) cm^{-1} are tentatively assigned $\nu(HgP)$, by comparison with the $\nu(HgP)$ data reported by Alyea *et al.*[97] for the analogous PBu^t_3 and $P(o\text{-tolyl})_3$ complexes, and are in agreement with the work of Deacon *et al.*[7] Finally, it is worthy to note that the $\nu(HgCl)$ assignments made here agree well with those reported for some related $[Hg_2Cl_6]^{2-}$ hexachlorodimercurate(II) salts.[96]

For $(PPh_3)HgBr_2$ the bands at 203 (IR)/200 (Ra) cm^{-1} and 190 (IR)/192 (Ra) cm^{-1} are assigned $\nu_a(HgBr)_t$ and $\nu_s(HgBr)_t$ respectively; however, it is likely that the bands at 203 (IR) and 192 (Ra) cm^{-1} contain some contribution from internal ligand modes. These assignments are essentially in agreement with those of Deacon *et al.*[7] Bands arising from one of the $\nu(HgBr)_b$ modes (which originate from the isolated molecule) have been assigned at 137 (IR) and 150 (Ra), but, because it is this region where $\nu(HgP)$ modes are also expected, some contribution from $\nu(HgP)$ is a possibility. The band at 117 (IR) cm^{-1} is also in a position reasonably attributable to $\nu(HgBr)_b$, and as such is assigned as the second IR-active $\nu(HgBr)_b$ mode (which originates from the isolated molecule). These assignments differ from those of Deacon *et al.*[7] only in that it is preferred to assign the bands at 137 (IR) and 117 (IR) cm^{-1} to individual $\nu(HgBr)_b$ modes rather than to a single $\nu(HgBr)_b$ mode [with the second $\nu(HgBr)_b$ mode at *ca.* 60 cm^{-1}].

Considering the spectra of the iodo complex, the bands at 163 (IR) and 160 (Ra) cm^{-1} are assigned $\nu_{as}(HgI)_t$ whereas the bands at 139 (IR) and 143 (Ra) cm^{-1} are assigned $\nu_s(HgI)_t$. This increased separation between antisymmetric and symmetric terminal modes from chloro through to iodo complexes is found, in the present work, to be a common phenomenon. It may also be expected that ν(HgP) modes will lie at ca. 140 cm^{-1}, so there is a possibility that the bands at 139 (IR) and 143 (Ra) cm^{-1} contain some contribution from ν(HgP) modes. The bands at 117 (IR) and 125 (Ra) cm^{-1} are almost certainly one set of $\nu(HgI)_b$ modes. There are no other bands in the Raman spectrum which immediately suggest that they may have arisen from the other Raman-active $\nu(HgI)_b$ mode, but the strong band at 89 cm^{-1} in the IR spectrum may possibly be the second IR-active $\nu(HgI)_b$ mode. Bands at comparable wavenumber positions have been assigned as $\nu(HgI)_b$ modes in the related $[Hg_2I_6]^{2-}$ species.[96] The assignments made here for ν(HgI) are similar to those of Deacon et al.[7], except that in the present work it is preferred to assign the bands at 117 and 89 cm^{-1} to individual IR-active $\nu(HgI)_b$ modes rather than to a single $\nu(HgI)_b$ mode [with the second $\nu(HgI)_b$ mode at 50 cm^{-1}].[7]

Finally one may note an outstanding feature of the Raman spectra of these complexes, in that the scattering ability of ν(HgX) modes is considerably dependent upon X and increases from X=Cl→Br→I. An artefact of this phenomenon is that internal modes of the ligand appear stronger in the spectra of these complexes as X changes in the sequence I→Br→Cl, because increased detector amplification has had to be used to observe these weaker scattering ν(HgX) modes. This phenomenon will be shown to be general for all the remaining $(PR_3)HgX_2$ complexes studied in this work.

(c) $(PEt_3)HgX_2$ (X=Cl, Br or I). The structure of the chloro complex may be described as a polymeric chain (Section 3.1). Mercury lies in a distorted trigonal bipyramidal environment with two short Hg-Cl contacts

(2.42 and 2.56 Å), a short Hg-P contact of 2.35 Å and two longer Hg-Cl contacts of 3.04 and 3.21 Å joining the '$PHgCl_2$ units' at either end. These chains are present in a monoclinic system, space group $P2_1/c$ (C_{2h}^5, No. 14).[112] The similarity of the patterns in the vibrational spectra indicate that the bromo and chloro complexes are isostructural, whereas the iodo complex may be of some different structure. Therefore, the spectra of the chloro and bromo complexes will be treated separately from those of the iodo complex. Examination of the spectra of the chloro and bromo analogues suggested that a simple line group C_i treatment would be adequate for full assignment of ν(HgX) modes (Appendix 4).

The number and activity of the internal modes of a single chain (taking PEt_3 as a point mass) is:-

$$\Gamma_{chain} = 11A_g(Ra) + 9A_u(IR)$$

while the number and activity of modes associated with ν(HgX) modes is:-

$$\Gamma\nu(HgX) = 4A_g(Ra) + 4A_u(IR)$$

Approximate forms of motion of each of these eight ν(HgX) modes have been derived by use of character tables[134] (Figure 3.3a).

As there are no terminal Hg-X bonds as such in this structure, all modes are denoted $\nu(HgX)_b$. The higher wavenumber bands observed in the spectra will be assigned to the modes associated with movement of the shorter bonds in the chain.

Vibrational spectra are shown in Figures 3.3b and 3.3c, while Table 3.5 contains wavenumber positions and vibrational assignments. Internal modes of PEt_3 have been eliminated using data reported by Green[142] for the free ligand and by comparison of the spectra of all three complexes. As noted by Allen and Wilkinson[141] in their studies on $(PR_3)_2NiX_2$ complexes, modes which were IR-active or Raman-active in the free ligand become both IR- and Raman-active on complexation, and a similar phenomenon is observed in the present case. The two pairs of $\nu(HgX)_b$ modes associated with vibration of the

Far infrared spectra (ca.30K) of $(PEt_3)HgX_2$ (X=Cl, Br or I) (cm^{-1})

X=Cl

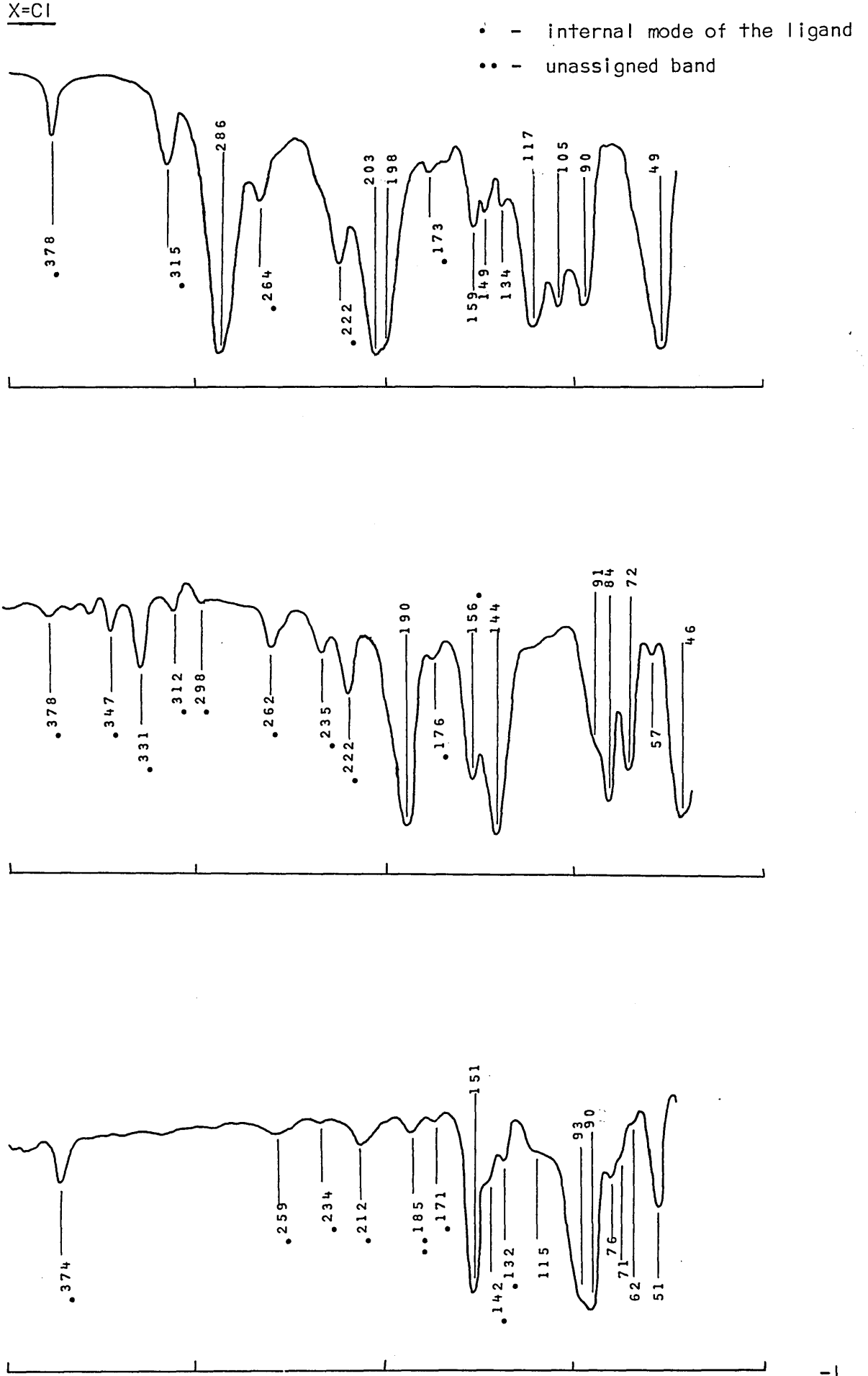

Figure 3.3c. Raman spectra (RT) of $AlEt_3/InX_2$ (X=Cl, Br or I) (cm^{-1})

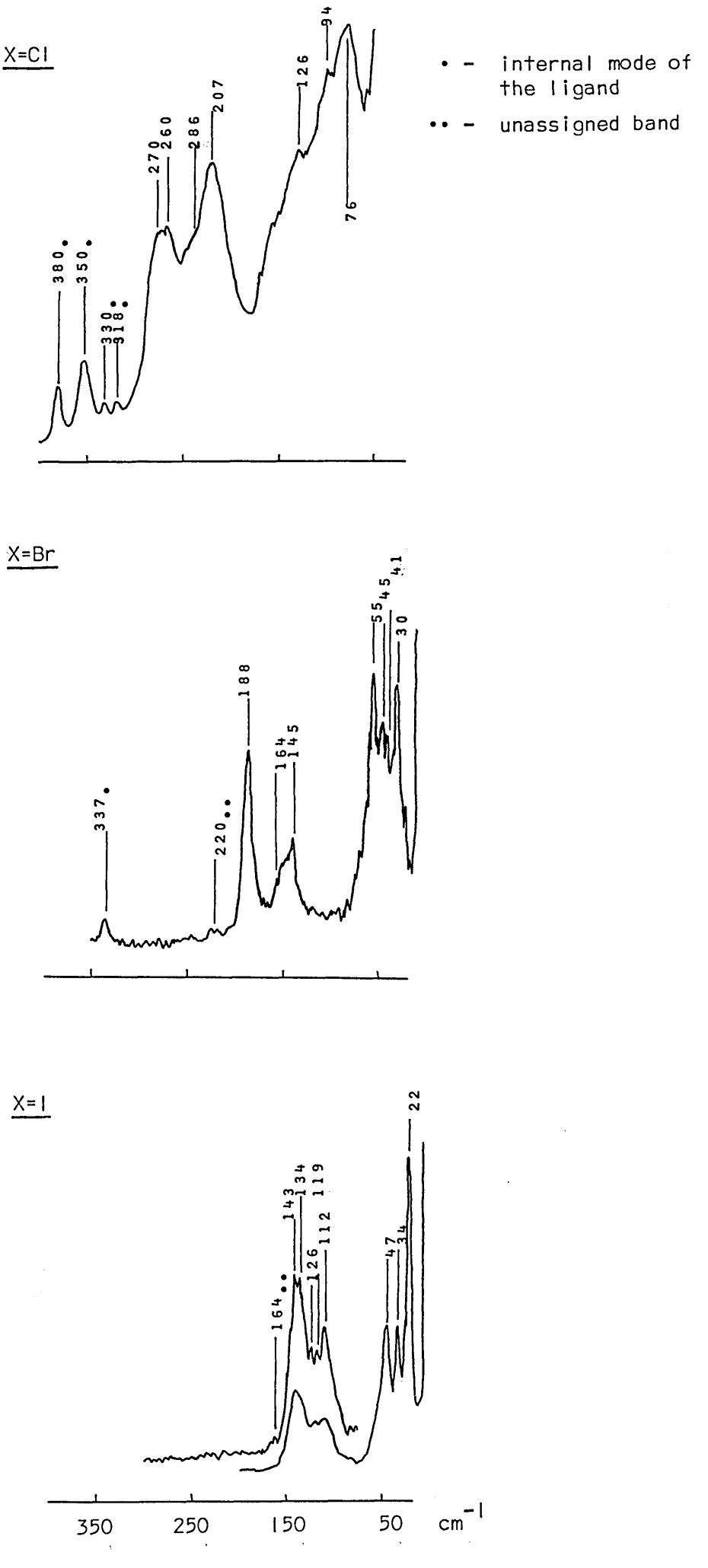

Table 3.5.

Vibrational assignments9 for (PEt^)HgX^ (X=C|, Br or I).

Cl		Br		Ib		
IRd	Ra6	1Rd	Rae	IR	Ra	Assi gnments0
				I85w	164w	
286s		190s		151		v 2 (HgX)b Au
	270s| 260s J		185		I43s| 134sj	v 1 (HgX)b Ag
203s | 198sh J		144s				v 6 <HgX)b Au
	207s		164sh J 145m J			^ 2 (HgX) b Ag
1I7s| 105s J		91 sh| 84s J		93shj 90s J		V7 (HgX)b Au
	126sh				1 12m	?V3 (H9X)b Ag
90s		72ms				(HgX)b Au
	94sh| 76vs|					?v4 (H9X)b Ag
49s	76vs	57w	55s	1 15sh	47m	\
		46s	45s	76w	34m	4
			4 1s	7 1sh	22vs	[Bending and lattice
			30s	62sh		Imodes etc.
				51 m		

a - omitting internal modes of the ligand

b see text

c - numbering of modes refers to Figure 3.3a.

d - recorded at ca. 30K

e - recorded at room temperature

? tentative assignment

shorter Hg-X bonds are easily assigned in both IR and Raman spectra of the chloro and bromo complexes. The modes associated with the longer Hg-X bonds are again quite readily located in the IR spectra of both compounds. However, the Raman spectra show little evidence of these modes except perhaps for the shoulders at 126 and 94 cm^{-1} and the strong band at 76 cm^{-1} in the Raman spectrum of the chloro complex. It would appear therefore that the IR spectrum is a better probe for locating these longer Hg-X interactions.

Assignments presented in Table 3.5 do not refer to the iodo complex, as this complex appears to have some different structure. Using wavenumber position as a guideline the bands at 143 (Ra), 134 (Ra) cm^{-1} and 151 (IR) cm^{-1} may be assigned to some form of ν(HgI) mode associated with relatively short Hg-I bonds. Similarly the bands at 112 (Ra) cm^{-1} and 93 (IR), 90 (IR) cm^{-1} are attributed to some form of ν(HgI) associated with relatively long Hg-I contacts. No structural inference can be made.

There are no bands in the spectra of any of the three complexes which immediately suggest they may have arisen from ν(HgP), so no ν(HgP) modes have been assigned.

(d) $\underline{(PMe_3)HgX_2\ (X=Cl,\ Br\ or\ I)}$. The structure of $(PMe_3)HgCl_2$ (Section 3.1) is essentially ionic, consisting of continuous zig-zag chains of alternating $[Cl\text{-}Hg\text{-}PMe_3]^+$ and Cl^- ions. These ions are present in a triclinic system, space group $P\bar{1}$ (C_i, No. 2).[112] Preliminary photographs show the bromo analogue to be isomorphous and most probably isostructural, whereas similar studies indicate the iodo complex is definitely not isomorphous and probably not isostructural. Consequently the spectra of the chloro and bromo complexes are discussed separately.

For an 'ionic' structure as found for chloro and bromo analogues, full unit cell group analysis is required (Appendix 4). The internal modes of the two cations in the unit cell (taking PMe_3 as a point mass) are:-

$$\Gamma_{int} = 3A_g(Ra) + 3A_u(IR)$$

and for internal modes due to ν(HgX) and ν(HgP):-

$$\Gamma\nu(HgX)_t = A_g(Ra) + A_u(IR)$$

$$\Gamma\nu(HgP) = A_g(Ra) + A_u(IR)$$

One may also predict the number and activity of the cation and anion translations within the unit cell to be:-

$$\Gamma_{ionic\ trans.} = 6A_g(Ra) + 3A_u(IR)$$

The experimental data are shown in Figures 3.4a and 3.4b and Table 3.6. The internal modes of the PMe_3 ligand have been eliminated by the use of data reported by Goggin *et al.*[106] for related $[X\text{-}Hg\text{-}PMe_3]^+$ ions and by comparison of spectra of the three complexes in question. The highest wavenumber halogen mass-dependent bands at 300 (IR) and 291 (Ra) cm^{-1} for the chloro complex, and at 216 (IR) and 208/193 (Ra) cm^{-1} for the bromo complex, are assigned to $\nu(HgX)_t$ modes. There is a possibility that the Ra-active $\nu(HgBr)_t$ bands at 208 and 193 cm^{-1} contain some contribution from the PC_3 symmetric deformation mode of PMe_3. The weak bands occuring at *ca.* 350-360 cm^{-1} in the IR and Ra spectra of both complexes are assigned to ν(HgP) on the basis of arguments already presented (Section 3.2.2).

Some of the assignments made in the present work are at variance to those of Schmidbaur *et al.*[4] For example, the band at 178 (Ra) cm^{-1} in the spectrum of the chloro complex is assigned as a PC_3 rocking mode in the present work, but as ν(HgCl) previously[4] (presumably a bridge mode). The bands at 168 (Ra) and 193 (Ra) cm^{-1} for the bromo complex now assigned as a PC_3 rocking mode and ν(HgBr) respectively are in reverse to the assignments made by Schmidbaur *et al.*[4] In view of the structural data available in the present work, and by comparison with the detailed assignments of Goggin *et al.*[106] for the related $[X\text{-}Hg\text{-}PMe_3]^+$ species, the present assignments are more justified and more consistent.

Figure 5.4a.

Far infrared spectra (ca. 30K) of $(PMe_3)HgX_2$ (X=Cl, Br or I) (cm^{-1})

X=Cl

• - internal mode of the ligand

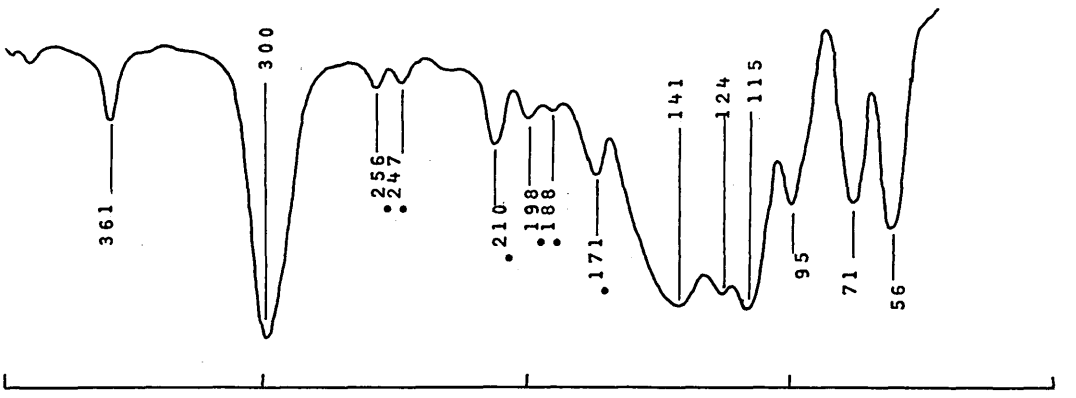

X=Br

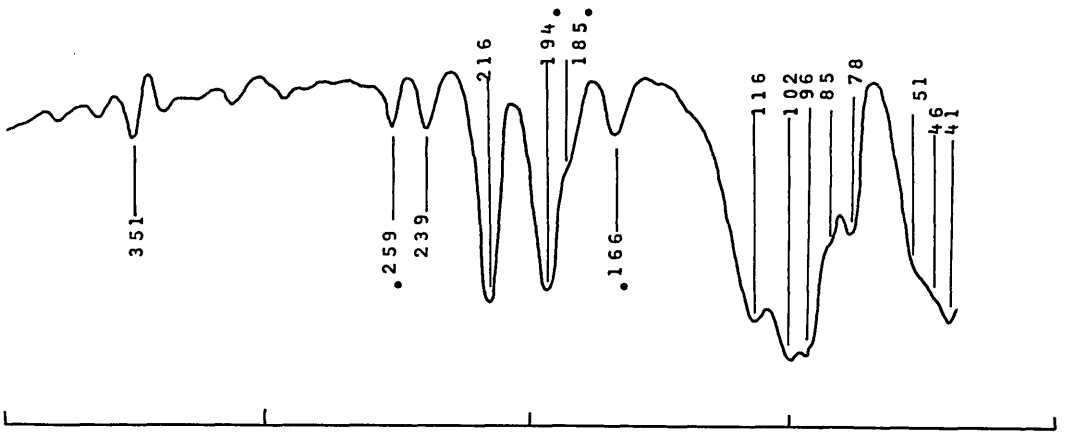

X=I

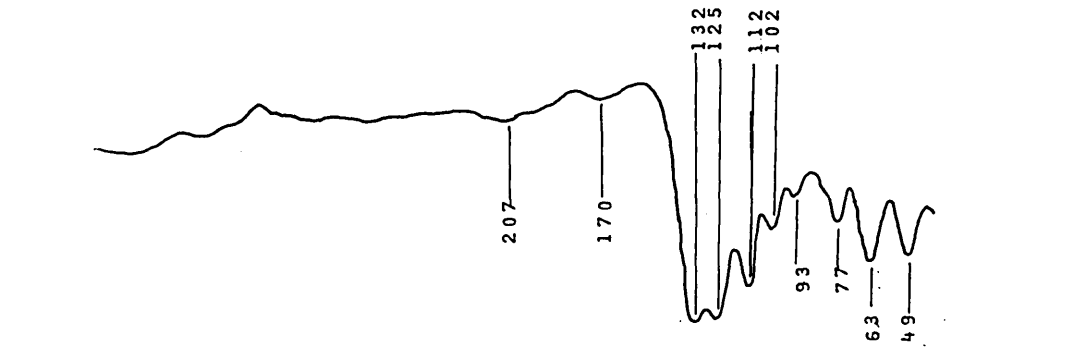

400 300 200 100 cm^{-1}

Raman spectra (RT) of $(PMe_3)HgX_2$ (X=Cl, Br or I) (cm^{-1})

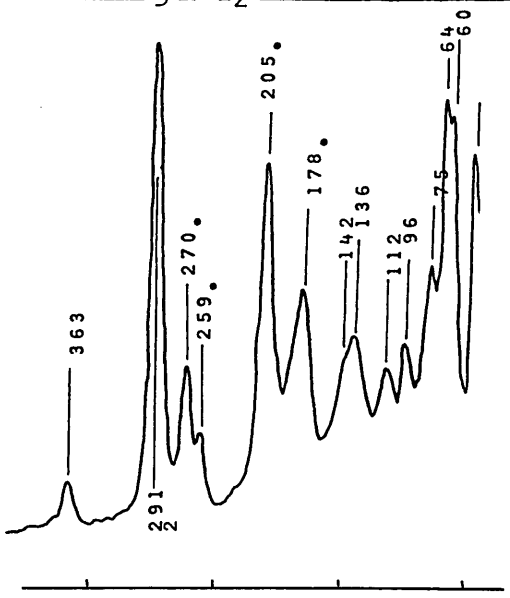

Table 3.6.

Vibrational assignments for $(PMe_3)_2HgX_2$ (X=Cl, Br or I)

Cl		Br		I		
IRb	RaC	1Rb	RaC	,Rb	RaC	Assignments
361 mw		35 lw				$\nu_{as}(HgP)$ A_u
	363w		354w			$\nu_{s}(HgP)$ A_g
300s		216s		132s		$\nu_{as}(HgX)$, A_u
	291s		208sh) 193s)	123s	123s	$\nu_{s}(HgX)$, A_g
141s,br	l42sh	116s	106m,br	112s	40s	Cation and anion translations, bending and other lattice modes
124s	136m	102s	86w,br	102mw		
115s	112m	96s	69m	93w		
95ms	96m	86sh	58m	77mw		
71 ms	75ms	78ms	48m	63m		
56ms	64s	51 sh		49m		
	60s	41 s				
						Ligand modes
	270m) 259w)	254w) 239w)	267vw) 260vw)			PC^ asymmetric def.
210m	205s	194s	208sh) 193s)	207vw		PC^ symmetric def.
171 m	178ms	166w	168ms	170vw	186vw	PC^ rock

a - see text

b - recorded at aa. 30K

c - recorded at room temperature

Because of the complicated nature of the spectra in the region of cation and anion translations no attempt has been made to assign each of the three IR-active and six Ra-active modes individually.

It should be mentioned at this point that the bands assigned to these ion translations are of comparable wavenumber to bands previously assigned asvOHgX)^. This is not surprising when one examines the bond lengths of the structures in question. It should be realized that, in some cases, one has a choice concerning the description of a structure. In the present instance the 'ionic' description is preferred in place of a bridged polymeric description because of the considerable distance (ca_.2.8 A) from the [Cl-Hg-PMe^] species to the next chlorine atom.

Assignments made in Table 3.6 do not refer to the (PMe^Hg^ complex; as already mentioned this compound appears to have a different structure to its other halo analogues. The Raman spectrum is extremely simple containing one very strong band at 123 cm ' and another medium strong band at 40 cm *. The IR spectrum is more complicated with two strong bands at 132, 123 cm * and a continuation of medium to medium-strong bands appearing from 112-49 cm *. It is interesting to note that the rather low wavenumber position of the highest wavenumber bands observed in both these spectra are close to those assigned to v(HgI) in the tetrahedral [HgI^3 2- ion contained in [NEt^^HgI^ [96] and also the [HgI^I species contained in [SMe^IHgI^. [96] One may tentatively propose, therefore, that similar [HgI 2- or 'monomeric (PMe^JHg^ 1 species are present in the (PMe^JHgI^ complex. The origin of the remaining bands in the IR spectrum is difficult to assess. There is no compelling evidence for the existence of v(HgP) modes in either IR or Ra spectra and so no such modes could be assigned. Finally, it should be mentioned that the phenomenon of large variation in intensity of internal ligand modes in the Raman spectra in the sequence Cl-»-Br-^I is outstandingly apparent in these series.

(e) (PBu^)HgX^ (X=Cl, Br or I). A te+rameric structure has been found for the a~(PBu^)$HgCl_2$ complex. This tetramer consists of two identical non-centrosymmetric dimers related by a centre of symmetry and joined via a very long mercury-chlorine contact of ca. 3.4 Å (Section 3.1). These tetramers crystallize in a monoclinic system, space group P2(/n (EP2j/c). Preliminary photographs indicate the bromo and iodo complexes are isomorphous with one another but not with a"(PBu^)HgCl2. The very similar patterns of the vibrational spectra, especially IR spectra, however, suggest that all three compounds may still be isostructural. Whilst this work was in progress, Kessler[90] reported the existence of a different form of the chloro complex, hereinafter referred to as 3"(PBu^)$HgCl_2$*. The room temperature spectra of the bromo and iodo complexes prepared in this work are in complete agreement with those of Kessler[90] indicating that they are in fact the same compounds. The complexes prepared in the present work shall be discussed initially.

Examination of the vibrational spectra suggest that a simple point group analysis is adequate (Appendix 4). The number and activity of the internal modes of the tetramer (taking PBu^ as a point mass) are:-

$$\Gamma_{int} = 21A_g(Ra) + 21A_u(IR)$$

For the internal modes solely associated with v(HgX):-

$$Tv(HgX)_t = A_g(Ra) + A_u(IR)$$

and

$$Tv(HgX)b = 6Ag(Ra) + 6Ay(IR)$$

whi le

$$Tv(HgP) = 2Ag(Ra) + 2Ay(IR)$$

* This complex was prepared in a similar manner to cr(PBu^)HgCl2. However, mixture of the stoicheiometric proportions of PBu^ and $HgCl_2$ was carried out to completion, and the complex was precipitated from the reaction mixture by addition of ether. Further details may be found in reference 90.

The prediction for ν(HgX) modes corresponds to one IR- and Ra-active pair for each distinct Hg-Cl bond. To a first approximation therefore the wavenumber values of these modes might well be expected to relate to the bond lengths involved during vibration, and assignments have been made on this basis.

The data are summarized in Figures 3.5a and 3.5b and Table 3.7. The low intensity internal modes of PBu^n_3 do not appear to cause any problems in spectral interpretation. The halogen mass-dependence of the spectra is striking especially for the IR spectra of chloro and bromo compounds. The wavenumber positions of the modes in both the IR and Raman spectra of all three complexes seem to mirror one another, which suggests the forms of motion of each IR/Ra-active pair are energetically very similar. The higher wavenumber modes in the IR and Ra spectra of all three complexes are readily assigned. However, due to the complexity of the spectra in the lower wavenumber regions (less than ca.140, 110 and 90 cm^{-1} for chloro, bromo and iodo complexes respectively), no further definite assignments can be made.

Although the appearance of the vibrational spectra of the bromo and iodo complexes are similar to those reported by Kessler,[90] the vibrational assignments made here are markedly different. This may be explained by the fact that Kessler[90] approached assignment from the view that these complexes were dimeric in the solid state. Kessler[90] has again approached assignment of β-$(PBu^n_3)HgCl_2$ assuming the structure to be dimeric. The far IR-spectrum of Kessler's actual β-$(PBu^n_3)HgCl_2$ sample has also been recorded in this laboratory and is in complete agreement with the spectrum reported by Kessler.[90] By comparison with the spectra of other dimeric structures studied in the present work Kessler's assignments, with which the present author concurs, seem reasonable. There is strong absorption at ca.300 cm^{-1} which may be assigned $\nu(HgCl)_t$ and also strong bands at ca. 173 cm^{-1} and 147 cm^{-1} which

Figure 5.2a.

Far infrared spectra (ca. 30K) of $(PBu^n_3)HgX_2$ (X=Cl, Br or I) (cm^{-1})

X=Cl (α-form)

• - internal mode of the ligand

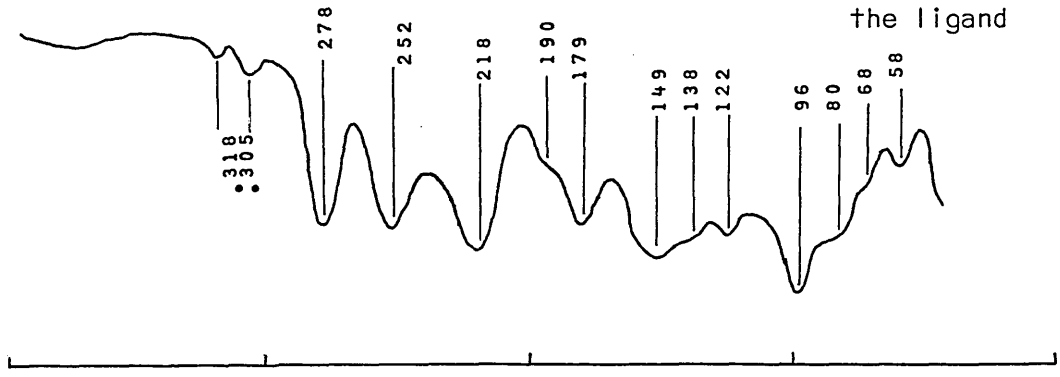

X=Cl (β-form)

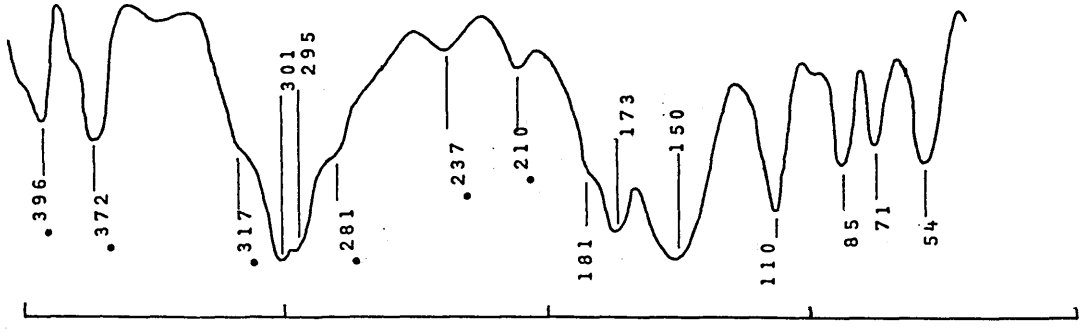

X=Br

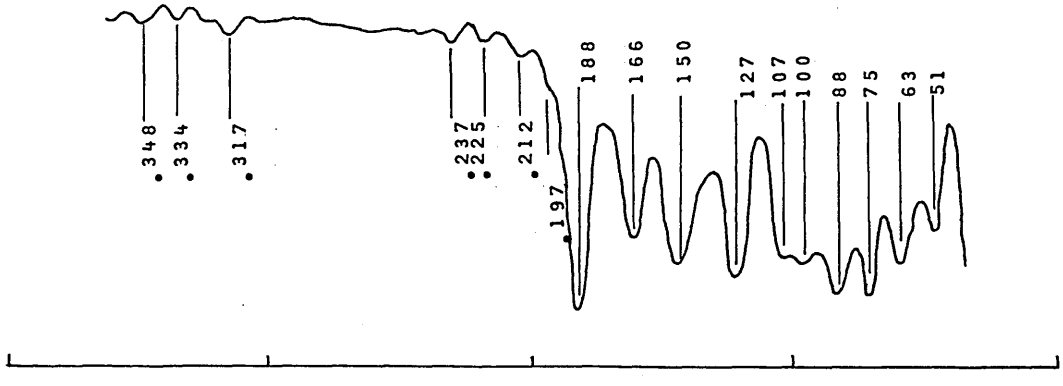

X=I

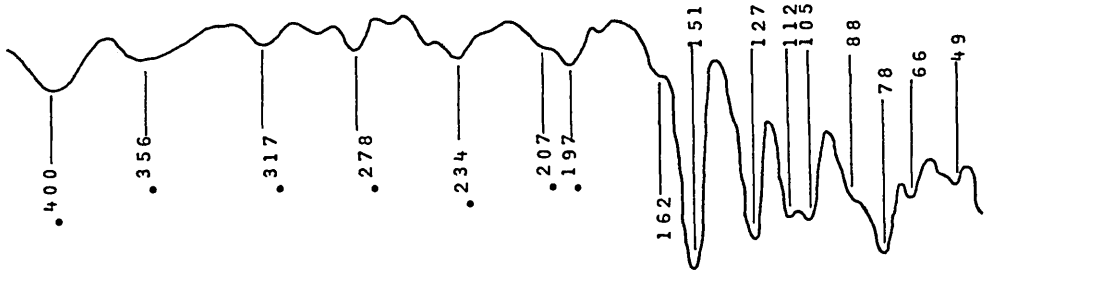

Figure 3.5b.

Raman spectra (RT) of $(PBu^n_3)HgX_2$ (X=Cl, Br or I)

X=α-Cl

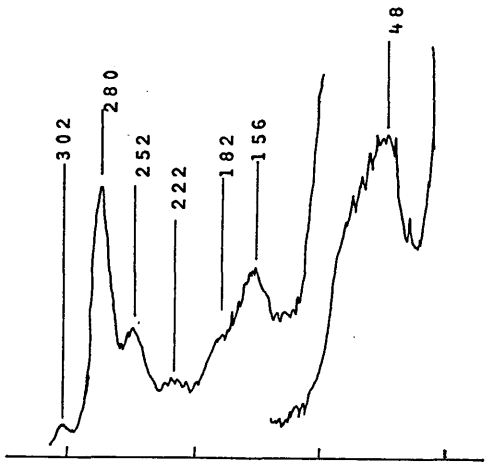

X=Br

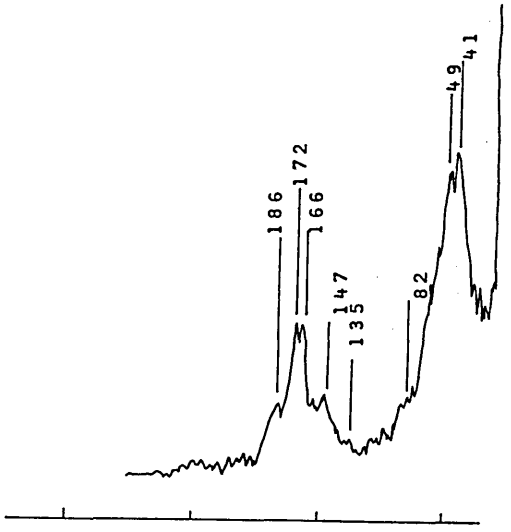

X=I

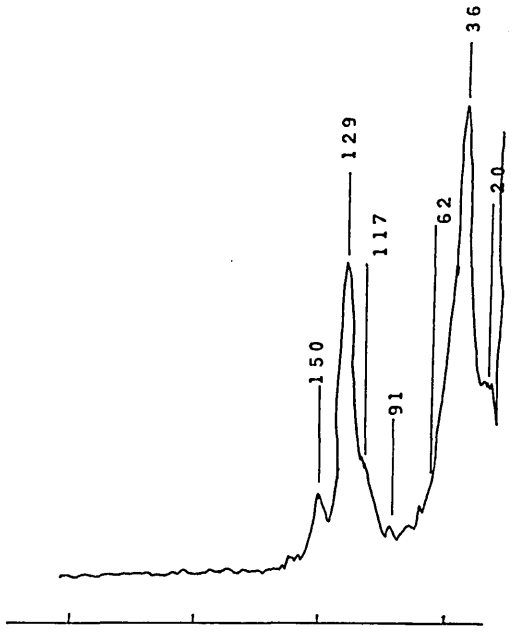

Table 3.7.

Vibrational assignments for $(PBu^n_3)HgX_2$ (X=Cl, Br or I)

Cl[a]		Br		I		
IR[b]	Ra[c]	IR	Ra	IR	Ra	Assignments
278s		188s		151s		$\nu(HgX)_t$ A_u
	280s		186m		150m	$\nu(HgX)_t$ A_g
252s		166s		127s		$\nu(HgX)$ A_u
	252m		172s) 166s)		129s	$\nu(HgX)$ A_g
218s		150s		112s		$\nu(HgX)$ A_u
	222w,br		147m		117sh	$\nu(HgX)$ A_g
179m		127s		105s		$\nu(HgX)$ A_u
	182sh		135vw		91vw	$\nu(HgX)$ A_g
149s,br	156s	107s	82sh	88sh	62sh	$\nu(HgX)$, bending
138sh	150sh	100s	49s	78s	36s	and lattice
122w	48vs,br	88s	41s	66w	20sh	modes
96s		75s		49w		
80sh,br		63ms				
68sh		51m				
58w						

a - α-form (see text)

b - recorded at ca. 30K

c - recorded at room temperature

can be assigned to the two IR-active $\nu(HgCl)_b$ modes. However, because of quite strong absorption below ca. 140 cm^{-1} one cannot rule out the possibility of further association beyond the dimer stage.*

It is interesting to note that the far IR spectra of the α-form (in benzene) and the β-form (in chloroform) suggest that both forms have similar dimeric structures in solution.

Finally it must be recorded that information concerning the presence of ν(HgP) modes was not immediately apparent.

(f) Summary of structure/spectra relationships. At least five separate structures have been shown to exist in the $(PR_3)HgX_2$ series viz. an asymmetric dimer, an almost symmetric dimer, a chain polymer, a tetramer and an 'ionic' chain. Irrespective of the way one wishes to describe these structures and further make vibrational assignments, the vibrational spectra of these complexes, especially IR spectra, show spectral features which are considered to be characteristic of these structures. Raman spectra are not as informative as IR spectra because of more severe interference from internal modes of the ligand.

Spectral features characteristic of molecular structure will be discussed and used for tentative structural proposals concerning other $(PR_3)HgX_2$ complexes.

In the structures of $(PR_3)HgCl_2$ (PR_3=TPP, PPh_3, PBu^n_3, PEt_3 or PMe_3) there is one common structural feature i.e. at least one short Hg-Cl bond. The vibrational spectra reflect this feature in that bands occur at ca. 280-300 cm^{-1} in both IR and Ra spectra arising from some form of ν(HgCl) mode associated with the short Hg-Cl bond (Table 3.8).

Specific structures within the chloro series can only be distinguished by examination of the lower wavenumber regions (ca. 200 cm^{-1} and below) for

* Subsequent experiments, using far-IR spectroscopy, have indicated that α-$(PBu^n_3)HgCl_2$ when recrystallized from the melt is converted, in part at least, to β-$(PBu^n_3)HgCl_2$.

Table 3.8.

ν(HgX) modes associated with 'short' Hg-X bonds

Compound	d(HgX)/Å	IR-active ν_{MAX}(HgX)/cm^{-1}*	Ra-active ν_{MAX}(HgX)/cm^{-1}*
(TPP)$HgCl_2$	2.41(3)	283	282
(PPh_3)$HgCl_2$	2.37(1)	290	286
(PEt_3)$HgCl_2$	2.40(1)	286	270
(PMe_3)$HgCl_2$	2.36(1)	300	291
(PBu^n_3)$HgCl_2$	2.28(3)	278	280
(TPP)$HgBr_2$		195	195
(PPh_3)$HgBr_2$		203	200
(PEt_3)$HgBr_2$		190	185
(PMe_3)$HgBr_2$		216	193
(PBu^n_3)$HgBr_2$		188	186
(PPh_3)HgI_2		163	160
(PBu^n_3)HgI_2		151	150

* - the notation ν_{MAX}(HgX) refers to the highest observed mercury-halogen stretching mode observed in each spectrum.

Table 3.9.

IR-active $\nu(HgX)_b$ modes associated with Hg-X bridge bonds

Compound	Structure	d(HgX)/Å	$\nu(HgX)_b/cm^{-1}$
$(TPP)HgCl_2$	asymmetric dimer	2.54 (1),2.75 (1)	219 and 156
$(PPh_3)HgCl_2$	symmetric dimer	2.623(8),2.658(8)	188 and 183
$(PEt_3)HgCl_2$	polymeric chain	2.56 (1),3.04 (1), 3.21 (1)	203,198sh and 117,105,90sh
$(PMe_3)HgCl_2$	'ionic chain'	2.782(4),2.941(4), 3.489(4)	141 and below*
$(TPP)HgBr_2$	asymmetric dimer		151 and 117
$(PPh_3)HgBr_2$	symmetric dimer		137 and 117
$(PEt_3)HgBr_2$	polymeric chain		144 and 91sh,84,72
$(PMe_3)HgBr_2$	'ionic chain'		116 and below*
$(PPh_3)HgI_2$	symmetric dimer		117 and 89

* - although denoted as $\nu(HgX)_b$ modes here, these bands are more correctly termed cation and anion translatory modes (Section 3.3.1d)

the existence of bands arising from $\nu(HgCl)_b$ modes associated with longer Hg-Cl contacts (Table 3.9). It can be seen that the wavenumber positions of $\nu(HgCl)$ modes vary in a manner dependent on the type and extent of mercury-chlorine bridging.

The $(PMe_3)HgCl_2$ 'ionic' chain can be distinguished from the other structures due to the lack of $\nu(HgCl)$ mode absorption in its IR spectrum between 140 and 300 cm^{-1}. The remaining compounds show strong absorption in their infrared spectra between 150 and 220 cm^{-1} corresponding to some form of $\nu(HgCl)_b$ mode. It is rather more difficult to differentiate between dimeric and polymeric chain structures without considering the lower, more complicated, wavenumber region of the spectrum, i.e. at ca. 100 cm^{-1} and below. The $(PEt_3)HgCl_2$ complex, which has a chain structure, contains strong bands at 117 and 90 cm^{-1} in its IR spectrum whereas the two dimeric structures $(PR_3)HgCl_2$ (PR_3=TPP or PPh_3) do not contain bands of comparable intensity in this region. If one accepts previous arguments (Section 3.2.1) the structures of $(PPh_3)HgCl_2$ and $(TPP)HgCl_2$ can be recognised by the degree of separation of the two IR-active $\nu(HgCl)_b$ modes. The more complicated nature of the α-$(PBu^n_3)HgCl_2$ spectrum does not allow one to deduce any further information which could be used for identification purposes, unless of course, one observed a comparable spectrum for some other $(PR_3)HgCl_2$ complex.

Consideration of $\nu(HgBr)$ mode data for the corresponding $(PR_3)HgBr_2$ complexes suggests that similar relationships exist between structure and vibrational spectra (Tables 3.8 and 3.9) Thus $\nu(HgBr)$ modes have been observed at ca. 200 cm^{-1}, which arise from modes associated with short Hg-Br bonds. The $\nu(HgBr)_b$ modes are found to range from ca. 150 cm^{-1} to lower values.

In view of the small number of structural data available for the corresponding iodo complexes, only the structure of $(PPh_3)HgI_2$ being known

(inferred from photographic studies), there is a far lesser understanding of their vibrational spectra. Therefore great caution must be exercised when making structural inference. From the present work ν(HgI) modes associated with terminal Hg-I bonds in a dimer appear at ca. 150 cm^{-1}, whereas $\nu(HgI)_b$ modes have been located at 117 and 89 cm^{-1} for $(PPh_3)HgI_2$ (Tables 3.8 and 3.9).

3.3.2. Solid-state vibrational spectra of some tertiary phosphine complexes of unknown structure.

(a) Introduction. Tentative vibrational assignments and structural proposals have been made in the light of the findings of the previous Section. It should be emphasized that structural proposals made in the following Sections are by no means definite. Considering that the complexes studied crystallographically cover only a rather limited range of possible $(PR_3)HgX_2$ complexes, with respect to electronic and steric properties, the five structural types shown in Section 3.1 are by no means exhaustive. Indeed, some spectra suggest that other completely different structures may exist.

A major problem encountered when interpreting these spectra was elimination of modes arising from the complexed ligand. Ideally one should be able to eliminate these modes by the halogen mass-dependence method together with a knowledge of the spectra (IR and Ra) of the free ligand. However, different structures probably occur within some halo series. The possible results of this are two-fold. Firstly, shifts in ligand modes (and/or intensity changes) may occur because of different coordination environments of these ligands about mercury, and secondly, varying degrees of splitting of these ligand modes may occur as a result of site symmetry differences.

In spite of these problems some vibrational assignments and structural proposals have been attempted and literature data have been used wherever possible to help eliminate internal modes of the ligands.

(b) $(PPr^n_3)HgX_2$ (X=Cl, Br or I). The vibrational spectra of these complexes are shown in Figures 3.6a and 3.6b. Wavenumber positions and tentative vibrational assignments are contained in Table 3.10.

The white (α-form) and yellow (β-form) isomers of $(PPr^n_3)HgI_2$ reported by Evans et al.[61] have been isolated and studied in the present work.

As observed by Allen et al.[141] for $(PPr^n_3)_2PdCl_2$ a number of modes of the ligand, originally not active in the spectra of the free ligand become active on complexation. By comparison with the work of Allen et al.[141], similar internal modes of the ligand have been eliminated from the present spectra. Examination of all four sets of spectra show no clear indication of normal halogen mass-dependence, except for perhaps those of the β-iodo isomer and the bromo compound. One can only assume therefore that at least three separate structures are present.

The chloro complex shows strong bands at 305 (IR) and 298 (Ra) cm^{-1} which can readily be attributed to ν(HgCl) modes associated with vibration of quite a short Hg-Cl bond of ca. 2.3 Å. The wavenumber position of the IR-active band (305 cm^{-1}) is indicative of a quite large Cl_s-Hg-P angle, by comparison with the work of Goggin et al.[106] on $[Cl\text{-}Hg\text{-}PMe_3]^+$ species and with the present work on $(PMe_3)HgCl_2$. Other bands at 205, 178, 169 and 144 cm^{-1} in the IR spectrum, and at 208, 189 and 169 cm^{-1} in the Ra spectrum, are of characteristic intensity and wavenumber to be tentatively assigned to $\nu(HgCl)_b$ modes. No further structural proposal could be made.

The bromo complex contains bands in its spectra at 196 (Ra) cm^{-1} and 203 (IR) cm^{-1} which can be assigned as $\nu_{as}(HgBr)_t$, and also bands at 179 (Ra) cm^{-1} and 181 (IR) cm^{-1} which can be assigned as $\nu_s(HgBr)_t$. There is a strong band at 144 (IR) cm^{-1} and a medium band at 145 (Ra) cm^{-1} which probably derive from $\nu(HgBr)_b$. The lack of any signal attributable to ν(HgBr) at less than ca. 140 cm^{-1} in the vibrational spectra of this complex

Far infrared spectra (ca. 30K) for (PPr^)HgX^ (X=Cl, Br or I) (cm)

X=Cl

to 00

• - interna! mode of the ligand

X=Br

X=I (a-form)

X* I ($-form)

i__

Raman spectra (RT) of $(PPr^n_3)HgX_2$ (X=Cl, Br or I) (cm^{-1})

X=Cl

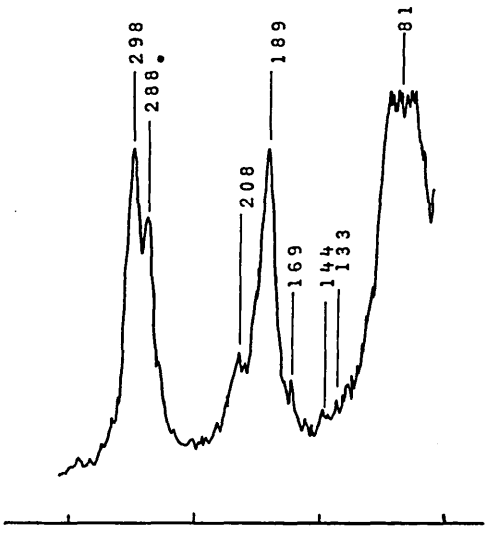

• - internal mode of the ligand.

•• - unassigned band.

X=Br

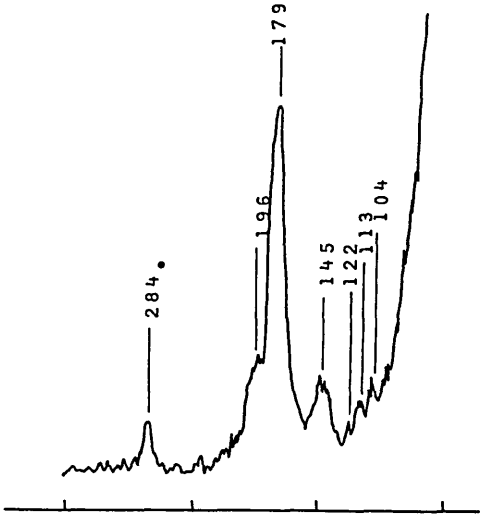

X=I (α-form)

X=I (β-form)

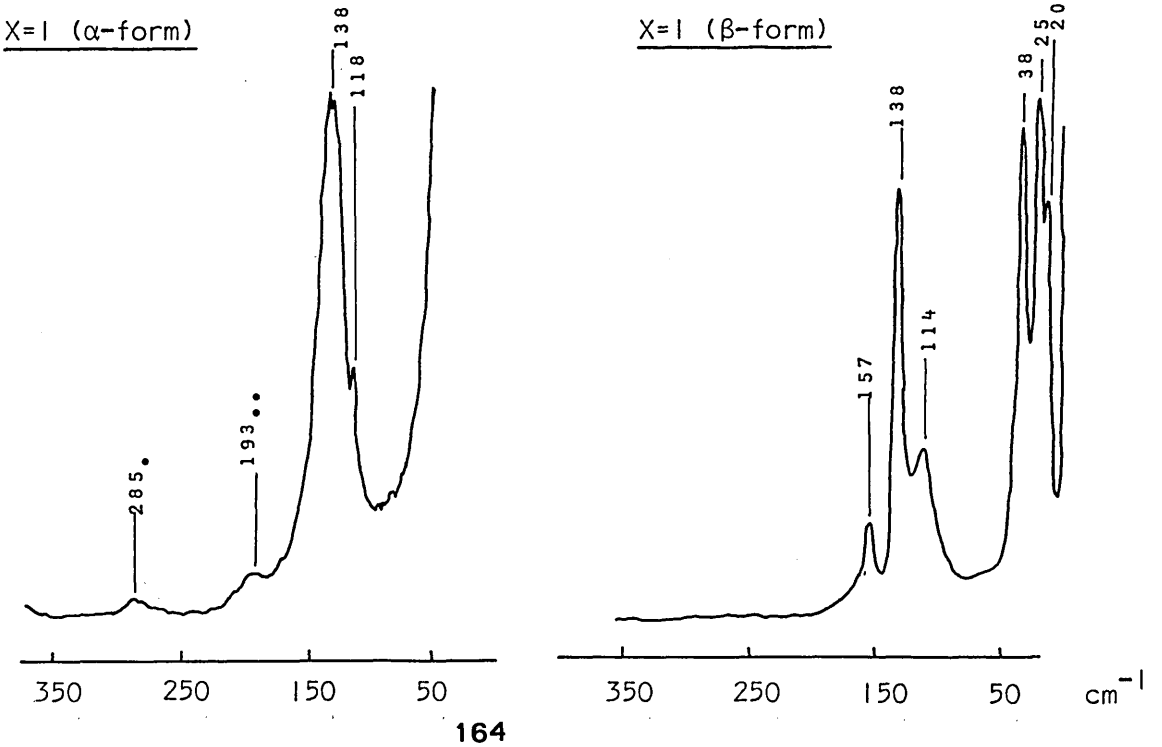

Table 3.10.

Vibrational assignments[a] for $(PPr^{n}_{3})HgX_2$ (X=Cl, Br or I)

Cl		Br		I(α-form)		I(β-form)		Assignments
IR[b]	Ra[c]	IR[b]	Ra[c]	IR[b]	Ra[c]	IR[b]	Ra[c]	
					193w,br			
305s		203s	196sh	139s	138s	153s	157m	$\nu_{as}(HgX)_t$
	298s	181m	179s	129m	118m	134s	138s	$\nu_{s}(HgX)_t$
205s	208m	144s	145s			90s	114m	$\nu(HgX)_b$
178sh	189s							
167s	169m							
144s								
115m	144w	112w,br	88vw		58w	38s		Bending and lattice modes
98m	133w	88w	113w	76sh	49vw	25s		
83mw	81s,br	76sh	104w	71sh			20s	
61w		66ms		61wm				
49w				51w				

a - omitting internal modes of the ligand.

b - recorded at ca. 30K

c - recorded at room temperature.

suggests that there is no further Hg-Br interaction. Therefore an asymmetric bromine-bridged dimeric structure is proposed.

The general appearances of the spectra of ft-CPPr^Hg^ are similar to those of the bromo complex, although some of the band shifts are not as one might expect e.g. the wavenumber separation between the IR-active vs(HgBr) mode andv(HgBr)b is 37 cm 1 whereas between vs(Hgl) and v(Hgl)^ it is larger at 44 cm '. However a dimeric structure may also be proposed in the present case. The bands at 151 (Ra) cm ' and 153 (IR) cm * are assigned as v_{as}(Hgl), whereas the bands at 138 (Ra) and 134 (IR) cm 1 are both assigned Vs(Hgl). The bands at 114 (Ra) and 90 (IR) cm ' are both assigned asv(Hgl)b modes. It is interesting to note that the vibrational spectra of 3"(PPr^)Hg12 are very similar to those observed for [NBu^j[Hgl^ which was proposed as being ionic and containing the dimeric $[Hg^I^3]^{2-}$ anion.

The surprisingly low wavenumber values of the v(Hgl) modes in both IR and Ra spectra of a-tPPr^Hg^ are of comparable wavenumber to those found for (PMe^Hg^ (Section 3.3. Id). Therefore there is again the possibility of the existence of similar species in the present case viz. $[HgI^]^{2-}$ or 'monomeric (PPr^Hg^ species'. Clearly there is no evidence of long range Hg—I interaction.

There was no evidence to indicate the presence of v(HgP) modes in the spectra of any of the four complexes studied.

(c) (PPh^Me)HgX^ (X=Cl, Br or I). It was found for the chloro complex that slow recrystallisation from DMFA^O resulted in the formation of a white a-isomer, whereas rapid recrystal lisat ion from the same solvent mixture resulted in the formation of a white 8-isomer (Section 7.1). Vibrational spectra of all four complexes are shown in Figures 3.7a and 3.7b, while Table 3.11 contains wavenumber positions and tentative vibrational assignments. These spectra strongly suggest that at least three separate

structures are present. As a result a variation is observed in the spectral activities and wavenumbers of the internal modes of the ligand, which makes their elimination difficult. Nevertheless an attempt has been made to eliminate these modes by comparison with the study of Allen *et al.*[141] on free PPh_2Me and $(PPh_2Me)_2PdCl_2$.

Comparison of the IR spectra of α- and β-forms of $(PPh_2Me)HgCl_2$ indicates two separate types of mercury-chlorine bridge interaction are present. Both compounds have strong bands at *ca.* 300 cm^{-1} indicating the presence of at least one short Hg-Cl bond of *ca.* 2.3 Å. The α-form contains a strong band at 203 cm^{-1} which is indicative of relatively short Hg-Cl bridge distances of *ca.* 2.6 Å (*cf.* $(PPh_3)HgCl_2$ and $(PEt_3)HgCl_2$), whereas, for the β-form there is no absorption attributable to $\nu(HgCl)_b$ until 165 cm^{-1} which suggests a much longer Hg-Cl interaction, comparable to that found for $(PMe_3)HgCl_2$.

The weak bands found in the vibrational spectra of the β-compound between *ca.* 290 and 160 cm^{-1} appear to mirror the spectrum of the α-compound in this region. These bands have been assigned to the ligand in the α-compound; however it is unlikely that these bands would fall in exactly the same position for the β-compound in view of its 'different structure'. One suspects, therefore, that the β-compound also contains some α-compound contamination.

The general appearance of the IR spectrum of α-$(PPh_2Me)HgCl_2$ is similar to that of $(PEt_3)HgCl_2$, suggesting an analogous structure. The Ra spectrum of α-$(PPh_2Me)HgCl_2$, however, is not so informative due to hindrance caused by internal modes of PPh_2Me. Assignments have been made (Table 3.11) using the same treatment, that of a polymeric chain, used for $(PEt_3)HgCl_2$ (Appendix 4).

The IR spectra of β-$(PPh_2Me)HgCl_2$ and $(PPh_2Me)HgBr_2$ appear to show normal halogen mass-dependence, and are reminiscent of spectra observed for $(PMe_3)HgX_2$ (X=Cl or Br), suggesting similar 'ionic' chain structures. There are strong bands at 310 (IR) and 304 (Ra), and at 221 (IR) and 216 (Ra) cm^{-1}

Figure 3.7a.

Far infrared spectra (ca. 30K) of $(PPh_2Me)HgX_2$ (X=Cl, Br or I) (cm^{-1})

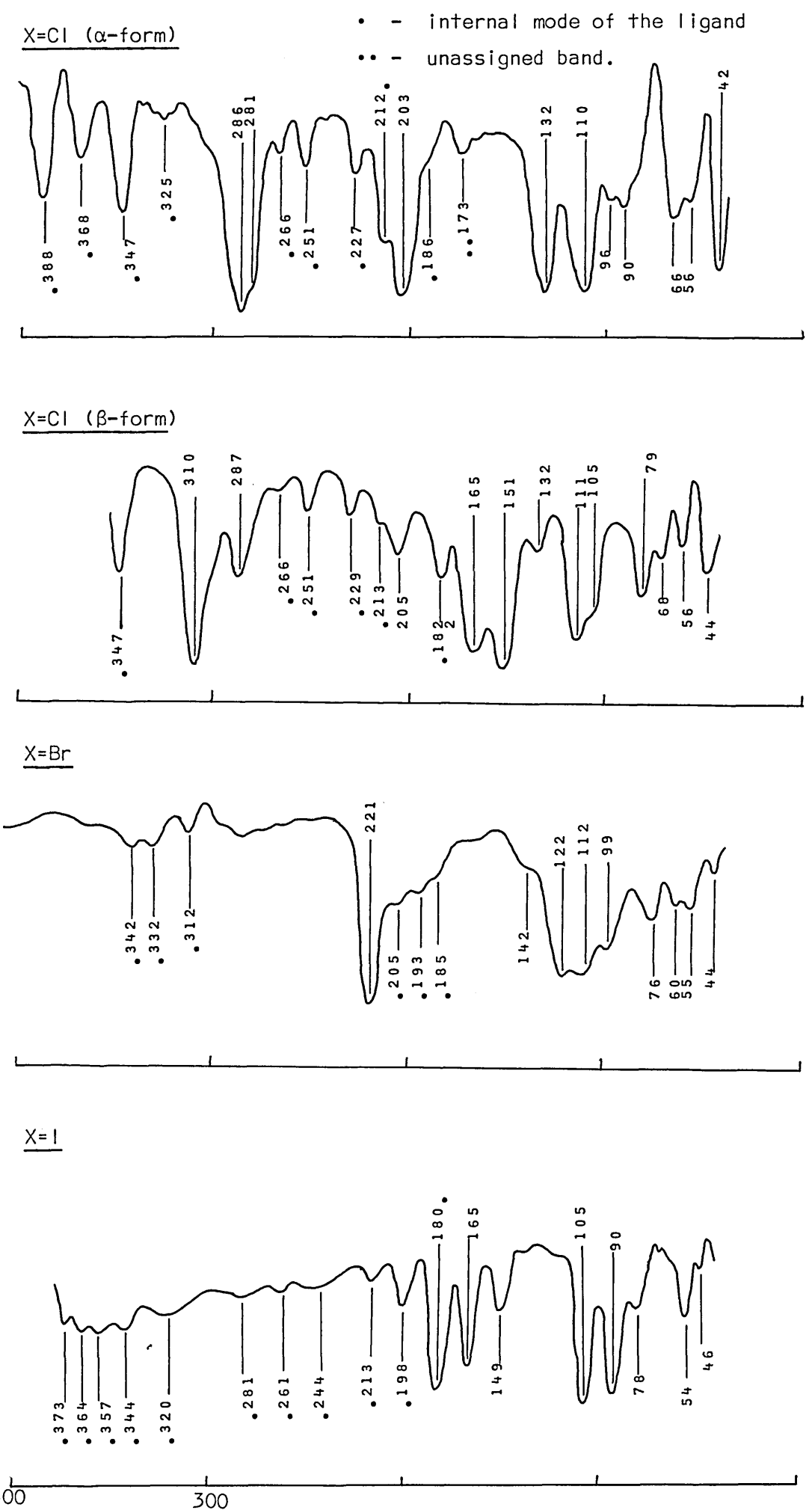

Raman spectra (RT) of $(PPh_2Me)HgX_2$ (X=Cl, Br or I) (cm^{-1})

• - internal mode of the ligand.

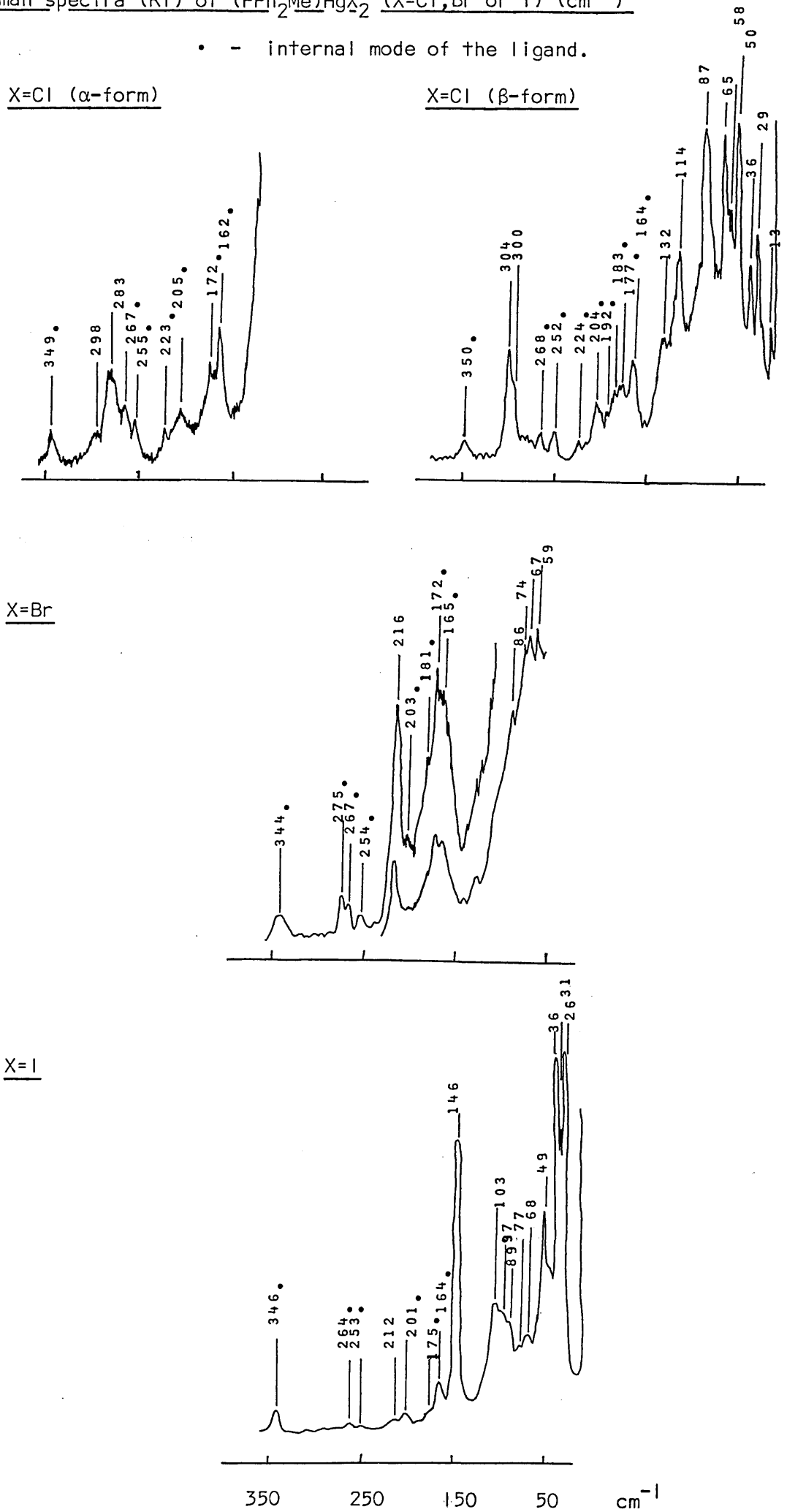

Table 3.1l.

Vibrational assignments3 for (PPh^Me)HgX^ (X=Cl, Br or I).

Cl (*a*-form)		Cl (&-form)		Br		I		
IRC	Rad	IRC	Rad	IRC	Rad	IRC	Rad	Assignments^
	298mw							
286s) 281sh)								v 5(HgCl)b Au
	283s							V |(H9C l)b Ag
		3 1Os		22 ls		165s	I64w	Vas<H9x)+
			304s) 300sh)		2 16	149m	I46s	Vs(HgX)+
						105s	103m	
						90s	97sh	v(H g l)b
							89sh	
		287m						See text
203s								V H9C l)b Au
I32s								V7(H9C l)b Au
I IOs								V H9C l)b Au
96sh		I32s	I32s	I_{22}s	$_{86}$sh	78mw	77w '	Cation and anion
90m		I IOs	I 14s	$I I_2$s	74sh	54m	$_{68}$w $_1$	trans$_1$ati ons,
$_{66}$m		96w	87vs	99s	67s	46w	49m	bending and
56sh		90w	65vs	76m	59s		36s (	lattice modes
42s		85sh	58s	60sh			31s	
		$_{66}$ms	50vs	55w			26s '	
		56ms	36s	44vw				
		42s	29s					
			I3ms				'	

a - omitting internal modes of the ligand,

b - numbering of modes is as in Figure 3.3a.

c - recorded at ca_. 30K.

d - recorded at room temperature.

in the spectra of the $-chloro and bromo complexes, respectively, which may be assigned v(HgX)^_. The relatively high wavenumber values of these v(HgX)^ modes suggest relatively large X-Hg-P angles. There are no further bands attributable to stretching modes between mercury and halogen until 165 cm * and 122 cm ^{1} in the IR spectra of $-chioro and bromo complexes, respectively where there are strong broad absorption bands which have been assigned to cation and anion translations.

The iodo complex shows bands at 165 (IR) and 164 (Ra) cm * and at 149 (IR) and 146 (Ra) cm * which are indicative of $v_{as}(HgI)_t$ and $v_s(HgI)_t$, respectively, in a discrete dimeric structure. The positions of the bands at 105 (IR) and 90 (IR), and at 103 (Ra), 97 (Ra) and 89 (Ra) cm * suggest they may have arisen from v(HgI)^ modes of a dimeric species. Consequently these bands are assigned v(HgI)^ and a discrete dimeric structure is proposed

It was not possible to deduce any information concerning v(HgP) modes,

(d) (PPhN^JHgX^ (X=CI, Br or I). Vibrational data obtained are shown in Figures 3.8a and 3.8b and Table 3.12. The infrared spectrum due to the complexed ligand appears to be consistent for the bromo and iodo complexes. When these bands are eliminated the spectra are much simplified.

There is a striking resemblance between the IR spectra of the bromo complex and that of (PMe-^HgB^ (Figure 3.8a). The highest wavenumber bands, at 225 (IR) and 225 (Ra) cm *, in the spectra of (PPhN^JHgBr^ have been assigned to v(HgBr), their exceptionally high wavenumber positions suggesting a large Br-Hg-P angle. The bands at 129, 120 and 99 cm * in the IR spectrum can be assigned to translations of *[Br-Hg-PPhN^l ' cations and 'Br anions No further information could be gained from the Ra spectrum.

The spectra of the iodo complex suggest a discrete dimeric structure by comparison with the spectra of (PPh^JHgl^, (PPl^MeJHg^ and B-tPPr^Hg^. The bands at 159 (IR) and 161 (Ra) cm * are assigned v (Hgl)^., whereas bands

Far infrared spectra (ca. 30K) for $(PPhMe_2)HgX_2$ (X=Cl, Br or I) (cm^{-1})

• - internal mode of the ligand.

•• - unassigned band.

X=Cl

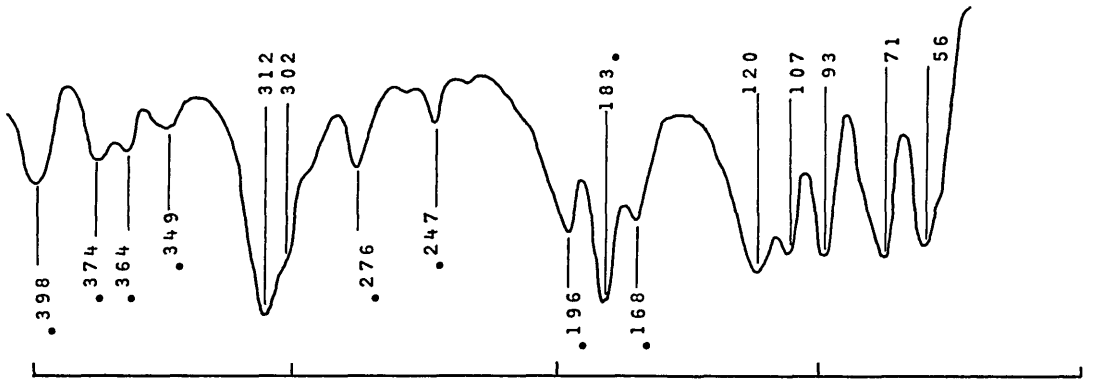

X=Br

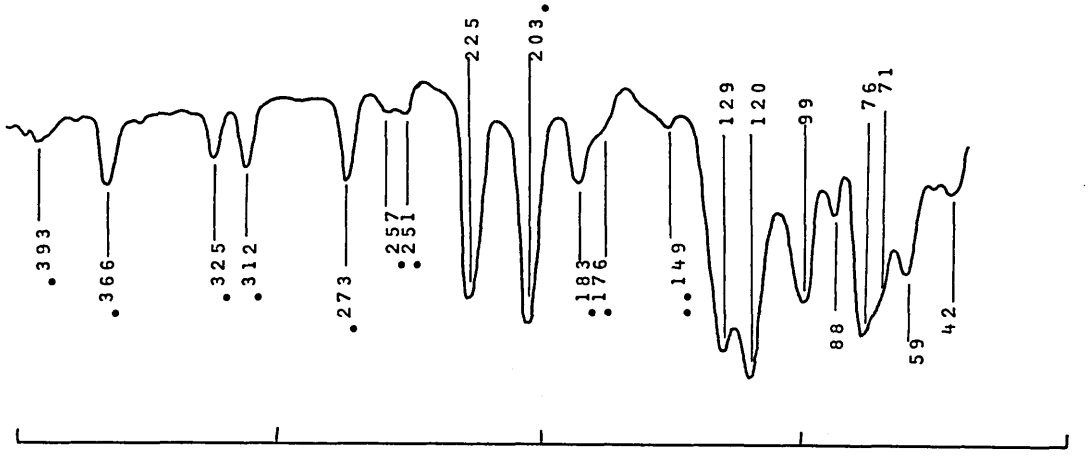

X=I

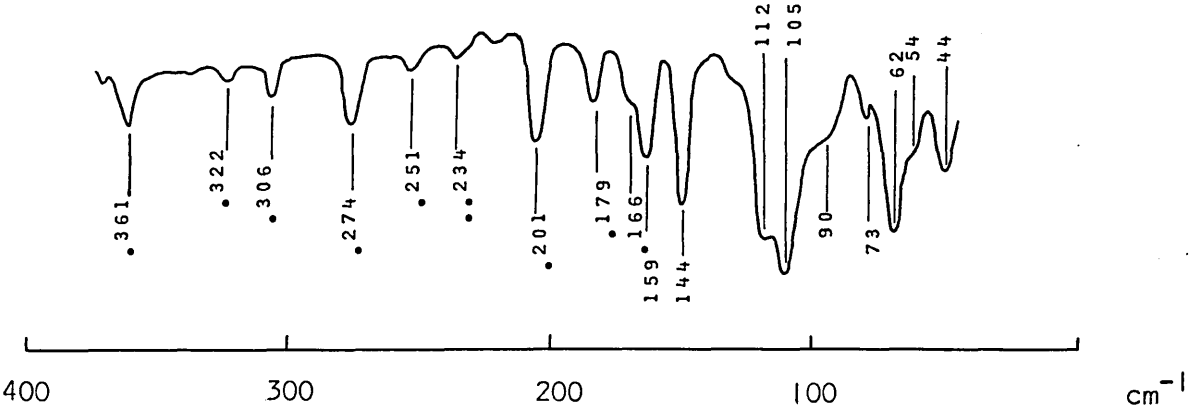

Raman spectra (RT) of $(PPhMe_2)HgX_2$ (X=Cl, Br or I) (cm^{-1})

• - internal mode of the ligand.

X=Cl

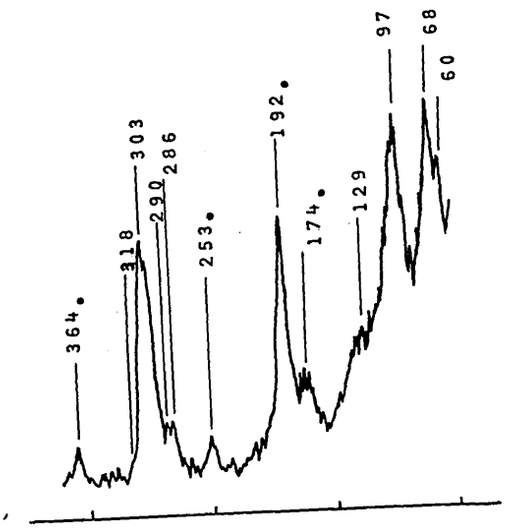

X=Br

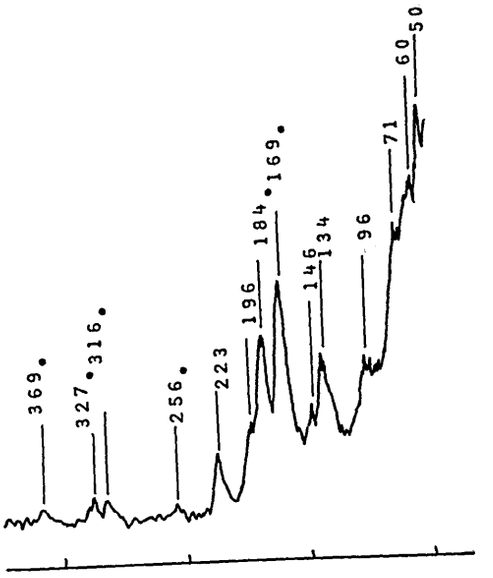

X=I

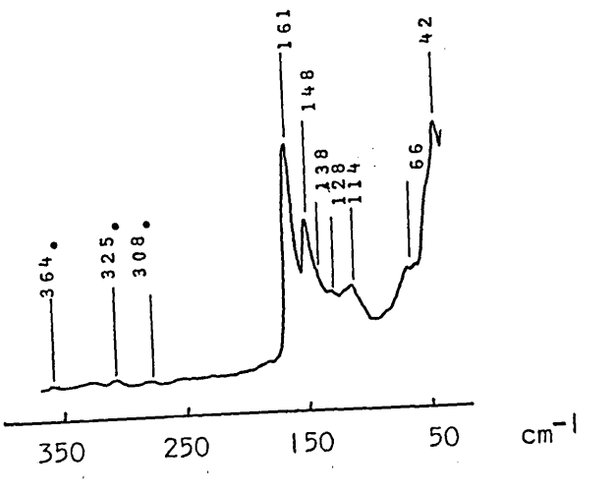

Table 3.12.

Vibrational assignments9 for (.PPhMeg)HgXg (X=Cl, Br or I).

Cl		Br		I		
IRb	Rac	1Rb	RaC	1Rb	RaC	Assi gnments
312s	318sh	225s		159m	161 s	v as<Hgx)+
302sh	303s		223m	144s	148m	Vs (HgX)t
				112 sh)	114m	>
				105s)		v(H g l)b
				90sh)		
120s	129sh	129s	146w	73w	66 sh	\ Cation and anion
107s	97s	122s	134m	62s	42s	translations,
93s	68 s	99s	96m	54sh		bending and
71s	60s	88w	71 sh	44mw		lattice modes.
56s		76s	60sh			
		71 sh	50s			
		59m				
		42w				i

a - omitting internal modes of the ligand,

b - recorded at ca_. 30K.

c - recorded at room temperature.

a+ 144 (IR) and 148 (Ra) cm $^{-1}$ are assigned $\nu_{3s}(HgI)_T$. The corresponding $\nu(HgI)_2$ modes are located at 112, 105 and 90 cm $^{-1}$, and at 114 cm $^{-1}$ in the infrared and Raman spectra respectively.

The spectra of the chloro complex are extremely difficult to interpret. The strong bands at *ca.* 310 cm $^{-1}$ in both IR and Ra spectra certainly arise from $\nu(HgCl_2)$ modes of some form, their high wavenumber values suggesting a large Cl-Hg-P angle. The region at ca. 200 cm $^{-1}$ causes difficulties. By comparison with the other two halo analogues one would expect quite strong signals in this region due to internal modes of the ligand, but this region is also that where bands arising from $\nu(HgCl)_2$ modes of a discrete dimeric species would occur. Although the relative intensity values of the bands in this region do not correspond to those bands attributed to the complexed ligand in bromo and iodo compounds, the wavenumber positions are very similar. Therefore these bands are tentatively assigned to internal ligand modes. Elimination of these bands means there are no further bands attributable to $\nu(HgCl)$ above ca. 130 cm $^{-1}$ in both IR and Raman spectra. This observation suggests a similar 'ionic' structure to that found for $(PMe_2Ph)_2HgCl_2$. This would be quite reasonable on the basis of the similarity between PMe_2Ph and $PPhMe_2$ ligands.

No information could be deduced concerning $\nu(HgP)$ modes.

3.4. STRUCTURAL STUDIES OF SOME $(PR_3)HgX_2$ COMPLEXES IN SOLUTION.

(a) Introduction. Information concerning the nature of $(PR_3)HgX_2$ species in solution is very useful for two reasons. Firstly, knowledge of their structure in solution would be useful whilst attempting to explain solid state structures (Section 2.3.1), and secondly, vibrational studies of solution phase species may help distinguish bands arising from solid state effects in the vibrational spectra of the solids. Therefore, wherever possible experiments were undertaken to gain such information. The experimental

techniques used for this purpose include relative molecular mass (M_r) determination, vibrational spectroscopy and ^{31}P n.m.r spectroscopy. Each of these techniques, especially the latter two, require quite high solubility of the complex in appropriate solvents. Unfortunately all the $(PR_3)HgX_2$ complexes studied in this work, with the exception of the PPr^n_3 and PBu^n_3 series, have limited solubilities in suitable solvents. Therefore solution phase studies have been restricted to $(PBu^n_3)HgX_2$ (X=Cl, Br or I) and $(PPr^n_3)HgX_2$ (X=Cl, Br or I).

(b) $(PBu^n_3)HgX_2$ (X=Cl, Br or I).

Relative molecular mass determinations in benzene. Table 3.13 contains the relative molecular (M_r) and formula (F_r) masses for the three complexes studied. The ratio M_r/F_r indicates that each halo analogue is dimeric in benzene. These results compare well with those of Kessler[90] who carried out similar studies in chloroform.

Far-infrared spectra in benzene. The far-infrared spectra together with vibrational assignments for the $(PBu^n_3)HgX_2$ complexes are shown in Figure 3.9. By comparison with data on the solid state (Section 3.3.1) the present spectra suggest the presence of halogen-bridged dimeric structures with ligands mutually trans, for which a simple point group analysis (C_i or C_{2h}) predicts that one $\nu(HgX)_t$ mode and two $\nu(HgX)_t$ modes are active in the IR spectrum. It should be mentioned that the broad absorption assigned as $\nu(HgI)_t$ could well consist of more than one component as already noted by Kessler.[90] The wavenumber positions of the remaining $\nu(HgX)_b$ modes may well be coincident with the first $\nu(HgX)_b$ mode in each case, thus suggesting symmetric four-membered rings, and this further suggests that the lower wavenumber bands in each spectrum (less than 101, 68, 61 cm^{-1} for chloro, bromo and iodo complexes, respectively) are due to bending modes. Alternatively these lower absorptions may be due to the second $\nu(HgX)_b$ mode which

Far infrared spectra (RT) of $(PBu^n_3)HgX_2$ (X=Cl, Br or I) in benzene

X=Cl (α-form) (conc^n ~ 35 mg cm^{-3})

303 - $\nu(HgCl)_b$, 163 - $\nu(HgCl)_b$, 101, 78 - '?$\nu(HgCl)_b$', bending modes + solvent.

X=Br (conc^n ~40 mg cm^{-3})

208, 198 - $\nu(HgBr)_t$, 109 - $\nu(HgBr)_b$, 68 - $\nu(HgBr)_b$, bending modes + solvent.

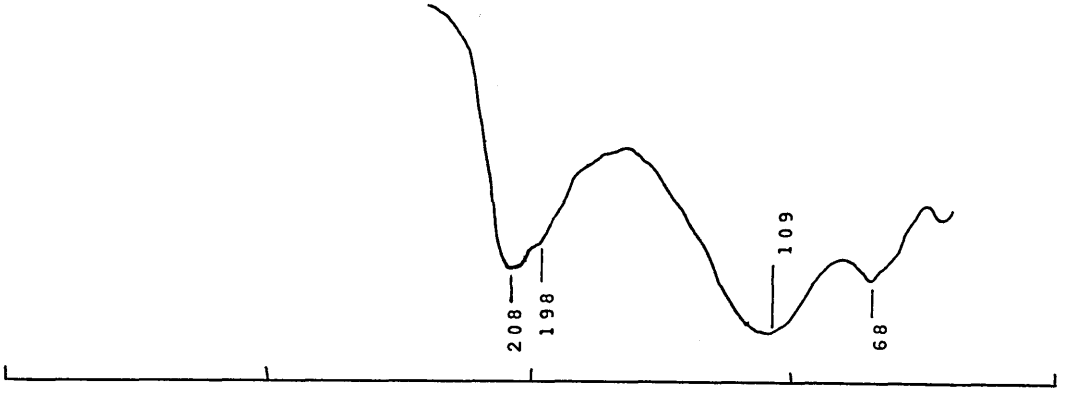

X=I (conc^n ~50 mg cm^{-3})

166, 159, 149, 144 - $\nu(HgI)_t$, 90, 76 - $\nu(HgI)_b$, 61 - '?$\nu(HgI)_b$', bending modes + solvent.

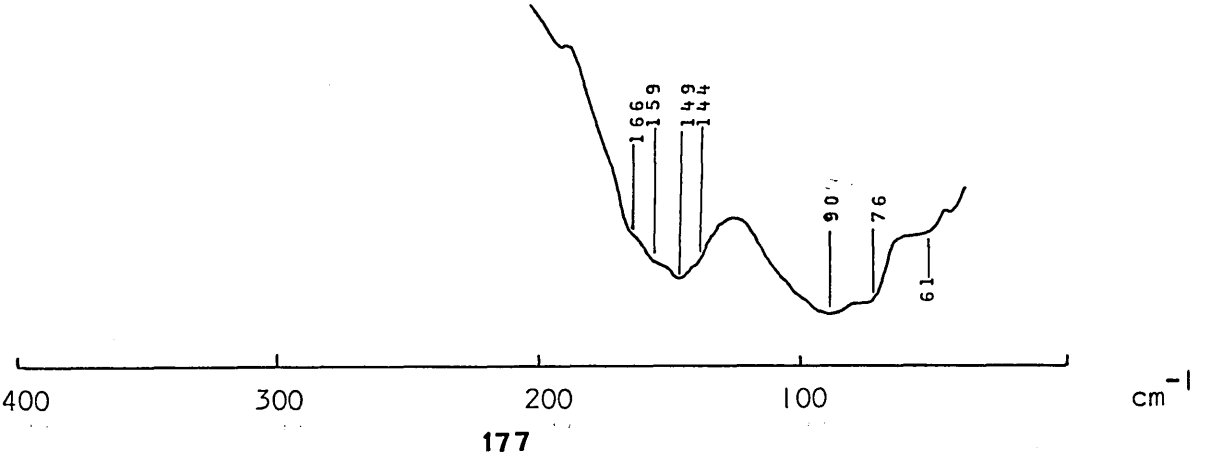

Table 3.13.

Relative molecular masses determined for $(PBu^n_3)HgX_2$ (X=Cl, Br or I) in benzene.

Compound	M_r	F_r	M_r/F_r
α-$(PBu^n_3)HgCl_2$	971	473	2.05
$(PBu^n_3)HgBr_2$	1122	562	2.00
$(PBu^n_3)HgI_2$	1252	656	1.91

Table 3.14.

Relative molecular masses determined for $(PPr^n_3)HgX_2$ (X=Cl, Br or I) in benzene.

Compound	M_r	F_r	M_r/F_r
$(PPr^n_3)HgCl_2$	864	432	2.00
$(PPr^n_3)HgBr_2$	1044	521	2.00
α-$(PPr^n_3)HgI_2$	1176	615	1.91

Table 3.15.

$\delta(^{31}P)$ and $^1J(Hg-P)$ data for $(PPr^n_3)HgX_2$ complexes.

Complex	$\delta(^{31}P)$/ppm [a]		$^1J(Hg-P)$/Hz [b]	
	300 K	183 K	300 K	183 K
$(PPr^n_3)HgCl_2$	33.0	32.7	7389	7524
$(PPr^n_3)HgBr_2$	27.2	27.7	6611	6836
α-$(PPr^n_3)HgI_2$	6.2	7.5	5071	5476
β-$(PPr^n_3)HgI_2$	6.9	7.5	5053	5481

a ± 1ppm b ± 5Hz.

would suggest the presence of asymmetric rings. It is worthy to note that these results are in complete agreement with the work of Kessler[90] who carried out similar experiments in $CDCl_3$.

(c) $(PPr^n_3)HgX_2$ (X=Cl, Br or I).

Relative molecular mass determinations in benzene. The relative molecular masses of the chloro, bromo and α-iodo complexes have been determined and indicate that each compound is essentially dimeric in solution.

Far-infrared spectra in benzene. The far-infrared spectra and vibrational assignments for $(PPr^n_3)HgX_2$ (X=Cl, Br or I) are shown in Figure 3.10. These spectra are very similar to those observed for the PBu^n_3 complexes and so similar structures are proposed, i.e. halogen-bridged dimers with ligands mutually trans. A similar point group treatment has been adopted. The more complicated nature of the $(PPr^n_3)HgBr_2$ spectrum, may well indicate the presence of more than one structural form.

^{31}P n.m.r spectra. ^{31}P n.m.r spectra have been recorded using CH_2Cl_2/CD_2Cl_2 (80/20) as solvent. Chemical shift, $\delta(^{31}P)$, and coupling constant, $^1J(Hg-P)$ data, recorded at room temperature and -90^oC are shown in Table 3.15.

These results correspond to those observed by Kessler[90] and Grim[125] for $(PBu^n_3)HgX_2$ complexes. By comparison with previous data[90,125,127] the $^1J(Hg-P)$ values are typical of a structure consisting of one phosphine ligand bonded to each mercury atom in a trans halogen-bridged dimeric arrangement.

3.5. VIBRATIONAL STUDIES OF 1:1 ADDITION COMPLEXES CONTAINING NITROGEN-, SULPHUR- OR OXYGEN-DONOR LIGANDS.

3.5.1. Nitrogen-donor ligands.

Crystallographic data available for complexes formed between nitrogen-donor ligands and the mercuric halides include the structures of

Figure 3.10.

Far infrared spectra of $(PPr^n_3)HgX_2$ (X=Cl, Br or I) in benzene.

X=Cl (conc^n ~30 mg cm^{-3})

305 - $\nu(HgCl)_t$, 156, 144 - $\nu(HgCl)_b$, 100 - '?$\nu(HgCl)_b$', bending modes + solvent.

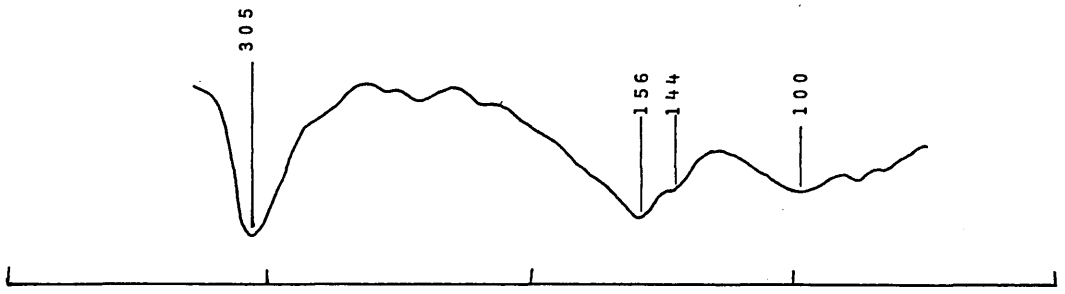

X=Br (conc^n ~40 mg cm^{-3})

225, 212, 200 - $\nu(HgBr)_t$, 144, 107, 96 - $\nu(HgBr)_b$, 75, 64 - '?$\nu(HgBr)_b$', bending modes + solvent.

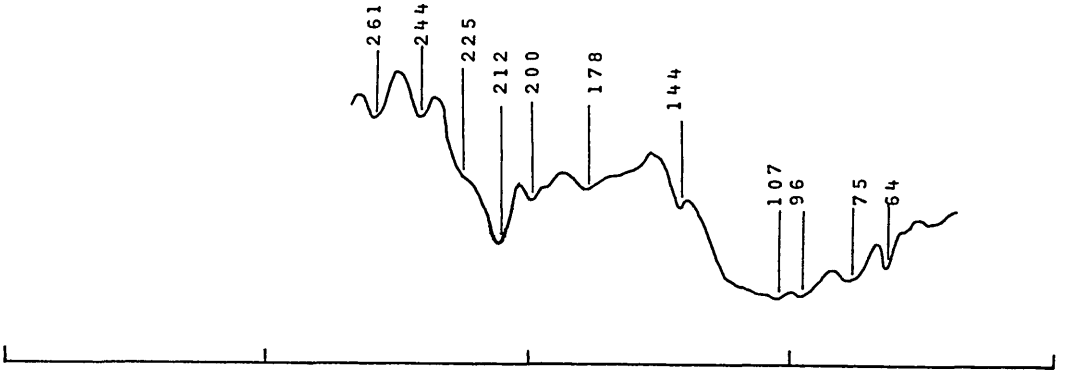

X=I(α-form) (conc^n ~50 mg cm^{-3})

171, 146 - $\nu(HgI)_t$, 88 - $\nu(HgI)_b$, 68, 59, 51 - '?$\nu(HgI)_b$', bending modes + solvent.

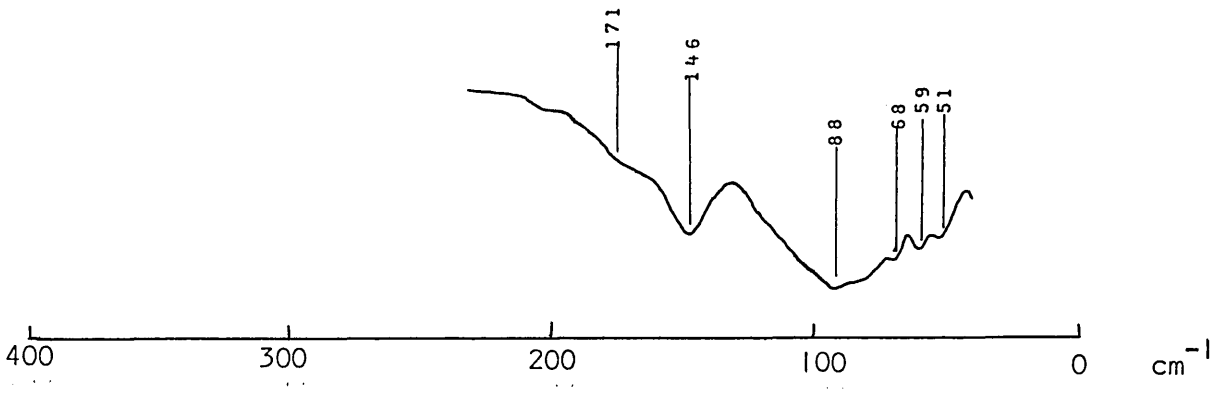

(2,4,6-trimethylpyridine)$HgCl_2$[62] and (guanosine-N^7)$HgCl_2$[63] (Section 1.3.3) and also that of (2,4-dimethylpyridine)$HgBr_2$ (Section 2.2.7). The vibrational spectra of a series of complexes of various methyl-substituted pyridines with mercuric halides have been recorded and where possible the aforementioned crystallographic data have been used as a basis for vibrational assignments.

The criteria employed to locate ν(HgX) modes are the same as those described in Section 3.2.1. In view of the unreliability of the literature with regard ν(HgN) modes in these compounds, attempts to locate these modes have been carried out disregarding these reports.

(a) <u>(2,4,6-trimethylpyridine)HgX_2 (X=Cl or Br)</u>. The equivalent iodo complex could not be prepared. The chloro complex is known to consist of almost trigonal planar '$NHgCl_2$' units stacked one upon another and joined at either end via two equivalent long range Hg-Cl contacts (Section 3.1).

The structure can be treated as a polymeric chain belonging to the C_i line group, i.e. a similar treatment to that used for $(PEt_3)HgCl_2$ (Appendix 4).

The line group analysis (taking the organic ligand as a point mass) predicts the total number and activity of the internal modes of the chain to be:-

$$\Gamma_{chain} = 11A_g(Ra) + 9A_u(IR)$$

The number and activity of modes associated with $\nu(HgCl)_b$ modes is:-

$$\Gamma\ \nu(HgCl)_b = 4A_g(Ra) + 4A_u(IR)$$

Far-infrared spectra are shown in Figure 3.11. Unfortunately attempts to record Raman spectra were unsuccessful due to severe fluorescence by the samples. Wavenumber positions and vibrational assignments are contained in Table 3.16. There are very strong bands in the region 200-300 cm^{-1} due to internal modes of the ligands but these may easily be eliminated in the conventional manner (free ligand spectra have been reported by Green and

Figure 3.11.

Far infrared spectra (ca. 30K) of (2,4,6-trimethylpyridine)HgX_2—(X=Cl or Br) (cm^{-1})

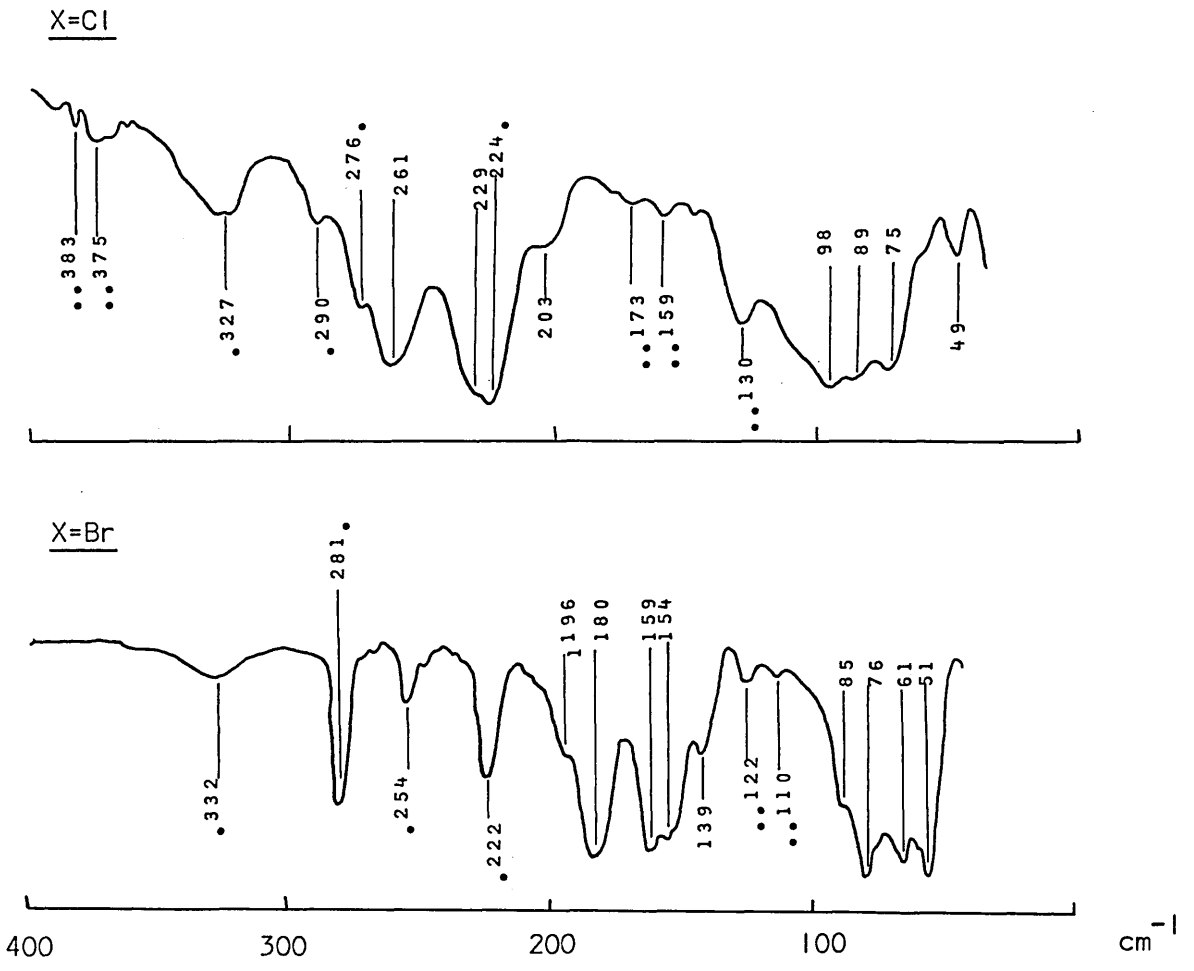

• - internal mode of the ligand.

•• - unassigned band.

Table 3.16.

Vibrational assionments[g] for (2.4.6-trimethylpyridine)HqXp (X=Cl or Br).

Cl IRb	Br IRb		Assignmentsc#ci
383vw			
375vw			
26 ls	l96sh) l80s)		V5(H3X)b Au
229s	l59s) l54s)		V H9X)b Au
98s	85sh	>	V H9X)b V
98sh	76s		v8(H9X)b Au.
75s	6 1s	1	bending and lattice
49w	5 1s	1!	modes.

a - omitting internal modes of the ligand,

b - recorded at ca^. 30K

c - Raman spectra could not be recorded because of severe fluorescence of samples,

d - numbering of modes as in Figure 3.3a.

Harrison[143]). Once the ligand modes are removed clear halogen mass-dependence of some of the bands in the spectra is found, suggesting chloro and bromo complexes are isostructural. The strong bands at 261 and 229 cm^{-1} in the spectrum of the chloro complex are readily assigned to the two highest frequency $\nu(HgCl)_b$ modes. Similarly, the strong pairs of bands at 196 and 180 cm^{-1} and at 159 and 154 cm^{-1} in the spectrum of the bromo complex can be assigned to the two corresponding $\nu(HgBr)_b$ modes. It is difficult to assign the remaining $\nu(HgX)_b$ modes unequivocally as the spectra in lower wavenumber regions are complicated by bands arising from the presence of bending and lattice modes. However, the bands which should arise from these $\nu(HgX)_b$ modes are most likely contained in the strong absorptions in the regions 75-98 and 51-85 cm^{-1} for the chloro and bromo complexes respectively.

No evidence of $\nu(HgN)$ modes was immediately apparent.

(b) <u>(2,4-dimethylpyridine)HgX_2 (X=Cl or Br)</u>. The equivalent iodo analogue could not be prepared. The structure of the bromo complex consists of approximately trigonal planar '$NHgBr_2$' units packed one upon another leading to a chain-like arrangement. There are two unequal Hg-Br bridge distances between each '$NHgBr_2$' unit which results in a different packing arrangement to that found for (2,4,6-trimethylpyridine)$HgCl_2$. Preliminary photographs indicate the equivalent chloro complex to be isomorphous and probably isostructural with the bromide.

The chain belongs to the C_1 line group. The line group analysis (taking the 2,4-dimethylpyridine ligand as a point mass) predicts the following internal modes of the chain:-

$$\Gamma_{chain} = 20A \text{ (IR, Ra)}$$

and:

$$\Gamma\nu(HgX)_b = 8A \text{ (IR, Ra)}$$

Vibrational data are recorded in Table 3.17 and Figure 3.12. Internal modes

Figure 3.12.

Far-infrared spectra (ca.30K) and Raman spectra (RT) of (2,4-dimethylpyridine)HgX_2 (X=Cl or Br) (cm^{-1})

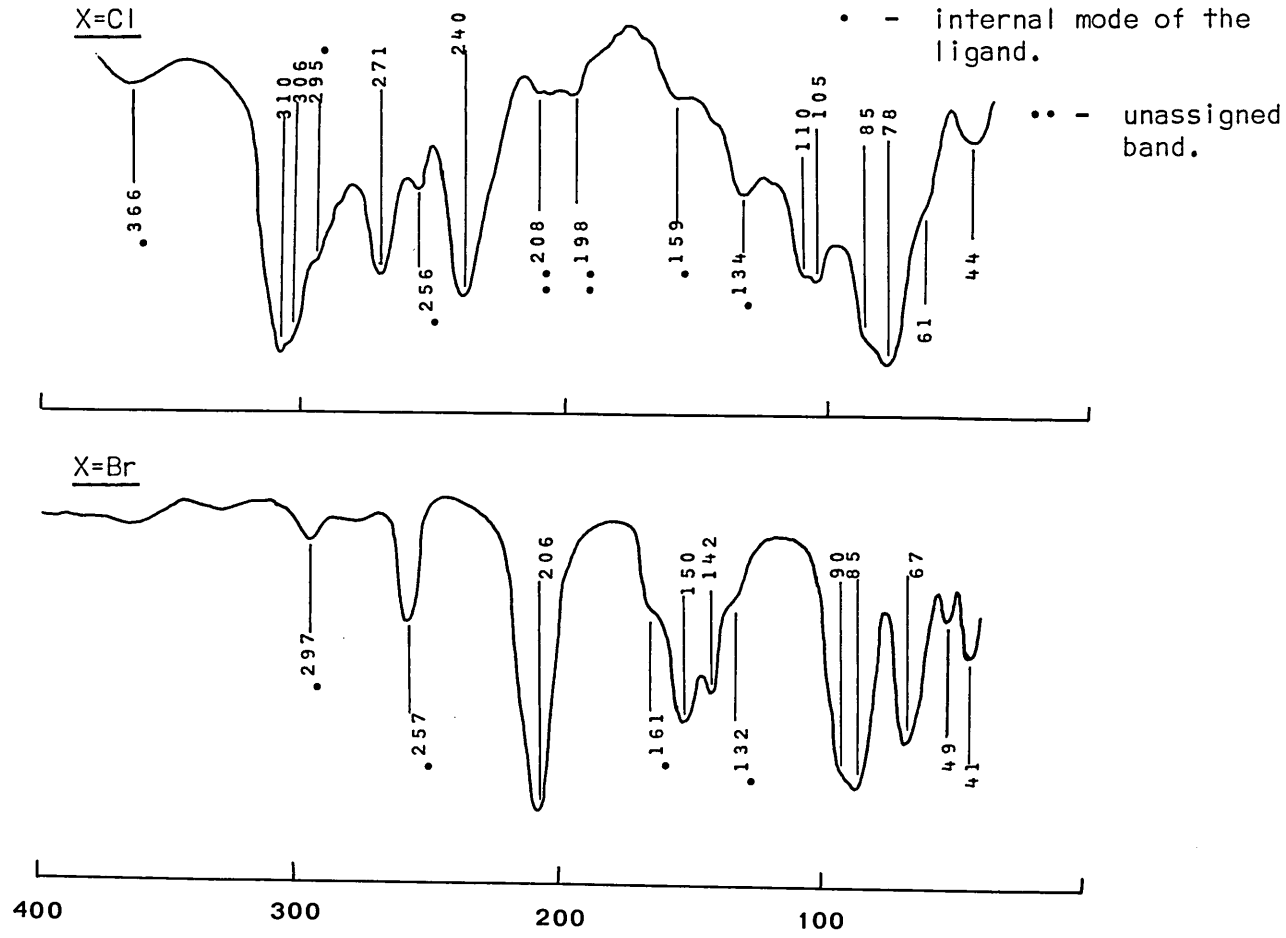

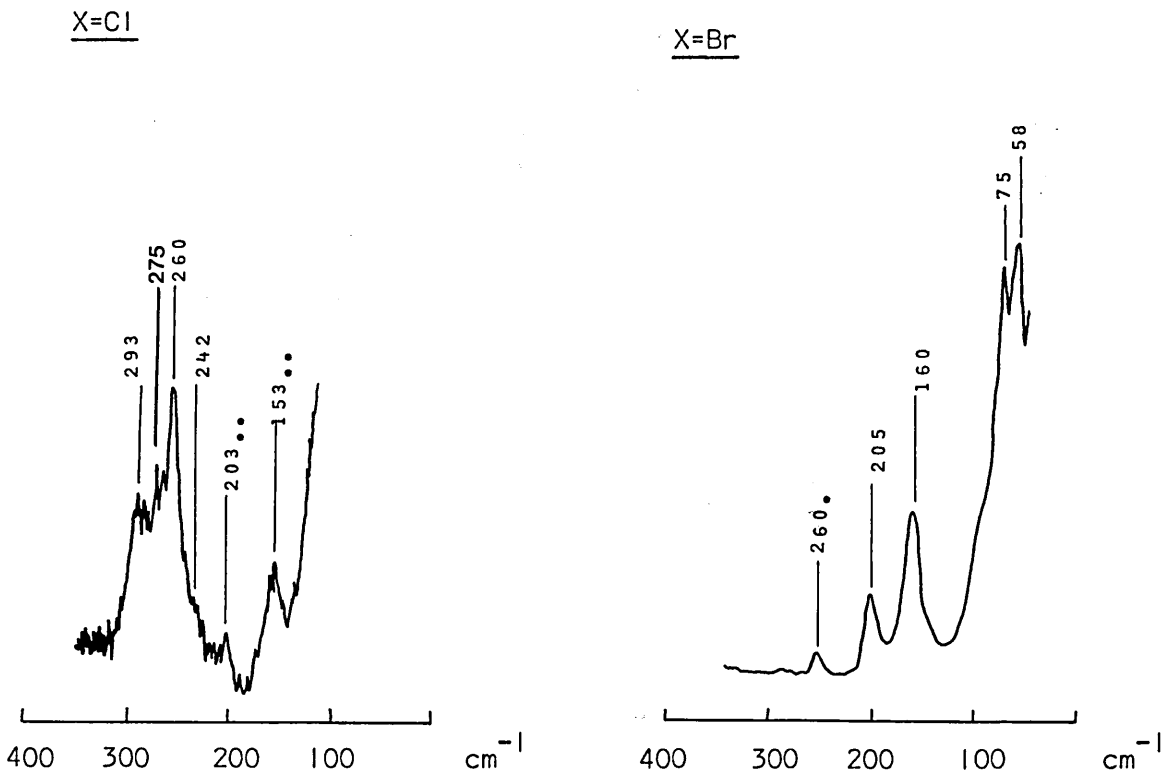

Table 3.17.

Vibrational assiqnments[0] for (2.4-dimethylpyr1dine)HqX^ (X =Cl or Br)

Cl		Br		
IRb	RaC	IRb	Rac	Ass ignments^
3 1Os) 306sh)		206s	205m	v ((HgX)b
	293se	I50s) 142m)	I60s	v 2(H9X)b
27 1m	275s			v 3(HgX)b
240s	242sh			V4(HgX)b
I lOsh)		85s	75s	\ V V H2X)b'
I05m)		67s	58s	bend i ng and
85sh				lattice modes
78s				
61 sh				
44w				

a - omitting internal modes of the ligand,

b - recorded at ca. 30K.

c - recorded at room temperature.

d - numbering of modes is as in Figure 3.3af
the numbering is not significant but used to differentiate between individual modes.

e - plus some contribution from an internal mode of the ligand.

of the ligand have been eliminated as usual, the free ligand spectra having been reported by Green et al.[144] The appearance of the vibrational spectra are far simpler than expected, not all the predicted modes being observed. For the chloro complex the bands at 310, 306, 271 and 240 cm^{-1} (IR) and 293, 275 and 242 cm^{-1} (Ra) are assigned to modes associated with vibration of the shorter Hg-Cl bonds, although the band at 293 (Ra) probably contains some contribution from an internal ligand mode. The appearance of much stronger internal ligand modes for the chloro complex is the result of a higher amplification being used whilst recording the spectrum (see Section 3.3.1b).

The spectra of the bromo complex are even simpler. The bands at 206 (IR) and 205 (Ra) cm^{-1}, and at 150, 142 (IR) and 160 (Ra) cm^{-1} are assigned to two ν(HgBr) modes associated with vibration of the shorter mercury-bromine bridges.

The remaining $\nu(HgX)_b$ modes cannot be assigned individually, but are expected to be contained in the bands appearing below 105 and 90 cm^{-1} in the vibrational spectra of the chloro and bromo compounds respectively.

There was no evidence of the presence of ν(HgN) modes in any of the spectra.

(c) (2,6-dimethylpyridine)HgX_2 (X=Cl or Br). The analogous iodo compound could not be prepared. No crystallographic data are available for these complexes. However, examination of their vibrational spectra indicate a similar structure to that found for (2,4,6-trimethylpyridine)$HgCl_2$, so consequently the spectra have been interpreted using the same line group (C_i) treatment for a polymeric chain (taking the ligand as a point mass) (Appendix 4).

For a chain polymer of this type one predicts the activity and number of internal modes to be:-

$$\Gamma_{chain} = 11A_g\ (Ra) + 9A_u\ (IR)$$

Figure 3.13.

Far-infrared spectra (ca.30K) and Raman spectra (RT) of (2,6-dimethylpyridine)HgX_2 (X=Cl or Br) (cm^{-1})

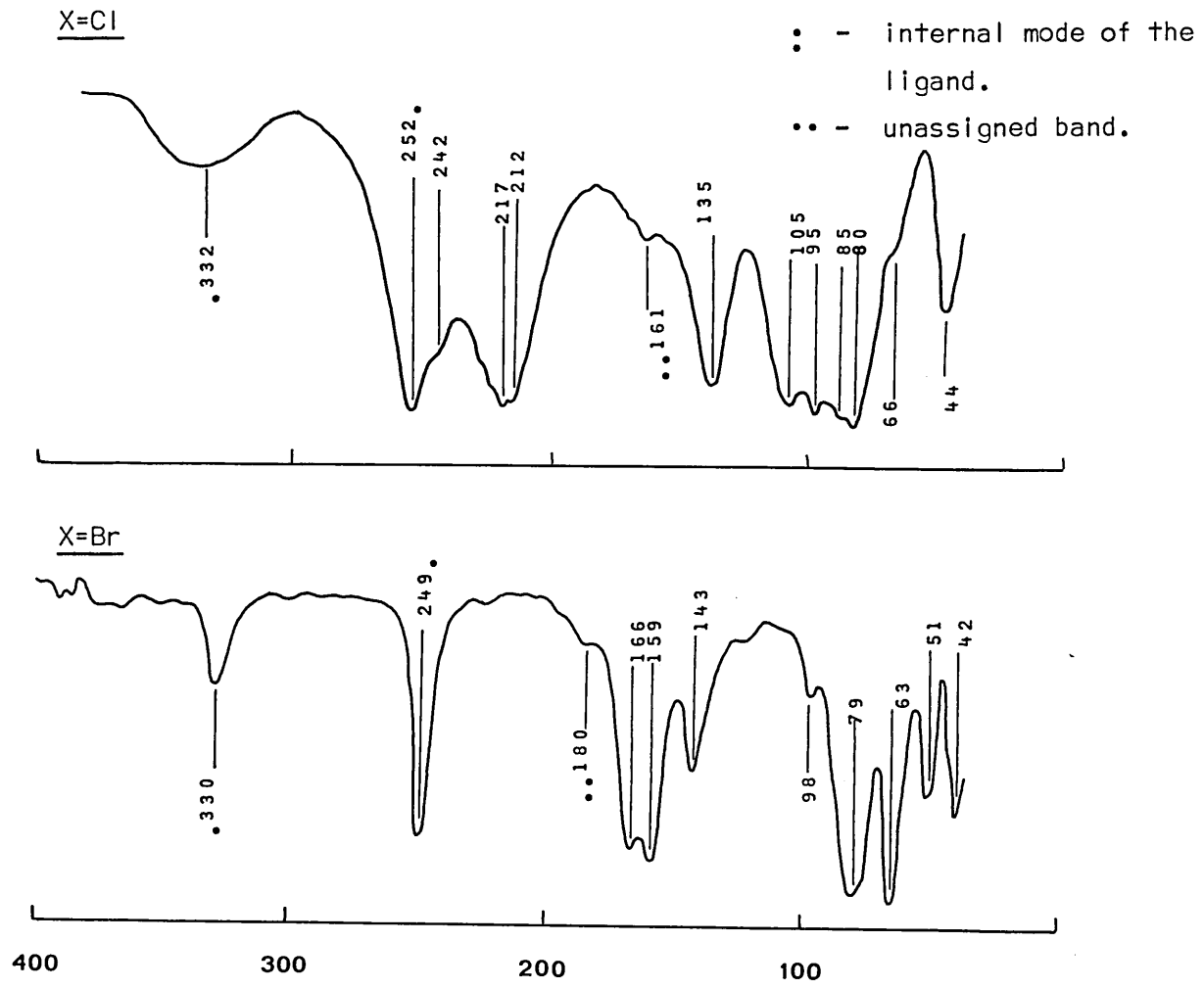

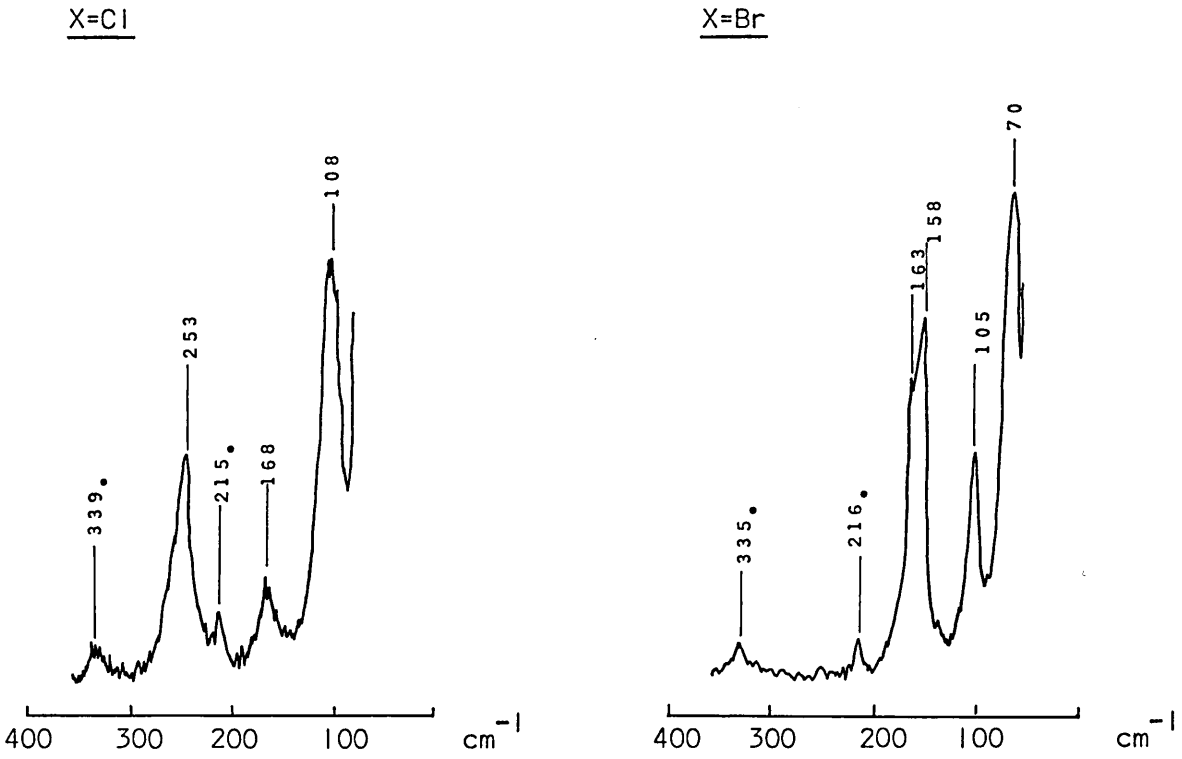

Table 3.18.

Vibrational assignments[0] for (2,6-dimethylpyridine)$_2$HgX$_2$ (X=Cl or Br)

Cl		Br		
IRb	Raᵒ	IRb	RaC	Assignments^
242sh		166s) 159s)		V H 9X)b \
	253		163s) 158s)	V|(H9X)b Au
217s) 212s)		143s		V H9X)b Au
	168m		105m	V H9X)b Ag
135s	108vs	98sh	70vs	> v(HgX)^, bending
105s		79s		and lattice modes.
95s		63s		
85sh		51m		
80s		42m		
66sh				
44m				

a - omitting internal modes of the ligand,

b - recorded at ca. 30K.

c - recorded at room temperature,

d - numbering of modes is as in Figure 3.3a.

The number of modes described as $\nu(HgX)_b$ are predicted to be:-

$$\Gamma\nu(HgX)_b = 4A_g(Ra) + 4A_u(IR)$$

Vibrational data are shown in Figure 3.13 and Table 3.18. Internal modes of the ligand are eliminated as usual (the free ligand spectra have been recorded by Green et al.[144]). The assignments made here agree quite well with those of (2,4,6-trimethylpyridine)HgX_2 complexes. There is a notable convergence of the two highest wavenumber IR-active $\nu(HgX)_b$ modes in the present case, however, which may be explained in terms of a near equivalence of Hg-X bonds in the '$NHgX_2$' units [Hg-Cl distances of 2.40 and 2.54 Å are found in (2,4,6-trimethylpyridine)$HgCl_2$.

Modes associated with $\nu(HgN)$ were not immediately apparent.

3.5.2. Sulphur-donor ligands.

To gain further information concerning the relationships between mercury-halogen spectra and structure, some S-donor complexes of known structure have been examined using infrared spectroscopy (40-400 cm^{-1}).

Sulphur-donor ligands can be of a range of steric and electronic type, including singly-bonded sulphur (e.g. dialkyl and diaryl suphides) and doubly-bonded sulphur (e.g. thiourea or Ph_3PS).

Crystallographic data available for sulphur-donor complexes include:-

*(MPC)$HgCl_2$[58] - an asymmetric dimer

(C_4H_8S)$HgCl_2$[64] - an 'ionic' chain

(Ph_3PS)HgX_2 (X=Cl or Br)[145] - asymmetric dimers (inferred from single crystal photographs)

(dehydrodithizone)$HgCl_2$[60] - a sulphur-bridged polymer

The far-IR spectra of the first three of these complexes and their halo analogues have been studied. The criteria used for vibrational assignments were as used for the (PR_3)HgX_2 complexes.

*MPC = methyl pyrrolidine-1-carbodithioate

(a) $\underline{(Ph_3PS)HgX_2\ (X=Cl,\ Br\ or\ I)}$. The complexes $(Ph_3PS)HgX_2$ (X=Cl or Br) are isomorphous[145] and probably isostructural with $(Ph_3PSe)HgCl_2$, which is known to be a halogen-bridged dimer.[57] The iodo complex is not isomorphous.[145] The spectra of the chloro and bromo complexes can be fully interpreted using a simple point group (C_1) analysis. The modes predicted (taking Ph_3PS as a point mass) are:-

$$\Gamma\nu(HgX)_t = A_g\ (Ra) + A_u\ (IR)$$
$$\Gamma\nu(HgX)_b = 2A_g\ (Ra) + 2A_u\ (IR)$$
$$\Gamma\nu(HgS) = A_g\ (Ra) + A_u\ (IR)$$

Relevant results are contained in Figure 3.14 and Table 3.19. Internal modes of the Ph_3PS ligand have been eliminated using normal procedures. The bands at 304 and 200 cm^{-1} in the chloro and bromo spectra, respectively, are assigned to the $\nu(HgX)_t$ modes, and the bands at 194, 142 (chloro complex) and 139, 98 cm^{-1} (bromo complex) are assigned to the two $\nu(HgX)_b$ modes in each case. The bands at 142 and 139 in the chloro and bromo complexes, respectively, may also contain some contribution from a mode of the Ph_3PS ligand as this does absorb in this region. However, comparison of the relative intensities of the ligand modes within each halo complex spectrum and a similar comparison within the spectrum of free Ph_3PS suggest that this contribution would be comparatively weak. The bands at 294 cm^{-1} (chloro complex) and 295 cm^{-1} (bromo complex) are tentatively assigned as $\nu(HgS)$ by comparison with other reports of $\nu(HgS)$ modes in this region.[16,103]

As already mentioned, the iodo complex is not isomorphous with its other halo analogues. However, internal modes of the ligand have been eliminated leaving a spectrum which also suggests a dimeric structure. Tentative vibrational assignments are contained in Table 3.19 in terms of an iodine-bridged dimer.

(b) $\underline{(MPC)HgX_2\ (X=Cl,\ Br\ or\ I)}$. The structure of $(MPC)HgCl_2$[58] is that

Figure 3.14.

Far-infrared spectra (ca.30K) of $(Ph_3PS)HgX_2$ (X=Cl, Br or I) (cm^{-1})

X=Cl

• - internal mode of the ligand.

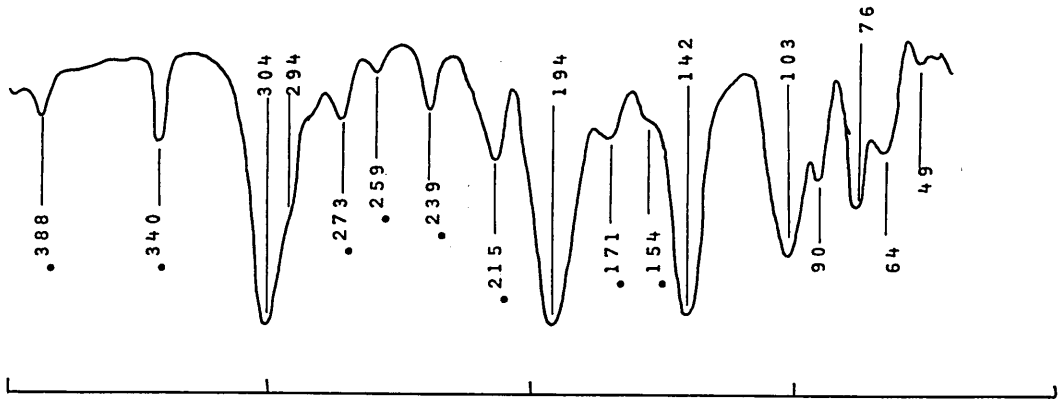

X=Br

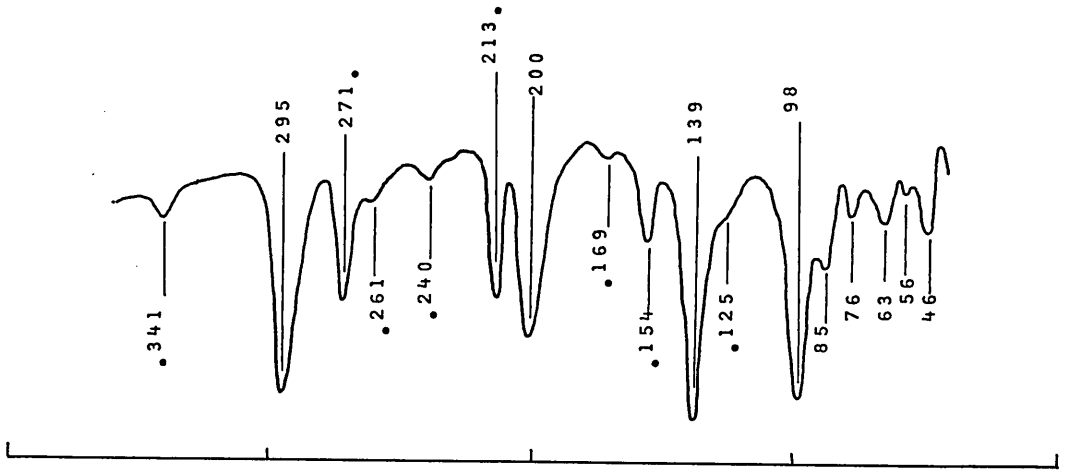

X=I

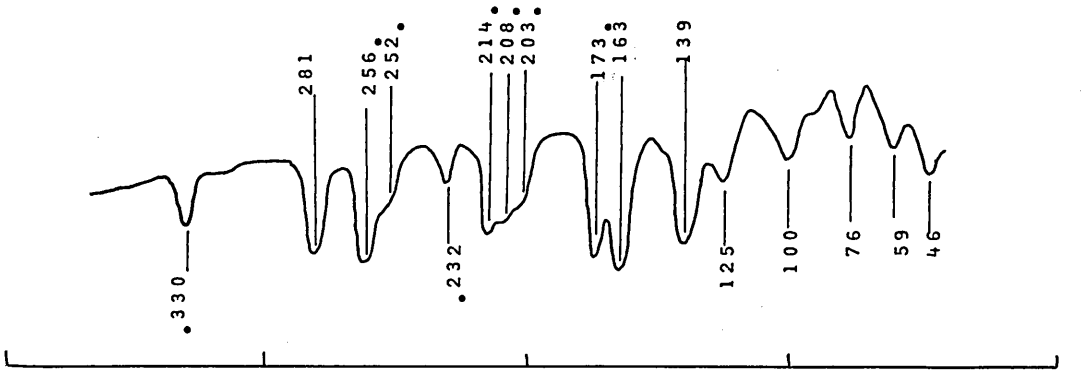

400 300 200 100 cm^{-1}

Table 3.19.

Vibrational assignments[a] for $(Ph_3PS)HgX_2$ (X=Cl, Br or I) (cm^{-1}).

Cl	Br	I	
IR[b]	IR[b]	IR[b]	Assignments
304s	200s	163s	$\nu_{as}(HgX)_t$
		139ms[c]	$\nu_s(HgX)_t$
194s	139s[c]	100m	$\nu(HgX)_b$
142s[c]	98s		
294sh	295s	281s	$\nu(HgS)$
103s	85m	76w	Bending and lattice modes etc.
90m	76w	59w	
76ms	63w	46w	
64m	56vw		
49vw	46w		

a - omitting internal modes of the ligand.

b - recorded at ca. 30K.

c - containing some contribution from an internal mode of the ligand.

of an asymmetric dimer, with one dimer per unit cell. The compound crystallizes in a triclinic system, space group $P\bar{1}$, and consequently solid state effects are not envisaged (cf. $(TPP)HgCl_2$, Section 3.3.1a). Vibrational data are reported in Table 3.20 and Figure 3.15. When internal modes of the MPC ligand have been eliminated the spectra of chloro and bromo compounds appear to be halogen mass-dependent in the manner expected for an isostructural pair. The spectrum of $(Ph_3PS)HgI_2$ is difficult to interpret as the positions of ligand modes appear to be shifted drastically and are very different to those located in the chloro and bromo analogues. Very little can be said about this spectrum other than the bands at 155 and 129 are probably due to some form of $\nu(HgI)$ modes, plus possibly some contribution from the ligand. It seems likely that the MPC ligand is coordinated to mercury in a manner different to that in chloro and bromo compounds.

With regards the chloro and bromo compounds, using a simple point group analysis (C_i) (taking the MPC ligand as a point mass) one may predict:-

$$\Gamma\nu(HgS) = A_g\ (Ra) + A_u\ (IR)$$

$$\Gamma\nu(HgX)_t = A_g\ (Ra) + A_u\ (IR)$$

and

$$\Gamma\nu(HgX)_b = 2A_g\ (Ra) + 2A_u\ (IR)$$

The bands at 291 cm^{-1} (chloro complex) and 195 cm^{-1} (bromo complex) are assigned to $\nu(HgX)_t$, whereas, the bands at lower wavenumber at 206 cm^{-1} (chloro complex) and 149 cm^{-1} (bromo complex) are assigned to one of the two $\nu(HgX)_b$ modes, in each case.

The second $\nu(HgCl)_b$ mode is assigned to the band at 132 cm^{-1}. The corresponding mode for the bromo compound could not be assigned due to strong ligand absorption in the region where it is likely to occur, i.e. ca. 90 cm^{-1}.

Modes due to $\nu(HgS)$ have been tentatively assigned at 283 and 271 cm^{-1} for bromo and iodo complexes, respectively, which leads to the reasonable

Figure 3.15.

Far-infrared spectra (ca.30K) of (MPC)HgX_2 (X=Cl, Br or I) (cm^{-1})

X=Cl

• - internal mode of the ligand.

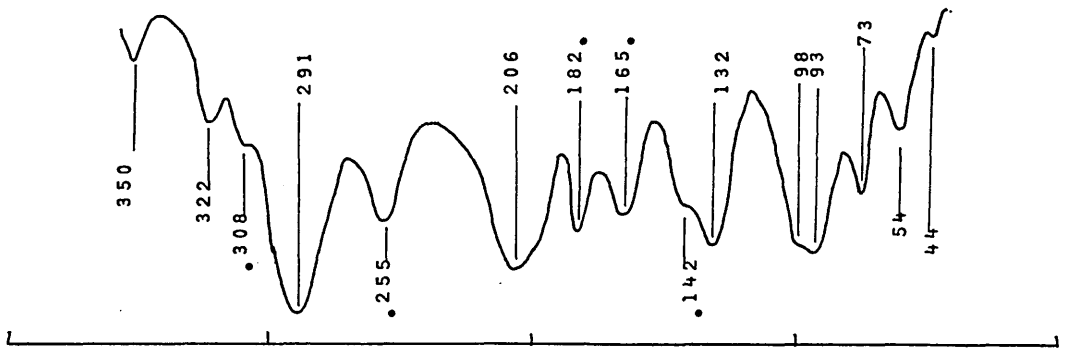

X=Br

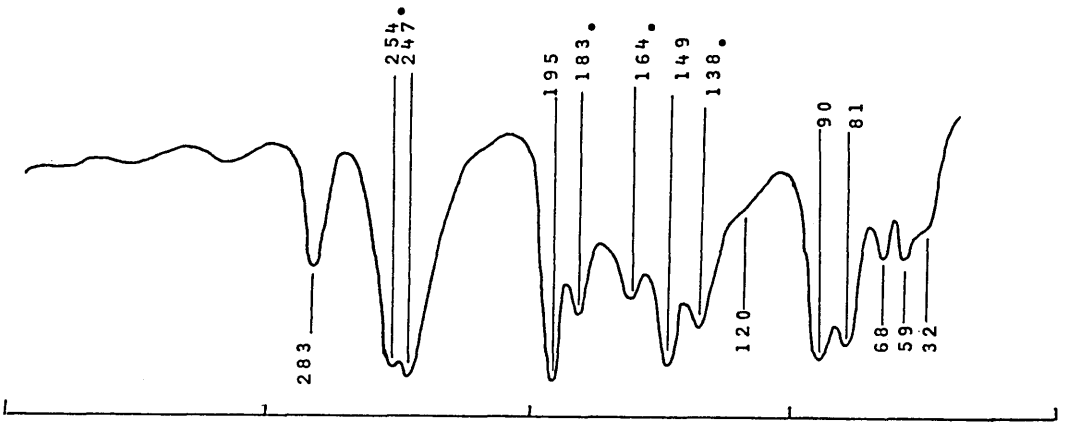

X=I

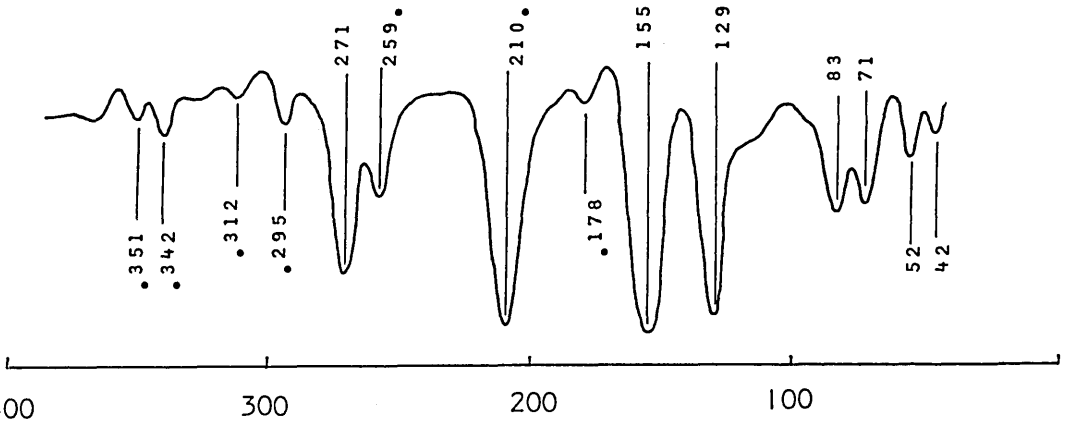

Table 3.20.

Vibrational assignments[a] for (MPOHqX^ (X=C1, Br or I) (cm^{-1}).

Cl	Br	Ib		
IRC	IRC	IRC		Ass ignments
291sd	283ms	27 Is		v(HgS)
291sd	I95s	I55s) I29s)		V(HgX),
206s	149			v(HgX)b
I32s				v(HgCI)b
98s	90s	83m	^	Bending i
93s	8 1s	7 1m	1	and
73ms	68w	52w		lattice modes
54m	59w	42w		
44w	32sh			
			>	

a - omitting internal modes of the ligand,

b - see text,

c - recorded at ca_. 30K.

d - coincident bands.

conclusion that the band assigned $\nu(HgCl)_t$ at 291 cm^{-1} probably contains some contribution from $\nu(HgS)$.

(c) $\underline{(C_4H_8S)HgX_2\ (X=Cl\ or\ Br)}$. The structure of the chloro complex[64] is similar to the 'ionic' chain structure found for $(PMe_3)HgCl_2$. However, in the present case each 'Hg---Cl^-' distance is slightly shorter. A similar vibrational treatment has been used as for $(PMe_3)HgCl_2$ (Appendix 4) i.e. a factor group analysis with two cations and two anions per unit cell.

The stretching modes associated with the $[S-Hg-Cl]^+$ cation (taking C_4H_8S as a point mass) are:-

$$\Gamma\nu(HgCl)_t = A_g\ (Ra) + A_u\ (IR)$$

$$\Gamma\nu(HgS) = A_g\ (Ra) + A_u\ (IR)$$

The number and activities of modes due to cation and anion translations are predicted to be:-

$$\Gamma_{ionic\ trans.} = 6A_g\ (Ra) + 3A_u\ (IR)$$

The IR spectra are shown in Figure 3.16. It should be mentioned that because of the instability of both these complexes the IR spectra were recorded immediately after preparation using the 'sandwich disc method' described in Section 7.2.

Internal modes of the ligand have been eliminated by comparison of chloro and bromo spectra. The remaining bands show typical halogen mass-dependence suggesting the bromo complex is isostructural with the chloro complex. The $(C_4H_8S)HgCl_2$ spectrum is similar to that of $(PMe_3)HgCl_2$, the one significant difference being the higher wavenumber positions of the ion translatory modes. This is not surprising when one considers the shorter Hg---Cl^- distances found for the $(C_4H_8S)HgCl_2$ complex. Vibrational assignments and wavenumber positions are contained in Table 3.21.

Figure 3.16.

Far-infrared spectra (ca. 30K) of $(C_4H_8S)HgX_2$ (X=Cl or Br) (cm^{-1})

• - internal mode of the ligand.

•• - unassigned band.

X=Cl

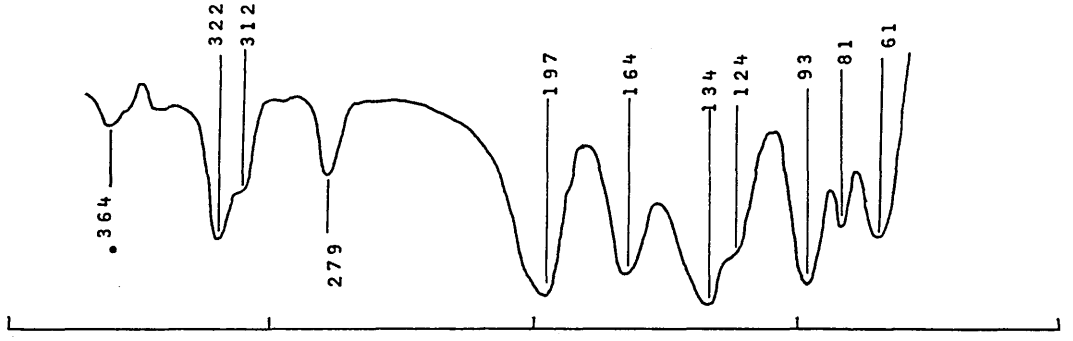

X=Br

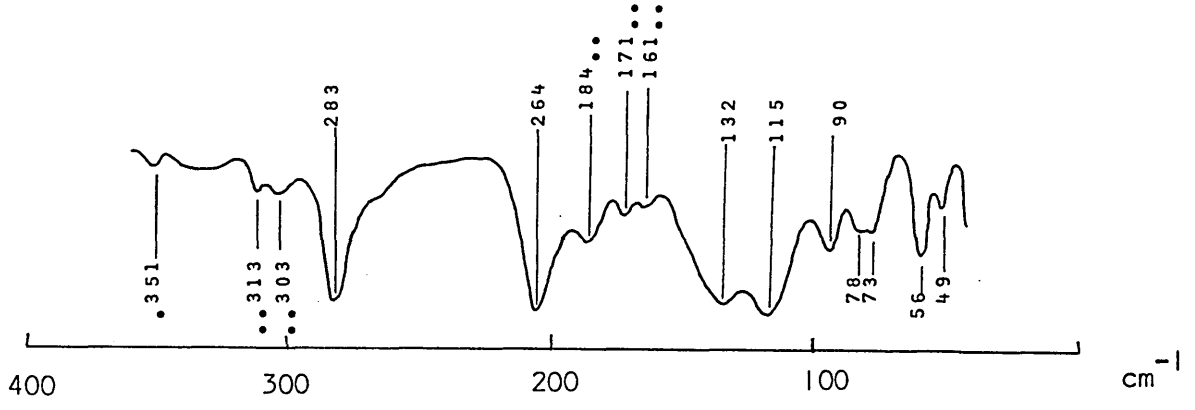

Table 3.21.

Vibrational assignments[a] for $(C_4H_8S)HgX_2$ (X=Cl, Br or I) (cm^{-1}).

Cl	Br	
IR[b]	IR[b]	Assignments
322s) 312sh)	204s	$\nu(HgX)_t$ A_u
279m	283s	$\nu(HgS)$ A_u
197s	132s	Cation and anion
164s	115s	translations,
134s	90m	bending and
124sh	78w	lattice modes.
93s	73w	
81mw	56m	
61s	49w	

a - omitting internal modes of the ligand.

b - recorded at ca. 30K.

3.5.3. Oxygen-donor ligands.

A number of complexes formed between oxygen-donor ligands and $HgCl_2$ have been studied crystallographically. Most of these structures contain almost undistorted $HgCl_2$ units, with Cl-Hg-Cl angles of ca. 170°, loosely held together by Hg-Cl contacts of ca. 3 Å. To study the vibrational properties of such structures the three complexes $(Ph_2SO)HgCl_2$, (Coumarin)$HgCl_2$ and (quinoline-N-oxide)$HgCl_2$ have been examined using far-infrared spectroscopy.

To a first approximation the structures shall be treated as discrete '$OHgCl_2$' units in which the $HgCl_2$ portion is only slightly bent. The symmetry of these tetratomic species is C_{2v}. One would therefore expect to observe three modes of vibration all both IR- and Raman-active, corresponding to the motions shown on p201. The infrared spectra and vibrational assignments for the compounds studied are shown in Figure 3.17. Internal modes of the ligands have been eliminated by comparison with free ligand spectra.

The stretching modes of linear $HgCl_2$ (point group $D_{\infty h}$) have been shown to occur[92] at 368 cm^{-1} for ν_a(HgCl) and at 330/310 cm^{-1} for ν_s(HgCl). One would not have expected to observe the ν_s(HgCl) mode in the IR-spectrum for a molecule of this symmetry (rule of mutual exclusion); its presence is a result of solid state effects. The wavenumber position of the δ(ClHgCl) mode for linear $HgCl_2$ has been characterized using matrix isolation methods[148] and is found to occur at ca. 100 cm^{-1}.

The present three spectra are similar to that found for solid $HgCl_2$. The ν_a(HgCl) mode is readily assigned in all three complexes, the positions

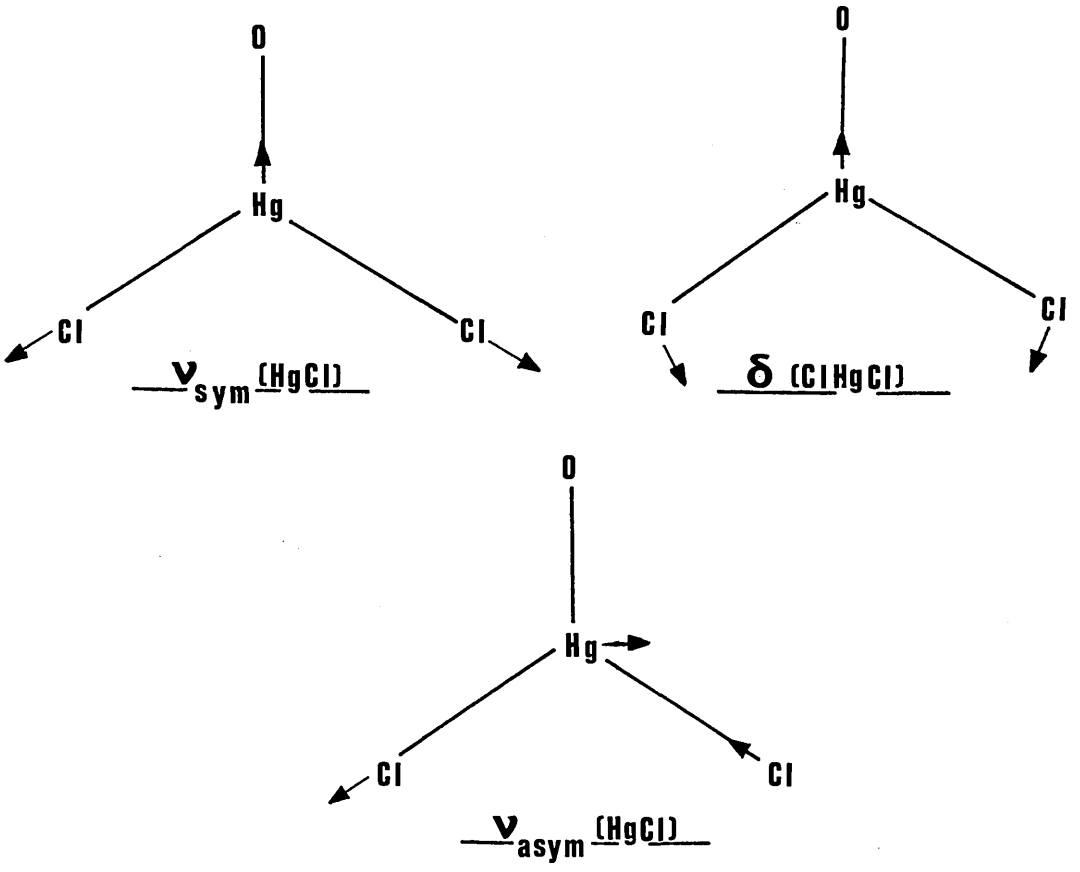

of these modes however appear at ca. 20-30 cm^{-1} lower in each case. For the Ph_2SO and quinoline-N-oxide complexes there are two bands in the ν_a(HgCl) region. This phenomenon may be attributed to correlation effects; Raman spectra would help clarify this situation.

Bands at 290 and 281 cm^{-1} for (quinoline-N-oxide)$HgCl_2$ may be assigned to ν_s(HgCl), these bands are ca. 30 cm^{-1} lower than found in solid $HgCl_2$. The appearance of two bands may again be due to solid state effects.

The ν_s(HgCl) mode in the other two complexes could not be assigned, because of intereference due to internal ligand modes in the region ca. 300 cm^{-1}.

Far-infrared spectra (ca.30K) of some (o-donor)$HgCl_2$ complexes.

$(Ph_2SO)HgCl_2$ • - internal mode of the ligand.

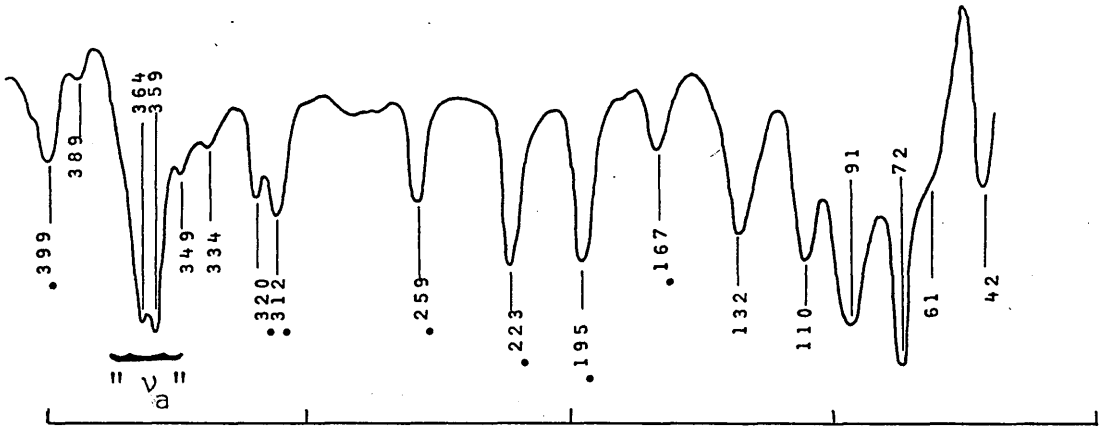

(Coumarin)$HgCl_2$

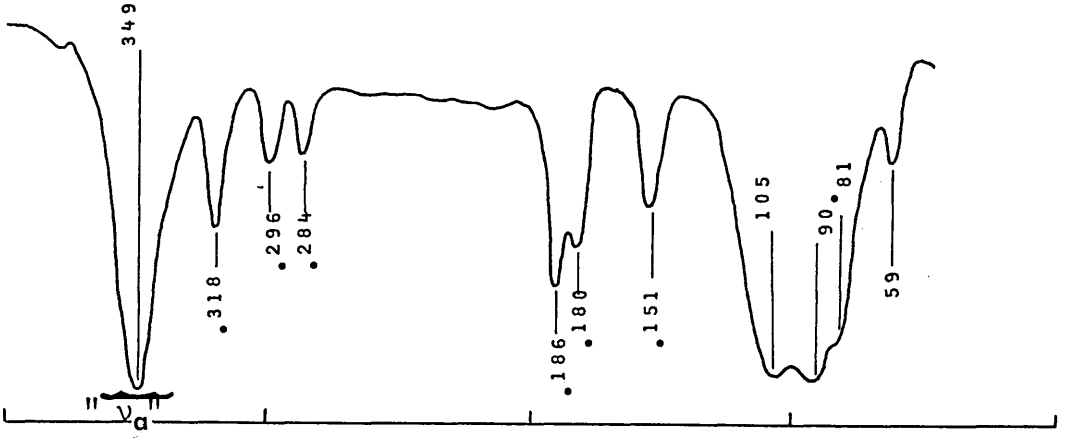

(quinoline-N-oxide)$HgCl_2$

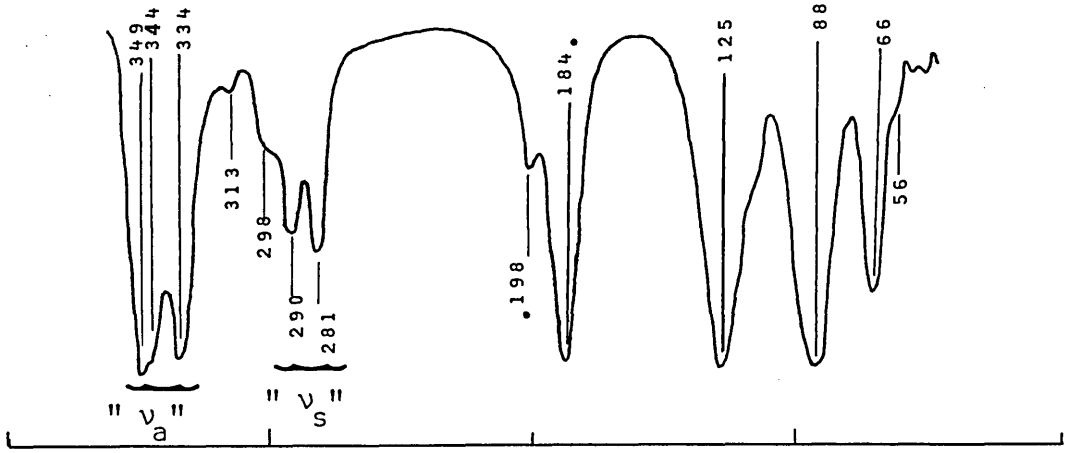

The lower reaches of the spectra ($< 120\ cm^{-1}$) become very complicated. Here, one would expect to observe the δ(ClHgCl) mode, modes associated with the long range Hg-Cl contacts and lattice modes. It was not possible to make any further vibrational assignment. There was no evidence of modes due to ν(HgO).

Although only a few ν(HgCl) modes have been assigned in the spectra of the above three complexes it is significant that there are similarities between them, and the spectrum of $HgCl_2$ itself, which, would seem to reflect the very weak Hg-O interactions.

3.6. GENERAL DISCUSSION

Throughout this work on the $(L)HgX_2$ systems elimination of bands arising from internal modes of ligands has been a major problem. Such bands often appear in regions where they 'mask' ν(HgX) modes. In isolation this 'masking' would not be a difficult problem, for comparison of a halo series should allow their elimination. However, for some of the halo series studied different structures are probable and consequently the numbers, wavenumber positions and intensities of these modes will vary within a series thus making their elimination difficult. Raman spectra appear to be more susceptible to interference of this kind than are IR spectra (Section 3.3.1b); consequently examination of IR data allows structure/spectra correlations to be made more readily than do Raman data. As far as it is possible to tell, the Raman data obtained were compatible with the conclusions reached using the IR data.

In spite of the aforementioned difficulties concerning spectral interpretation, a number of ν(HgX) assignments have been compiled (Table 3.22) from which structure/spectra relationships have been derived. The ν(HgX) mode data for the general case of complexes $(L)HgX_2$ (L=N-, P-, S- or O-donor ligand) (Section 3.5) are in agreement with correlations presented in

Section 3.3.1f for $(PR_3)HgX_2$ complexes; Table 3.22 has been expanded to include some further structures observed for the 1:1 system.

Consideration of the structure and spectra of some $(L)HgX_2$ complexes of known structure indicates that a similar pattern is emerging as found for comparable chloromercurate(II) complexes[96] (Section 1.4.1). Table 3.23 contains structural descriptions and vibrational data of some addition complexes and chloromercurate(II) salts whose mercury-chlorine skeletal structures are similar. One may note the similarity in wavenumber positions of ν(HgCl) modes which to some extent reflect the similarities in coordination environment about mercury and the degree of Hg-Cl bridging. The highest wavenumber ν(HgCl) modes are dependent upon the coordination environment about mercury, which in turn is dependent upon the nature of the donor ligand. For the O-donor complexes such as $(Ph_2SO)HgCl_2$[72] where the mercury-ligand interaction is very weak, the $HgCl_2$ unit remains virtually unaffected, and consequently the IR spectra contain bands at wavenumbers just below that found for $HgCl_2$ (solid) (Table 3.23). For complexes formed between mercuric chloride and ligands containing N-, P- or S-donor atoms, where there is a stronger mercury-ligand interaction the $HgCl_2$ unit is considerably perturbed giving rise to a number of structural possibilities, e.g. dimeric, polymeric, 'ionic' chain or tetrameric. These structures may be characterized to some extent by the wavenumber positions of the highest occuring ν(HgCl) mode. The wavenumber values decrease progressively as the coordination environment of the short Hg-Cl bonds changes from linear, to distorted tetrahedral (in a dimer) through to trigonal bipyramidal (Table 3.23). Further characterization of these structures may be observed by examination of $\nu(HgCl)_b$ data. One may note the similarity in wavenumber position of $\nu(HgCl)_b$ modes assigned for $[(PPh_3)HgCl_2]_2$ and $[Hg_2Cl_6]^{2-}$ species on the one hand, and for $[NHgCl_2]_n$ and $[HgCl_3]_n^{n-}$ species on the other

(Table 3.23).

As a consequence of the variation in Hg-Cl bridge bond length observed for the range of $(L)HgCl_2$ structures [e.g. as short as 2.56 Å for $(PEt_3)HgCl_2$ and as long as 3.489 Å for $(PMe_3)HgCl_2$], a similarly wide wavenumber range is observed within which $\nu(HgX)_b$ modes have been assigned (Table 3.22). It should be mentioned that a correlation exists between the length of Hg-Cl bonds, both terminal and bridging, and the wavenumber positions of bands assigned to $\nu(HgCl)$ modes (Figure 3.18a). It is almost as if each Hg-Cl bridge bond behaves as a single independent bond, and the wavenumber position of the vibrational stretching mode associated with this 'single' bond is dependent on bond length. Although this correlation appears to be consistent for Hg-Cl ranging from ca. 2.3 - 3.0 Å and $\nu(HgCl)_b$ modes assigned between ca. 100 and 360 cm^{-1}, the situation for Hg-Cl bonds longer than ca. 3 Å is difficult to assess. The spectra in this lower region are complicated by the possibility of various deformation, bending and lattice modes, so that assignments have been limited. Presumably, when a Hg-Cl distance is greater than the sum of the van der Waals' radii for mercury and chlorine, bonding interaction will cease. We would then have 'lost' a $\nu(HgCl)_b$ mode and 'gained' an external lattice mode. It may be envisaged that around this point the curve would 'flatten' as shown in Figure 3.18b. Obviously the wavenumber position of the mode associated with these longer Hg-Cl distances cannot decrease simply as a function of the curve because at ca. 3.3 Å a zero wavenumber value would be observed, which has no physical meaning for a solid.

The use of this curve for predicting Hg-Cl bond lengths is to be warned against because the situation is probably more complicated than it appears, as one finds when one attempts to fit the vibrational data for α-$(PBu^n_3)HgCl_2$ to this curve (Figure 3.18a).

Equivalent bromo complexes (L=N-, P-, or S-donor ligand) appear to show similar spectral trends to their chloro counter-parts; ν(HgBr) modes associated with vibrations of 'short' Hg-Br bonds have been assigned at ca. 200 cm^{-1} for polymeric chain, 'ionic' chain and dimeric structures (Table 3.22). The wavenumber positions of $\nu(HgBr)_b$ modes are found to vary considerably from ca. 50-170 cm^{-1} depending on the structural type (Table 3.22). Detailed comparison of bond length and wavenumber data is not possible due to the lack of precise Hg-Br bond length results.

Due to the lack of crystallographic data for the $(L)HgI_2$ complexes (only the crystal structure of $(PPh_3)HgI_2$ is known, inferred from single-crystal X-ray photographs) only tentative structure/spectra correlations can be made at the present time. It appears that for an iodine-bridged dimer $\nu(HgI)_t$ modes occur at ca. 150 cm^{-1} whereas $\nu(HgI)_b$ modes occur between ca. 90 and 120 cm^{-1}.

The general relationships between crystal structure and vibrational spectra outlined above have allowed a number of structural proposals to be made based solely on vibrational data. Some of these proposals are only very tentative (Table 3.22). Many of the proposed structures are similar to those already observed, while other complexes show (at the present time) quite inexplicable vibrational spectra [e.g. $(PEt_3)HgI_2$ and $(PPr^n_3)HgCl_2$], suggesting that other completely different structures exist. An interesting situation exists for β-$(PPr^n_3)HgI_2$ and $(PMe_3)HgI_2$, where the positions of the highest wavenumber bands attributable to ν(HgI) are relatively low for complexes of this stoicheiometry (ca. 130 cm^{-1}). It is this region where one observes ν(HgI) modes for $[HgI_4]^{2-}$ [96] and sometimes $[HgI_3]^-$ [96]. The possibility of the existence of the $[HgI_4]^{2-}$ ion or discrete 'monomeric $(PR_3)HgI_2$' species in these adducts should not be dismissed.

Information concerning ν(HgL) modes has generally been disappointing.

Data have been limited to tentative assignments for

ν(HgP) at ca. 165 cm^{-1} for $(TPP)HgX_2$ (X=Cl or Br),

at ca. 137-157 cm^{-1} for $(PPh_3)HgX_2$ (X=Cl, Br or I),

and at ca. 350 cm^{-1} for $(PMe_3)HgX_2$ (X=Cl, Br or I);

and for ν(HgS) at ca. 281-295 cm^{-1} for $(Ph_3PS)HgX_2$ (X=Cl, Br or I),

at ca. 280 cm^{-1} for $(C_4H_8S)HgX_2$ (X=Cl or Br).

As a result of the present work, previous vibrational spectroscopic reports for $(L)HgX_2$ complexes may be considered (Table 1.5). Crystallographic data presented in Chapter 2 have shown that many of the vibrational spectroscopic data in Table 1.5 have been based on false premise[2-6,11-15]; instead of the existence of solely discrete trans halogen-bridged dimeric structures a range of structural arrangements exist. These structures cannot be distinguished **at all** by the location of a single IR-active $\nu(HgCl)_t$ mode. Spectral information is required covering the entire far-IR region of the spectrum and even then caution should be exercised when making structural proposals.

In other cases a single $\nu(HgX)_b$ mode has been located in addition to a $\nu(HgX)_t$ mode, e.g. in the 'thiourea' complexes.[16] Whilst the assignment of these $\nu(HgX)_b$ modes may be correct, the structural inferences should still be treated with caution, because, as has been shown for dimeric $(PPh_3)HgCl_2$ and polymeric $(PEt_3)HgCl_2$, the IR spectra above ca. 150 cm^{-1}, which includes $\nu(HgCl)_t$ and $\nu(HgCl)_b$ modes, are not that dissimilar and study of the even lower, more complicated, wavenumber regions is required. Crystallographic data could help provide the necessary basis to enable interpretation of these systems.

Fig. 3.18a Correlation between ν(HgCl) and bond length

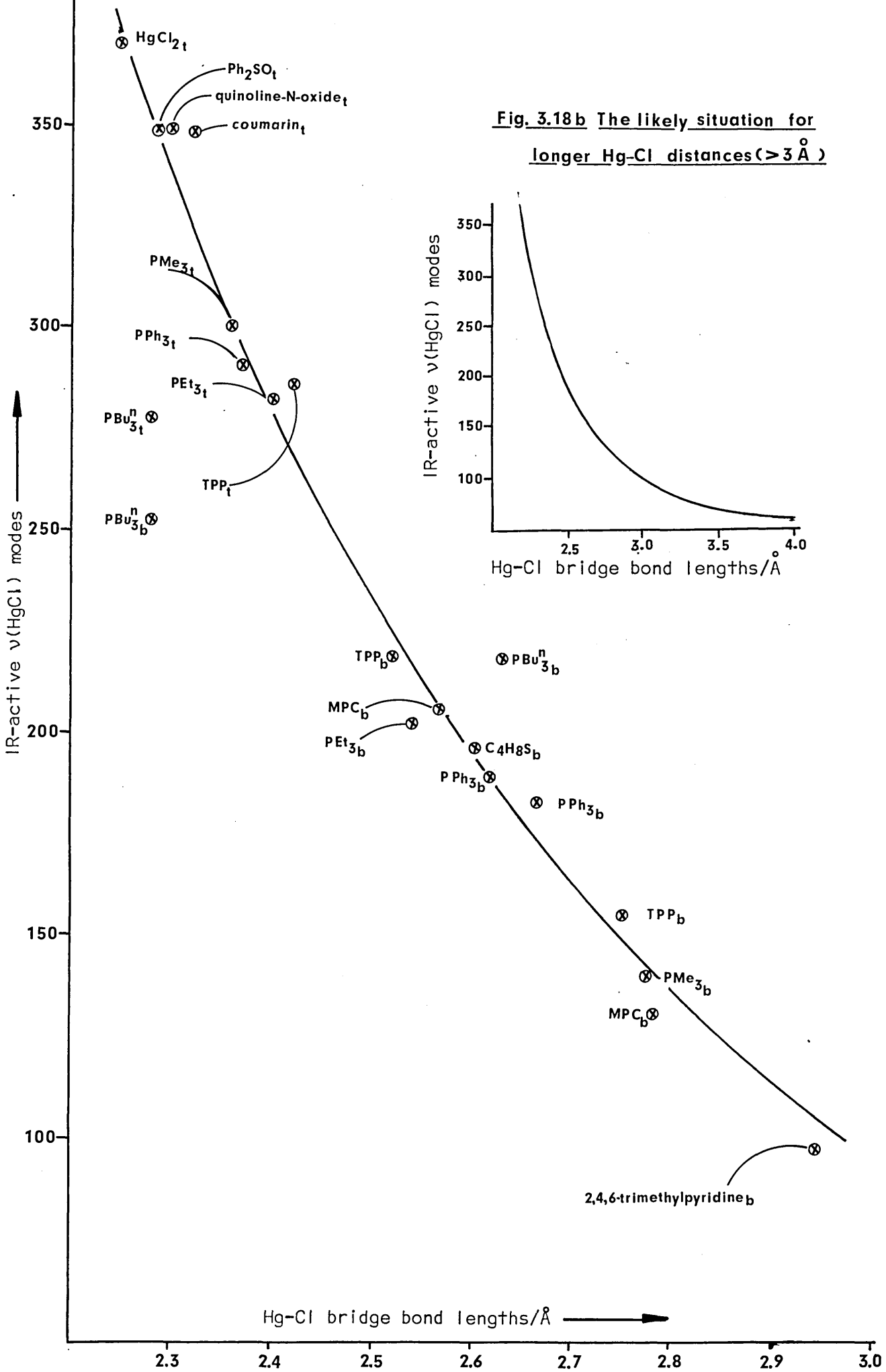

Fig. 3.18b The likely situation for longer Hg-Cl distances (> 3 Å)

Table 3.22.

Summary of ν(HgX) mode data for $(L)HgX_2$ complexes.

Compound	Structure*	ν(HgX)/cm^{-1}		ν(HgX)$_b$/cm^{-1}	
		IR	Ra	IR	Ra
$(L)HgCl_2$ complexes					
L=					
TPP	asymmetric dimeric	283		219,156	204,168
			282		
PPh_3	symmetric dimeric	291		188,183	n.a
		288	286		
PEt_3	polymeric chain	286		203 198, 117,105	207,126,94,76
			270	90	
			260		
PMe_3	'ionic' chain	300		141	142
			291		
PPr^n_3	?	305		205,178,169	208,189,169
			298	144	
α-PPh_2Me	(polymeric chain)?	286		203,132,110	n.a
		281	283		
β-PPh_2Me	('ionic' chain)?	310		165	
$PPhMe_2$	('ionic' chain)?	312	318	120	129
		302	303		
2,4,6-$Me_3C_5H_2N$	polymeric chain	261	n.r	229, 130	n.r
2,4-$Me_2C_5H_3N$	polymeric chain	310		240,105,85	275
		306		110 78	260
			292.5		
2,6-$Me_2C_5H_3N$	polymeric chain	242		217,135 212	167.5,108
			252.5		
Ph_3PS	dimeric	304	n.r	194,142	n.r
MPC	dimeric	291	n.r	206,132	n.r
C_4H_8S	'ionic' chain	315	n.r	197	n.r
Ph_2SO	polymeric structures	364	n.r	n.a	
	containing almost	359			
Coumarin	linear	349	n.r	n.a	n.r
Quinoline-N-oxide	Cl-Hg-Cl units	349	n.r	n.a	n.r
		344			

Table 3.22, continued

Compound	Structure*	ν(HgX)/cm^{-1} IR	ν(HgX)/cm^{-1} Ra	ν(HgX)$_b$/cm^{-1} IR	ν(HgX)$_b$/cm^{-1} Ra
(L)HgBr$_2$ complexes					
L=					
TPP	asymmetric dimeric	195	195	151,117	153,122
PPh_3	symmetric dimer	203 190	200 192	137,117	150
PEt_3	(polymeric chain)	190	185	91 144, 84 72	164 145
PMe_3	'ionic' chain	216	208 193	116	106
PPr^n_3	(dimeric)?	203 181	196 179	144	145
PPh_2Me	('ionic' chain)?	221	216	129	n.a
$PPhMe_2$	('ionic' chain)?	225	223	96	129
2,4,6-$Me_3C_5H_2N$	(polymeric chain)	196 180	n.r	159, 85 154	n.r
2,4-$Me_2C_5H_3N$	polymeric chain	206	205	150,85,67	160,75,67.5
2,6-$Me_2C_5H_3N$	(polymeric chain)	166 159	162.5 157.5	143, 98	105,70
Ph_3PS	dimeric	200	n.r	139,98	n.r
MPC	dimeric	195	n.r	149	
C_4H_8S	('ionic' chain)	204	n.r	132	n.r
(L)HgI_2 complexes					
L=					
PPh_3	dimeric	163 139	160 142.5	117,89	125
PEt_3	?	151	143 134	93 90	112

Table 3.22, continued

Compound	Structure*	ν(HgX)/cm^{-1} IR	ν(HgX)/cm^{-1} Ra	ν(HgX)$_b$/cm^{-1} IR	ν(HgX)$_b$/cm^{-1} Ra
(L)HgI_2 complexes, (continued)					
L=					
PMe_3	(HgI_4^{2-} present	132		n.a.	n.a.
	or 'monomeric	125	123		
α-PPr^n_3	(PR_3)HgI_2	134	137.5	n.a.	n.a.
	species')?	129	117.5		
β-PPr^n_3	(dimeric)?	157	157	90	114
		134	138		
PPh_2Me	(dimeric)?	165	164	105,90	103,97,89
		149	146		
$PPhMe_2$	(dimeric)?	159	161	112,105,90	114
		144	148		

* - Structural descriptions contained in parentheses are those inferred from vibrational studies and when followed by a question mark are only tentative proposals; remaining descriptions are either derived from full crystallographic analysis or from single crystal photographic studies.

n.a. - not assigned.

n.r. - not recorded.

Table 3.23.

Comparison of some ν(HgCl) mode data for some structurally similar addition and chloromercurate(II) complexes.

Coordination geometry	Remarks	Addition complexes			Chloromercurate(II) complexes		
		Example	$\nu(HgCl)_s/cm^{-1}$	$\nu(HgCl)_b/cm^{-1}$	Example	$\nu(HgCl)_s/cm^{-1}$	$\nu(HgCl)_b/cm^{-1}$
near-linear Cl-Hg-Cl units.	Extended structures containing long Hg-Cl contacts	$(Ph_2SO)HgCl_2$	364,359	n.a	$HgCl_2$(solid)	368	n.a
Distorted tetrahedral	Chlorine-bridged dimers	$(PPh_3)HgCl_2$	291	188,183	β-$[NET_4]_2[Hg_2Cl_6]$	280	188
Distorted trigonal bipyramidal	Chlorine-bridged polymeric chains containing $(NHgCl_2)$ or $[HgCl_3]^-$ units	(2,4,6-$Me_3C_5H_2N)HgCl_2$	261	75-98	$[SMe_3][HgCl_3]$	263	100*

n.a - not assigned

* - denotes assignment made in the present work.

Chapter 4.

Crystallographic studies of some $(PR_3)_2HgX_2$ complexes.

Contents

4.1. CRYSTALLOGRAPHIC STUDIES OF SOME $(PR_3)_2HgX_2$ COMPLEXES.

4.1.1. Introduction.

On the basis of vibrational spectroscopic studies (Section 1.4.2) complexes of 2:1 stoicheiometry have generally been inferred to have discrete tetrahedral monomeric structures or polymeric structures in which mercury lies in a distorted octahedral environment, as in $(Py)_2HgCl_2$.[84] In the main these inferences have no basis, because only for $(Py)_2HgCl_2$ have spectroscopic studies been based on sound crystallographic data. Therefore, present knowledge regarding relationships between vibrational spectra and crystal structure for $(L)_2HgX_2$ complexes would benefit from a systemmatic spectroscopic and crystallographic study. Towards this end crystallographic and spectroscopic studies of some $(PR_3)_2HgX_2$ complexes have been undertaken.

Whilst this work was in progress the first $(PR_3)_2HgX_2$ structure, that of $(PPh_3)_2HgI_2$,[74] which is a discrete tetrahedral monomer, was reported. This structure confirms the previously reported structural proposal by Deacon *et al.*,[7] on the basis of far-infrared data. Similar monomeric structures have been proposed for $(PPh_3)_2HgX_2$ (X=Br or Cl)[7] and $(PR_3)_2HgX_2$ (PR_3=PBu^n_3[90] or PCy_3[6]; X=Cl, Br or I).

The existence of other different structures have also been reported. Schmidbaur *et al.*[4] inferred that $(PMe_3)_2HgX_2$ complexes contain linear $[P\text{-}Hg\text{-}P]^{2+}$ cations and two X^- anions, on the basis of vibrational spectroscopic and conductivity data. Kessler,[90] on the basis of ^{31}P n.m.r data and of very low lying $\nu(HgX)$ modes, which were assigned $\nu(HgX)_b$, proposed that $(PEtMe_2)_2HgX_2$ (X=Br or I) complexes contain linear P-Hg-P species, along an apical axis, surrounded by halogen-bridges in the equatorial plane. Vibrational data recorded in this work, some previously reported and some new, show a very wide wavenumber range within which $\nu(HgX)$ modes may be assigned. This observation further suggests different structures exist for $(PR_3)_2HgX_2$

complexes.

In view of the structural effects of varying PR_3 in $(PR_3)HgX_2$ compounds (Chapter 2), and also considering that a range of structures overall are known for $(L)_2HgX_2$ compounds (Section 1.3.3), it did not seem unlikely that different structures may be found in 2:1 phosphine adducts.

In an attempt to verify the proposals of Kessler concerning 'monomeric' $(PBu^n_3)_2HgX_2$ (X=Cl, Br or I) and 'associated' $(PEtMe_2)_2HgX_2$ (X=Br or I) the crystal structure of $(PEtMe_2)_2HgBr_2$ and the preliminary crystallographic analysis of $(PBu^n_3)_2HgCl_2$ have been carried out. Also, in order to explain the low wavenumber positions of bands assigned ν(HgX) in the $(PEt_3)_2HgX_2$ series, the crystal structure of $(PEt_3)_2HgCl_2$ has been determined. As well as providing information for the spectroscopist regarding structure/spectra relationships some further aspects of the coordinating behaviour of HgX_2 with PR_3 ligands may be examined.

4.1.2. The crystal structure of $(PEt_3)_2HgCl_2$

Crystal Data.

$C_{12}H_{30}P_2HgCl_2$, M_r=507.80, Tetragonal,

a=b=12.060(10), c=14.199(12) Å;

α=90.00 . β=90.00 . γ=90.00 .

D_m=1.60 g cm^{-3} (by flotation in a $CHBr_3/CHCl_3$ mixture), D_c=1.63 g cm^{-3}.

Z=4 (molecules lie on special positions and so there are four molecules/unit cell)

$F_{(ooo)}$=983.82 μ(Mo-K_α)=75.48 cm^{-1}

Systematic absences:-

hoo reflections are absent for h=2n + 1

ool " " " " l=2n + 1

In addition to these absences certain reflections appear systematically weak:-

hkl reflections appeared very weak for l =2n

hk0 " " " " " h+k =2n.

It was deduced from these absences and systematic weakness that that the crystals belonged to space group $P4_22_12$ (D_4^6, No. 94)[112] with mercury atoms located on 'special positions' along the two-fold rotation axes.

Data Collection and Structure Refinement. All unique diffraction data for a crystal of this symmetry is contained in a segment $1/16^{th}$ of the sphere of reflection. In order to collect only unique diffraction data the tetragonal unit cell was modified to:

a=17.056, b=12.060, c=14.199 Å

$\alpha=\beta=90$, $\gamma=135^\circ$

As a result of collecting the data in this way some reflections had to be reindexed before subsequent structure solution. The relationship between the indices of collected data and the correct indices was:

$$hkl_{correct} = (h+k)\ k\ l_{collected}$$

Colourless crystal, approximate dimensions 0.42x0.08x0.25 mm , mounted about c.Fifteen layers,hk0→hk14, were collected; 902 reflections with $2\theta < 50^\circ$; 488 had $I/\sigma(I) \geq 2.0$ and were used for refinement. Unit weights were used, and no absorption correction was applied.

The temperature factors of the carbon atoms in this structure are quite high, as found for some of the $(PR_3)HgCl_2$ structures reported in this work. This phenomenon may again be attributed to genuinely high thermal motion of the carbon atoms, or domination of diffraction data by Cl, P and especially Hg within the 2θ range recorded. The former explanation is thought to be more appropriate in the present case as location of carbon atoms provided no difficulties. Full-matrix refinement with anisotropic temperature factors for all non-carbon atoms gave R = 0.054. Final atomic and thermal parameters may be found in Table A2.7 (Appendix 2). Calculated and observed structure

factors are contained in Table A3.7 (Appendix 3). A complete set of bond distances and angles may be found in Table 4.1.

Description of structure. The structure consists of four discrete monomers per unit cell. The mercury atoms lie along two-fold rotation axes; the coordinates of these special positions are:-

0, 1/2, **z** 1/2, 0, **z**

0, 1/2, 1/2 + z 1/2, 0, 1/2 - Z

Joined to each mercury atom are two PEt^ ligands which are related by the two-fold rotation and two chlorine atoms which are similarly related. The Hg-P and Hg-Cl distances are 2.39(1) and 2.68(1) A, respectively. It should be noted that these termi na1 Hg-Cl bonds are longer than those br?dgi ng bonds found for (PPh^)HgCl £ (which are 2.62 and 2.66 A, Section 2.2.2). The mercury atom lies in an irregular four-coordination environment with the angles P-Hg-P' = 158.5(5)° and Cl-Hg-Cl* =105.5(4)° (Figure 4.1).

The monomers within the unit cell are related to one another by screw tetrads along the £-directi on i.e. each monomer may be rotated 90° about an axis parallel with the£-axis, and translated one-half a unit cell along £, to become directly superimposable upon another identical monomer. The Hg-Hg distance between each monomer is ca_. 7 Å so there is no possibility of long range mercury-chl orine interaction (Figure 4.2).

The four-coordination geometry about mercury is very similar to that found for (thiosemicarbazide^HgCl$_2$[83] (Section 1.3.3) (S-Hg-S angle=l60.7°, Hg-Cl distances 2.8 Å). However in this structure there was further Hg Cl contact (3.25 A).

The conformation of the PE$_3$ ligand in the present complex is (skew, skew, skew), which is different to that found for (PEt^)HgCl^ but similar to that found in other transition metal complexes.[116]

Fig. 4.1 The molecular structure of $(PEt_3)_2HgCl_2$

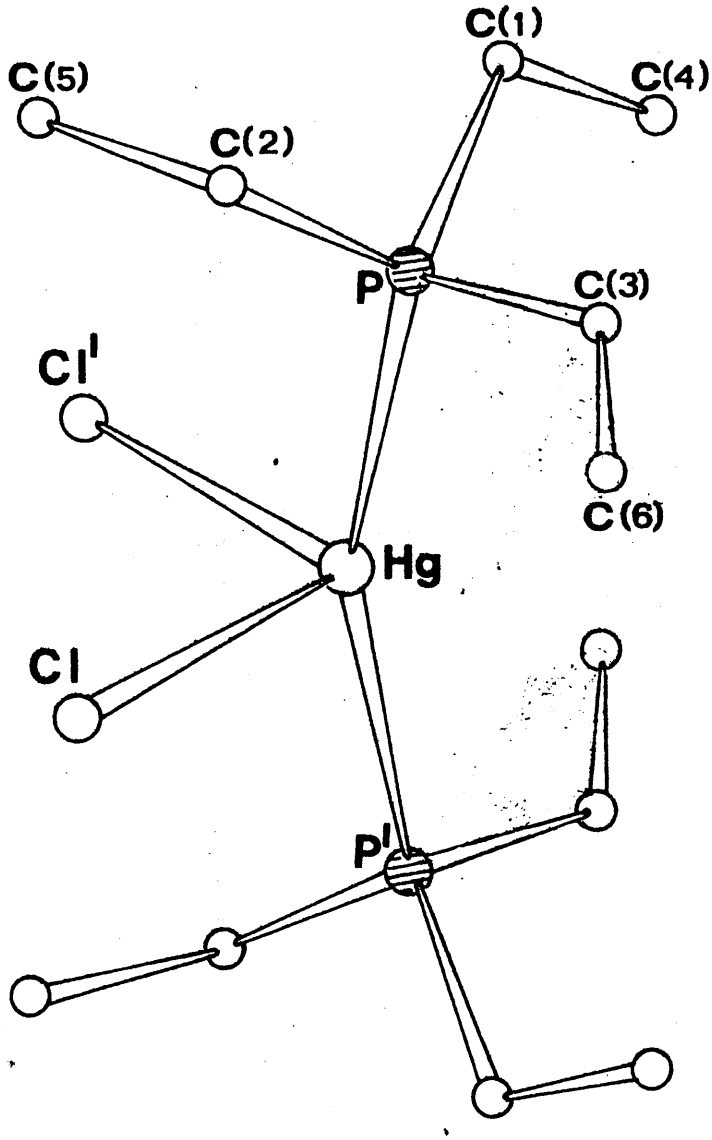

— viewed along the a-axis

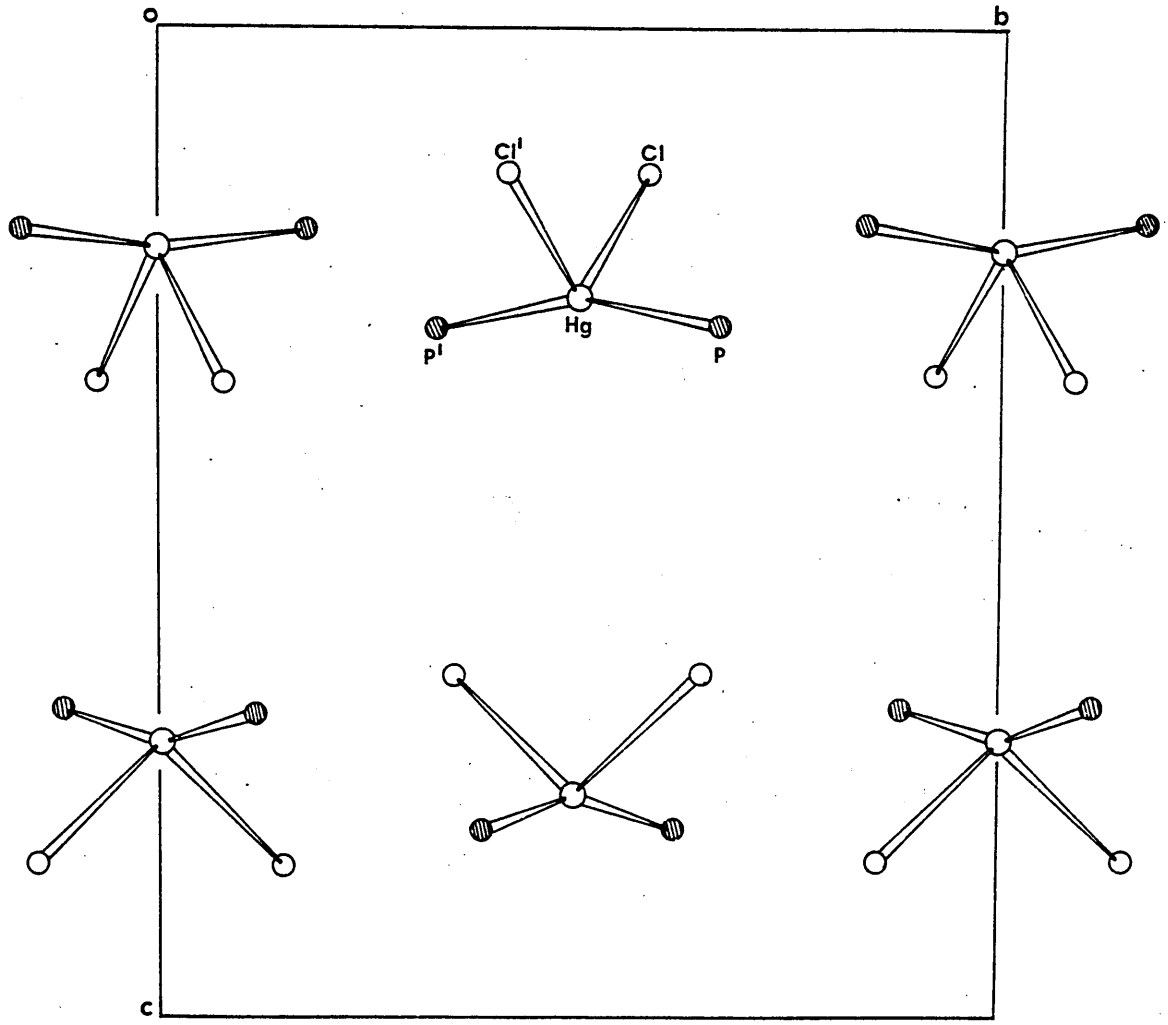

a—Omitting carbon atoms

Table 4.1.

Bond distances and angles for $(PEt_3)_2HgCl_2$ with standard deviations in parentheses.

(a) Distances/Å

Hg-Cl	= 2.68(1)	P-C(1)	= 1.94(8)
Hg-Cl'	= 2.68(1)	P-C(2)	= 1.62(1)
Hg-P	= 2.39(1)	P-C(6)	= 1.84(7)
Hg-P'	= 2.39(1)		
		C(1)-C(4)	= 1.11(9)
		C(2)-C(5)	= 1.46(8)
		C(3)-C(6)	= 1.28(6)

(b) Angles/Å

Cl-Hg-Cl'	= 105.5(5)	C(1)-P-C(2)	= 105(3)
P-Hg-P'	= 158.5(5)	C(1)-P-C(3)	= 105(4)
Cl-Hg-P	= 93.5(5)	C(1)-P-Hg	= 115(3)
Cl-Hg-P'	= 97.5(5)	C(2)-P-C(3)	= 103(2)
		C(2)-P-Hg	= 115(1)
		C(3)-P-Hg	= 114(2)
		P-C(1)-C(4)	= 124(6)
		P-C(2)-C(5)	= 121(3)
		P-C(3)-C(6)	= 120(5)

4.1.3. The Crystal Structure of $(PEtMe_2)_2HgBr_2$

Crystal Data.

$C_8H_{22}P_2HgBr_2$ M_r=540.60 Orthorhombic

a=12.532(11), b=20.801(17), c=12.694(12) Å;

$\alpha=\beta=\gamma=90.00°$.

D_m=2.14 g cm^{-3} (by flotation in a $CHBr_3/CHCl_3$ mixture) D_c=2.17 g cm^{-3}, Z=8 (with two independent molecules per asymmetric unit).

$F_{(ooo)}$=1999.65, $\mu(Mo\text{-}K_\alpha)$=138.55 cm^{-1}.

Systematic absences:-

hoo reflections are absent for h=2n + 1.

oko " " " " k=2n + 1.

ool " " " " l=2n + 1.

These absences uniquely define the crystals as belonging to the space group $P2_12_12_1$ (D_2^4, No. 19).[112]

Data Collection and Structure Refinement. The temperature factors of all atoms in this structure are extremely high. It is difficult to assess the reason for this phenomenon, however, one may propose two possible explanations:-

(a) 'unresolvable disorder'

or (b) the temperature factors do in fact reflect genuinely high thermal motion.

Difficulty was encountered on trying to locate some of the carbon atoms. This may be attributable to the same reasons as above but also because the diffraction data in the 2θ range recorded may be dominated by the bromine and mercury atoms, which provide little information concerning the lighter carbon atoms. It has been possible to fix 'chemically sensible' carbon atoms in positions of adequate electron density.

A colourless crystal, approximate dimensions 0.35x0.27x0.19 mm , was mounted about c. Fourteen layers, hk0 →hk13, were collected; 2675 reflections were recorded with $2\theta < 50^{\circ}$ of which 809 had $I/\sigma(I) \geq 2.0$ and were used for refinement. Unit weights were used and no absorption correction was applied.

Full-matrix refinement with anisotropic temperature factors for all non-carbon atoms gave R=0.123. Final atomic and thermal parameters are given in Table A2.8 (Appendix 2). Calculated and observed structure factors are contained in Table A3.8 (Appendix 3). A complete set of bond distances and bond angles may be found in Table 4.2.

Description of Structure. This complex crystallizes with eight monomers (falling into two crystallographically independent types) per unit cell. The geometry of each of these types is similar but different (Figure 4.3). Each crystallographically independent unit contains one four-coordinate mercury atom joined to two phosphorus atoms at distances of ca. 2.4-2.5 Å and two bromine atoms at ca. 2.8 Å. It is significant that these terminal Hg-Br bonds are longer than Hg-Br bridge bonds found for $[Hg_2Br_6]^{2-}$ species.[50,52,54] The coordination polyhedra about both mercury atoms are very distorted tetrahedra with angles ranging from ca.150° for P-Hg-P to ca.90-98° for the smallest angles (Br-Hg-P). The two independent monomers are oriented so that Br(1), attached to Hg(1), approaches Hg(2) at a distance of 3.83(3) Å and almost bisects the P(1)-Hg(2)-P(2) angle; similarly, the Br(4) atom attached to Hg(2) approaches Hg(1) at a distance of 4.00(3) Å. These Hg-Br distances are just outside the sum of the van der Waals' radii for mercury and bromine (3.68 Å), and so if there is any form of contact between these molecules it is only very weak.

The manner in which the eight monomers are arranged within the unit cell is shown in Figure 4.4.

Little can be said about the $PEtMe_2$ ligands because of the high errors associated with the positional parameters of the carbon atoms which they contain.

Fig. 13 Intermolecular distances in $(PEtMe_2)_2HgBr_2$

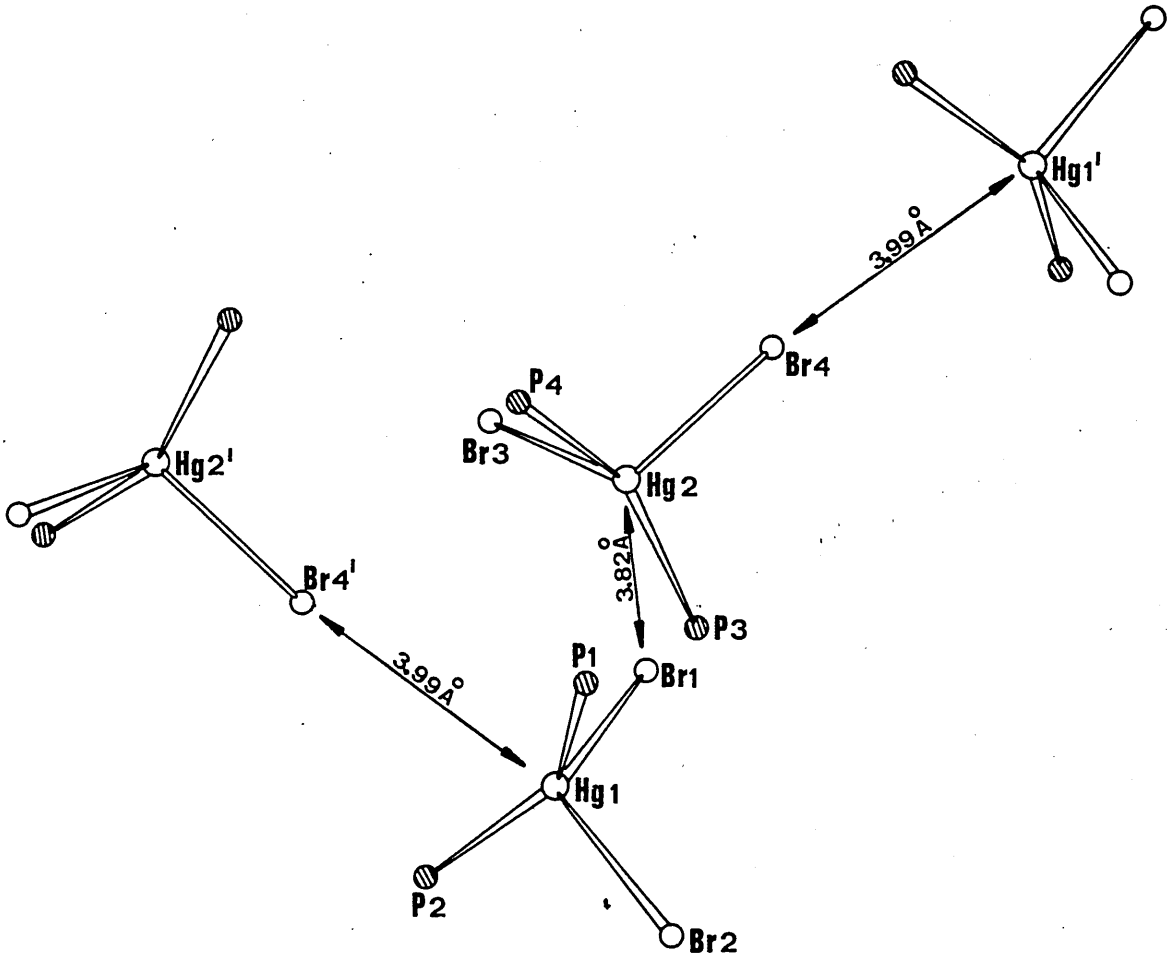

—viewed along the b—axis

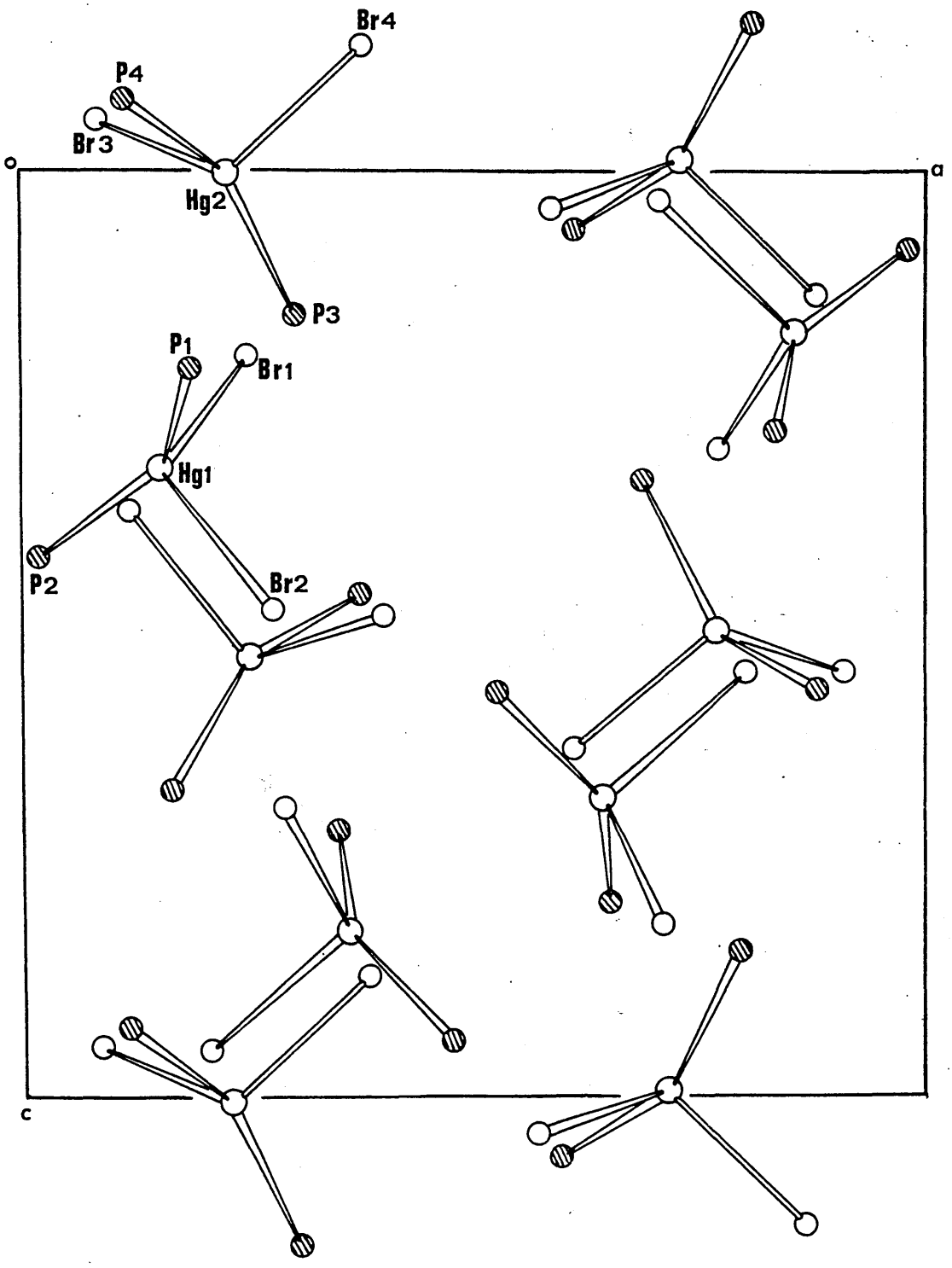

a—Omitting carbon atoms

Table 4.2.

Bond distances and angles for $(PEtMe_2)_2HgBr_2$ with standard deviations in parentheses.

(a) Distances/Å

Hg(1)-Br(1)	= 2.79(2)	Hg(2)-Br(3)	= 2.88(2)
Hg(1)-Br(2)	= 2.72(2)	Hg(2)-Br(4)	= 2.79(3)
Hg(1)-P(1)	= 2.50(5)	Hg(2)-P(3)	= 2.48(6)
Hg(1)-P(2)	= 2.44(6)	Hg(2)-P(4)	= 2.39(5)
av. P-C distance	= 2.0 Å	No β-carbon atoms were located	

(b) Angles/°

Br(1)-Hg(1)-Br(2)	= 101.7(8)	Br(3)-Hg(2)-Br(4)	= 106.9(8)
Br(1)-Hg(1)-P(1)	= 101(2)	Br(3)-Hg(2)-P(3)	= 99(1)
Br(1)-Hg(1)-P(2)	= 102(1)	Br(3)-Hg(2)-P(4)	= 90(1)
Br(2)-Hg(1)-P(1)	= 99(1)	Br(4)-Hg(2)-P(3)	= 103(1)
Br(2)-Hg(1)-P(2)	= 100(2)	Br(4)-Hg(2)-P(4)	= 101(1)
P(1)-Hg(1)-P(2)	= 147(2)	P(3)-Hg(2)-P(4)	= 150(2)
av. C-P-C angle	= 108°	av. Hg-P-C angle	= 110°

4.1.4. The preliminary crystallographic analysis of $(PBu^n_3)_2HgCl_2$

Crystal Data.

$C_{24}H_{54}P_2HgCl_2$ M_r=676.13 Orthorhombic

a=14.470(13), b=13.594(14), c=17.279(19) Å;

α=90.00° β=90.00° γ=90.00°

D_m=1.32 g cm^{-3} (by flotation in a $CHCl_3/CHBr_3$ mixture), D_c=1.32 g cm^{-3}.

Z=4, $F_{(000)}$=1367.82, μ(Mo-K_α)=45.95 cm^{-1}

Systematic absences:-

hoo reflections are absent for h=2n + 1

oko " " " " k=2n + 1

ool " " " " l=2n + 1.

These absences uniquely define the crystals as belonging to the space group $P2_12_12_1$ (D_2^4, No. 19).[112]

Structure Determination. A colourless crystal, approximate dimensions, 0.5 x 0.5 x 0.3 mm, was mounted about a. Sixteen layers, 0kl→15kl were collected; 2675 reflections were recorded with $2\theta < 50°$ of which 809 had $I/\sigma(I) \geq 2.0$ and were used for refinement. Unit weights were used and no absorption correction was applied.

This structure is thought to be disordered but the nature of this disorder could not be resolved. The temperature factors of the atoms located are extremely high, thus reflecting the disorder perhaps also a high degree of thermal motion. It was not possible to distinguish between chlorine and phosphorus atoms because carbon atoms could not definitely be located.

The only definite inference which can be made from this study is that $(PBu^n_3)_2HgCl_2$ exists as discrete distorted tetrahedral monomeric units with no possibility of further mercury-chlorine contact (Figure 4.5). The data in Table 4.3 define the geometry of the monomer. The phosphorus and chlorine atoms have been assigned on the basis of what is thought to be 'chemically

Figure 4.5.

The structure of the 'P_2HgCl_2' unit of $(PBu^n_3)_2HgCl_2$.

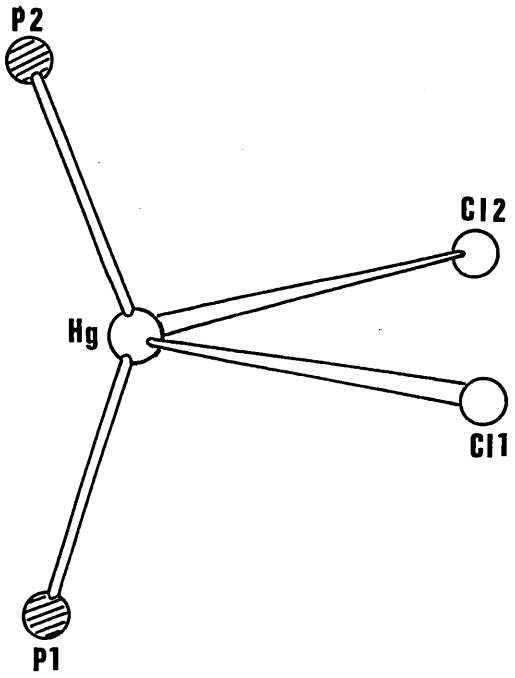

Table 4.3.

Bond distances and angles for the 'P_2HgCl_2' unit of $(PBu^n_3)_2HgCl_2$.

(a) Distances/ Å		(b) Angles/°	
Hg-Cl(1)	= 2.55(5)	Cl(1)-Hg-Cl(2)	= 105(2)
Hg-Cl(2)	= 2.66(5)	Cl(1)-Hg-P(1)	= 99(2)
Hg-P(1)	= 2.34(6)	Cl(1)-Hg-P(2)	= 103(2)
Hg-P(2)	= 2.64(6)	Cl(2)-Hg-P(1)	= 105(2)
		Cl(2)-Hg-P(2)	= 102(2)
		P(1)-Hg-P(2)	= 139(2)

sensible' in terms of the $(PR_3)_2HgX_2$ structures reported in this work, and of the structure of $(PPh_3)_2HgI_2$. Consequently, the large angle of ca. 139° is attributed to P(1)-Hg-P(2).

This compound awaits data collection at low temperature, which, it is hoped will help to resolve the problems associated with 'disorder', and subsequently allow complete structure determination.

4.1.5. General discussion.

The crystal structures of the $(PR_3)_2HgX_2$ complexes now known are summarized in Table 4.4. All structures are monomeric with varying degrees of distortion from a regular tetrahedral geometry.

The factors which influence these different coordination arrangements around phosphorus include:-

a) the nature of substituents joined to phosphorus;

b) the halogen atom;

c) solid-state effects.

It is extremely unlikely that solid-state effects have any influence at all in views of the large inter-monomer distances found for these structures.

Unfortunately it is not possible clearly to separate the effects of substituents joined to phosphorus and those due to the presence of different halogen atoms. However, discussed below are structural trends which suggest that substituent effects and the way these influence the donor properties of the PR_3 ligands are a major factor determining the stereochemistry of the monomer.

Consideration of all four $(PR_3)_2HgX_2$ structures indicates there is a wide variation in P-Hg-P angle (Table 4.4). A further significant feature of these monomers are their very long Hg-X distances (Table 4.4) which for

Table 4.4.

Summary of the crystal structures* of some $(PR_3)_2HgX_2$ complexes

Compound	d(Hg-X)/ Å	d(Hg-P)/ Å	X-Hg-X/°	P-Hg-P/°
$(PPh_3)_2HgI_2$ [74]	2.733(1),2.763(1)	2.574(1),2.574(1)	110.43(9)	108.95(4)
$(PBu^n_3)_2HgCl_2$	2.55 (5),2.66 (5)	2.34 (6),2.64 (6)	105(2)	139(2)
$(PEtMe_2)_2HgBr_2$	2.72 (2),2.79 (2)	2.44 (6),2.50 (5)	102(1)	147(2)
	2.79 (3),2.88 (2)	2.39 (5),2.48 (6)	107(1)	150(2)
$(PEt_3)_2HgCl_2$	2.68 (1),2.68 (1)	2.39 (1),2.39 (1)	105.5(5)	158.5(5)

* - All structures are distorted tetrahedral monomers.

$(PEt_3)_2HgCl_2$ and $(PEtMe_2)_2HgBr_2$ are of comparable length to some Hg-X bridge bonds found in other HgX_2 complexes (e.g. 2.62 and 2.66 Å for the $(PPh_3)HgCl_2$ dimer;* 2.75 and 2.75 Å for the dimeric anion in $[NEt_4]_2[Hg_2Br_6]$ [96]). The percentage increases in the Hg-X bonds due to complexation for the present $(PR_3)_2HgX_2$ compounds have been calculated relative to the Hg-X distances of the mercuric halides in the gas-phase[146] [2.28(4), 2.40(4) and 2.57(4) for $HgCl_2$, $HgBr_2$ and HgI_2, respectively] and are found to be:-

7% for $(PPh_3)_2HgI_2$

14% for $(PBu^n_3)_2HgCl_2$

16% for $(PEtMe_2)_2HgBr_2$

17% for $(PEt_3)_2HgCl_2$

The above observations regarding P-Hg-P angles and percentage increases in Hg-X bonds may be rationalized by regarding the reaction,

$$2PR_3 + HgX_2 \longrightarrow (PR_3)_2HgX_2$$

as approaching a substitution reaction, whereby the PR_3 ligands are attempting to displace the halogen atoms and ultimately achieve a linear P-Hg-P arrangement. The final geometry of the $(PR_3)_2HgX_2$ units are therefore controlled by the donor strengths of the PR_3 ligands and the ease of elimination of the halogen atoms.

On the basis of pK_a values, cone angles and Taft constants (Section 2.3.1) it is possible to arrange the present series of PR_3 ligands into the approximate order of donor strength shown:-

$$PEtMe_2 > PEt_3 \sim PBu^n_3 > PPh_3$$

Also, based on the relative electronegativities of the halogens one may arrange Cl, Br and I in the following order of 'ease of elimination' from the initial HgX_2 unit:-

$$I < Br < Cl$$

* - the present work (Section 2.2.2).

Therefore the larger P-Hg-P angle observed for $(PEtMe_2)_2HgBr_2$ as compared to that observed for $(PPh_3)_2HgI_2$ and also the greater percentage increase of Hg-X bonds for $(PEtMe_2)_2HgBr_2$ (Table 4.4) can be explained in terms of the stronger donor properties of $PEtMe_2$ relative to PPh_3 and also by the greater 'ease of elimination' of bromine relative to iodine.

Comparison of P-Hg-P angles and percentage increase in Hg-Cl bonds for the two chloro compounds viz. $(PBu^n_3)_2HgCl_2$ and $(PEt_3)_2HgCl_2$, clearly indicate that there is a difference in the extent of P-Hg-P interaction, which, can only be explained in terms of the PEt_3 ligand being a stronger donor than PBu^n_3 towards $HgCl_2$ in these 2:1 complexes.

Considering solely the 'donor strengths of the ligands PEt_3 and $PEtMe_2$, one may have expected to observe a smaller P-Hg-P angle in $(PEt_3)_2HgCl_2$ than in $(PEtMe_2)_2HgBr_2$; however, this is not the case. This observation would seem to suggest that the 'ease of elimination' of the halogen atoms also has some influence in these compounds.

In conclusion, therefore, it has been indicated that the extent of P-Hg-P interaction is a major factor controlling the stereochemistry about mercury in these monomers, and also that the nature of the halogen atom should also be taken into consideration. Further, the above observations indicate that phosphorus in a sufficiently reactive environment, which is controlled by the substituents joined to phosphorus, has a higher affinity for Hg(II) than do the halogens. It would appear that as the donor strength of the PR_3 ligands increase they 'attempt' to replace the two halogen atoms of the original HgX_2 unit and take up the common digonal coordination arrangement. This is a similar situation to that observed for $(PR_3)HgCl_2$ complexes where the Cl_t-Hg-P angle approaches linearity as the donor strength of the phosphine is increased.

The limited solution-phase data available for $(PR_3)_2HgX_2$ compounds are

summarized in Table 4.5, and are generally in line with the solid-state observations just described.

The relative molecular mass (M^) determinations of Farhanghi and Graddon,*^"- for $(PBu_3)_2HgX_2$ (X=Cl, Br or I) and of Kessler^ for $(PEtMe_2)_2HgX_2$ (X=Cl or I), indicate that the species present in solution are neutral monomers. On the other hand Schmidbaur et al.[4] on the basis of conductivity measurements propose that the compounds $(PMe_3)_2HgX_2$ (X=Cl, Br or I), exist as [PMe^-Hg-PMe^]2+ cations and 2X anions in solution, whereas, from similar studies Coates and Lauder suggest that (PEt^^HgC^ in solution exists as $[(PEt_3)_2Hg(H_20)2]$ 2+ + 2CI" ions.[147]

These conductivity data are understandable in view of the crystal structures contained in Table 4.4. It is reasonable to suppose that ^PEtj^HgC^ in aqueous solution might readily lose its two weakly held chlorine atoms. Also, judging by the large P-Hg-P angle in the solid, it is likely that a linear $[PEt_3$~Hg-PEt3]2+ cation may result in aqueous solution, perhaps with some degree of solvation. A similar situation may be envisaged for the $(PMe_3)_2HgX_2$ (X=Cl, Br or I) complexes in methanol.[4]

The 'J(Hg-P) coupling constant data in Table 4.5 are worthy of mention because they are consistent with the idea that varying degrees of P-Hg-P donor-acceptor interaction occur as a result of the differing donor properties of the PR_3 ligands. For example, consider the *J(Hg-P) coupling constants for:-

	Compound	Solution-phase structure	*J(Hg-P)/Hz
(a)	$(PMe_3)_2HgCl_2$	$[PMe_3$-Hg-PMe3]2+ + 2Cl"[4]	55054
(b)	(PEtI^^^HgCI2	monomeric[go]	5606[QO]
(c)	(PBu^^HgC^	monomeric*^	5125^
(d)	$[P(CgH^CMe_3-P)_3I_2HgCl_2$[127]	monomeric*^7,	4602*^7

* - Although not confirmed by M determination, the author[127] assumes that this compound is monomeric in solution. In retrospect, as a result of the crystal structure analysis of (PPfu^Hg^ and vibrational studies for (PPI^^HgCl2 (Section 5.2a) it is felt that this is a reasonable assumption.

The higher $^{1}J(Hg-P)$, the stronger is the coupling between mercury and the two phosphorus atoms, and the stronger will be the P-Hg-P donor-acceptor interaction.

Consideration of $^{1}J(Hg-P)$ for the latter three complexes (b), (c) and (d) show a decrease in the sequence (b) (c) (d), which can be correlated with the donor properties of the PR_3 ligands. It is interesting to note that the coupling constants for (a) $[PMe_3-Hg-PMe_3]^{2+}$ and (b) monomeric $(PEtMe_2)_2HgCl_2$ are of the same order. This result indicates a similar P-Hg-P donor-acceptor interaction even though the solution phase species are not exactly the same. It may be suggested that a near-linear $(PEtMe_2-Hg-PEtMe_2)$ arrangement is present in the $(PEtMe_2)_2HgCl_2$ monomer in $CDCl_3$ and that the chlorine atoms are only very weakly held by mercury, thus having little influence on $^{1}J(Hg-P)$ [cf. the solid-state structure of $(PEt_3)_2HgCl_2$].

Thermodynamic data are available,[132] in the form of enthalpies of ligation (ΔH_L) for the reaction:-

$$HgX_2 + 2PR_3 \longrightarrow (PR_3)_2HgX_2$$

Although only PPh_3 and PBu^n_3 from the present series have been studied, the results indicate that stronger P-Hg-P donor-acceptor interactions are found for the reactions between PBu^n_3 and HgX_2 than between PPh_3 and HgX_2, and also that ΔH_L values for the reaction between a particular phosphine and the mercuric halides decrease in the sequence

$$Cl > Br > I$$

As far as it is possible to tell these results are consistent with the crystallographic data (Table 4.4). Only for $(PEtMe_2)_2HgBr_2$ is there any 'sign' of further Hg-X interaction beyond the monomer stage, with Hg-Br distances of ca. 3.8 and 4.0 Å. However, as these distances are greater than the sum of the van der Waals' radii of mercury and bromine it

is unlikely that the atoms are in contact. The lack of further Hg-X association is not surprising for $(PPh_3)_2HgI_2$ and $(PBu^n_3)_2HgCl_2$ in view of the large steric bulk of the PR_3 ligands involved. However, it is difficult to find a reason for the lack of further association for $(PEt_3)_2HgCl_2$, especially when one considers that further association exists in the very similar (thiosemicarbazide)$_2HgCl_2$ complex.[83]

Consideration of the $(PR_3)_2HgX_2$ complexes in the more general context of $(L)_2HgX_2$ indicates that, as for the 1:1 system, there are essentially two separate types of mercury-ligand interaction:-

a) A relatively weak interaction - for example as in $(Py)_2HgCl_2$,[84] (phenoxathiin)$_2HgCl_2$[86] and $(CH_3OH)_2HgCl_2$,[85] all of which contain virtually undistorted $HgCl_2$ units to which are weakly attached two donor ligands. Extra Hg-Cl contacts, of ca. 3 Å, between 'monomers' result in polymeric arrangements, in which mercury atoms lie in distorted octahedral environments.

b) A range of stronger interactions - for example, for S- or P- donor ligands, which result in structures ranging from discrete monomers for $(PPh_3)_2HgI_2$[74] and (o-ethylthiocarbamate)$_2HgCl_2$,[75] to arrangements in which the donor-ligands appear to displace the halogen atoms and adopt digonal coordination environments, such as in (thiosemicarbazide)$_2HgCl_2$[83] and $(PEt_3)_2HgCl_2$, to a structure like (thiourea)$_2HgCl_2$[81] in which a chlorine atom has actually been displaced resulting in an ionic structure consisting of $[S_2HgCl]^+ + Cl^-$ ions.

The importance of the halogen atom in determining the structures of $(L)_2HgX_2$ compounds has been indicated by the (thiourea)$_2HgX_2$ (X=Cl, Br or I) series (Section 1.3.3), where it has been shown that the bromo compound[80] gives rise to a more associated structure, containing a larger S-Hg-S angle, than the corresponding iodo compound,[79] where the chloro compound[81] turns out to be a completely different ionic structure.

Table 4.5.

Solution phase data for some (PR^)oHqX^ complexes.

Compound	Proposed solution-phase structure	Solvent	^1J(Hg-P)/Hz	Other experimental techniques	Ref.
(L)0HgC10 complexes					
L=					
PBu^	Monomeric	benzene		Mr	132
PBun	Monomeric	$CDCl_3$ or CH_2Cl_2	5125	IR,Ra	90
PBu^	Monomeric		5100		126
PBu^	Monomeric	CH_2Cl_2	5078		125
PPhBu^	Monomeric	CH_2Cl_2	5035		125
PPh2Bun	Monomeric	CH_2Cl_2	4754		125
PEtMe2	Monomeric	$CDCl_3$	5606	1R,Ra,Mr	90
•PMe3	tP-Hg-Pl2+ + 2Cl"	CH3CH		Conductivity	4
PMe3	[P-Hg-P]2+ + 2Cl"	H20	5505		4
P(C6H4SiMe3-p)3	Monomeric	CH_2Cl_2	4653		127
P(C6H4CMe3-p)3	Monomeric	CH_2Cl_2	4602		127
P(Octyl)3	Monomeric		5160		126
PE+3	[P2Hg(H20)2]2++2Cl“	H20		Conductivity	147
(L)0HgBr0 complexes					
L=					
PBu3	Monomeric	benzene		Mr	132
PBu3	Monomeric	$CDCl_2$	4829	IR,Ra	90
PBu§	Monomeric		4780		126
PBu3	Monomeric	CH_2Cl_2	4741		125
PPhBu2	Monomeric	CH_2Cl_2	4629		125
PPh2Bun	Monomeric	CH_2Cl_2	4216		125
PEtMe2	Monomeric	$CDCl_3$	5560	IR,Ra	90
PMe3	[P-Hg-Pl 2+ + 2Br”	CH30H		Conductivity	4
PPh2(C6H4CgH|?-p)	Monomeric	CH_2Cl_2	4130		127
P(C6H4CMe3-P)3	Monomeric	CH_2Cl_2	4228		127
P(Octyl)3	Monomeric		4800		126

Table 4.5, continued

Compound	Proposed solution-phase structure	Solvent	^1J(Hg-P)/Hz	Other experimental techniques	Ref.
$(L)_2HgI_2$ complexes					
L=					
PBu^n_3	Monomeric	benzene		Mr	132
PBu^n_3	Monomeric	$CDCl_3$	4101	IR,Ra	90
PBu^n_3	Monomeric		4040		126
PBu^n_3	Monomeric	CH_2Cl_2	4100		125
$PPhBu^n_2$	Monomeric	CH_2Cl_2	3726		125
$PEtMe_2$	Monomeric	$CDCl_3$	4788	IR,Ra,Mr	90
PMe_3	$[P\text{-}Hg\text{-}P]^{2+} + 2I^-$	CH_3OH		Conductivity	4
$P(Octyl)_3$	Monomeric		3960		126

Chapter 5.

Spectroscopic studies of some $(PR_3)_2HgX_2$ complexes.

Contents.

5.1. BASIS FOR VIBRATIONAL ASSIGNMENTS FOR $(PR_3)_2HgX_2$ COMPLEXES.

The poor quality of spectroscopic data available in the literature for the $(L)_2HgX_2$ system (Section 1.4.2) suggested that perhaps, as for the 1:1 system, a systematic study of a series of closely related complexes of known structure would improve our knowledge of structure/spectra relationships. Unfortunately, data relating to such a series of complexes were not available. Spectroscopic studies carried out in this work and elsewhere[4,90] suggested that the $(PR_3)_2HgX_2$ complexes would be suitable for such a systematic study. The results of these spectroscopic studies indicated that the $(PR_3)_2HgX_2$ complexes give rise to associated or otherwise unusual structures depending on the nature of the PR_3 ligand. Therefore to define these different structures and to explain the spectroscopic observations it was decided to determine the crystal structures of $(PBu^n_3)_2HgCl_2$, $(PEt_3)_2HgCl_2$ and $(PEtMe_2)_2HgBr_2$, suitable crystals of which could be prepared.

The crystallographic data so obtained, together with the recently reported[74] $(PPh_3)_2HgI_2$ structure then formed a basis from which vibrational assignments were made.

The structures of all these complexes were shown to be monomeric but with the coordination polyhedron about mercury varying from one structure to another (Table 5.1).

In spite of the different stereochemical arrangements about the mercury atoms all monomers are essentially of C_{2v} symmetry. Point group analysis predicts the following molecular modes for a C_{2v} monomer:

$$\Gamma_{int} = 4A_1(IR,Ra) + A_2(Ra) + 2B_1(IR,Ra) + 2B_2(IR,Ra)$$

These modes may be described as follows:-[134]

A_1 : $\nu_s(HgX)$
$\nu_s(HgP)$
$\delta_s(XHgX)$
$\delta_s(PHgP)$

A_2 : $\rho_t(HgP_2)$

Table 5.1.

Summary of the geometries of some $(PR_3)_2HgX_2$ monomers.

Compound	d(Hg-P)/Å	d(Hg-X)/Å	P-Hg-P/°	X-Hg-X/°
$(PBu^n_3)_2HgCl_2$	2.34 (6),2.64 (6)	2.55 (5),2.66 (5)	139(2)	105(2)
$(PEt_3)_2HgCl_2$	2.39 (1),2.39 (1)	2.68 (1),2.68 (1)	158.5(5)	105.5(5)
$(PEtMe_2)_2HgBr_2$	2.44 (6),2.50 (5) 2.39 (5),2.48 (5)	2.72 (2),2.79 (2) 2.79 (3),2.88 (2)	147(2) 150(2)	102(1) 107(1)
$(PPh_3)_2HgI_2$ [74]	2.574(1),2.574(1)	2.733(1),2.763(1)	108.95(4)	110.43(9)

Figure 5.1.

The approximate forms of motion of ν(HgX) and ν(HgP) modes for a C_{2v} monomer.

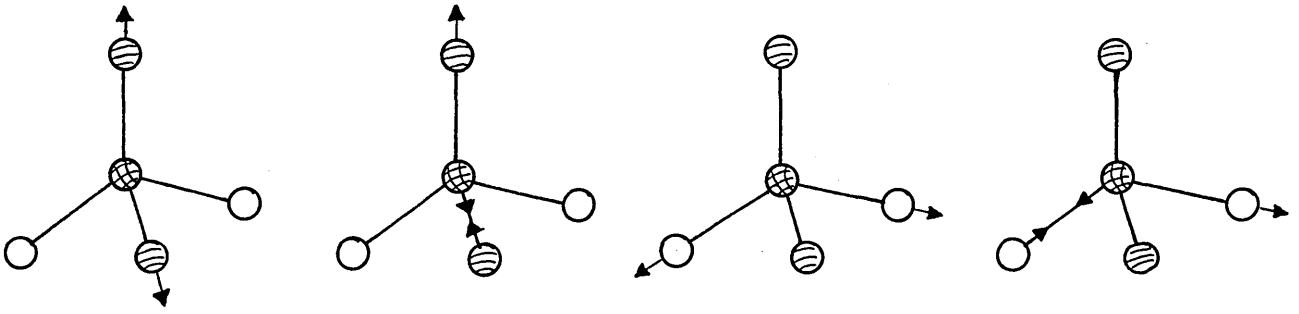

$\nu_s(HgP)(A_1)$ $\nu_a(HgP)(B_2)$ $\nu_s(HgX)(A_1)$ $\nu_a(HgX)(B_1)$

● - Hg ◍ - P ○ - X

Table 5.2.

Solid state ν(HgX) data for $(Et_4N)_2HgX_4$ (X=Cl, Br or I)(cm^{-1})[96]

Compound	ν_s(HgX)	ν_a(HgX)
$(Et_4N)_2HgCl_4$	265s Ra	229m Ra
	i.a.	230s,br IR
$(Et_4N)_2HgBr_4$	168s Ra	159m Ra
	i.a.	157s,150sh IR
$(Et_4N)_2HgI_4$	122s Ra	122[a] Ra
	i.a.	123s IR

Ra - recorded at room temperature.

IR - recorded at ca. 100K.

a - coincident with the ν_s(HgX) mode.

i.a. - inactive.

B_1 : $\nu_a(HgX)$ $\quad$ B_2 : $\nu_a(HgP)$

$\rho_r(HgX_2)$ $\quad$ $\delta_a(PHgP)$

The most informative of these modes, as far as the present work is concerned are the $\nu(HgX)$ and $\nu(HgP)$ modes. The approximate forms of motion of these modes may be determined from the C_{2v} character table and are shown in Figure 5.1.

The question arises as to the wavenumber positions of both sets of modes.

Reliable spectroscopic data for some tetrahedral $[HgX_4]^{2-}$ monomers (X=Cl, Br or I)[96] (Table 5.2) should provide a clue as to the positions of $\nu(HgX)$ modes in an 'ideal' $(PR_3)_2HgX_2$ monomer. The positions of the mercury-halogen stretching modes observed for the remaining crystallographically characterized complexes which deviate from ideal tetrahedral are easily interpreted in terms of their specific structural features.

The approximate wavenumber positions of $\nu(HgP)$ modes arising from tetrahedrally coordinated Hg-P bonds and the difficulties encountered in their location have been discussed previously in Section 3.2.2. Using similar arguments as presented for $(PR_3)HgX_2$ complexes, where the position of $\nu(HgP)$ modes are dependent on the Cl_s-Hg-P angle, the wavenumber position of $\nu(HgP)$ modes in the $(PR_3)_2HgX_2$ complexes might be expected to increase as the P-Hg-P angle is increased.

5.2. THE SOLID-STATE VIBRATIONAL SPECTRA OF SOME $(PR_3)_2HgX_2$ COMPLEXES OF KNOWN STRUCTURE.

(a) $(PPh_3)_2HgX_2$ (X=Cl, Br or I)

$(PPh_3)_2HgI_2$[74] has been shown to be a slightly distorted tetrahedral monomer of C_{2v} symmetry. The regular halogen mass-dependence of the vibrational spectra (Figures 5.2a and 5.2b) indicate that chloro and bromo

complexes are isostructural.

As shown in the previous Section, using the point group approach one may expect to observe the following ν(HgX) and ν(HgP) modes for a 'tetrahedral' monomer of this symmetry:-

$$\Gamma\nu(HgX) = A_1(IR,Ra) + B_1(IR,Ra)$$

and $$\Gamma\nu(HgP) = A_1(IR,Ra) + B_2(IR,Ra)$$

Room temperature IR spectra recorded in the present work are in complete agreement with a previous report by Deacon et al.[7], but at low temperature the IR spectra (Figure 5.2a) show improved resolution and expected band shifts to higher wavenumber values. The present study also includes room temperature Raman data obtained for the first time. Wavenumber positions and vibrational assignments are contained in Table 5.3. Internal modes of the PPh_3 ligand have been eliminated using the halogen mass-dependence method and by comparison with the free ligand spectra. Assignments of the IR-active modes are essentially in agreeement with those of Deacon et al.,[7] but because of the improved resolution more detailed assignments are now possible. The X-sensitive bands at ca. 230, 160 and 135 cm^{-1} for chloro, bromo and iodo complexes, respectively, in both IR and Ra spectra are readily assigned to ν(HgX) modes. The higher wavenumber bands in each case have been assigned ν_s(HgX), by comparison with some polarisation data recorded by Kessler[90] for other $(PR_3)_2HgX_2$ complexes in solution. The lower wavenumber value of the ν_s(HgCl) mode found for $(PPh_3)_2HgCl_2$ as compared to that found for $[NEt_4]_2[HgCl_4]$[90] may be attributed to longer Hg-Cl bonds in the present case.

Comparison with the ν(NiP) mode assignments of Allen and Wilkinson[141] for some $(PR_3)_2NiX_2$ complexes allows one tentatively to assign the bands at 161 and 145(IR) and 140 cm^{-1} (Ra) for the chloro complex, and also the bands at 140(IR) and 139(Ra) for the bromo complex as ν(HgP) modes. The ν(HgP)

Far infrared spectra (ca. 30K) of $(PPh_3)_2HgX_2$ (X=Cl, Br or I) (cm^{-1})

X=Cl

• - internal mode of the ligand.

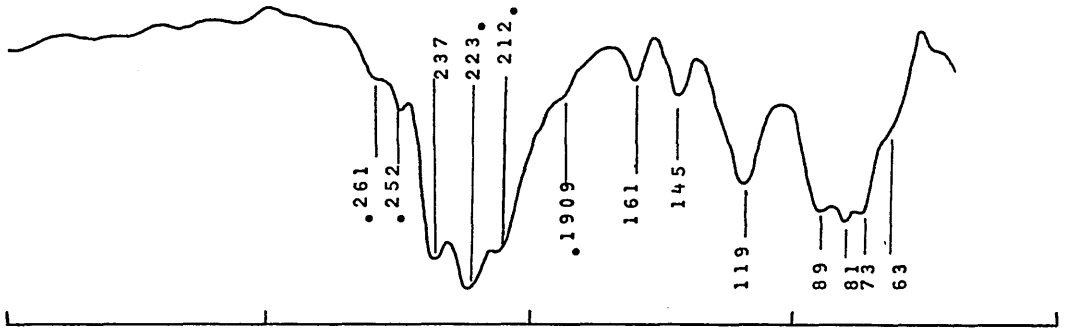

X=Br

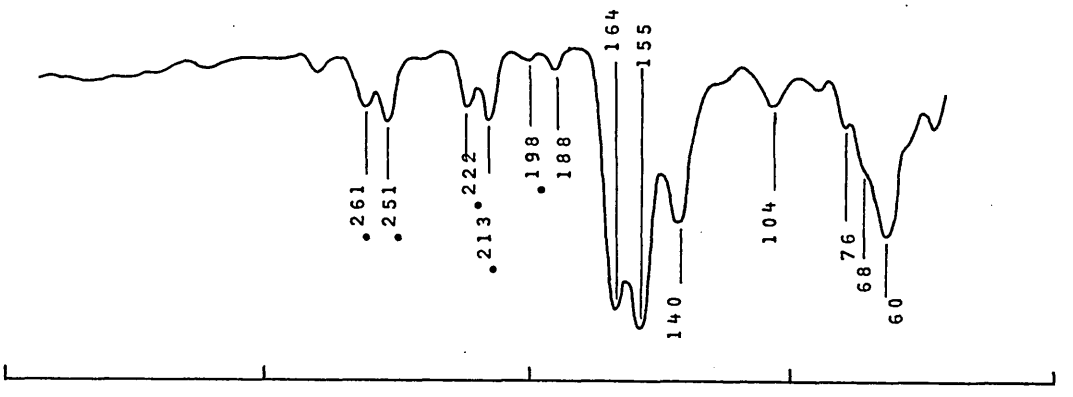

X=I

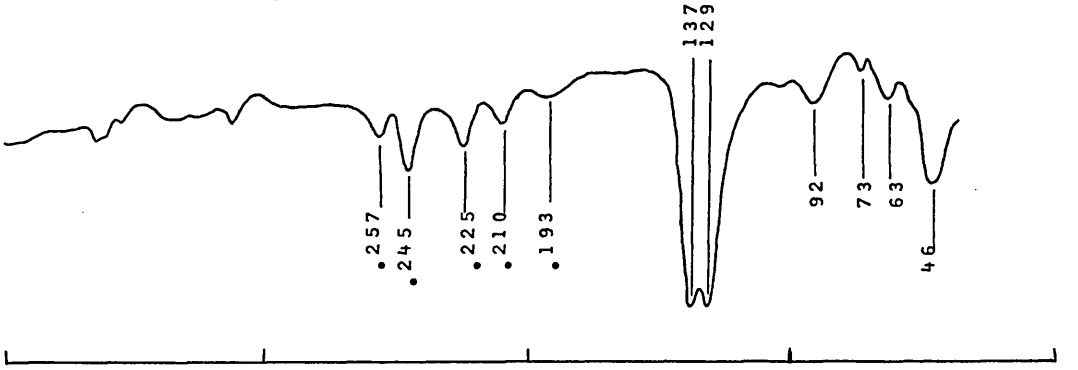

400 300 200 100 cm^{-1}

Raman spectra (RT) of $(PPh_3)_2HgX_2$ (X=Cl, Br or I) (cm^{-1})

• - internal mode of the ligand.

X=Cl

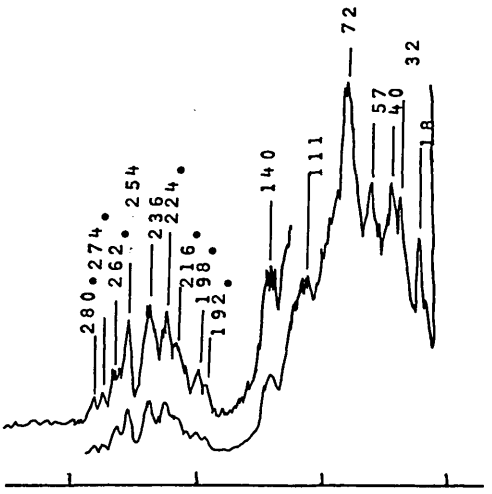

X=Br

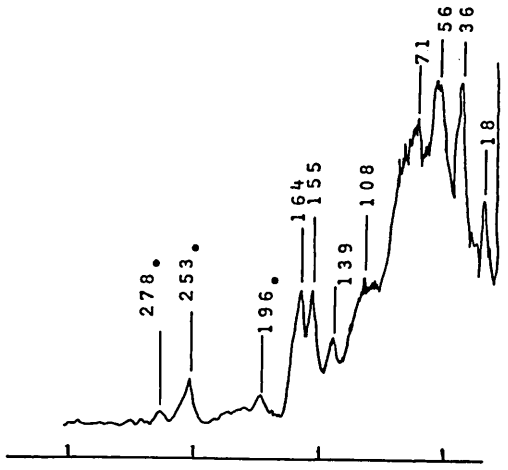

X=I

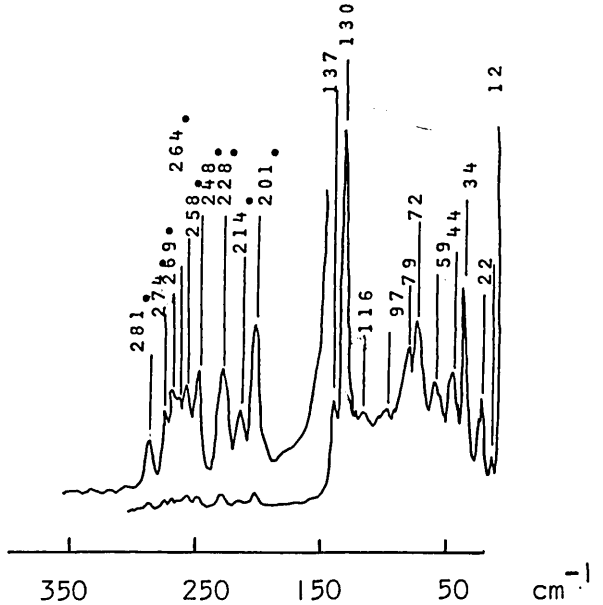

Table 5.3.

Vibrational assignments[a] for $(PPh_3)_2HgX_2$ (X=Cl, Br or I) (cm^{-1})

Cl		Br		I		
IR[b]	Ra[c]	IR[b]	Ra[c]	IR[b]	Ra[c]	Assignments
237s	236vw	164s	164m	137s	137m	ν_s(HgX)
223s[d]	224vw[d]	155s	155m	129s	130s	ν_a(HgX)
161w		164s[e]				ν_s(HgP)
145w	140m	140m	139w	137s[e]	137m[e]	ν_a(HgP)
					116m	
119m	111s	104w	108m	92w	97m	Deformation,
89s	72s	76w,sh	71s	73vw	79s	rocking,wagging,
81s	57s	68sh	56s	63w	72s	twisting and
73s	40s	60m	36s	46m	59m	external modes.
63sh	32s		18m		44m	
	18m				34s	
					22m	
					12w	

a - omitting internal ligand modes.

b - recorded at ca. 30K.

c - recorded at room temperature.

d - coincident with an internal ligand mode.

e - assumed coincident with ν_s(HgX)

modes of the iodo complex are evidently accidentally coincident with the ν(HgI) modes at ca. 137 cm^{-1}.

Detailed assignment of the deformation modes has not been attempted. However by comparison with similar modes of $[HgX_4]^{2-}$ species[96] these modes may be assigned to the bands occuring below 119, 108 and 97 cm^{-1}, in the IR and Ra spectra of chloro, bromo and iodo complexes, respectively. At very low wavenumber values in the Ra spectra (<40 cm^{-1}) one is almost certainly beginning to observe external modes.

One may note that the Raman spectra of the chloro and iodo complexes have been recorded at two separate amplifier gains. The problem which arose because of the weak Ra signals for ν(HgCl) modes for the 1:1 complexes (Section 3.3.1b) is again apparent for the $(PR_3)_2HgCl_2$ complexes. The amplified spectra were recorded to help with elimination of the internal modes of the PPh_3 ligand.

(b) $(PEt_3)_2HgX_2$ (X=Cl, Br or I)

The structure of $(PEt_3)_2HgCl_2$ has been shown to be monomeric and of C_{2v} symmetry but with a large P-Hg-P angle and relatively long Hg-Cl bonds (Table 5.1).

The regular halogen mass-dependence of both IR and Ra spectra indicate that the bromo and iodo complexes both have similar structures to the chloride.

The number and activity of the vibrational modes predicted by point group analysis for this structure, that of a C_{2v} monomer, has been stated in the previous Section.

Vibrational spectra are shown in Figures 5.3a and 5.3b. Internal modes of the ligand have been eliminated so that modes arising from ν(Hg-X) are readily assigned in both IR and Ra spectra at ca. 190, 150 and 110 cm^{-1} for chloro, bromo and iodo complexes, respectively. The ν_s(HgX) and ν_a(HgX) have been assigned in the same wavenumber order as previously. The low wave-

Figure 5.3(a).

Far infrared spectra (ca. 30K) of $(PEt_3)_2HgX_2$ (X=Cl, Br or I) (cm^{-1})

• - internal mode of the ligand.

X=Cl

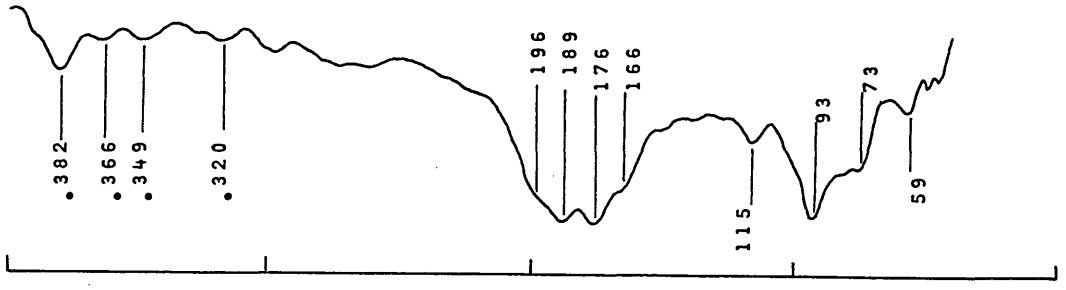

X=Br

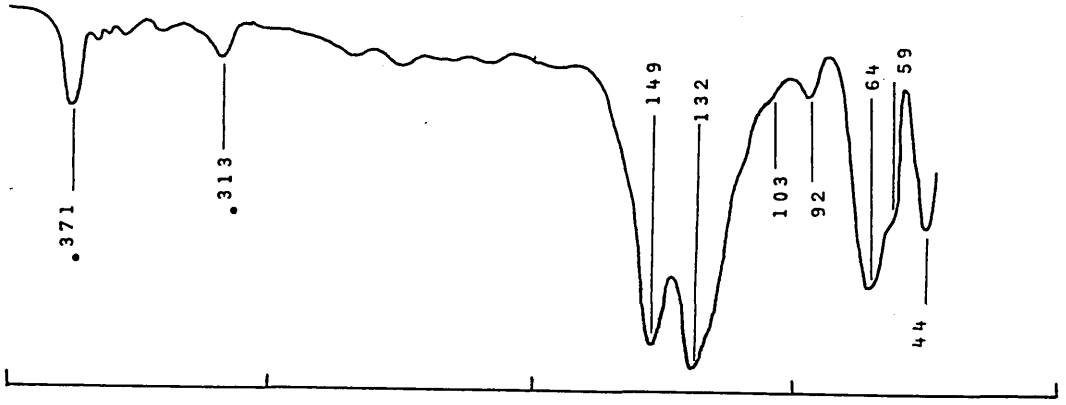

X=I

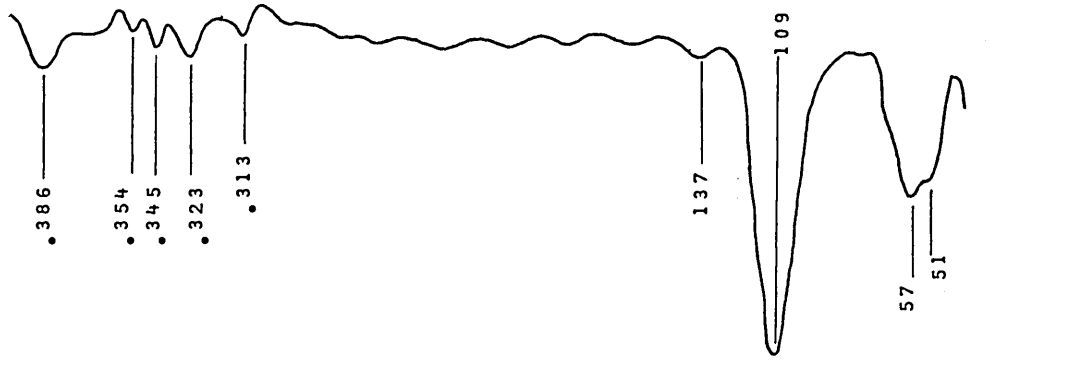

400 300 200 100 cm^{-1}

Raman spectra (RT) of $(PEt_3)_2HgX_2$ (X=Cl, Br or I) (cm^{-1})

X=Cl

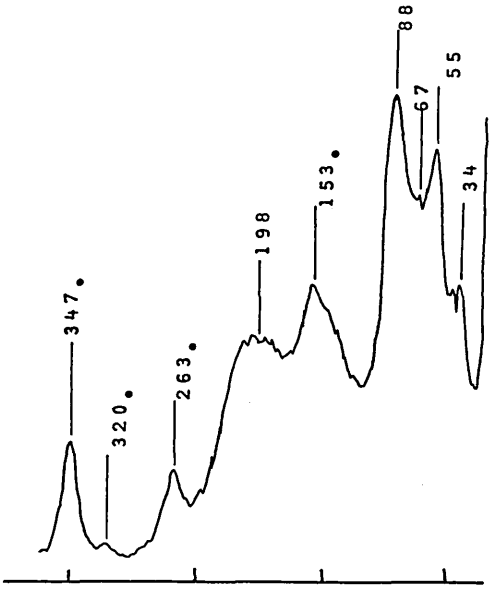

• - internal mode of the ligand.

X=Br

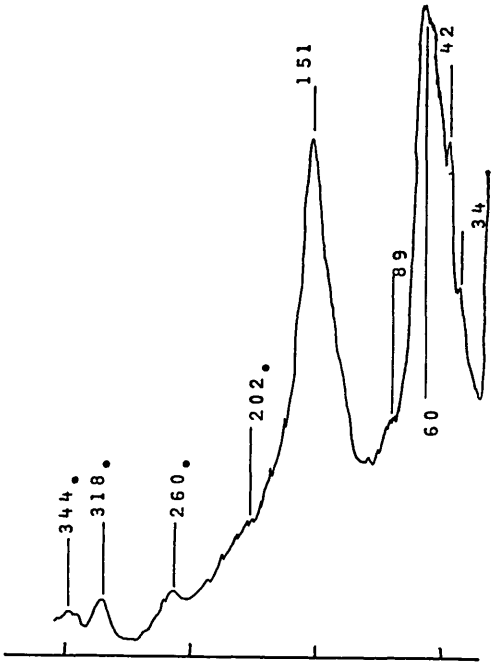

X=I

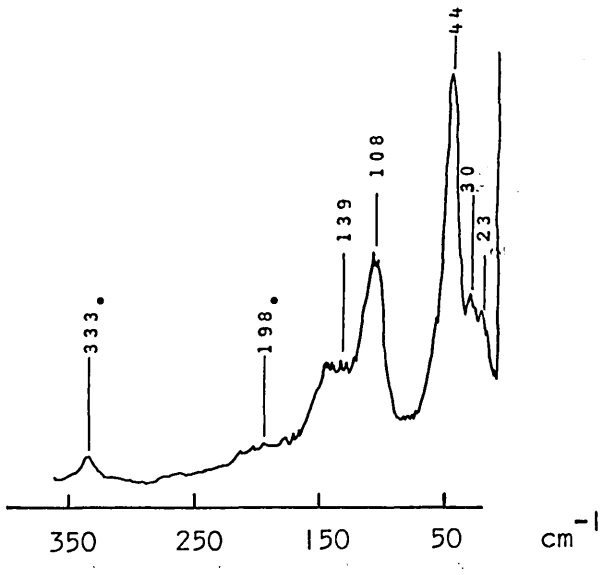

Table 5.4.

Vibrational assiqnments[9] for $(PEt_3)_2H9^2$ ^=Cl, Br or I) (cm 1)

c.		Br		[1]		
IRb	Rac	1Rb	RaC	IRb	Rac	Ass ignments
					139m	
196sh) 189s)	198s,br	149s	[1]51 vs	109s	108s	\MHgX)
176s) 166sh)		132s		109s	108s	Vg(HgX)
	153s					
[1]I5w	[8 8] vs	92w	89sh	57m	44vs	Deformation,
93s	67sh	64s	60vs	51 sh	30m	twisting, wagging
73sh	55s	59sh	42s		23m	and external
59w	34m	44m	32sh			modes.

a - omitting internal ligand modes,

b - recorded at ca. 30K.

c - recorded at room temperature.

number values of these modes, as compared to the equivalent modes observed for the $(PPh_3)_2HgX_2$ complexes, reflect the longer bond lengths which are known for the chloro complex and inferred for bromo and iodo complexes. Bands arising from ν_a(HgX) have only been observed in the IR spectra of the bromo and chloro compounds, whereas, ν_a(HgI) and ν_s(HgI) modes are probably coincident in both IR and Ra spectra. Certainly, this phenomenon of decrease in wavenumber separation of ν_s and ν_a modes as X changes from Cl→Br→I is quite common within the present series of $(PR_3)_2HgX_2$ complexes and has been reported on a number of occasions for related systems viz. $[HgX_4]^{2-}$ species,[90,96] $(PR_3)_2NiX_2$ complexes,[141] and $(Py)_2CoX_2$ complexes.[18]

The origin of bands which occur at 153(Ra) cm^{-1}, and 134(Ra) and 137(IR) cm^{-1} in the spectra of the chloro and iodo complexes respectively is difficult to assess. There is the possibility that these modes may have arisen from ν(HgP) modes, the corresponding modes for the bromide being 'masked' by the ν(HgBr) modes (at ca. 151 cm^{-1}). However, one may have expected ν(HgP) modes to appear at higher values, especially for $(PEt_3)_2HgCl_2$ in view of its large P-Hg-P angle.

(c) $(PBu^n_3)_2HgX_2$ (X=Cl, Br or I)

Preliminary crystallographic analysis indicates that $(PBu^n_3)_2HgCl_2$ is a distorted tetrahedral monomer of C_{2v} symmetry (Table 5.1). Vibrational spectra (Figures 5.4a and 5.4b) suggest that the equivalent bromo and iodo compounds are isostructural with the chloride. The Raman spectrum of the bromo complex appeared to undergo decomposition in the laser beam, presumably to the 1:1 complex, consequently this spectrum is not shown.

Room temperature IR and Ra spectra recorded in the present work are in agreement with those reported by Kessler.[90] The corresponding far IR spectra at ca. 30K (Figure 5.4a), however, showed improved spectral resolution, which allowed more detailed vibrational assignments.

Far infrared spectra (ca.30K) of $(PBu^n_3)_2HgX_2$ (X=Cl, Br or I) (cm^{-1})

X=Cl

• - internal mode of the ligand.

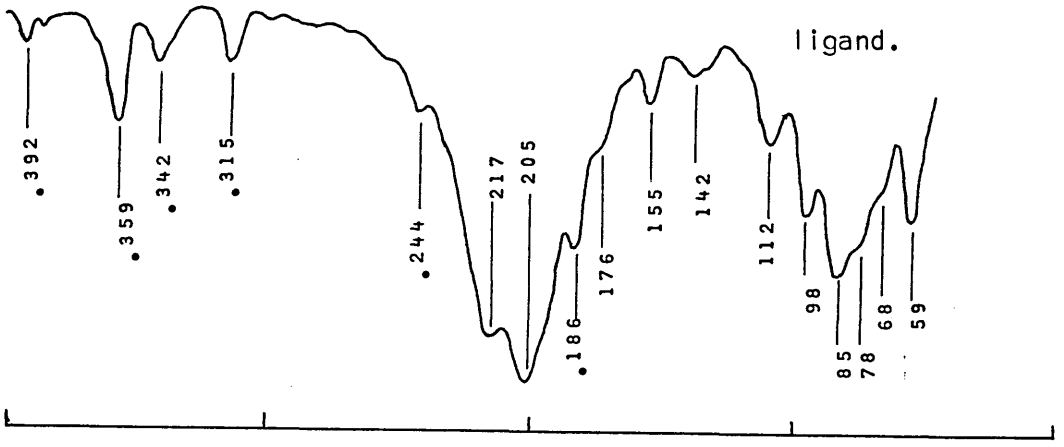

X=Br

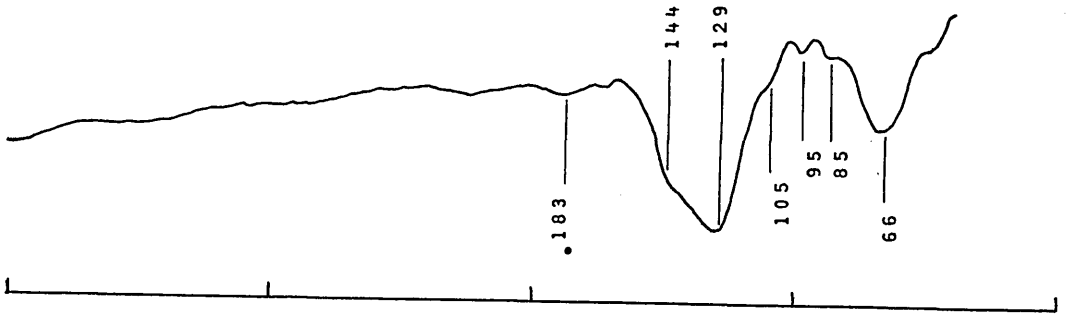

X=I

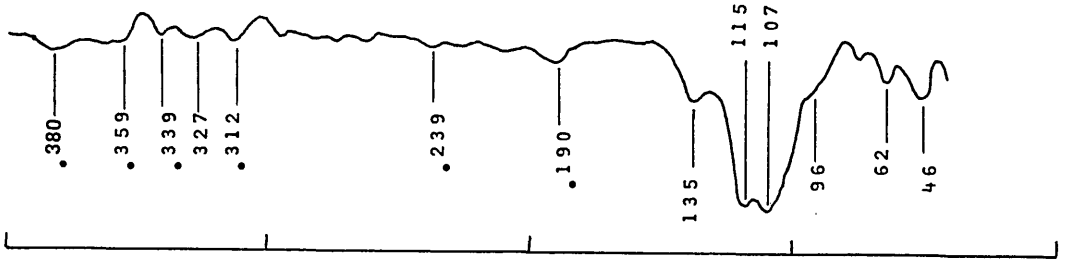

400 300 200 100 cm^{-1}

Raman spectra (RT) of $(PBu^n_3)_2HgX_2$ (X=Cl, or I) (cm^{-1})

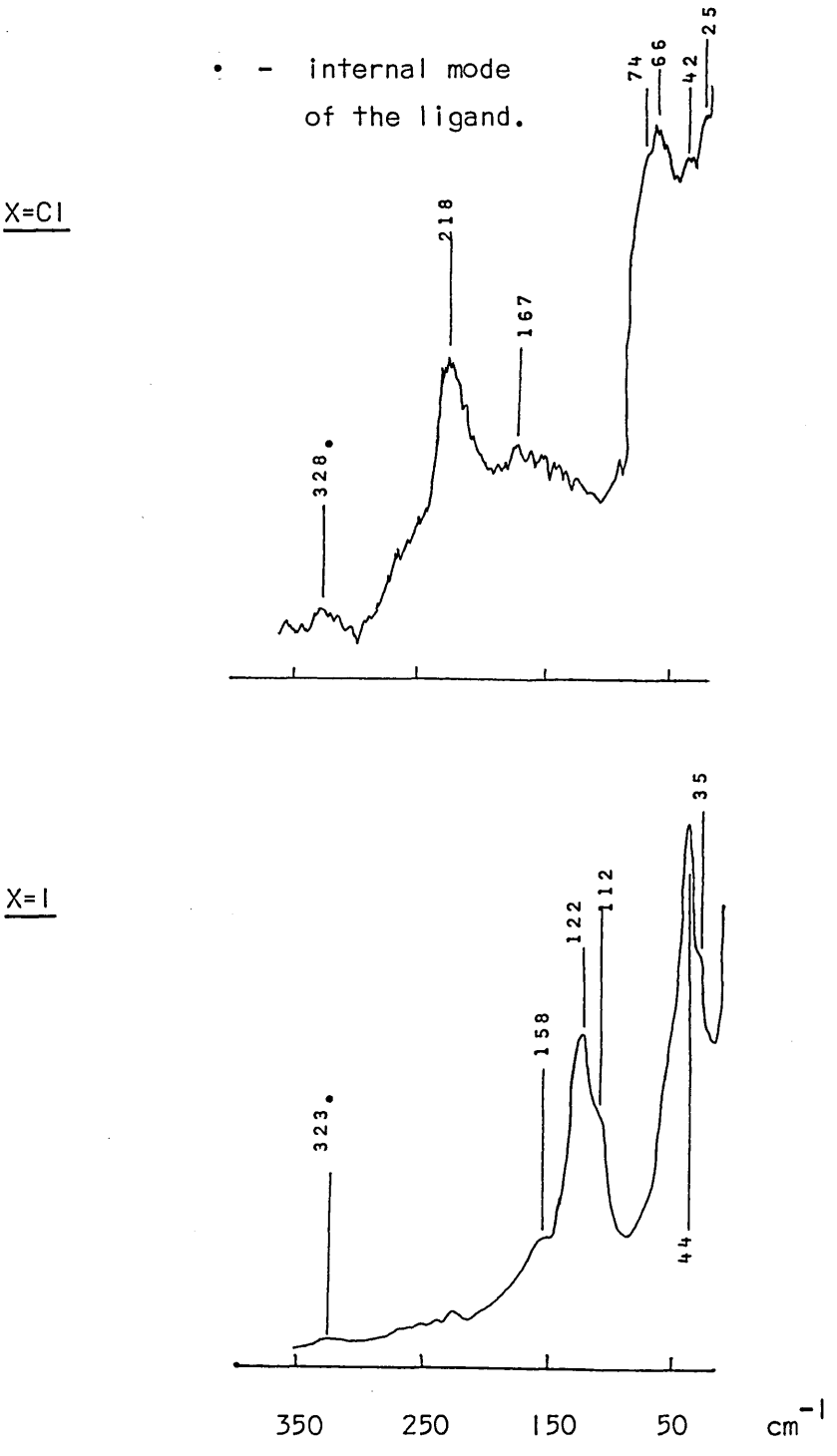

Table 5.5.

Vibrational assignments[a] for (PBu^)^HqX^ (X=Cl, Br or I) (cm *)

Cl		Br		I		
IRb	Rac	IRb	Rad	1Rb	RaC	Assignments
217s	218s	144sh		115s	122s	Vs (HgX)
205s		127s		107s	112sh	va (HgX)
176sh	167m,br					
155w						
142w				135w		
		110sh		96sh		
112mw	76sh	95w		62w	44vs	> Deformation,
98m	66vs	85sh		46w	35sh	rocking, wagging,
85ms	42vs	66m,br				twisting and
78sh	25sh					external modes.
68sh						
59m						

a - omitting internal ligand modes,

b - recorded at £a. 30K.

c - recorded at room temperature,

d - see text.

Internal modes of the PBu^n_3 ligand are easily eliminated by comparison of the spectra of all three complexes.

The number and activity of the vibrational modes predicted for ν(HgX) and ν(HgP) has already been stated (Section 5.1).

The ν_s(HgX) modes of the chloro and iodo complexes have been assigned as the strong halogen mass-dependent bands at ca. 218, 120 cm^{-1}, respectively, whereas bands at ca. 205, 127 and 110 cm^{-1} have been assigned ν_a(HgX) modes, for chloro, bromo and iodo complexes respectively.

Deformation, wagging modes etc., are likely to be contained within bands occuring lower than ca. 112, 95 and 62 cm^{-1} for chloro, bromo and iodo complexes, respectively.

Bands in the IR spectra at 142(Cl) and 135 cm^{-1} (I) are possibly due to ν(HgP), the corresponding mode for the bromo complex being masked by the ν(HgBr) mode. Again, however, on the basis of P-Hg-P angle, it is anticipated that ν(HgP) modes would occur at higher wavenumber values for the $(PBu^n_3)_2HgX_2$ series than for the $(PPh_3)_2HgX_2$ series.

(d) $(PEtMe_2)_2HgX_2$ (X=Cl, Br or I)

Crystallographic analysis shows that the structure of $(PEtMe_2)_2HgBr_2$ consists of two similar monomeric units of approximately C_{2v} symmetry (Table 5.1). The closest approach of these two monomers is through a mercury-bromine distance of ca. 3.8 Å, which is just outside the sum of the van der Waals' radii of mercury and bromine, and therefore little if any bonding between these two atoms is considered to take place. Consideration of the vibrational spectra of the equivalent chloro and iodo complexes indicates that similar structures are present to the bromide (Figures 5.5a and 5.5b).

The simplicity of the vibrational spectra of all three complexes allows one to use a simple point group analysis based on a structure of C_{2v} symmetry. The number and activity of the modes predicted for a molecule of this symmetry

Far infrared spectra (ca. 30K) of $(PEtMe_2)_2HgX_2$ (X=Cl, Br or I) (cm^{-1})

X=Cl

• - internal mode of the ligand.

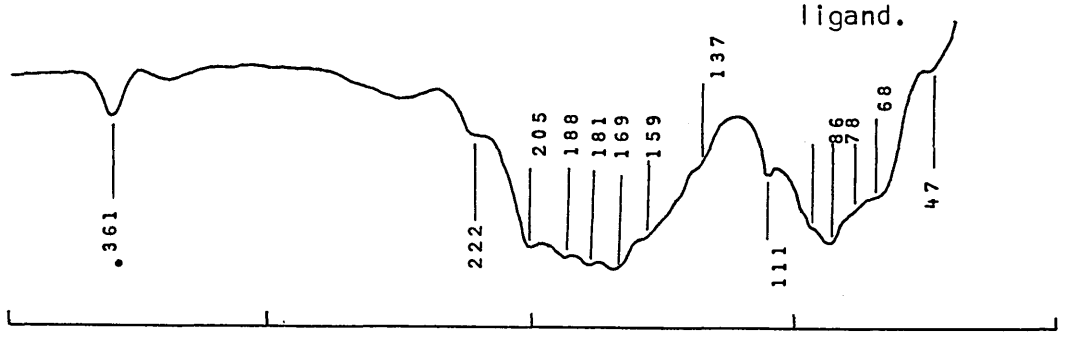

X=Br

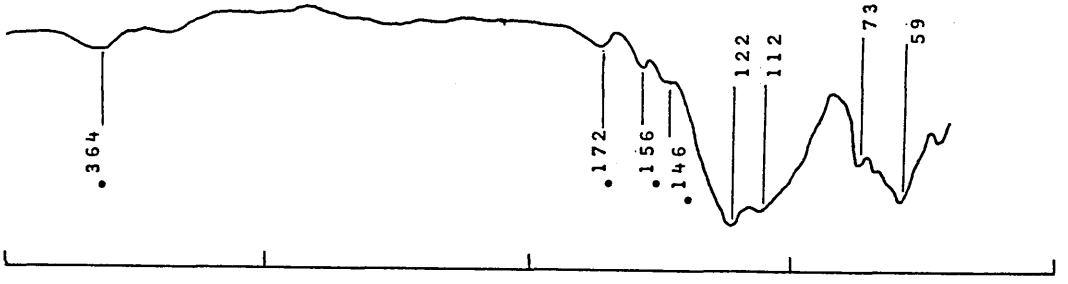

X=I

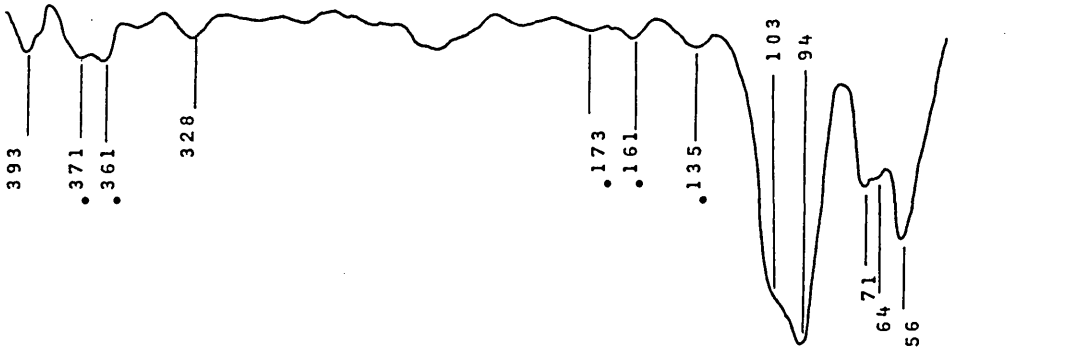

400 300 200 100 cm^{-1}

Raman spectra (RT) of $(PEtMe_2)_2HgX_2$ (X=Cl, Br or I) (cm^{-1})

X=Cl

• - internal mode of the ligand.

? - uncertainty as to the existence of this band.

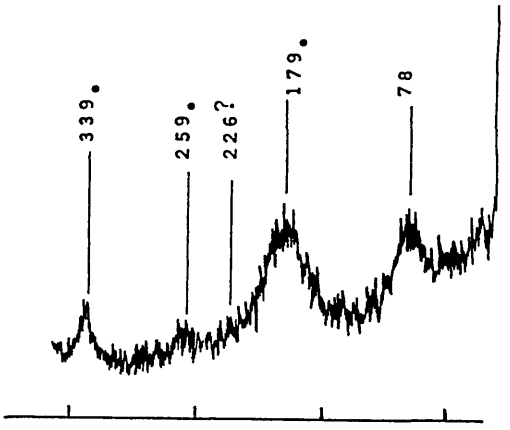

X=Br

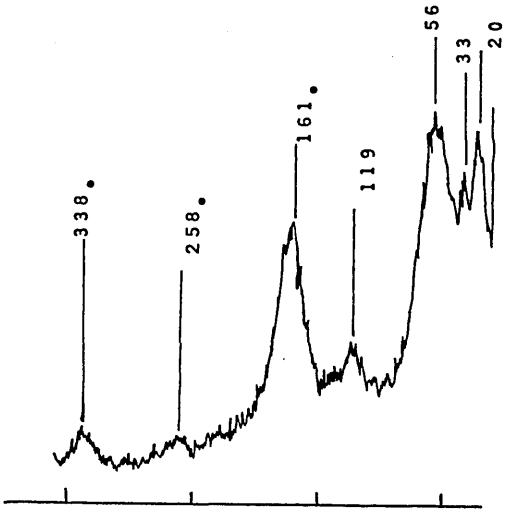

X=I

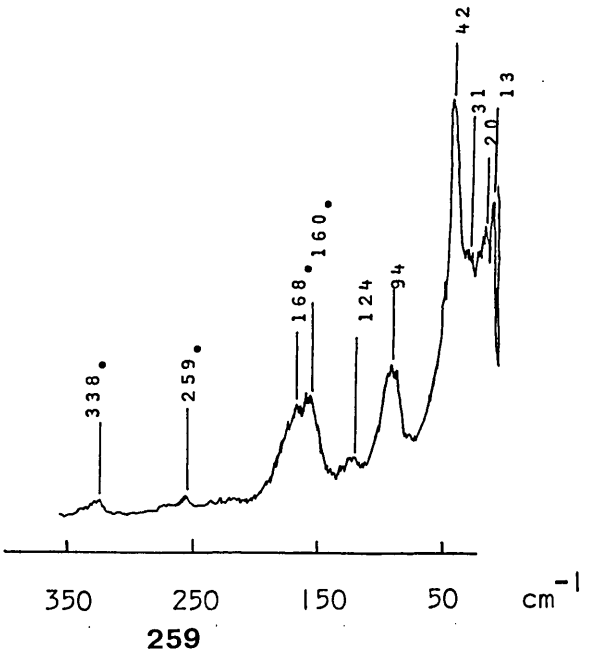

Table 5.6.

Vibrational assiqnments[a] for (PEtMe^)$_2$^$_9$X$_2$ (X=Cl, Br or 1) (cm^{-1})

Cl		Br		1		
1Rb	RaC	1Rb	RaC	.Rb	RaC	Assignments
	226vwd				124w	
205		$_{122}$s	$_{1}$19mw	103sh		\MHgX)
188	179s,br6					
181 s,br		$_{112}$sh		94s	94s	Vg(HgX)
169						
159						
137						
$_{11}$lw	78s,br	73w	56vs	71m	42vs	jDeformation,
93sh		59ms	33s	64sh	31 sh	lrocking, wagging,
$_{86}$s			$_{20}$vs	56ms	$_{20}$s	[twisting and
$_{68}$sh					13s	lexternal modes.
47sh						)

a - omitting internal ligand modes,

b - recorded at ca. 30K.

c - recorded at room temperature.

d - uncertainty as to the existence of this band (see text),

e - coincident with an internal ligand mode.

have been stated previously (Section 5.1).

These complexes have also been studied by Kessler,[90] but again the low-temperature IR spectra recorded here allow more detailed vibrational assignments. The assignments made here are essentially in agreement with those of Kessler,[90] the one notable difference occuring in the Ra spectrum of $(PEtMe_2)_2HgCl_2$ where a medium intense band at 233 cm^{-1} has been assigned[90] to $\nu_s(HgX)$. It was difficult to distinguish this band in the present study, probably due to high spectral noise. However, because in the present study one has the benefit of the crystallographic data for $(PEtMe_2)_2HgBr_2$, one may suggest the relatively high wavenumber position of this band is not consistent with the likely structure of $(PEtMe_2)_2HgCl_2$, and also not consistent with Kessler's own polarization data.

The few internal modes of the $PEtMe_2$ ligand have been eliminated by the halogen mass-dependence method. The very strong absorption from 137 to 205 cm^{-1} in the IR spectrum of the chloro complex is assigned to $\nu_a(HgX)$ and $\nu_s(HgX)$. The equivalent Raman bands are thought to be masked by the strong ligand band between 150 and 200 cm^{-1}. The low wavenumber values of these $\nu(HgCl)$ modes suggests that the Hg-Cl bonds are quite long, while the broad nature of the IR band perhaps suggests overlap of bands which may have arisen from vibration of a range of Hg-Cl bonds, some of which may be bridge bonds. Further inter-monomer contact is quite likely when one considers the structure of $(PEtMe_2)_2HgBr_2$; however the proposal for further association remains tentative without the necessary crystallographic evidence.

Assignments of $\nu(HgX)$ modes for bromo and iodo complexes are straightforward and are shown in Table 5.6. The wavenumber position of the $\nu(HgBr)$ modes are consistent with the Hg-Br bond lengths found; similarly, the low wavenumber position of $\nu(HgI)$ modes suggest correspondingly long Hg-I bond lengths for the iodo complex.

Finally, it should be mentioned that no evidence for ν(HgP) modes was immediately apparent.

(e) Summary.

As indicated in Section 4.1.5 the distortion of the 'P_2HgX_2' unit from regular tetrahedral appears to be dependent upon the donor strength of the PR_3 ligand. The degree of this distortion and thus the extent of mercury-phosphorus interaction may be indicated by each of two seemingly complementary parameters, viz. P-Hg-P angle and Hg-X bond length.

The magnitude of the Hg-X bond lengths, and consequently the P-Hg-P angles, are reflected in the vibrational spectra of the complex by the position of the mercury-halogen stretching modes (Table 5.7). The regular halogen mass-dependence in the vibrational spectra of each of the four series of compounds already studied suggests that equivalent halo analogues have similar structures (Table 5.7).

Therefore location of ν(HgX) modes in the regions 160-240 cm^{-1} for chloro, 110-160 cm^{-1} for bromo and 90-140 cm^{-1} for iodo complexes, and the absence of other bands attributable to mercury-halogen stretching indicate the presence of monomeric 'P_2HgX_2' species with the detailed geometries determining the precise wavenumber positions.

Although initial interpretation of these vibrational spectra, prior to crystallographic examination indicated long Hg-X bonds, a further inference from the results was the possibility of mercury-halogen associated structures.[90] There is no evidence for the existence of associated structures for $(PR_3)_2HgX_2$ complexes. Therefore it has been shown that the very low ν(HgX) modes observed for some structures is simply a function of the long Hg-X bond lengths, and that even such very low wavenumbers for ν(HgX) cannot be used to postulate association via halogen-bridging.

Although there is no evidence for association via halogen-bridging from

Table 5.7.

rhe relat'onship between the structures and vibrational spectra of some (PR-z)^HgX^ complexes.

Parameter	$(PR_3)_2HgCl_2$				$(PR_3')_2HgBr_2$				$(PR_3)_5Hg_2X_2$			
	PPh_3	PBu_3	$PEtMe_2$	PE+3	PPh_3	PBu_3	$PEtMe_2$	PEt_3	PPh_3	PBu_3	$PEtMe_2$	PEt_3
P-Hg-P angle/°		139		158.5			av. 148.5		110.43			
av. Hg-X length/A		2.60		2.68			2.79		2.75			
vas(H_gX) /cm	223	205	181-169	176	155	127	112	132	129	107	94	109

crystallographic studies, in one case, $(PEtMe_2)_2HgCl_2$, the breadth of the IR-active band assigned to ν(HgCl) has tentatively been attributed to band overlap caused by bands arising from vibration of a range of different Hg-Cl bonds, some of which may be Hg-Cl bridge bonds.

Evidence compiled concerning wavenumber regions where one might expect to observe ν(HgP) modes is again very meagre, as found for complexes of 1:1 stoicheiometry. Only the tentative assignments for the series $(PPh_3)_2HgX_2$, $(PBu^n_3)_2HgX_2$ and $(PEt_3)_2HgX_2$ have been possible.

5.3. THE SOLID-STATE VIBRATIONAL SPECTRA (cm^{-1}) OF SOME $(PR_3)_2HgX_2$ COMPLEXES OF UNKNOWN STRUCTURE.

(a) $(PPr^n_3)_2HgX_2$ (X=Cl, Br or I)

The general appearance of each spectrum indicates that all three complexes exist as monomers (Figures 5.6a and 5.6b). There are similarities in the wavenumber positions of ν(HgX) modes between the chloro complex and $(PEtMe_2)_2HgCl_2$, the bromo complex and $(PBu^n_3)_2HgBr_2$, and the iodo complex and $(PEt_3)_2HgI_2$. Similar coordination tetrahedra about mercury may therefore be envisaged although their precise nature are unknown.

Internal modes of the PPr^n_3 ligand have been eliminated by the usual methods. Specific wavenumber positions and vibrational assignments follow naturally from the similarities noted above and may be found in Table 5.8. The bands at 156, 161 and 155 cm^{-1} in the Ra spectra respectively of the chloro, bromo and iodo complexes have been tentatively assigned to ν_s(HgP). However, one should not dismiss the possibility that these bands contain some contribution from an internal ligand mode, because Allen and Wilkinson[141] have noted ligand bands in this region for $(PPr^n_3)_2PdCl_2$.

(b) $(PPh_2Me)_2HgX_2$ (X=Cl, Br or I)

The vibrational spectra of the chloro complex are very similar to those observed for $(PPh_3)_2HgCl_2$, suggesting a similar monomeric structure

Far infrared spectra (ca. 30K) of $(PPr^n_3)_2HgX_2$ (X=Cl, Br or I) (cm^{-1})

X=Cl

• - internal mode of the ligand.

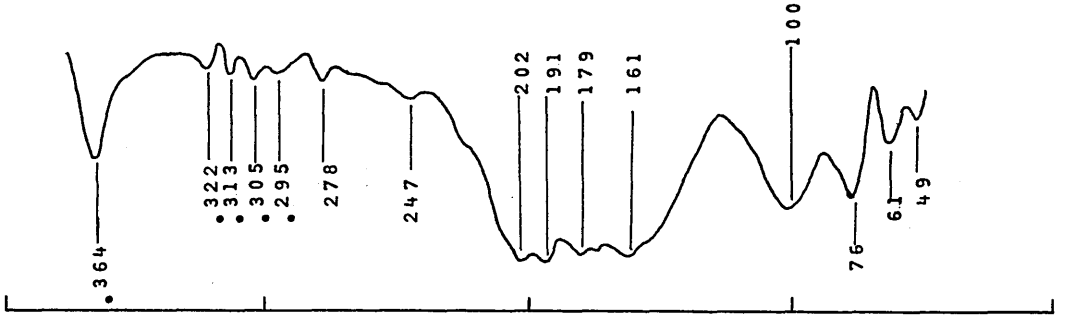

X=Br

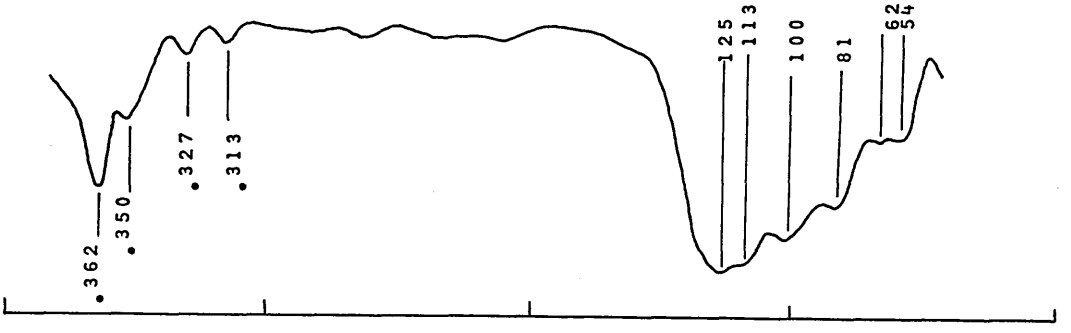

X=I

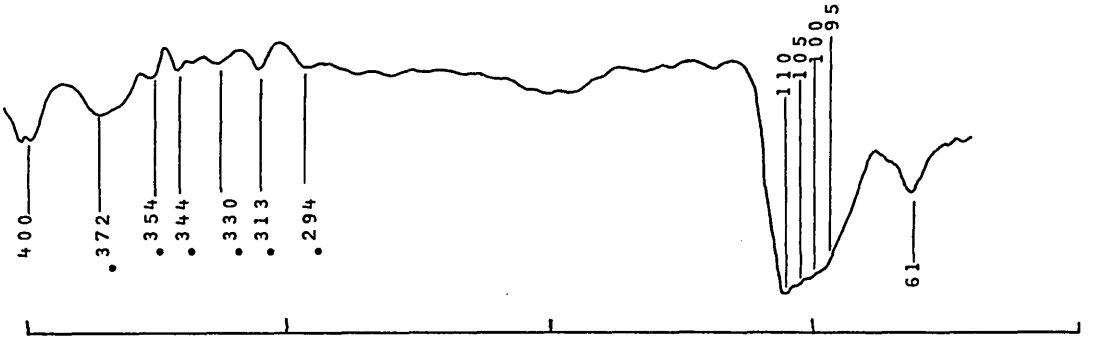

400 300 200 100 cm^{-1}

Raman spectra (RT) of $(PPr^n_3)_2HgX_2$ (X=Cl, Br or I) (cm^{-1})

X=Cl

internal mode of the ligand.

X=Br

350 250 150 50 cm"1

Table 5.8.

Vibrational assignments[3] for (PPr^)oHqXo (X=Cl, Br or I) (cm *)

Cl		Br		1		
1Rb	RaC	IRb	RaC	1Rb	RaC	Assignments
278w						
247w						
/ 202				/I 10	108s	
19!	197s	\\25s,br	132m	'I05sh	100sh	v(HgX)
s,br				s,br		
179		!l 13s,br		100sh	t 88sh	
161				{ 95sh		
	156m		161s		155m	v (HgP)
I00m,br	100sh	IOOsh	50vs	61mw	80w	]Deformation,
76m	72vs	81sh	38s		42vs	1rocking, wagging,
61mw	58sh	62sh			24s	Itwisting and
94m	44sh	54sh				1external modes.

a - omitting internal ligand modes,

b - recorded at ca. 30K.

c - recorded at room temperature.

Far infrared spectra (ca.30K) of $(PPh_2Me)_2HgX_2$ (X=Cl, Br or I) (cm^{-1})

X=Cl

• - internal mode of the ligand.

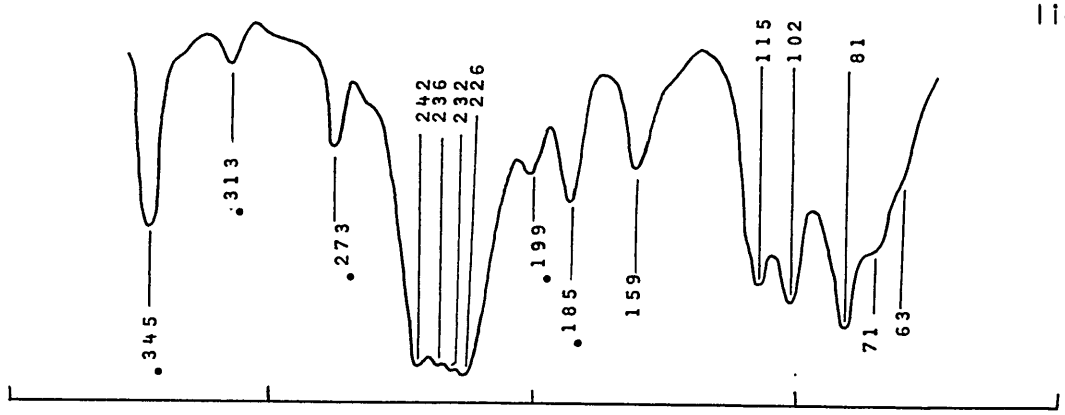

X=Br

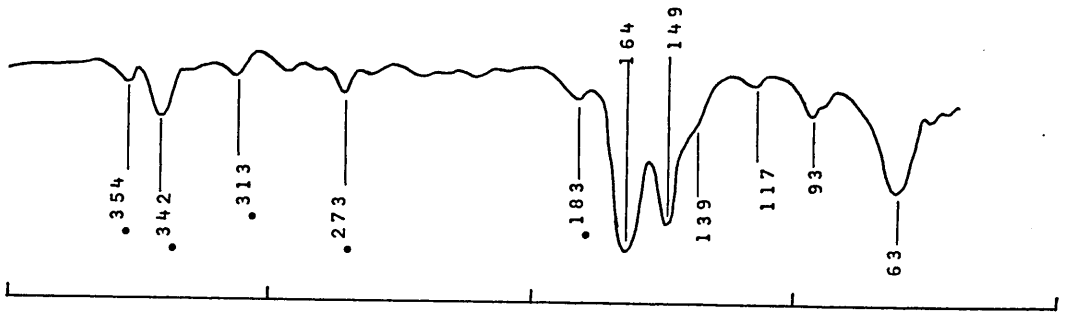

X=I

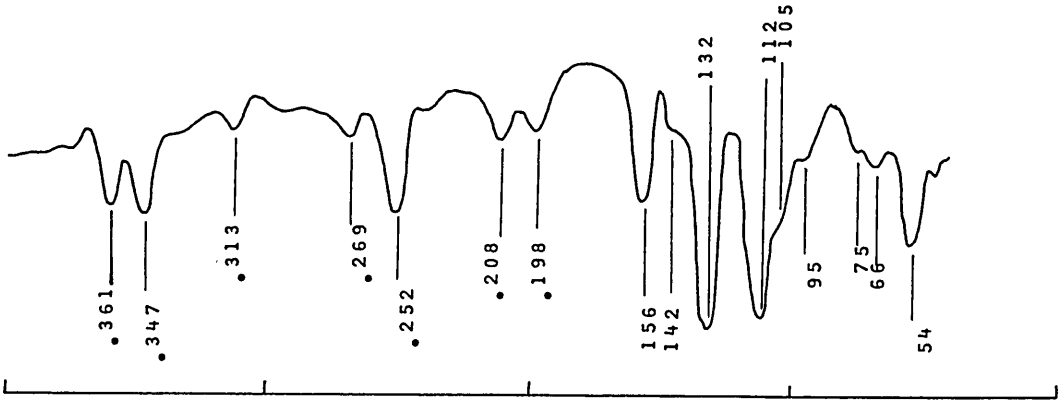

400 300 200 100 cm^{-1}

Raman spectra (RT) of $(PPh_2Me)_2HgX_2$ (X=Cl, Br or I) (cm^{-1})

X=Cl

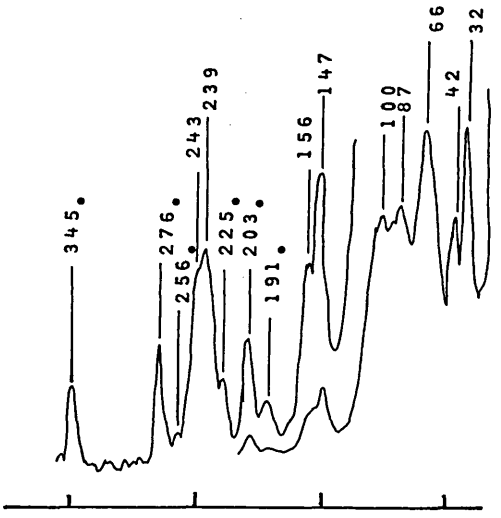

• - internal mode of the ligand.

X=Br

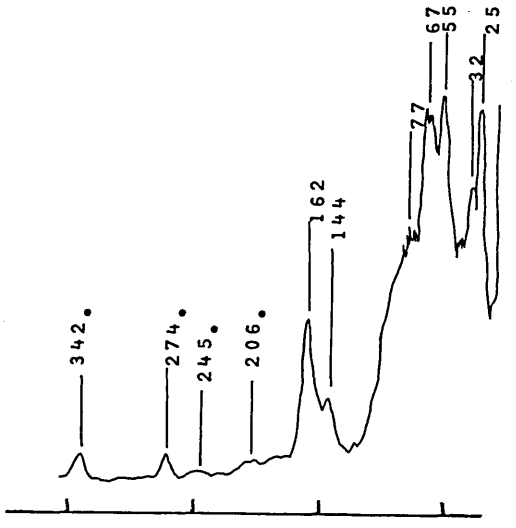

X=I

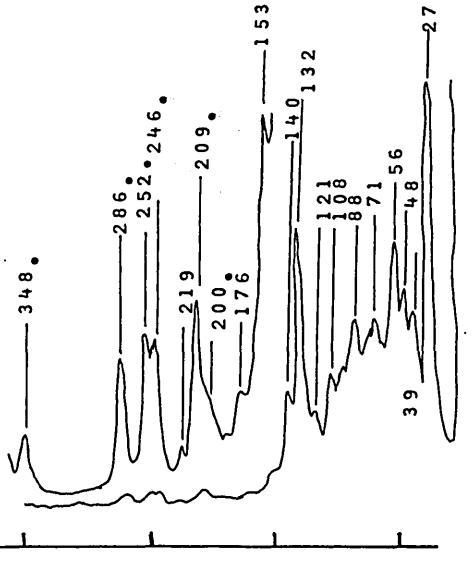

350 250 150 50 cm^{-1}

Table 5.9.

Vibrational assignments[3] for (PPh^ M e) (X=Cl, Br or I) (cm 1)

Cl		Br				
1Rb	RaC	1Rb	RaC	1Rb	Ra°	Assignments
242s ; 236s ;	243shj 239s j	164s	162s	132s	132s	1 v s (HgX)
232s ; 226s !	225mw	149s	144m	112 m	108m	1) v 3 (HgX)
159m	156m	149- 164s	144- 162s	156m	I53w	; v s (HgP)
	147s	139sh			140m	v g (HgP)
				142sh	121 m	
				105sh		
				95sh		
115s	100 s	93w	77sh	75sh	**88m**	\Deformation,
102 s	87s	63m	67vs	66 w	71m	Crocking, wagging,
81s	66 vs		55vs	54w	56s	Itwisting and
71 sh	42s		32s		48ms	Jexternal modes.
	32vs		25vs		39m	1
					27vs	}

a - omitting internal ligand modes,

b - recorded at ca. 30K.

c - recorded at room temperature.

(Figures 5.7a and 5.7b). According to assignments presented in Table 5.9 the positions of bands attributable to v(HgX) modes for bromo and iodo complexes are again of wavenumbers characteristic of the 'monomeric$_1$ $(PPh^{\wedge})_2 HgX_2$ (X=Br or I) complexes. However, in the present case there is a far wider separation between symmetric and anti symmetric v(HgX) modes. This separation is likely to be significant in terms of the precise coordination environment of mercury, but in exactly what way it is difficult to assess. Possible explanations include; (i) the presence of two Hg-X bonds of different length, or (ii) the presence of a relatively large X-Hg-X angle as indicated by Baran[137] from his work on a number of C2v systems. Of course the possibility of different structures and alternative assignments should not be dismissed, but alternative (ii) seems most likely.

Modes arising fromv(HgP) have been tentatively assigned at *ca_.* 150 cm for chloro and iodo complexes, thev(HgP) modes of $(PPh_2 Me)_2 HgBr_2$ being assumed to be accidentally coincident with v(HgBr) modes between 144 and 164 cm *. Wavenumber positions and vibrational assignments, omitting internal ligand modes , are contained in Table 5.9.

(c) $(PPhMe_2)_2 HgX_2$ (X=Cl, Br or I)

As for the $(PPhMe_2)HgX_2$ complexes, the appearance of strong ligand modes in the Ra spectra of $(PPhMe_2)_2 HgX_2$ complexes makes assignment of Ra-active modes very difficult.

In overall appearance, the vibrational spectra of the iodo complex (Figures 5.8a and 5.8b) are very similar to those of $(PPh_2 Me)_2 HgI_2$ and there fore similar structural possibilities are envisaged (Section 5.3b).

The lack of a well defined 'window' region between v(HgBr) modes and deformation modes etc., in the IR and Ra spectra of $(PPhMe_2)_2 HgBr_2$ perhaps indicates that further Hg Br interactions are present. The positions of the v(HgBr) modes suggests the existence of bond lengths of the same order as those found for $(PEtMe_2)_2$ HgBr2.

Far infrared spectra (ca.30K) of $(PPhMe_2)_2HgX_2$ (X=Cl, Br or I) (cm^{-1})

X=Cl

• - internal mode of the ligand.

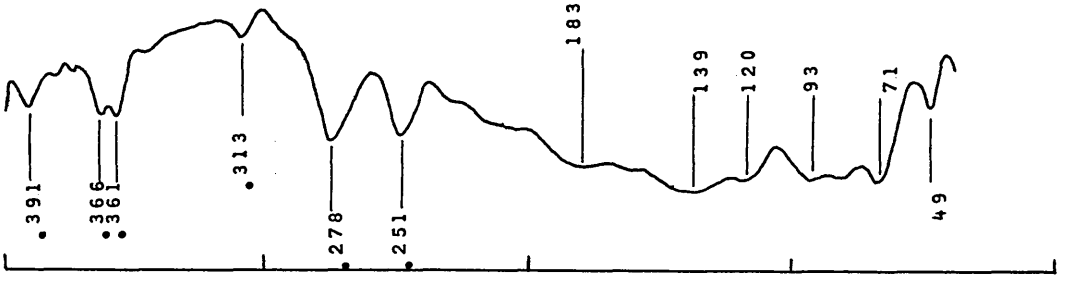

X=Br

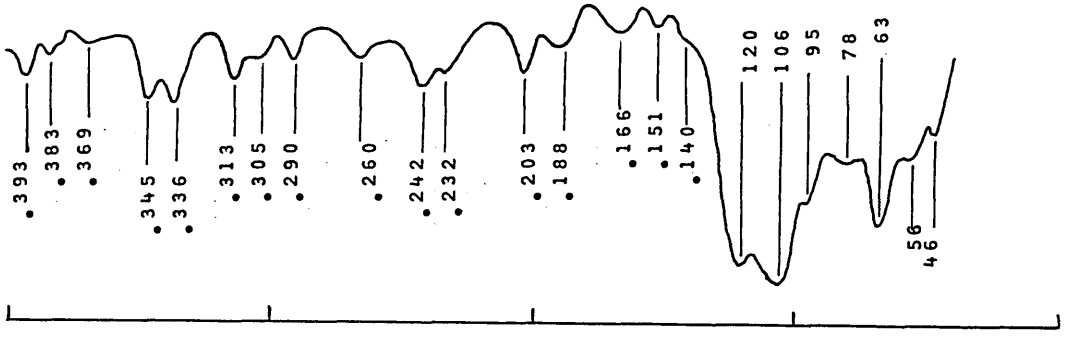

X=I

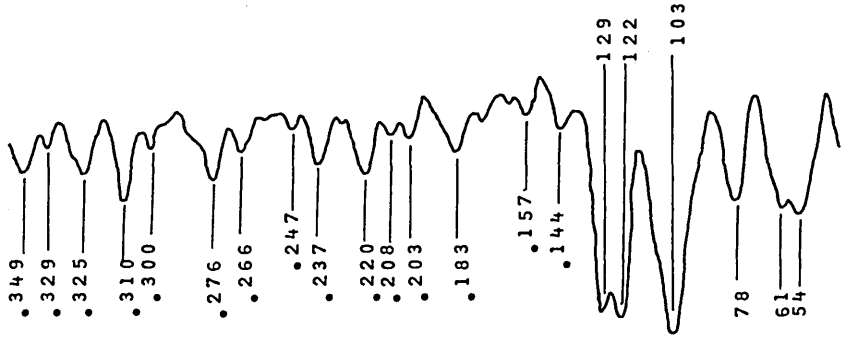

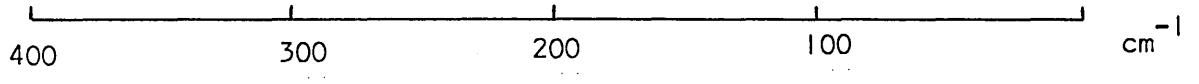

Figure 5.3(b).

Raman spectra (RT) of $(PPhMe_2)_2HgX_2$ (X=Cl, Br or I) (cm^{-1})

• - internal mode of the ligand.

X=Cl

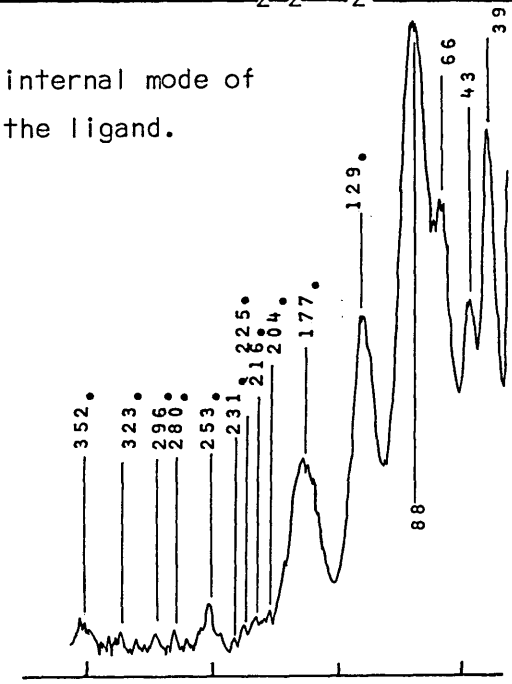

X=Br

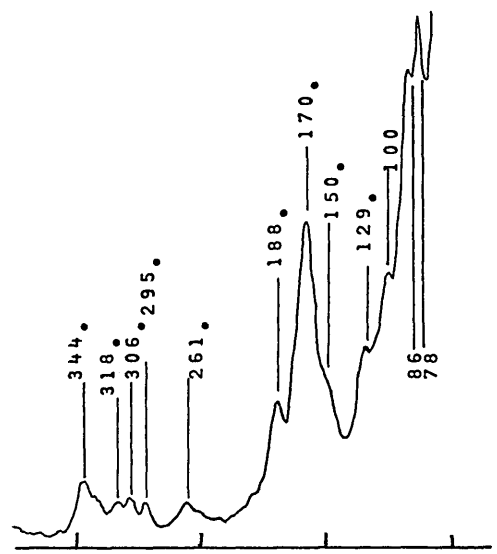

X=I

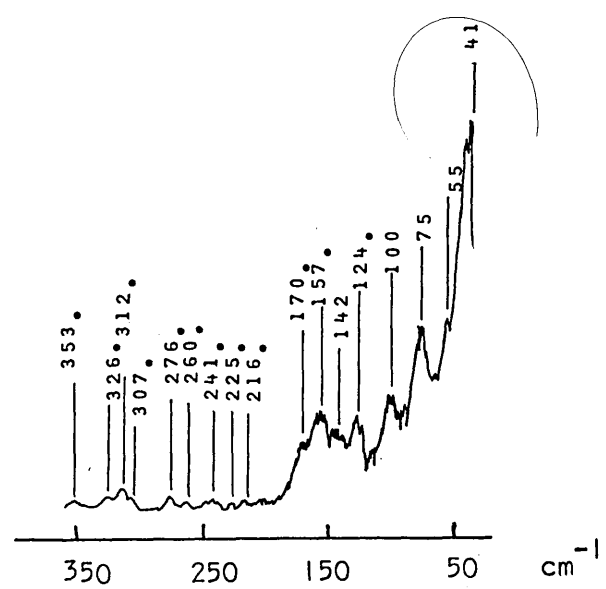

Table 5,10. ,

Vibrational assignments9 for (PPhMe^)^HqX^ (X=Cl, Br or I) (cm *)

Cl		Br		I		
1Rb	RaC	IRb	RaC	1Rb	RaC	Assignments
183		120 s		f 129s [122 s	124m	Vs(Hgx)
139 s, br 120		[106sh | 95sh	100 sh	103s	100 m	Va(HgX)
;93 s, vbr	88 vs	78sh	86 sh	78m	75s	>Deformation,
|7I	66 s	63m	78vs	61 m	55sh	wagging, twisting,
49w	43s	56sh		54m	41 vs	rocking and
	39vs	46w				external modes.

a - omitting internal modes of the ligand,

b - recorded at _ca. 30K.

c - recorded at room temperature.

The vibrational spectra of $(PPhMe_2)_2HgCl_2$ are unusual, but neither spectrum is obviously informative. However, it appears there is no absorption attributable to ν(HgCl) in the IR spectrum above ca. 183 cm^{-1}, and the very broad absorption below this value possibly suggests a bridged structure, for similar reasons as previously described. The Ra spectrum of this complex at wavenumbers above ca. 88 cm^{-1} is obliterated by what are thought to be internal ligand modes and so no assignments were possible in this region of the spectrum.

The large number of weak absorptions in the higher wavenumber regions of the IR spectra (> 180 cm^{-1}) of all three complexes most probably arise from internal modes of the $PPhMe_2$ ligand, and are assigned as such.

It was not possible to gain information concerning ν(HgP) modes. Wavenumber positions and vibrational assignments may be found in Table 5.10.

5.4. GENERAL DISCUSSION.

For the series of complexes $(PR_3)_2HgX_2$ examined in this work the general structural type appears to be that of a C_{2v} monomer. The precise stereochemistry of these monomers is apparently dependent on the donor properties of the PR_3 ligand.

It has been shown (Section 5.2) that the wavenumber positions of ν(HgX) modes for these monomers reflect their stereochemistry, and ν(HgX) modes may be found within a range of wavenumbers viz. 160-240, 110-166 and 90-140 cm^{-1} for chloro, bromo and iodo complexes, respectively. The ν(HgX) modes which occur at the lower wavenumber ends of these ranges indicate larger P-Hg-P angles and longer Hg-X bonds.

These structure/spectra relationships presented in Section 5.2 allow one to make some quite confident structural proposals. For example, that the structures of $(PPh_2Me)_2HgCl_2$ and $(PPh_3)_2HgCl_2$ are very similar and are probably slightly distorted tetrahedral monomers, and also that $(PPr^n_3)_2HgI_2$

and $(PBu^n_3)_2HgI_2$ are structurally very similar containing distorted tetrahedral monomers.

The vibrational spectra of other complexes, notably $(PPhMe_2)_2HgX_2$ (X=Cl or Br), suggest that other structural arrangements exist. The tentative proposals to the effect that associated structures are present can only be corroborated by complete crystallographic analysis. Unfortunately crystals of $(PPhMe_2)_2HgCl_2$ suitable for X-ray analysis could not be prepared.

With the knowledge which is now available concerning the wavenumber positions of ν(HgX) modes for a 'P_2HgX_2' C_{2v} monomeric structure, previous literature data can be examined. In some cases, such as the closely related complexes $(PCy_3)_2HgX_2$ (X=Cl, Br or I), quite detailed re-interpretation is possible. In view of the position of ν(HgX) modes at ca. 200, 140 and 100 cm^{-1} for chloro, bromo and iodo complexes, respectively, monomeric structures slightly more distorted than those found for $(PBu^n_3)_2HgX_2$ complexes may be envisaged. In other cases it is obvious that previous assignments and proposals of tetrahedral monomeric structures are erroneous viz. the (primary amine)$_2HgX_2$ complexes,[10] the (arylamine)$_2HgX_2$ complexes,[3] $[PhNHCS(NH_2)]_2HgCl_2$,[25] and $[Me_2NCS(H)]_2HgI_2$,[100] (Table 1.6). In all these compounds the positions of bands assigned to ν(HgX) are far too high to have arisen from regular tetrahedrally coordinated Hg-X bonds in a $(L)_2HgX_2$ complex.

The majority of other previous data have been interpreted in terms of a distorted octahedral polymeric structure, similar to that found crystallographically for $(Py)_2HgCl_2$.[84] Because of a limited crystallographic basis, one cannot comment upon these data other than re-emphasize the spectral properties of $(Py)_2HgCl_2$,[98] for which no ν(HgX) modes are observed above ca. 200 cm^{-1}, whereas most other reports propose this structure assign bands at ca. 290 cm^{-1} or above for chloro complexes,[2] and ca. 200 cm^{-1} and above for bromo complexes.[2,18-20] The high positions of these ν(HgX) modes are

not consistent with the assignments reported, evidently without ambiguity, for $(Py)_2HgCl_2$.[98]

The proposal of Kessler[90] that $(PEtMe_2)_2HgX_2$ (X=Br or I) adopt bridged structures with linear P-Hg-P units, is certainly in part correct because a P-Hg-P angle of ca. 150°, approaching linearity has been found for $(PEtMe_2)_2HgBr_2$. However, evidence concerning mercury-halogen bridging has not been definitely found crystallographically.

On the basis of the present work Schmidbaur's[4] proposal for the existence of linear $[P-Hg-P]^{2+}$ cations and $2X^-$ anions for $(PMe_3)_2HgX_2$ complexes in the solid state, can be stated probably to be correct, as far as the presence of linear P-Hg-P units are concerned. However, the nature of Hg-X interaction is still in doubt.

Contents

6.1. THE CRYSTALLOGRAPHIC EXAMINATION OF $(PEtMe_2)_3(HgCl_2)_2$

6.1.1. Introduction.

Although the literature contains very many reports of the existence of mercuric halide complexes of neutral unidentate ligands of varied stoicheiometry, very few definitive data are available concerning their actual structure. Evans *et al.*[61] have long since reported the existence of 3:2 (ligand:mercuric halide) complexes *viz.* $(PR_3)_3(HgI_2)_2$ (R=Pr^n or Bu^n) and $(AsR_3)_3(HgI_2)_2$ (R=Et, Pr^n or Bu^n). However, no crystallographic data are available for complexes of this type.

During the present work a compound of 3:2 stoicheiometry, $(PEtMe_2)_3(HgCl_2)_2$, was isolated from a sample which in bulk analysed as a 2:1 complex, $(PEtMe_2)_2HgCl_2$.

The crystal structure of this 3:2 complex has been determined thus providing the first crystallographic report for this stoicheiometry.

6.1.2. Structure determination of $(PEtMe_2)_3(HgCl_2)_2$

Crystal Data.

$C_{12}H_{33}P_3Hg_2Cl_4$ M_r=813.31 Orthorhombic

a=18.755(3), b=13.749(3), c=9.740(2) Å;

$\alpha=\beta=\gamma=90.00^\circ$.

D_m=2.19 g cm^{-3} (by flotation in a $CHBr_3/CHCl_3$ mixture), D_c=2.15 g cm^{-3}

Z=4, $F_{(000)}$=1511.65, μ(Mo-K_α)=123.41 cm^{-1}

Systematic absences:-

hoo reflections are absent for h=2n + 1

oko " " " " k=2n + 1

ool " " " " l=2n + 1

These absences uniquely define the crystals as belonging to the space group, $P2_12_12_1$ (D_2^4, No.19).[112]

Data Collection and Structure Refinement. The data set used for this

structure was collected on a Nonius Cad-4 diffractometer (at Rothamsted Experimental Station) using Mo-K radiation, $k = 0.71069$ Å.

A colourless crystal, approximate dimensions, 0.46x0.31x0.31 mm was mounted. There were 2702 reflections recorded with $2\theta < 40°$ of which 2552 had 1/ a(I) ^2,0 and were used for refinement. Interlayer scaling was used, but no absorption correction was applied.

The weighting scheme used was:-

$$w = 4.6289/(02|F_o| + 0.000297 |F_o|2)$$

Full-matrix refinement with anisotropic temperature factors for all non-carbon atoms gave Rw=0.064.% Final atomic and thermal parameters are given in Table A2.9 (Appendix 2). Calculated and observed structure factors are given in Table A3.9 (Appendix 3). A finalset ofbonddistances and bond angles may be found in Table 6.1.

Discussion and description of structure. The structure may be envisaged as a conti nous 'ionic' chain of [(PEtN^^HgCN + cations and [(PEtN^JHgCl ^ anions linked together via chlorine-bridges.

An unusual feature of this structure is the presence of alternating four- and five-coordinate mercury atoms.

The Hg(2) atom is joined to the threechlorineatoms, Cl(2), Cl(3) and Cl(4) at distances of 2.62(1), 2.52(1) and 2.45(1) Å, respectively, and to the P(3) atom at 2.40(2) Å. The Hg(2) atom lies in a distorted tetrahedral environment, the tetrahedral angles ranging from 98.2(5)° for Cl(2)-Hg(2)-Cl(3) to 132.9(6)° for P(3)-Hg(2)-Cl(4).

The characteristic coordination number of Hg(I) is three, with two short Hg-P bonds each 2.40 Å long separated by an angle of 172.3(5)°, and along Hg-Cl bond of 2.69(1) Å. The result is an unusual T-shaped geometry.

The effective coordination number of Hg(I) is increased from three to five by further contacts, Hg(I)—Cl(2)=3.07(I) A and Hg(I)-Cl(4)=3.25(I) A,

* - R= 0.057

which result in a very distorted trigonal bipyramidal arrangement.

The molecular packing diagram shows how the chains are arranged with respect to one another in the unit cell (Figure 6.2).

The P-C and C-C distances, and C-P-C angles of the $PEtMe_2$ ligands are typical of other phosphine ligands studied in this work.

It is difficult to draw any meaningful inferences with regards to factors influencing structures of this stoicheiometry on the basis of a single structure, but there is one striking feature of this structure which is analogous to previous findings for the 1:1, and especially the 2:1 systems, notably the large P-Hg-P angle ($172.3(5)^{\circ}$) contained in the $[P_2HgCl]^+$ cation. Mercury once again adopts the common linear coordination arrangement apparently favoured by the 'strong' donor properties of the $PEtMe_2$ ligand, as expressed by its cone angle, Taft constant and pK_a value.

Table 6.1.

Bond distances and angles for $(PEtMe_2)_3(HgCl_2)_2$ — with standard deviations in parentheses.

(a) Distances/ Å

Hg(1)-Cl(1)	= 2.69(1)	P(1)-C(11)	= 1.83(6)
Hg(1)---Cl(2)	= 3.07(1)	P(1)-C(12)	= 1.79(5)
Hg(1')---Cl(4)	= 3.25(2)	P(1)-C(13)	= 1.82(6)
Hg(1)-P(1)	= 2.40(1)	C(13)-C(14)	= 1.59(9)
Hg(1)-P(2)	= 2.40(1)		
Hg(2)-Cl(2)	= 2.62(1)	P(2)-C(21)	= 1.70(6)
Hg(2)-Cl(3)	= 2.52(1)	P(2)-C(22)	= 1.81(7)
Hg(2)-Cl(4)	= 2.45(1)	P(2)-C(23)	= 1.79(5)
Hg(2)-P(3)	= 2.40(1)	C(23)-C(24)	= 1.57(8)
		P(3)-C(31)	= 1.81(5)
		P(3)-C(32)	= 1.81(5)
		P(3)-C(33)	= 1.81(7)
		C(33)-C(34)	= 1.58(9)

(b) Angles/ °

Cl(1)-Hg(1)-P(1)	= 97.6(5)	C(11)-P(1)-Hg(1)	= 110(2)
Cl(1)-Hg(1)-P(2)	= 90.1(5)	C(11)-P(1)-C(12)	= 103(3)
P(1)-Hg(1)-P(2)	=172.3(5)	C(11)-P(1)-C(13)	= 111(3)
		C(12)-P(1)-Hg(1)	= 110(2)
Cl(4)-Hg(1)-Cl(2)	=140.1(4)	C(12)-P(1)-C(13)	= 104(3)
		C(13)-P(1)-Hg(1)	= 118(2)
Cl(2)-Hg(2)-Cl(3)	= 98.2(5)	C(14)-C(13)-P(1)	= 113(5)
Cl(2)-Hg(2)-Cl(4)	=103.1(5)		
Cl(2)-Hg(2)-P(3)	=101.0(5)	C(21)-P(2)-Hg(1)	= 110(2)
Cl(3)-Hg(2)-Cl(4)	= 98.5(5)	C(21)-P(2)-C(22)	= 108(3)
Cl(3)-Hg(2)-P(3)	=117.2(5)	C(21)-P(2)-C(23)	= 105(3)
Cl(4)-Hg(2)-P(3)	=132.9(6)	C(22)-P(2)-Hg(1)	= 115(2)
		C(22)-P(2)-C(23)	= 106(3)
Hg(1)-Cl(2)-Hg(2)	=133.1(5)	C(23)-P(2)-Hg(1)	= 112(2)
Hg(1)-Cl(4)-Hg(2)	=107.1(5)	C(24)-C(23)-P(2)	= 111(4)

Table 6.1, continued.

(b) Angles/ °

C(31)-P(3)-Hg(2)	= 113(2)
C(31)-P(3)-C(32)	= 109(3)
C(31)-P(3)-C(33)	= 102(3)
C(32)-P(3)-Hg(2)	= 107(2)
C(32)-P(3)-C(33)	= 113(4)
C(33)-P(3)-Hg(2)	= 113(2)
C(34)-C(33)-P(3)	= 107(5)

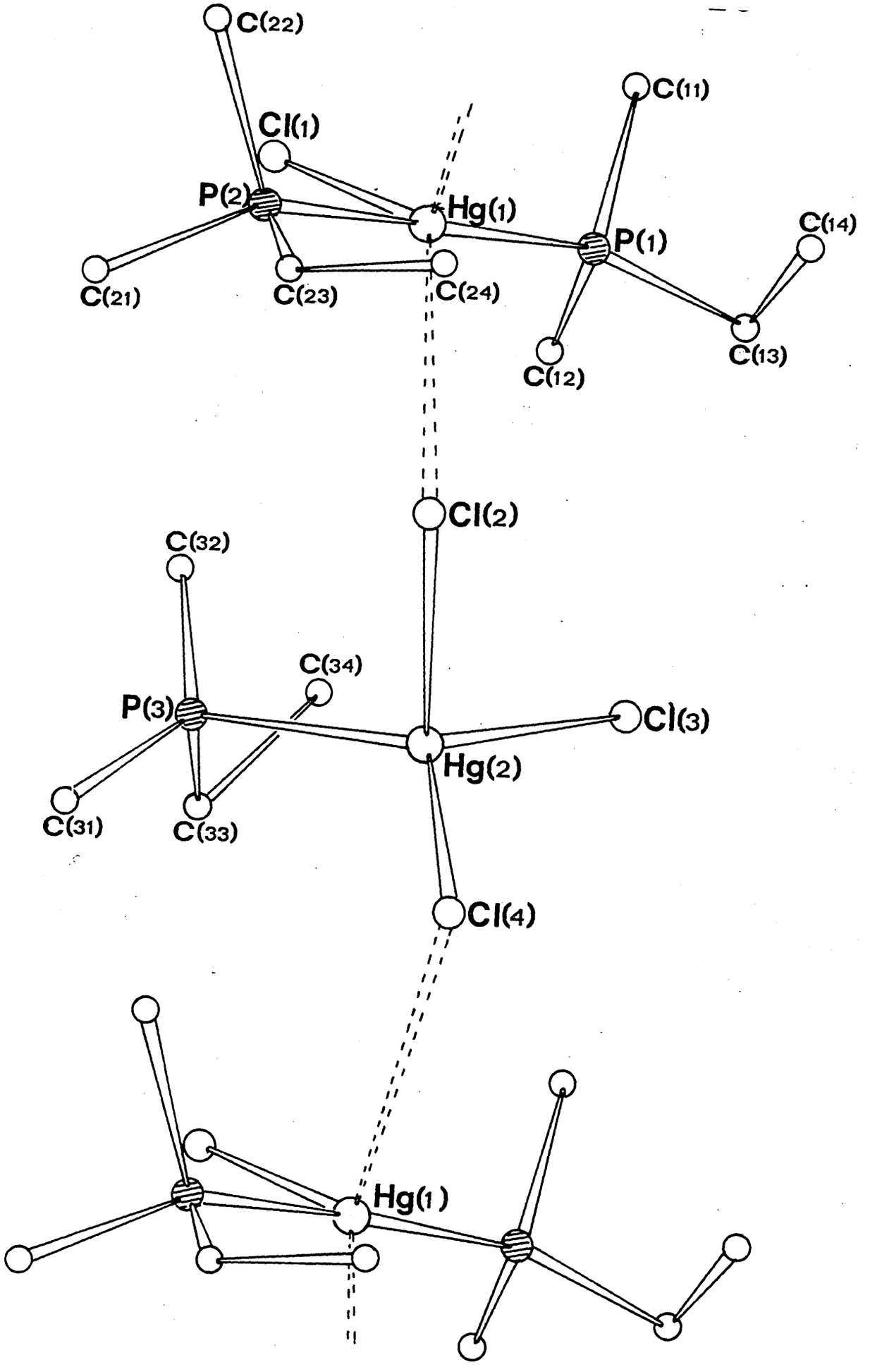
C(22)
C(11)
Cl(1)
P(2)
Hg(1)
P(1)
C(14)
C(21)
C(23)
C(24)
C(12)
C(13)
Cl(2)
C(32)
C(34)
P(3)
Cl(3)
Hg(2)
C(31)
C(33)
Cl(4)
Hg(1)

—viewed along the a-axis

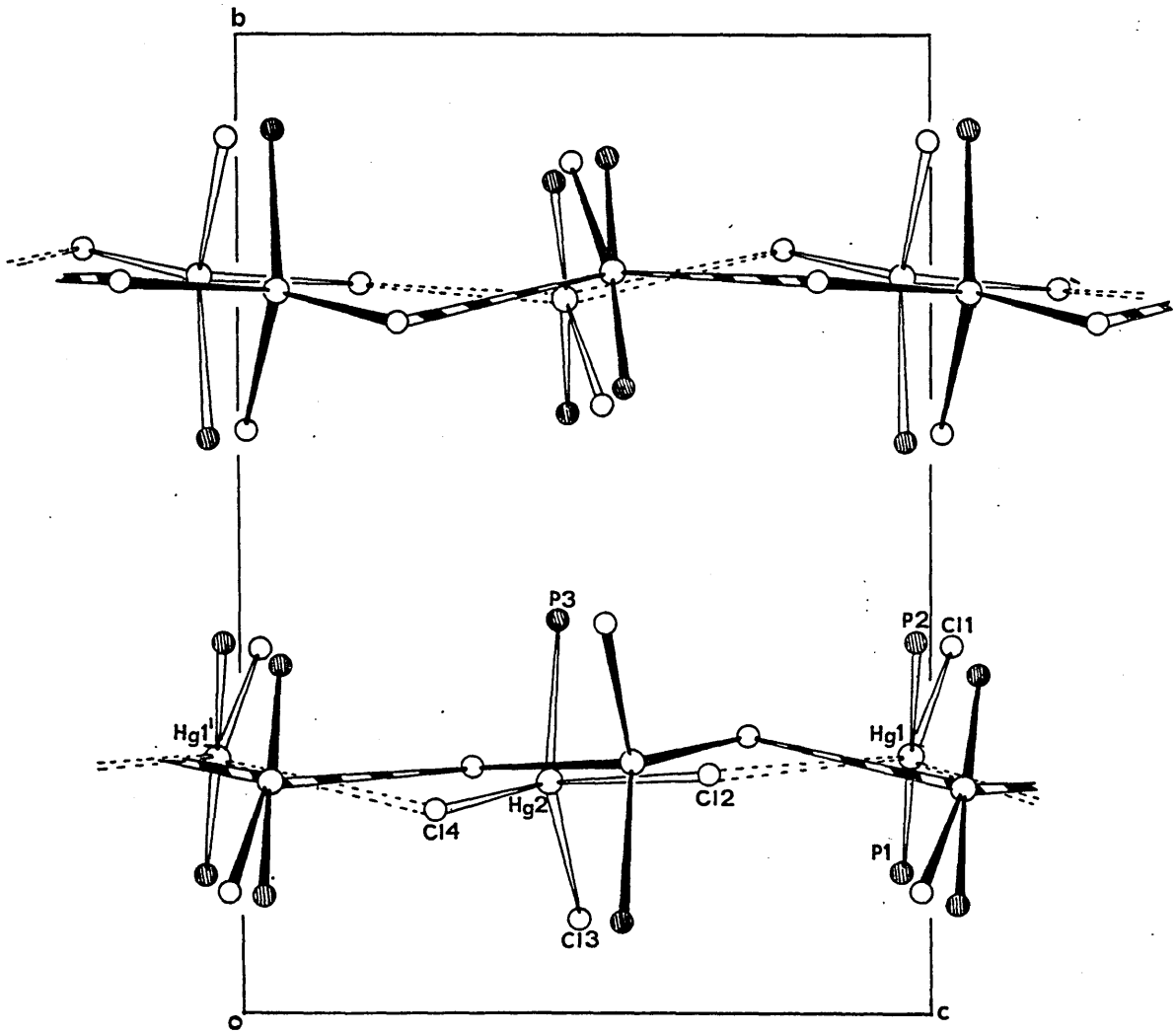

a—Omitting carbon atoms

Contents

7.1. PREPARATIVE METHODS

The tertiary phosphines PPh_3 and PMe_3 were prepared using standard Grignard syntheses. The $(PMe_3)AgNO_3$ complex was prepared as described by Goggin *et al.*[149] All other tertiary phosphines were supplied by Maybridge Chemicals (Tintagel, Cornwall) and were used as obtained.

The Ph_3PS was prepared as described by Dalziel *et al.*[145] All other ligands were commercially available, easily obtained and were used as received.

Sodium-dried Analar benzene was used for all molecular mass determinations.

Table 7.1 contains analytical data for all complexes prepared and studied in this work. The methods of preparation used for each complex are denoted A, B, C, etc. Details of each of these preparative methods are outlined below. The approximate quantity of mercuric halide used for each preparation was 1.35 g (0.005 mole) $HgCl_2$, 1.80 g (0.005 mole) $HgBr_2$ and 1.25 g (0.0025 mole) HgI_2. Because it was the structural properties of the complexes which were under investigation and not the properties of the actual reaction, product yields have been sacrificed at the expense of obtaining high purity of samples, and so, no percentage yields are quoted. Unless otherwise stated the final recrystallised sample was used for subsequent study.

A Equimolar proportions of ligand and mercuric halide were dissolved in minimal quantities of ethanol. When necessary, these mixtures were heated to enable complete dissolution of solute. The ligand solution was added dropwise to the mercuric halide solution and the precipitate which formed, immediately or on standing, was collected and dried by suction. A portion of this initial product was recrystallised from a DMF/H_2O mixture, and dried *in vacuo*.

B This method was very similar to method A; however, recrystallisation

consisted of five rapid recrystallisations using ethanol as solvent, as described by Evans *et al.*[56] Previous attempts to prepare $(PEt_3)HgBr_2$ and $(PEt_3)HgI_2$ showed that slow recrystallisation resulted in 2:3 complexes being formed.

C The method employed was that described by Goggin *et al.*[149] The PMe_3 ligand was released from the complex $(PMe_3)AgNO_3$ by heating under reflux in the presence of thiourea. The PMe_3 ligand was distilled under dry N_2, into a reaction vessel containing an ethanolic solution of mercuric chloride. Equimolar proportions of $(PMe_3)AgNO_3$ and mercuric chloride were used. The white precipitate which formed immediately on contact of PMe_3 and $HgCl_2$ was collected, dried by suction and recrystallised from DMF/H_2O.

D A solution of $(PMe_3)AgNO_3$ in water was added dropwise to an equimolar aqueous solution of $(NEt_4)_2HgX_4$* (X=Cl or Br). A yellow/white precipitate containing a mixture of AgCl and $(PMe_3)HgX_2$ formed immediately. After complete addition of the $(PMe_3)AgNO_3$ solution the precipitate was collected and dried by suction. The $(PMe_3)HgX_2$ complex was extracted from the AgCl using hot DMF. Distilled water was added dropwise to the DMF extract until it became cloudy. The DMF extract was heated until the cloudiness disappeared. On standing, white, well formed, rectangularly shaped crystals were obtained. These crystals were collected and dried *in vacuo*. For the preparation of $(PMe_3)HgI_2$, the $(NEt_4)_2HgI_4$ salt had to be dissolved in a considerable quantity of acetone. In the case of $(PMe_3)HgCl_2$, it was found that K_2HgCl_4 could be used in place of $(NEt_4)_2HgCl_4$.

E This method is very similar to method A but with recrystallisation carried out from ethanol rather than from DMF/H_2O.

F This method has previously been described by Evans *et al*[61] "The PPr^n_3 ligand (1 mol) and a solution of excess HgI_2 (2 mol) in 10% aqueous potassium iodide solution were vigorously shaken together; a pale yellow sticky product

* Prepared as described in Reference 96

deposited; recrystallisation from alcohol:acetone (4:1) gave the white α- form of the $(PPr^n_3)HgI_2$ complex. The mother liquor on standing deposited the β - form as yellow crystals."

G Equimolar quantities of $PPhMe_2$ and HgI_2 were dissolved separately in minimal quantities of ethanol. The ligand solution was added dropwise to the HgI_2 solution and a yellow oil was produced. The contents of the flask were heated so as to dissolve as much of the oil as possible. The ethanolic solution was then decanted to separate the remainder of undissolved oil. On standing, small white clusters of very fine needle shaped crystals appeared. On further standing yellow opaque deposits also formed together with more of the yellow oil. The white precipitate was collected and dried in vacuo; this product was found from elemental analysis to be the 1:1 complex and so was used for subsequent study. The yellow deposits were found to be $(PPhMe_2)_2(HgI_2)_3$ (found : C, 12.2; H, 1.5%. $C_{16}H_{22}P_2Hg_3I_6$ requires : C, 11.7; H, 1.4%).

H Equimolar quantities of PBu^n_3 and $HgCl_2$ were dissolved separately in minimal quantities of ethanol. The PBu^n_3 solution was added dropwise to the ethanolic solution of $HgCl_2$, whereupon a fine white precipitate formed immediately. When approximately half of the PBu^n_3 solution had been added, the precipitate then obtained was collected, washed in ethanol, then ether, and dried in vacuo; it was then recrystallised from benzene/heptane. Separate experiments showed that if all the PBu^n_3 solution was added to the $HgCl_2$ solution, the white precipitate initially formed redissolved and subsequent attempts to isolate a complex of 1:1 stoicheiometry led to the formation of what is most likely an impure sample of a 3:2 complex (found : C, 35.8; H, 6.8%. $C_{36}H_{81}P_3Hg_2Cl_4$ requires : C, 37.6; H, 7.1%).

I Stoicheiometric proportions of ligand and mercuric halide, in the ratio 2:1, were dissolved separately in minimal quantities of ethanol. The mercuric halide solution was added dropwise to that of the ligand solution. The precipitate which formed, immediately or on standing, was collected, dried by

suction, and recrystallised from DMF/H_2O.

J This method is similar to I; however, all the ethanol in the reaction mixture was allowed to evaporate off, leaving a sticky product at the bottom of the flask. This sticky product was taken up in hot pentane and several drops of ether were added. The solution was cooled in an ice bath and the white precipitate which formed was collected and dried in vacuo.

K Stoicheiometric proportions of ligand and mercuric chloride, in the ratio 3:1, were dissolved separately in minimal quantities of sodium-dried AnalaR benzene. The $HgCl_2$ solution was added dropwise to that of the ligand. On standing, white, well formed, rectangular block shaped crystals were produced which were collected and dried in vacuo. Attempts to form $(PEt_3)_2HgCl_2$ and $(PPr^n_3)_2HgCl_2$ using method L resulted in formation of the 1:1 complexes.

L This method is very similar to that described for method I but using ethanol as recrystallisation solvent rather than DMF/H_2O.

M These complexes were provided by Dr. P. L. Goggin (University of Bristol). Details of their preparation may be found in Reference 90.

N Stoicheiometric proportions of PPh_2Me and HgI_2, in the ratio 3:1, were dissolved separately in minimal quantities of acetone. The HgI_2 solution was added dropwise to that of the PPh_2Me solution. On standing, very large, well formed white crystals appeared which were collected, washed with ethanol, and dried in vacuo. Attempts to prepare $(PPh_2Me)_2HgI_2$ using method L resulted in the 1:1 complex being formed.

O The $(PEtMe_2)_3(HgCl_2)_2$ complex was provided by Dr. P. L. Goggin (University of Bristol) and was isolated from the bulk of a sample of $(PEtMe_2)_2HgCl_2$, the preparation of which may be found in Reference 90.

7.2. SPECTROSCOPIC TECHNIQUES

Infrared spectra. All infrared spectra (40-450 cm^{-1}) were obtained using a RIIC FS-720 interferometer at Sheffield City Polytechnic. Vibrational

information was collected on paper tape in the form of interferograms. Interferograms were transferred into spectra using conventional Fourier transform computation methods, using an IBM 1130 computer. All spectra were ratioed against an instrument background.

Most samples were ground to a fine powder, 7-10 mg of which was added to high density polyethylene powder (20 mg, B.D.H.). After thorough mixing, the sample plus polyethylene powder, was pressed into the form of a circular disc (£" diameter, using a force of 50 tons).

For samples which were unstable under vacuum, such as (C^HgS)$HgCl_2$ »two poly ethylene discs(iOmg) were prepared (45 tons force), and a mixture comprising 7-10 mg of finely ground sample plus 5 mg of polyethylene powder was distributed evenly between them. The discs were re-pressed (50 tons force) yielding a 'sandwich disc'. This procedure countered decomposition due to the vacuum environment of the interferometer.

Spectra of solutions and liquids were obtained using a RIIC FS-100 liquid cell with PTFE spacers and polyethylene windows. Cell preparation was as suggested by Goldstein and Willis.[1-^1] Spectra were recorded at room temperature and at ca. 30 K. The low temperature was obtained using a CTi cryogenic cooling unit model 20 (Cryogenic Tech. Inc., Massachusetts).

Raman spectra. All Raman spectra were recorded using a C0DERG T-800 Triple Monochromator spectrophotometer using Ar+ (488.0 mm) laser excitation, either at the University College Cardiff (Department of Physics) or the University of Leicester (Department of Chemistry). All samples were powders and sampled using 90° collection from a capillary tube.

^{31}P n.m.r spectra. ^{31}P n.m.r. spectra were recorded on a JE0L PFT-100 Fourier Transform spectrophotometer equipped with an EC-100 computer, Diablo disc drive and Schomandl ND l00M frequency synthesizer at the University of Sheffield (Department of Chemistry). Samples were prepared in 10 mm outside diameter tubes using a Ch^Cl^/CD^Cl_2 <ca. 4:1) mixture; the deuterium solvent signal was used for field/frequency locking. Chemical shifts are recorded

on the $_{6}$ scale, increasing $ corresponding to increasing frequency. Standard conditions for recording spectra were 40.48 MHz sweepwidth as required, noise decoupling, and 85$ external standard.

$_{7}$.3. CRYSTALLOGRAPHIC TECHNIQUES

Photographic techniques. Oscillation, Weissenberg and precession photographs were taken using conventional methods and using Mo - K_a radiation.

Oscillation and Weissenberg photographs were taken using a 'StiJe non-integrating Weissenberg goniometer' and precession photographs were taken using a 'St$_{8}$e Buerger precession goniometer'. Measurement of photographs involved the use of a ruler accurate to 0.5 mm for measurement of lengths and a Charles Supper measuring device for angles.

Data collection techniques. All data, unless otherwise stated, were collected using Mo - K_{α} radiation = 0.71069 A) using a St$_{8}$e Stadi 2, 2-circle diffractometer, which uses a graphite monochromator, a Philips PWI964/20/30 scintillation counter as a detector and a Digital PDP$_{8}$/f control unit.

Data were collected using the background, w-scan, background technique. Paper tape output was converted to cards and then stored on disc in a format compatible with the SHELX system of computer programs.**^ Computation was carried out using an IBM 370/135 computer. One data set, for (PEtMe$_{2}$)^HgCl*2^2* was collected using a Nonius Cad-4 diffractometer at Rothamsted Experimental Station. Mo - K_a radiation (A = 0.71069 κ) was used.

7.4, MOLECULAR MASS DETERMINATION

All relative molecular mass values quoted in this work have been detei—mined using a Hitachi Perkin-Elmer model 115 molecular weight apparatus and standardized against benzil solutions in benzene of concentrations in the range 3 - 16 x 10 ^ mol dm Sample solutions were of similar concentration ranges. The relative molecular mass values quoted are considered accurate

within ± 5%.

7.5. ANALYSES

All microanalyses were carried out at the laboratory of Dr. F. B. Strauss, 10 Carlton Road, Oxford. Results of carbon and hydrogen analyses are contained in Table 7.1.

TABLE 7.1

Preparative and Analytical Data.

COMPOUND	METHOD OF PREPARATION	% C		% H	
		CALCULATED	FOUND	CALCULATED	FOUND
$(PPh_3)HgCl_2$	A	40.5	40.6	2.8	2.8
$(PPh_3)HgBr_2$	A	34.7	34.9	2.4	2.4
$(PPh_3)HgI_2$	A	30.2	30.1	2.1	2.2
$(PEt_3)HgCl_2$	A	18.5	18.6	3.9	3.9
$(PEt_3)HgBr_2$	B	15.1	15.1	3.2	3.4
$(PEt_3)HgI_2$	B	12.6	12.7	2.6	2.6
$(PMe_3)HgCl_2$	C	10.4	10.4	2.6	2.9
	D	10.4	10.5	2.6	2.4
$(PMe_3)HgBr_2$	D	8.3	8.3	2.1	2.0
$(PMe_3)HgI_2$	D	6.8	6.8	1.7	1.8
$(PBu^n_3)HgCl_2$	H	30.4	30.4	5.7	5.7
$(PBu^n_3)HgBr_2$	E	25.8	25.8	4.9	4.9
$(PBu^n_3)HgI_2$	E	21.9	22.2	4.1	4.2
$(PPr^n_3)HgCl_2$	E	25.0	25.4	4.9	4.9
$(PPr^n_3)HgBr_2$	E	20.8	20.9	4.1	4.0
α-$(PPr^n_3)HgI_2$	F	17.6	17.7	3.4	3.6
β-$(PPr^n_3)HgI_2$		17.6	17.6	3.4	3.4
$(PPhMe_2)HgCl_2$	A	23.5	23.3	2.7	2.7
$(PPhMe_2)HgBr_2$	A	19.3	19.2	2.2	2.3
$(PPhMe_2)HgI_2$	G	16.2	16.2	1.9	1.8
β-$(PPh_2Me)HgCl_2$	A*	33.1	32.3	2.8	3.1
α-$(PPh_2Me)HgCl_2$	A	33.1	33.2	2.8	2.9
$(PPh_2Me)HgBr_2$	A	27.9	27.7	2.3	2.4
$(PPh_2Me)HgI_2$	A	23.9	23.6	2.0	2.0

* Rapid recrystallisation from DMF/H_2O

TABLE 7.1 (continued)

COMPOUND	METHOD OF PREPARATION	% C		% H	
		CALCULATED	FOUND	CALCULATED	FOUND
$(TPP)HgCl_2$	A	45.3	45.1	2.9	3.2
$(TPP)HgBr_2$	A	39.3	39.6	2.4	2.6
$(2,4,6\text{-}Me_3C_5H_2N)HgCl_2$	E	24.5	24.4	2.8	2.9
$(2,4,6\text{-}Me_3C_5H_2N)HgBr_2$	E	20.0	19.3	2.3	2.3
$(2,4\text{-}Me_2C_5H_3N)HgCl_2$	E	22.2	22.4	2.4	2.3
$(2,4\text{-}Me_2C_5H_3N)HgBr_2$	E	18.0	18.2	1.9	1.9
$(2,6\text{-}Me_2C_5H_3N)HgCl_2$	E	22.2	22.0	2.4	2.5
$(2,6\text{-}Me_2C_5H_3N)HgBr_2$	E	18.0	18.2	1.9	2.0
$(MPC)HgCl_2$	A	16.7	17.2	2.5	2.5
$(MPC)HgBr_2$	A	13.8	14.3	2.1	2.2
$(MPC)HgI_2$	E	11.7	12.4	1.8	2.2
$(C_4H_8S)HgCl_2$	E	13.4	13.6	2.2	2.4
$(C_4H_8S)HgBr_2$	E	10.7	11.1	1.8	2.1
$(Ph_2SO)HgCl_2$	E	30.1	30.4	2.1	2.3
$(C_9H_7NO)HgCl_2$ *	E	25.9	26.0	1.7	1.7
$(C_9H_6O_2)HgCl_2$ *	E	25.9	26.1	1.5	1.4
$(PPh_3)_2HgCl_2$	I	54.3	54.5	3.8	3.8
$(PPh_3)_2HgBr_2$	I	48.9	48.7	3.4	3.5
$(PPh_3)_2HgI_2$	I	44.2	44.3	3.1	3.2
$(PBu^n_3)_2HgCl_2$	J	42.6	42.2	8.0	7.7
$(PBu^n_3)_2HgBr_2$	J	37.7	38.0	7.1	7.0
$(PBu^n_3)_2HgI_2$	M	33.6	33.3	6.3	6.4

* C_7H_9NO =

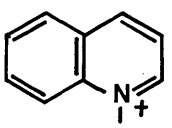

= quinoline-N-oxide

$C_9H_6O_2$ =

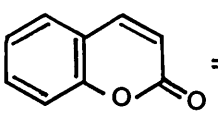

= coumarin

Table 7.1 (continued)

COMPOUND	METHOD OF PREPARATION	% C		% H	
		CALCULATED	FOUND	CALCULATED	FOUND
$(PPr^n_3)_2HgCl_2$	K	36.5	36.7	7.2	7.2
$(PPr^n_3)_2HgBr_2$	L	31.8	31.5	6.2	6.2
$(PPr^n_3)_2HgI_2$	L	27.9	28.2	5.4	5.6
$(PEt_3)_2HgCl_2$	K	28.4	28.5	6.0	6.0
$(PEt_3)_2HgBr_2$	L	24.2	24.1	5.1	5.2
$(PEt_3)_2HgI_2$	L	20.9	20.9	4.4	4.4
$(PEtMe_2)_2HgCl_2$	M	21.2	21.0	4.9	5.3
$(PEtMe_2)_2HgBr_2$	M	17.8	17.4	4.1	3.9
$(PEtMe_2)_2HgI_2$	M	15.1	15.2	3.5	3.6
$(PPh_2Me)_2HgCl_2$	L	46.5	46.4	3.9	3.9
$(PPh_2Me)_2HgBr_2$	L	41.0	40.8	3.4	3.5
$(PPh_2Me)_2HgI_2$	N	36.5	36.7	3.1	3.0
$(PPhMe_2)_2HgCl_2$	L	35.1	34.8	4.1	4.3
$(PPhMe_2)_2HgBr_2$	L	30.2	30.3	3.5	3.3
$(PPhMe_2)_2HgI_2$	L	26.3	26.2	3.0	3.3
$(Ph_3PS)HgCl_2$	A	38.2	38.3	2.7	2.7
$(Ph_3PS)HgBr_2$	A	33.0	33.1	2.4	2.3
$(Ph_3PS)HgI_2$	A	28.9	29.1	2.0	1.9
$(AsPh_3)HgCl_2$	A	37.4	32.4	2.6	2.8
$(AsPh_3)HgBr_2$	A	32.4	32.4	2.3	2.5
$(PEtMe_2)_3(HgCl_2)_2$	O	17.7	17.8	4.1	4.2

N.B. A solution of the yellow compound $(PBu^n_3)HgI_2$ in benzene when subjected to a vacuum very quickly lost its benzene leaving a residue of white powder. The carbon and hydrogen analysis of this white powder corresponded to a 1:1 complex. The appearance of a far-infrared spectrum of this white compound was different to that of the original yellow $(PBu^n_3)HgI_2$.

Summary and suggestions for future work.

The primary objective of this work has been to provide crystallographic data,

a) to aid in meaningful interpretation of the vibrational spectra of mercuric halide complexes.

b) to improve existing knowledge of the stereochemistry of mercury(II).

Unlike previously accepted it has been shown that $(L)HgX_2$ complexes, instead of exhibiting THD structures, show a range of structures varying from discrete THD structures e.g. $(PPh_3)HgX_2$ (X=Cl, Br or I) and $(TPP)HgX_2$ (X=Cl or Br), to a discrete tetramer for α-$(PBu^n_3)HgCl_2$ to various extended structures for $(PEt_3)HgCl_2$, $(PMe_3)HgX_2$ (X=Cl or Br) and (2,4-dimethylpyridine) (X=Cl or Br).

These changes in structure, for the $(PR_3)HgCl_2$ complexes at least, and most probably for the equivalent bromo complexes, are due to the donor strengths and size of the ligands. The smaller ligands, such as PMe_3 and PEt_3, which appear to interact strongly with HgX_2 give rise to extended structures , whereas, the larger PPh_3 and TPP ligands where Hg-P interaction is weaker yield the discrete dimeric structures.

It has been mentioned in this work that donor strengths of PR_3 ligands may arise as a result of solely steric effects (cone angle, θ[122]) or a combination of steric and electronic effects (C-P-C angles and Taft constants, σ^*[121]). Determination of the structure of for example $(PCy_3)HgCl_2$, where electronic properties favour strong interaction and thus an extended structure, and where steric properties ($\theta = 170^\circ$) favour weak interaction and thus an unassociated structure may help to elucidate the determining factor(s).

Only a small number of structural data is available for $(PR_3)HgI_2$ complexes. However, judging by the fact that from single crystal photographs $(PMe_3)HgI_2$ appears different from the chloro and bromo complexes, and that

$(TPP)HgI_2$ cannot even be prepared it seems likely that the halogen also plays an important role in determining the structure of these complexes, especially on changing X from Br to I.

Undoubtedly the donor-atom also plays its part in influencing the structure of $(L)HgX_2$ complexes. The mercury-donor atom interaction has been classified in two categories:

a) Very weak interactions, arising from the reaction between mercury and oxygen ligands, where X-Hg-X units remain virtually undistorted and weakly bound $(LHgX_2)_n$ 'polymers' are formed.

b) Stronger interactions, arising from, for example, mercury-sulphur, -phosphorus, -selenium, -arsenic, -nitrogen interaction where there is considerable distortion of the X-Hg-X unit. The result is that $(L)HgX_2$ distorted monomers can pack together in a number of ways giving rise to a variety of structures.

Although it has been shown in the present work on $(PR_3)HgX_2$ complexes that the R-substituents joined to phosphorus is an important parameter, it would be interesting to know if these substituent effects are paralleled by other donor atom systems e.g. $(L)HgX_2$ (where L= S-, As- or N-donor ligand).

Mainly on the basis of vibrational data three types of structure had been previously been predicted for $(PR_3)_2HgX_2$ complexes viz. discrete tetrahedral monomers, an ionic structure[4] $[Me_3PHgPMe_3]^{2+} + 2Cl^-$ and an extended structure[90] $(PEtMe_2)_2HgBr_2$.

Although $(PPh_3)_2HgI_2$ has been described[74] as a tetrahedral monomer, neither this structure nor the other two aforementioned structures have been found in this work. Each structure consists of extremely distorted four-coordinate monomers, ranging in their degree of distortion in the order $(PEt_3)_2HgCl_2$ > $(PEtMe_2)_2HgBr_2$ > $(PBu^n_3)_2HgCl_2$. The degree of distortion of the monomers is again due to the donor strengths of the PR_3 ligands.

For both $(PR_3)_2HgX_2$ and $(PR_3)HgX_2$ complexes it appears when PR_3 is a strong donor e.g. PMe_3, $PEtMe_2$, PEt_3, a 'phosphorus' competes with a chlorine atom for accomodation around mercury in a digonal arrangement. This phenomenon is also observed in the $[(PEtMe_2)_2HgCl]^+$ cation in the $(PEtMe_2)_3(HgCl_2)_2$ ionic structure.

As a result of these very strong Hg-P interactions observed for the discrete monomers it has been shown that some Hg-X bond lengths e.g. $(PEt_3)_2HgCl_2$ (2.68 Å) and $(PEtMe_2)_2HgBr_2$ (av. 2.77 Å) are larger than those Hg-X bridge bonds found in $(PPh_3)HgCl_2$ (2.62 and 2.66 Å) and $[Hg_2Br_6]^{2-}$ species (2x2.75 Å).

A major problem throughout this work has been elimination of internal ligand modes in the vibrational spectra of these complexes. A way in which this severe problem may be overcome is difficult to foresee at the present time. In spite of this problem during precise spectral interpretation it has been shown that certain general spectra/structure relationships do exist. Generally, for $(L)HgX_2$ complexes irrespective of their overall structure, ν(HgX) modes associated with vibration of short Hg-X bonds (close to those found in the mercuric halides themselves) are found to occur at ca. 300 (Cl), 200 (Br) and 150 cm^{-1} (I), whilst $\nu(HgX)_b$ modes vary in their wavenumber position and are located around and below values of 240 (Cl), 160 (Br) and 120 cm^{-1} (I). These wavenumber positions illustrate a remarkable $\nu(HgX)_b$/Hg-X bridge length dependence. It has been shown therefore that detailed investigation of the complete far-IR region of the spectrum, including <200 cm^{-1}, is necessary before making structural predictions concerning these complexes.

The ν(HgX) modes located for the discrete $(L)_2HgX_2$ monomers again showed a striking Hg-X bond length dependence and have been assigned in the ranges 169-223 (Cl), 112-155 (Br) and 94-129 cm^{-1} (I).

It was significant that ν(HgX) modes assigned for $(L)_2HgX_2$ complexes fell within the region associated with $\nu(HgX)_b$ modes observed for $(L)HgX_2$ complexes. This shows, therefore, that the appearance of low wavenumber ν(HgX) modes need not necessarily indicate the presence of Hg-X bridges.

The above structure/spectra relationships have allowed tentative structural proposals to be made, on the basis of solely vibrational data, some examples of which are listed below.

β-$(PPh_2Me)HgCl_2$
$(PPhMe_2)HgX_2$ (X=Cl or Br) } - 'ionic' type structures cf. $(PMe_3)HgCl_2$

$(PPh_2Me)HgI_2$ - discrete THD structure.

$(PPh_2Me)_2HgCl_2$
$(PPr^n_3)_2HgX_2$ (X=Cl, Br or I) } - distorted 4-coordinate monomers.

The location of ν(HgL) modes has been very disappointing and consists of only a few tentative assignments. This may be attributed to their very low intensity as was observed by Goggin *et al.*[106] for ν(HgP) modes and also to severe interference caused by internal modes of the ligands.

Location of ν(HgL) modes may be aided, in principle at least, by isotopic substitution experiments involving isotopes of mercury and ligand donor atom.

It has been mentioned that vibrational data in solution, particularly for $(PR_3)HgX_2$ complexes would be useful for two reasons:

a) It may help in spectral interpretation of the solid state spectra

b) It may yield information concerning precise structures of the stable solution phase species. The reason for the lack of such information is due to the low solubility of $(L)HgX_2$ complexes in suitable solvents.

It may be possible to overcome this difficulty, for the IR-active spectrum at least, by the use of a more sophisticated rapid scan Fourier transform spectrometer.

Appendices

Appendix I ; The Absorption correction

Absorption corrections have been made for (PMe^)HgCI2 and (TPP)HgCI2, using ABSCOR, written by N.W. Alcock.[152] A description of the manner in which the absorption correction for (PMe^)HgCI2 has been applied is outlined below.

Principle.

The measured intensity of the X-ray beam emergent from a crystal can have been diminished due to absorption of X-rays by the crystal. Equation (I) defines the extent of absorption.

$$I = I_o \exp(-\mu X) \quad \text{..... (1)}$$

where I measured intensity of emergent beam

I_o intensity of emergent beam at zero absorption

X total path length of the X-ray through the crystal (cm)

μ linear absorption coefficient (cm *) and is given by equation (2)

$$\mu = \frac{N}{V_c} \sum_i (\mu_a)_i \quad \text{..... (2)}$$

where N number of molecules per unit cell

V_c Volume of unit cell

$(\mu_a)_i$ atomic absorption coefficient

i the i^ atom.

The transmission factor T is equal to I/IQ and is obtained by integration over the volume of the crystal.

$$T = I / I_o = \frac{1}{V} \int \exp[-\mu(X_1 + X_2)] \, dV \quad (3)$$

where X_1 = length of incident beam from the point of entry to the element of volume dV

X_2 = length of diffracted beam from the point of emergence from element dV, to the point of emergence from the crystal.

The crystal is considered as a convex polyhedron, and for every reflection may be divided into a number of tetrahedra. The absorption correction for one tetrahedron is found and summing over all tetrahedra gives the total absorption correction needed for that particular reflection.

Definition of crystal shape.

For the absorption correction to be made the crystal shape has to be defined. The faces of the crystal can be defined in terms of their Miller indices. An origin point is chosen within the crystal and the perpendicular distance from all the faces to this origin are measured. All crystal faces are therefore defined.

Figure AI.1.

Schematic diagram of the $(PMe_3)HgCl_2$ crystal.

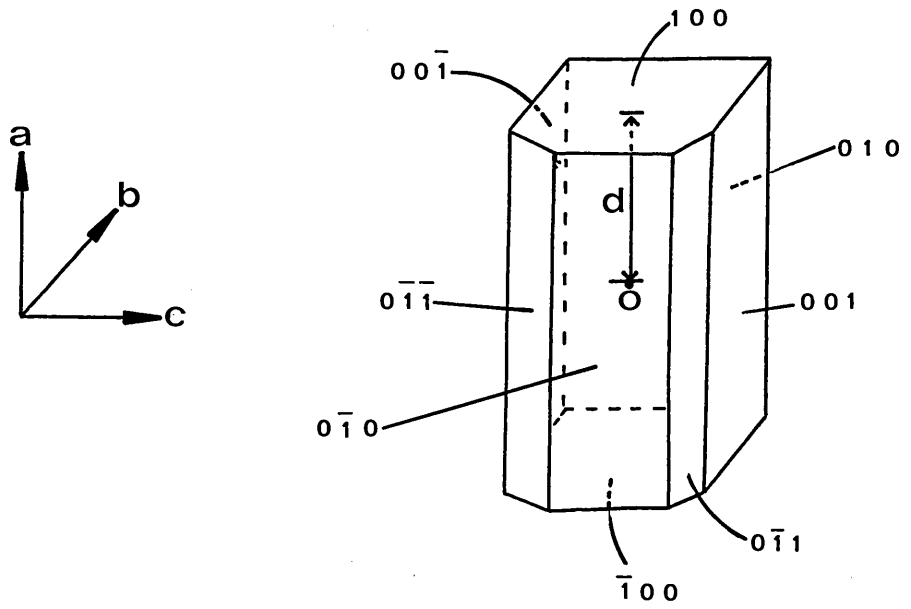

d= perpendicular distance (cm) from crystal face (100) to origin point O

Thus having fully defined the crystal shape the program is able to use equation (3) to calculate T and further supply corrected intensities for each reflection.

Appendix 2 : Final positional parameters (fractional) and thermal parameters

This Appendix contains Tables of final positional parameters (fractional) and thermal parameters for all the structures determined in this work.

Isotropic temperature factors are always of the form:-

exp -8π2 U2 (sin20)/X2

where $\tilde{u}^2$ = the mean square amplitude of atomic vibration»

and anisotropic temperature factors are always in the form:-

exp [-2π (U11h a + U92k b + U-^l c + 2Uj2hka b + 2U|^hla c + 2U23klb c)]

where U's are the mean square amplitudes of vibration which describe the ellipsoidal electron distribution of the anisotropical ly vibrating atom.

For all parameters, estimated standard deviations are given directly below.

Tab le A2.1.

Final positional parameters (fractional) and thermal parameters for the structure of (PPhUHgCI2.

Atom	X/A	Y/B	z/c	UII	U22	U33	U23	U13	U12
Hg	0.1325	0.0899	-0.0143	0.0607	0.0352	0.0436	-0.0151	-0.0156	-0.0069
	0.0001	0.0001	0.0001	0.0009	0.0049	0.0008	0.0007	0.0006	0.0008
CU	0.2219	0.0239	-0.1566	0.0617	0.1500	0.0526	-0.0248	-0.0000	0.0305
	0.0009	0.0013	0.0007	0.0065	0.0122	0.0056	0.0068	0.0048	0.0071
CL2	0.9241	0.1055	0.9263	0.0549	0.0364	0.0639	0.0133	-0.0297	0.0140
	0.0007	0.0007	0.0006	0.0054	0.0068	0.0054	0.0042	0.0043	0.0041
P	0.1908	0.2365	0.1058	0.0366	0.0272	0.0336	-0.0074	-0.0121	-0.0002
	0.0006	0.0007	0.0006	0.0047	0.0062	0.0044	0.0035	0.0035	0.0036
Cl 1	0.3398	0.2251	0.1329	0.0345					
	0.0012	0.0018	0.0015	0.0071					
C12	0.4012	0.3243	0.1598	0.0495					
	0.0012	0.0018	0.0015	0.0088					
Cl 3	0.5121	0.3131	0.1839	0.0728					
	0.0012	0.0018	0.0015	0.0116					
C14	0.5617	0.2027	0.1810	0.0624					
	0.0012	0.0018	0.0015	0.0104					
C15	0.5003	0.1035	0.1541	0.0680					
	0.0012	0.0018	0.0015	0.0108					
C16	0.3893	0.1147	0.1300	0.0551					
	0.0012	0.0018	0.0015	0.0094					
C2I	0.1241	0.2272	0.2180	0.0307					
	0.0015	0.0019	0.0012	0.0069					

Table A2.1, continued.

Atom	X/A	Y/B	Z/C	U_{11}	U_{22}	U_{33}	U_{23}	U_{13}	U_{12}
C22	0.0173	0.1859	0.2173	0.0517					
	0.0015	0.0019	0.0012	0.0090					
C23	-0.0392	0.1854	0.3050	0.0738					
	0.0015	0.0019	0.0012	0.0116					
C24	0.0111	0.2262	0.3934	0.0839					
	0.0015	0.0019	0.0012	0.0133					
C25	0.1179	0.2675	0.3941	0.0585					
	0.0015	0.0019	0.0012	0.0097					
C26	0.1744	0.2680	0.3064	0.0491					
	0.0015	0.0019	0.0012	0.0087					
C31	0.1680	0.3808	0.0532	0.0462					
	0.0019	0.0015	0.0016	0.0087					
C32	0.1259	0.4720	0.1096	0.0514					
	0.0019	0.0015	0.0016	0.0091					
C33	0.1168	0.5851	0.0696	0.0617					
	0.0019	0.0015	0.0016	0.0100					
C34	0.1496	0.6071	-0.0266	0.0769					
	0.0019	0.0015	0.0016	0.0156					
C35	0.1916	0.5160	-0.0829	0.0764					
	0.0019	0.0015	0.0016	0.0122					
C36	0.2008	0.4028	-0.0430	0.0679					
	0.0019	0.0015	0.0016	0.0107					

Table A2.2.

Final positional parameters (fractional) and thermal parameters for the structure of $(TPP)HgCl_2$

Atom	X/A	Y/B	Z/C	U_{11}	U_{22}	U_{33}	U_{23}	U_{13}	U_{12}
Hg	0.0722	0.1573	0.1380	0.0390	0.0281	0.0377	-0.0020	0.0104	0.0163
	0.0002	0.0003	0.0002	0.0008	0.0076	0.0008	0.0006	0.0005	0.0006
CL1	0.2907	0.2799	0.1209	0.0488	0.0703	0.0862	0.0339	0.0201	0.0239
	0.0010	0.0017	0.0014	0.0061	0.0123	0.0086	0.0073	0.0057	0.0062
CL2	0.0202	0.8848	0.1563	0.0634	0.0544	0.0223	0.0062	0.0072	0.0401
	0.0011	0.0014	0.0009	0.0062	0.0109	0.0045	0.0045	0.0041	0.0062
P	-0.0517	0.2502	0.2410	0.0452	0.0331	0.0411	0.0095	0.0165	0.0246
	0.0009	0.0013	0.0011	0.0054	0.0100	0.0056	0.0049	0.0043	0.0050
C1	-0.1458	0.3336	0.1022	0.0325					
	0.0031	0.0046	0.0037	0.0085					
C2	-0.0845	0.4791	0.1243	0.0405					
	0.0035	0.0051	0.0041	0.0095					
C3	0.0419	0.5375	0.2399	0.0391					
	0.0034	0.0050	0.0041	0.0093					
C4	0.0575	0.4262	0.3192	0.0329					
	0.0031	0.0048	0.0037	0.0083					
C5	-0.1477	0.1345	0.3652	0.0422					
	0.0023	0.0028	0.0026	0.0098					
C6	-0.1618	-0.0102	0.3907	0.0337					
	0.0023	0.0028	0.0026	0.0085					
C7	-0.2380	-0.0976	0.4853	0.0803					
	0.0023	0.0028	0.0026	0.0159					
C8	-0.3001	-0.0403	0.5544	0.0486					
	0.0023	0.0028	0.0026	0.0106					
C9	-0.2860	0.1045	0.5289	0.0491					
	0.0023	0.0028	0.0026	0.0104					
C10	-0.2098	0.1919	0.4343	0.0622					
	0.0023	0.0028	0.0026	0.0130					
C11	0.1667	0.4387	0.4455	0.0296					
	0.0019	0.0033	0.0021	0.0081					
C12	0.2873	0.5367	0.4297	0.0288					
	0.0019	0.0033	0.0021	0.0080					

Table A2.2, continued.

Atom	X/A	Y/B	Z/C	U_{11}	U_{22}	U_{33}	U_{23}	U_{13}	U_{12}
C13	0.3895	0.5666	0.5479	0.0971					
	0.0019	0.0033	0.0021	0.0190					
C14	0.3711	0.4985	0.6819	0.0686					
	0.0019	0.0033	0.0021	0.0136					
C15	0.2504	0.4005	0.6977	0.0501					
	0.0019	0.0033	0.0021	0.0107					
C16	0.1483	0.3706	0.5795	0.0557					
	0.0019	0.0033	0.0021	0.0117					
C17	-0.2647	0.2424	0.0065	0.0337					
	0.0019	0.0029	0.0026	0.0087					
C18	-0.3536	0.3021	-0.0491	0.0558					
	0.0019	0.0029	0.0026	0.0115					
C19	-0.4664	0.2208	-0.1434	0.0575					
	0.0019	0.0029	0.0026	0.0122					
C20	-0.4903	0.0798	-0.1820	0.0590					
	0.0019	0.0029	0.0026	0.0119					
C21	-0.4014	0.0200	-0.1264	0.0434					
	0.0019	0.0029	0.0026	0.0096					
C22	-0.2886	0.1013	-0.0321	0.0599					
	0.0019	0.0029	0.0026	0.0123					

Table A2.3.

Final positional parameters (fractional) and thermal parameters for the structure of $(PEt_3)HgCl_2$

Atom	X/A	Y/B	Z/C	U_{11}	U_{22}	U_{33}	U_{23}	U_{13}	U_{12}
Hg	-0.2185	0.0142	0.0608	0.0681	0.0729	0.0548	-0.0031	0.0429	-0.0007
	0.0002	0.0001	0.0001	0.0009	0.0010	0.0008	0.0007	0.0007	0.0008
CL1	0.4371	0.5878	0.6063	0.0678	0.0970	0.0612	-0.0208	0.0319	0.0074
	0.0014	0.0009	0.0007	0.0063	0.0069	0.0053	0.0049	0.0048	0.0050
CL2	0.1047	0.3415	0.5023	0.0717	0.0730	0.0821	-0.0037	0.0548	-0.0062
	0.0013	0.0008	0.0007	0.0065	0.0057	0.0062	0.0047	0.0053	0.0046
P	0.8005	0.3695	0.7040	0.0744	0.1327	0.0624	0.0282	0.0473	0.0028
	0.0016	0.0012	0.0008	0.0076	0.0098	0.0064	0.0064	0.0059	0.0066
C1	-0.0052	0.7101	0.2553	0.0879					
	0.0066	0.0036	0.0034	0.0120					
C2	0.1680	0.5132	0.1808	0.1542					
	0.0130	0.0079	0.0065	0.0327					
C3	0.3801	0.7301	0.3196	0.1518					
	0.0093	0.0058	0.0050	0.0218					
C4	-0.2050	0.6377	0.2095	0.1263					
	0.0085	0.0050	0.0042	0.0188					
C5	0.2300	0.5792	0.0933	0.1533					
	0.0092	0.0052	0.0045	0.0196					
C6	0.4141	0.8071	0.4015	0.1399					
	0.0089	0.0054	0.0049	0.0205					

Table A2.4.

Final positional parameters (fractional) and thermal parameters for the structure of $(PMe_3)HgCl_2$

Atom	X/A	Y/B	Z/C	U_{11}	U_{22}	U_{33}	U_{23}	U_{13}	U_{12}
Hg1	0.1928	0.0099	0.2989	0.0492	0.0250	0.0648	-0.0008	0.0053	0.0027
	0.0001	0.0001	0.0001	0.0004	0.0003	0.0004	0.0002	0.0003	0.0002
CL1	0.7334	-0.0132	0.3218	0.0344	0.0440	0.0549	-0.0010	0.0037	0.0012
	0.0006	0.0004	0.0006	0.0019	0.0019	0.0024	0.0016	0.0016	0.0014
CL2	0.2032	0.2727	0.2482	0.0563	0.0271	0.0632	0.0010	0.0003	0.0042
	0.0007	0.0004	0.0006	0.0024	0.0015	0.0027	0.0016	0.0019	0.0015
P1	0.2099	-0.2510	0.2525	0.0276	0.0282	0.0484	-0.0022	0.0026	0.0030
	0.0006	0.0004	0.0006	0.0017	0.0016	0.0023	0.0015	0.0015	0.0013
C1	1.0498	0.3529	0.7622	0.0440					
	0.0026	0.0018	0.0024	0.0035					
C2	0.6616	0.3359	0.5535	0.0513					
	0.0028	0.0020	0.0026	0.0041					
C3	0.6538	0.2915	0.9550	0.0628					
	0.0033	0.0023	0.0030	0.0050					

Table A2.5.

Final positional parameters (fractional) and thermal parameters for the structure of α-$(PBu^n_3)HgCl_2$

Atom	X/A	Y/B	Z/C	U_{11}	U_{22}	U_{33}	U_{23}	U_{13}	U_{12}
Hg1	0.4787	0.1815	0.2140	0.1387	0.0655	0.1066	0.0025	0.0265	-0.0041
	0.0002	0.0001	0.0003	0.0025	0.0016	0.0023	0.0017	0.0018	0.0018
CL1	0.3283	0.1735	0.0789	0.1606	0.0838	0.1942	0.0077	0.0494	0.0182
	0.0016	0.0007	0.0024	0.0188	0.0125	0.0237	0.0139	0.0180	0.0128
CL3	0.5777	0.1006	0.1499	0.1962	0.0764	0.1106	0.0075	0.0805	0.0138
	0.0016	0.0006	0.0019	0.0202	0.0109	0.0168	0.0104	0.0148	0.0118
P1	0.6079	0.2373	0.3140	0.1144	0.1299	0.1698	0.0184	0.0158	0.0161
	0.0016	0.0009	0.0024	0.0164	0.0169	0.0214	0.0156	0.0153	0.0140
C11	0.6902	0.2767	0.2446	0.2842					
	0.0117	0.0062	0.0181	0.0702					
C12	0.6499	0.2703	0.0864	0.1879					
	0.0075	0.0040	0.0116	0.0393					
C13	0.6944	0.3049	-0.0144	0.2057					
	0.0081	0.0042	0.0123	0.0429					
C14	0.6875	0.2967	-0.1466	0.1867					
	0.0064	0.0033	0.0097	0.0336					
C21	0.5712	0.2929	0.4331	0.2886					
	0.0119	0.0055	0.0150	0.0656					
C22	0.4671	0.2995	0.4111	0.1729					
	0.0081	0.0039	0.0103	0.0377					
C23	0.4406	0.3338	0.5440	0.2785					
	0.0128	0.0066	0.0181	0.0796					
C24	0.3510	0.3455	0.5530	0.2752					
	0.0091	0.0042	0.0115	0.0468					
C31	0.7184	0.1986	0.3346	0.3155					
	0.0109	0.0060	0.0164	0.0703					
C32	0.7213	0.1807	0.4340	0.1785					
	0.0088	0.0046	0.0138	0.0451					
C33	0.7990	0.1531	0.5391	0.3562					
	0.0151	0.0069	0.0176	0.0817					
C34	0.8745	0.1336	0.5409	0.2162					
	0.0128	0.0068	0.0170	0.0863					

Table A2.5, continued.

Atom	X/A	Y/B	Z/C	U_{11}	U_{22}	U_{33}	U_{23}	U_{13}	U_{12}
Hg2	0.4870	0.0403	0.3283	0.1625	0.0704	0.0882	-0.0006	0.0226	-0.0032
	0.0003	0.0001	0.0003	0.0029	0.0016	0.0020	0.0017	0.0018	0.0019
CL2	0.4326	0.1309	0.4195	0.1800	0.0798	0.1052	-0.0136	0.0669	0.0021
	0.0015	0.0006	0.0018	0.0191	0.0110	0.0155	0.0101	0.0141	0.0112
CL4	0.6327	0.0271	0.4727	0.1567	0.1056	0.1929	0.0201	0.0551	-0.0041
	0.0017	0.0007	0.0023	0.0191	0.0149	0.0227	0.0144	0.0178	0.0130
P2	0.3504	0.0074	0.1846	0.0935	0.0887	0.1425	-0.0137	0.0199	0.0075
	0.0014	0.0007	0.0023	0.0148	0.0130	0.0197	0.0123	0.0143	0.0110
C41	0.3555	0.0252	0.0157	0.0930					
	0.0051	0.0024	0.0067	0.0221					
C42	0.2610	0.0147	-0.0661	0.1155					
	0.0054	0.0026	0.0074	0.0239					
C43	0.2753	0.0429	-0.2108	0.2082					
	0.0057	0.0030	0.0076	0.0263					
C44	0.1804	0.0387	-0.3229	0.2465					
	0.0060	0.0031	0.0079	0.0278					
C51	0.2657	0.0453	0.2545	0.1995					
	0.0077	0.0038	0.0100	0.0362					
C52	0.1798	0.0186	0.1976	0.2914					
	0.0097	0.0046	0.0126	0.0516					
C53	0.0863	0.0456	0.2889	0.2820					
	0.0090	0.0045	0.0120	0.0467					
C54	-0.0121	0.0309	0.1807	0.3043					
	0.0066	0.0033	0.0087	0.0312					
C61	0.3373	-0.0666	0.1855	0.1129					
	0.0061	0.0029	0.0080	0.0276					
C62	0.4476	-0.0876	0.2051	0.1197					
	0.0071	0.0037	0.0097	0.0375					
C63	0.4305	-0.1589	0.2058	0.1603					
	0.0066	0.0034	0.0086	0.0329					
C64	0.5474	-0.1753	0.2341	0.1418					
	0.0059	0.0030	0.0075	0.0265					

Table A2.6.

Final positional parameters (fractional) and thermal parameters for the structure of (2,4-dimethylpyridine)$HgBr_2$.

Atom	X/A	Y/B	Z/C	U_{11}	U_{22}	U_{33}	U_{23}	U_{13}	U_{12}
Hg	0.0	0.0372	0.2500	0.0439	0.0419	0.0470	0.0008	-0.0052	-0.0047
	0.0	0.0001	0.0	0.0007	0.0007	0.0010	0.0014	0.0006	0.0011
Br1	0.1455	-0.0425	0.4779	0.0377	0.0563	0.0314	-0.0010	-0.0002	0.0066
	0.0003	0.0004	0.0005	0.0020	0.0022	0.0023	0.0021	0.0015	0.0019
Br2	-0.1396	-0.1007	0.1189	0.0399	0.0729	0.0546	-0.0182	0.0000	-0.0115
	0.0003	0.0005	0.0007	0.0021	0.0028	0.0030	0.0025	0.0019	0.0021
N	0.0040	0.2414	0.2656	0.0381					
	0.0033	0.0021	0.0060	0.0056					
C1	-0.0738	0.3187	0.2384	0.0331					
	0.0025	0.0033	0.0050	0.0076					
C2	-0.0651	0.4444	0.2524	0.0442					
	0.0030	0.0036	0.0055	0.0087					
C3	0.0241	0.5015	0.3063	0.0325					
	0.0025	0.0029	0.0046	0.0073					
C4	0.1144	0.4175	0.3541	0.0388					
	0.0028	0.0034	0.0052	0.0078					
C5	0.1002	0.2912	0.3228	0.0334					
	0.0026	0.0030	0.0048	0.0076					
C6	0.0405	0.6362	0.3215	0.0805					
	0.0046	0.0053	0.0085	0.0154					
C7	-0.1787	0.2567	0.1758	0.0543					
	0.0033	0.0041	0.0064	0.0101					

Table A2.7.

Final positional parameters (fractional) and thermal parameters for the structure of $(PEtMe_2)_2HgBr_2$ —

Atom	X/A	Y/B	Z/C	U_{11}	U_{22}	U_{33}	U_{23}	U_{13}	U_{12}
Hg1	0.1518	0.3541	0.3183	0.1445	0.0608	0.1087	0.0008	-0.0141	0.0130
	0.0009	0.0004	0.0009	0.0090	0.0049	0.0089	0.0059	0.0087	0.0060
Hg2	0.2246	0.1208	0.0034	0.1007	0.0581	0.0866	0.0033	0.0023	0.0154
	0.0007	0.0004	0.0010	0.0069	0.0042	0.0072	0.0068	0.0081	0.0054
Br1	0.2525	0.2588	0.2004	0.1934	0.0569	0.1713	-0.0173	0.0607	-0.0010
	0.0029	0.0010	0.0028	0.0320	0.0136	0.0309	0.0167	0.0293	0.0181
Br2	0.2953	0.3741	0.4754	0.2115	0.1003	0.1498	0.0025	-0.0522	0.0166
	0.0017	0.0011	0.0020	0.0172	0.0137	0.0218	0.0143	0.0149	0.0132
Br3	0.0819	0.0195	-0.0590	0.1598	0.0703	0.1314	-0.0105	-0.0396	-0.0166
	0.0025	0.0011	0.0025	0.0269	0.0170	0.0265	0.0153	0.0213	0.0179
Br4	0.3930	0.1208	0.8600	0.1452	0.0852	0.1285	0.0024	0.0250	0.0206
	0.0021	0.0013	0.0023	0.0247	0.0158	0.0281	0.0179	0.0201	0.0178
P1	0.1913	0.4513	0.2087	0.0677	0.1066	0.0865	0.0001	-0.0182	0.0123
	0.0050	0.0027	0.0057	0.0503	0.0391	0.0569	0.0370	0.0410	0.0326
P2	0.0171	0.2924	0.4134	0.1838	0.1300	0.1633	0.0048	0.0681	-0.0010
	0.0057	0.0029	0.0057	0.0544	0.0477	0.0658	0.0434	0.0475	0.0419
P3	0.3027	0.0701	0.1620	0.1547	0.0440	0.0701	0.0095	-0.0289	0.0312
	0.0053	0.0029	0.0060	0.0542	0.0442	0.0622	0.0410	0.0462	0.0394
P4	0.1087	0.1982	-0.0755	0.0929	0.0544	0.1055	0.0168	-0.0373	0.0187
	0.0050	0.0027	0.0055	0.0499	0.0416	0.0601	0.0354	0.0407	0.0340
C1	-0.0706	0.0233	1.2823	0.0900					
	0.0136	0.0073	0.0150	0.0522					
C6	0.6181	0.7289	0.9826	0.0744					
	0.0127	0.0069	0.0153	0.0544					
C9	0.4527	0.1038	1.2093	0.0439					
	0.0190	0.0098	0.0212	0.0837					
C10	0.1953	0.0764	1.2762	0.0277					
	0.0134	0.0069	0.0144	0.0530					
C11	0.3711	-0.0163	1.1485	0.1486					
	0.0138	0.0070	0.0141	0.0510					
C13	0.0679	0.1616	0.7958	0.0798					
	0.0125	0.0072	0.0145	0.0503					
C14	-0.0193	0.2013	0.9998	0.1190					
	0.0125	0.0067	0.0161	0.0456					
C15	0.1828	0.2811	0.9412	0.1211					
	0.0141	0.0073	0.0151	0.0520					

Table A2.8.

Final positional parameters (fractional) and thermal parameters for the structure of $(PEt_3)_2HgCl_2$—

Atom	X/A	Y/B	Z/C	U_{11}	U_{22}	U_{33}	U_{23}	U_{13}	U_{12}
Hg1	0.0	0.5000	0.2725	0.0621	0.0514	0.0596	0.0	0.0	0.0
	0.0	0.0	0.0001	0.0022	0.0020	0.0010	0.0	0.0	0.0
P1	0.1087	0.6617	0.3043	0.0823	0.0679	0.0573	0.0111	-0.0024	-0.0155
	0.0011	0.0010	0.0010	0.0084	0.0081	0.0092	0.0060	0.0063	0.0076
CL1	0.1532	0.4115	0.1582	0.0861	0.0855	0.1212	0.0010	0.0128	0.0382
	0.0010	0.0010	0.0011	0.0089	0.0087	0.0151	0.0079	0.0078	0.0075
C1	0.0255	0.7869	0.3525	0.1706					
	0.0069	0.0064	0.0067	0.0371					
C2	0.1762	0.7113	0.2147	0.1226					
	0.0049	0.0047	0.0044	0.0197					
C3	0.2194	0.6400	0.3916	0.1353					
	0.0051	0.0054	0.0054	0.0250					
C4	0.0312	0.2164	0.4144	0.2199					
	0.0092	0.0092	0.0090	0.0191					
C5	0.1186	0.7475	0.1300	0.1689					
	0.0058	0.0055	0.0064	0.0285					
C6	0.2782	0.5522	0.3888	0.0884					
	0.0043	0.0043	0.0046	0.0167					

Table A2.9.

Final positional parameters (fractional) and thermal parameters for the structure of $(PEtMe_2)_3(HgCl_2)_2$

Atom	X/A	Y/B	Z/C	U_{11}	U_{22}	U_{33}	U_{23}	U_{13}	U_{12}
Hg1	0.4175	-0.2561	0.9794	0.0287	0.0307	0.0438	0.0008	0.0018	0.0057
	0.0000	0.0001	0.0001	0.0006	0.0006	0.0006	0.0006	0.0004	0.0004
CL1	0.3082	0.6242	1.0377	0.0568	0.0447	0.0942	0.0090	0.0146	-0.0093
	0.0004	0.0005	0.0010	0.0049	0.0043	0.0065	0.0050	0.0052	0.0037
P1	0.3361	0.8783	0.9617	0.0451	0.0369	0.0375	0.0033	0.0068	0.0129
	0.0004	0.0005	0.0008	0.0043	0.0041	0.0042	0.0040	0.0040	0.0035
P2	0.5109	0.6251	0.9888	0.0425	0.0369	0.0409	0.0030	0.0004	0.0096
	0.0004	0.0005	0.0007	0.0041	0.0041	0.0044	0.0036	0.0036	0.0033
C11	0.2903	0.8974	1.1248	0.0491					
	0.0015	0.0021	0.0031	0.0080					
C12	0.2653	0.8483	0.8470	0.0441					
	0.0014	0.0018	0.0028	0.0074					
C13	0.3703	0.9923	0.8946	0.0633					
	0.0016	0.0020	0.0031	0.0085					
C14	0.4386	1.0301	0.9751	0.0998					
	0,0021	0.0027	0.0040	0.0123					
C21	0.4864	0.5243	0.8993	0.0562					
	0.0014	0.0019	0.0029	0.0080					
C22	0.5361	0.5877	1.1602	0.0668					
	0.0015	0.0022	0.0033	0.0091					
C23	0.5910	0.6662	0.9073	0.0451					
	0.0013	0.0019	0.0029	0.0078					
C24	0.6101	0.7718	0.9558	0.0883					
	0.0018	0.0023	0.0034	0.0103					
Hg2	0.3849	0.7642	0.4477	0.0557	0.0293	0.0412	0.0034	-0.0041	-0.0045
	0.0001	0.0001	0.0001	0.0007	0.0006	0.0006	0.0006	0.0005	0.0006
CL2	0.4592	0.7552	0.6747	0.0609	0.0684	0.0377	0.0029	-0.0083	0.0021
	0.0003	0.0005	0.0006	0.0043	0.0051	0.0032	0.0047	0.0032	0.0048
CL3	0.3242	0.9254	0.4901	0.0464	0.0481	0.0563	0.0050	0.0075	0.0122
	0.0004	0.0005	0.0007	0.0042	0.0042	0.0054	0.0036	0.0043	0.0034
CL4	0.4727	0.8180	0.2780	0.0649	0.0632	0.0536	0.0023	0.0123	0.0103
	0.0004	0.0006	0.0008	0.0048	0.0051	0.0047	0.0040	0.0043	0.0042

Table A2.9, continued

Atom	X/A	Y/B	Z/C	U_{11}	U_{22}	U_{33}	U_{23}	U_{13}	U_{12}
P3	0.3132	0.6204	0.4676	0.0553	0.0465	0.0493	-0.0025	-0.0069	-0.0166
	0.0004	0.0006	0.0009	0.0051	0.0046	0.0050	0.0044	0.0046	0.0040
C31	0.3492	0.5183	0.3733	0.0511					
	0.0013	0.0019	0.0030	0.0078					
C32	0.3090	0.5902	0.6481	0.0810					
	0.0019	0.0027	0.0038	0.0116					
C33	0.2260	0.6344	0.3901	0.0874					
	0.0019	0.0025	0.0041	0.0120					
C34	0.1836	0.7116	1.4788	0.1143					
	0.0023	0.0030	0.0044	0.0141					

Table A3.1.

Observed and calculated structure factors for $(PPh_3)HgCl_2$

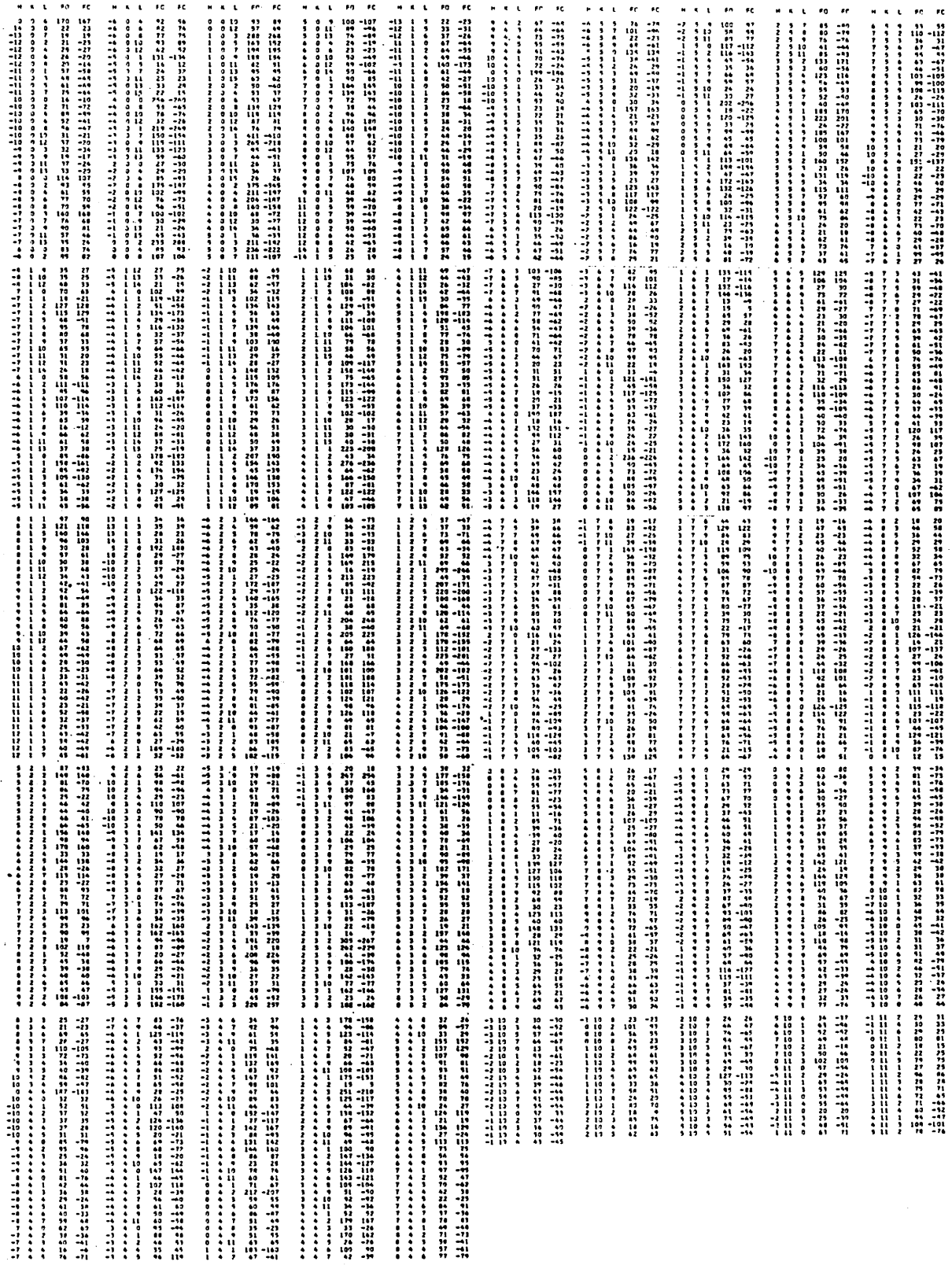

Table A3.2.

Observed and calculated structure factors for $(TPP)HgCl_2$

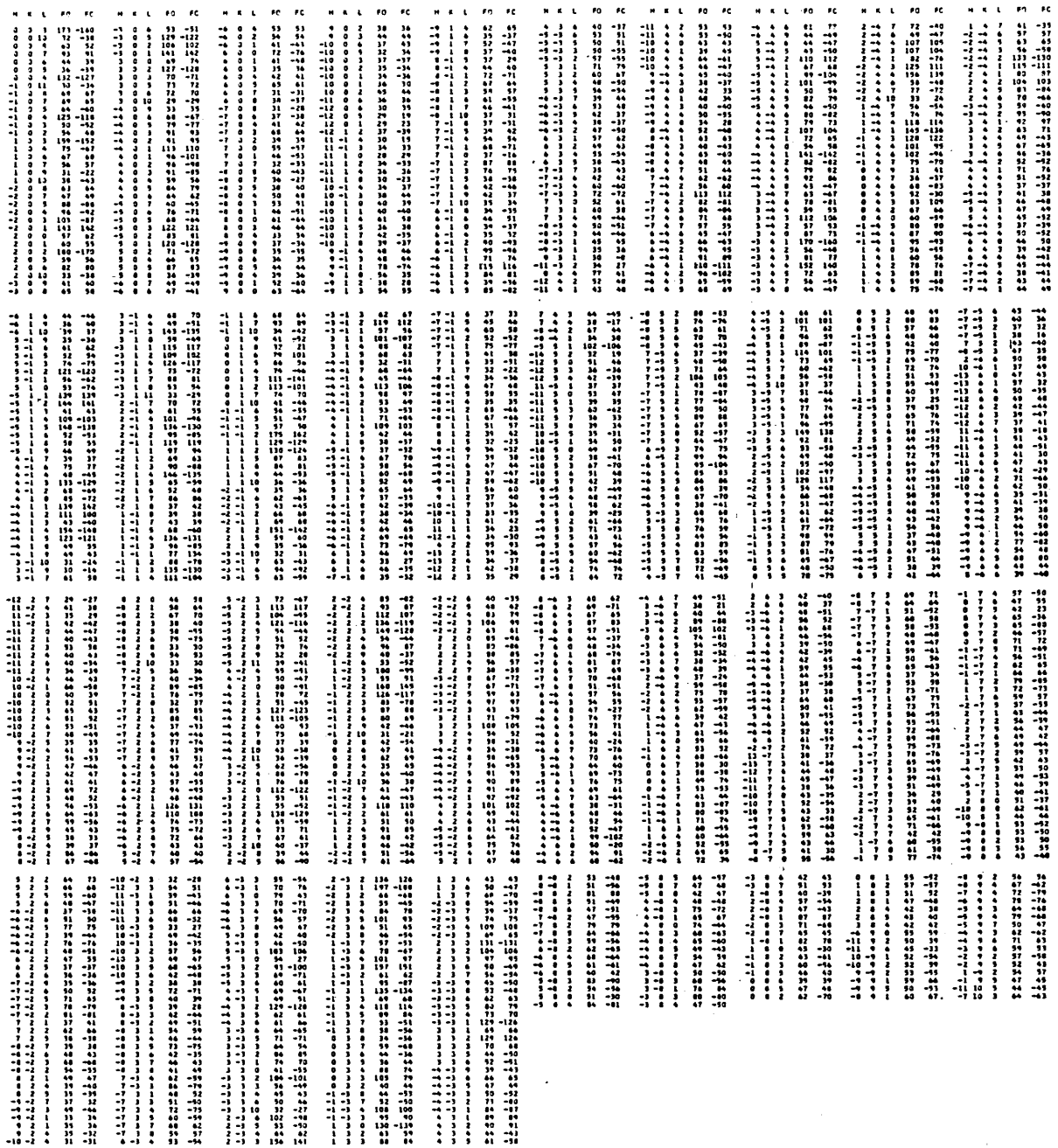

Table A3.3.

Observed and calculated structure factors for $(PEt_3)HgCl_2$

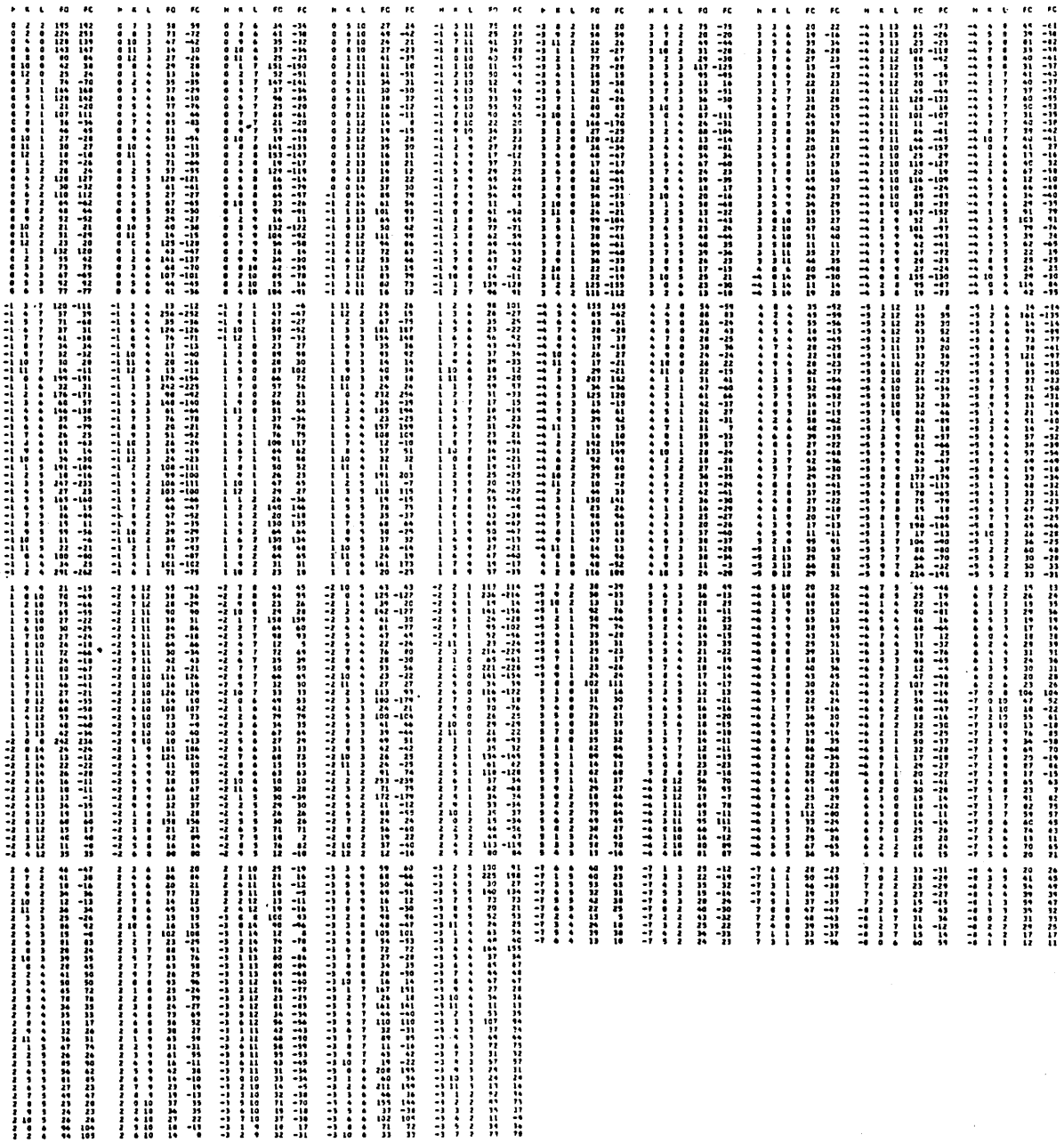

Table A3.4.

Observed and calculated structure factors for $(PMe_3)HgCl_2$

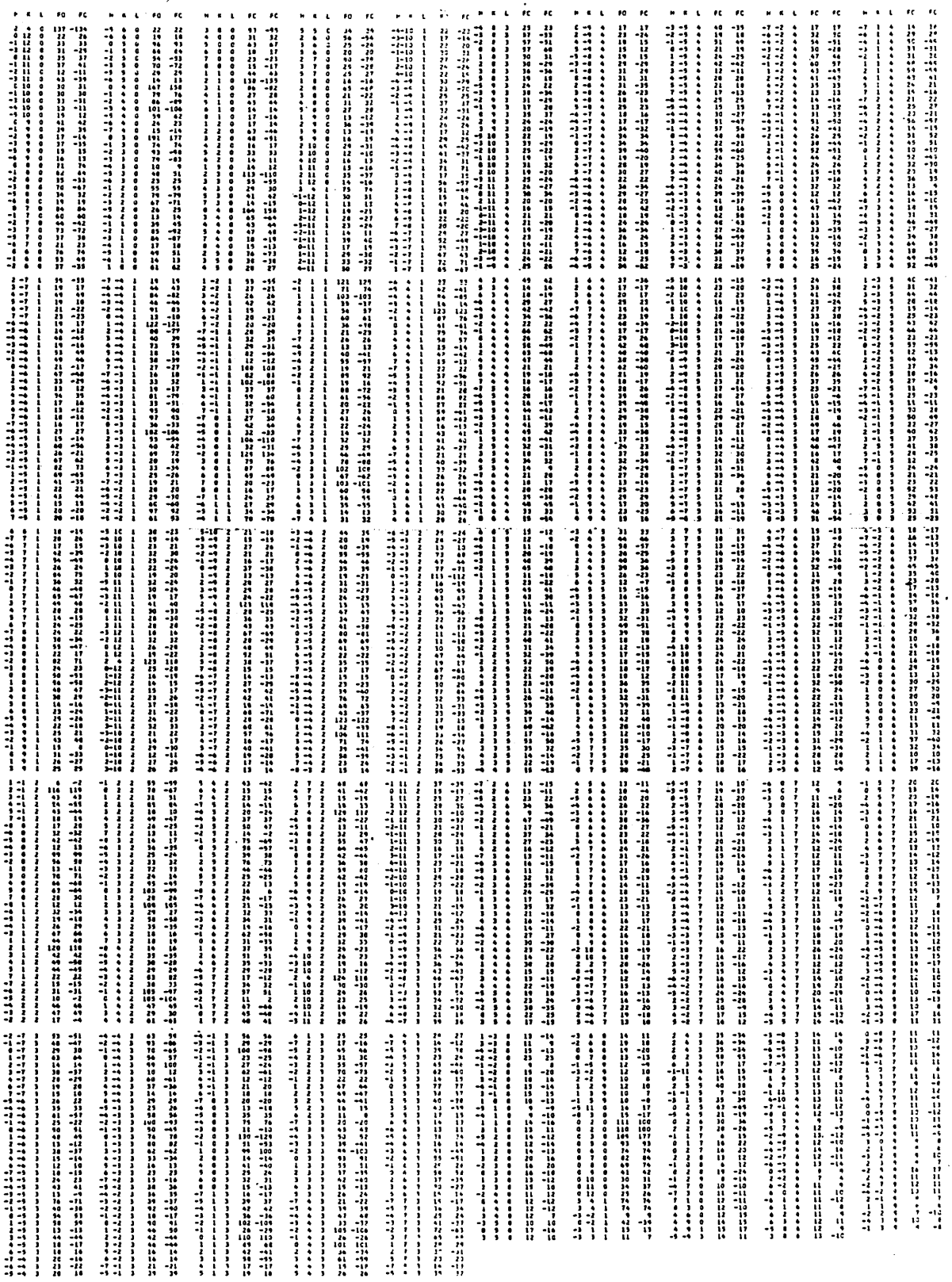

Table A3.5.

Observed and measured structure factors for α-(PBu^n_3)$HgCl_2$

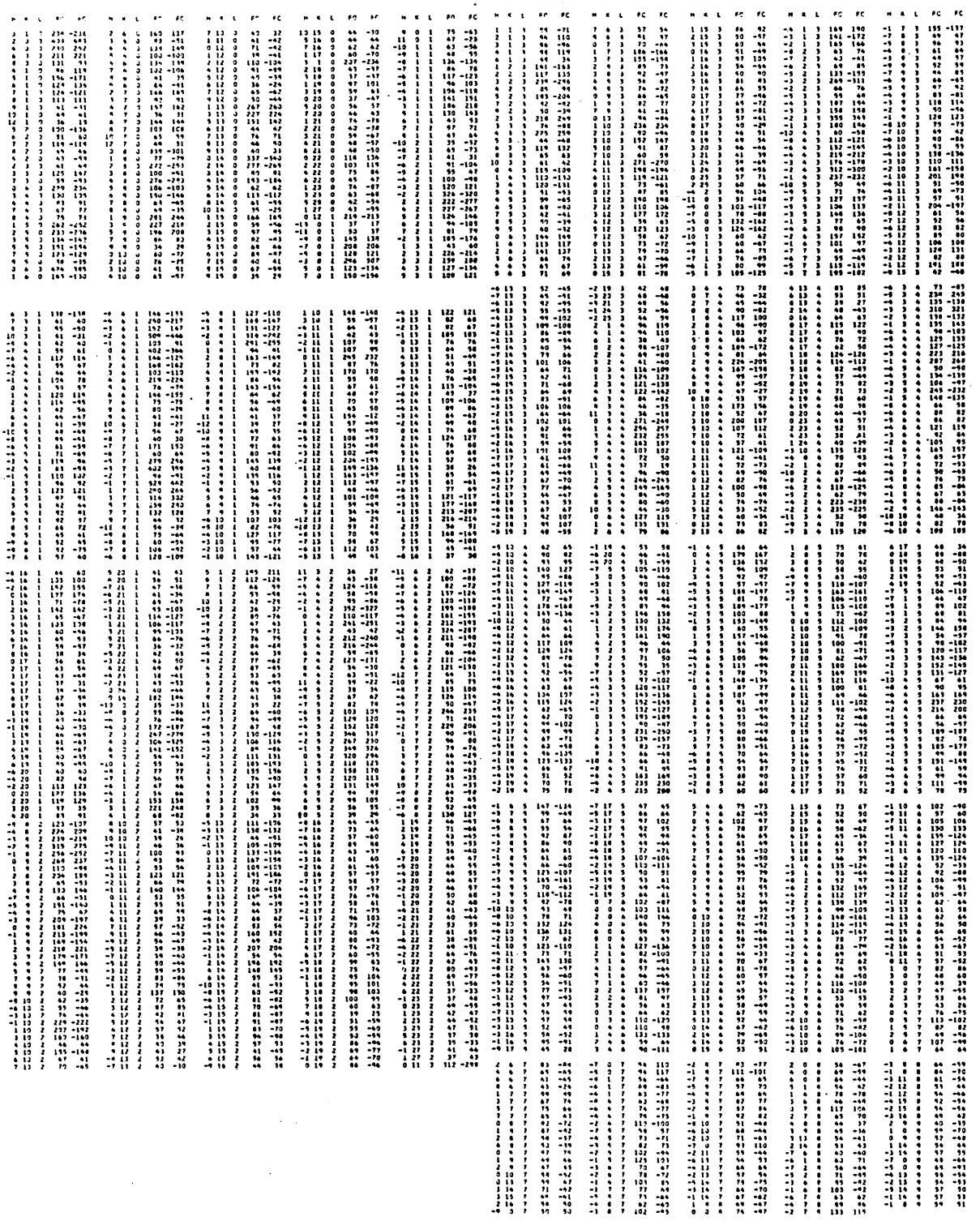

Table A3.6.

Observed and calculated structure factors for (2,4-dimethylpyridine)$HgBr_2$

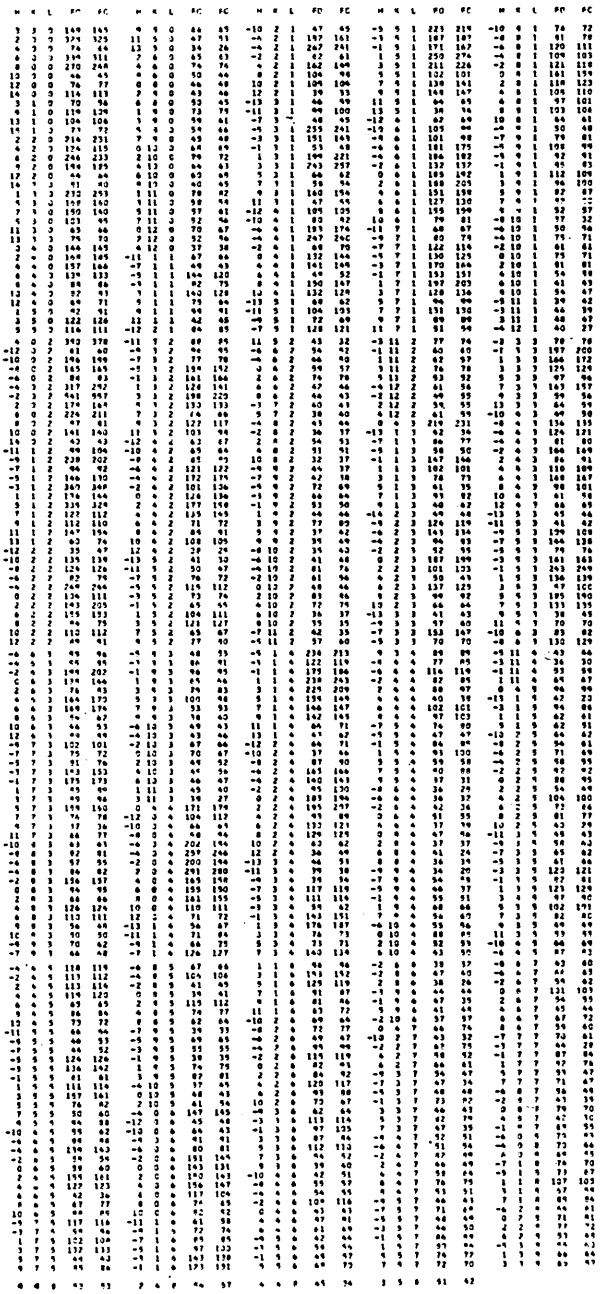

Observed and calculated structure factors for $(PEt_3)_2HgCl_2$

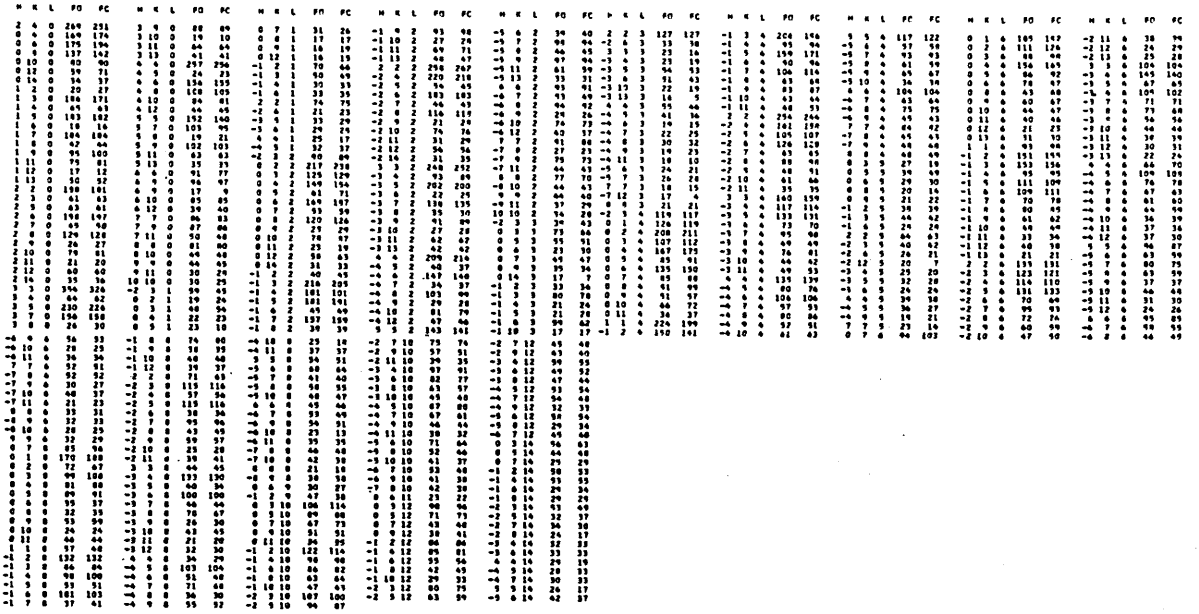

Table A3.8.

Observed and calculated structure factors for $(PEtMe_2)_2HgBr_2$

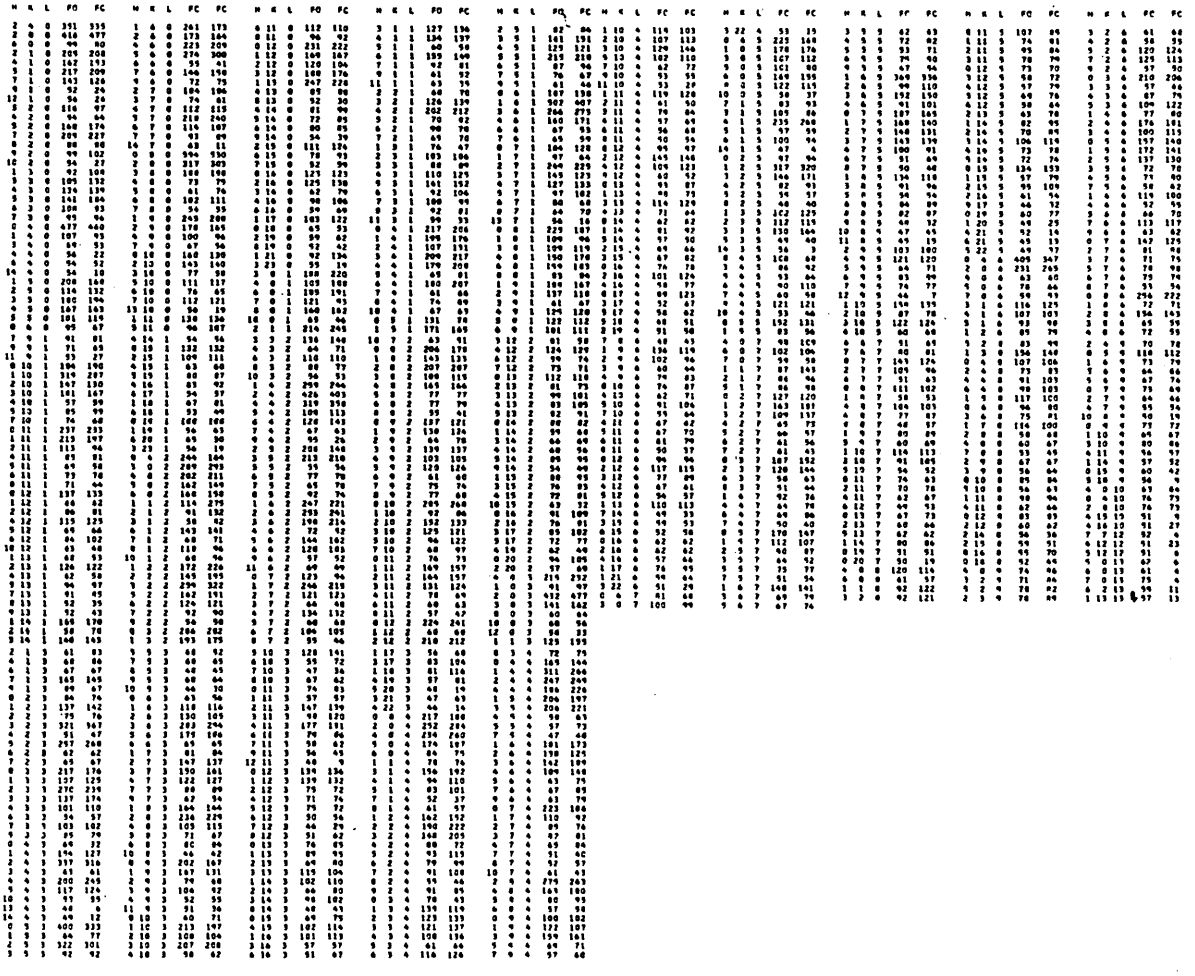

Table A3.9.

Observed and calculated structure factors for $(PEtMe_2)_3(HgCl_2)_2$

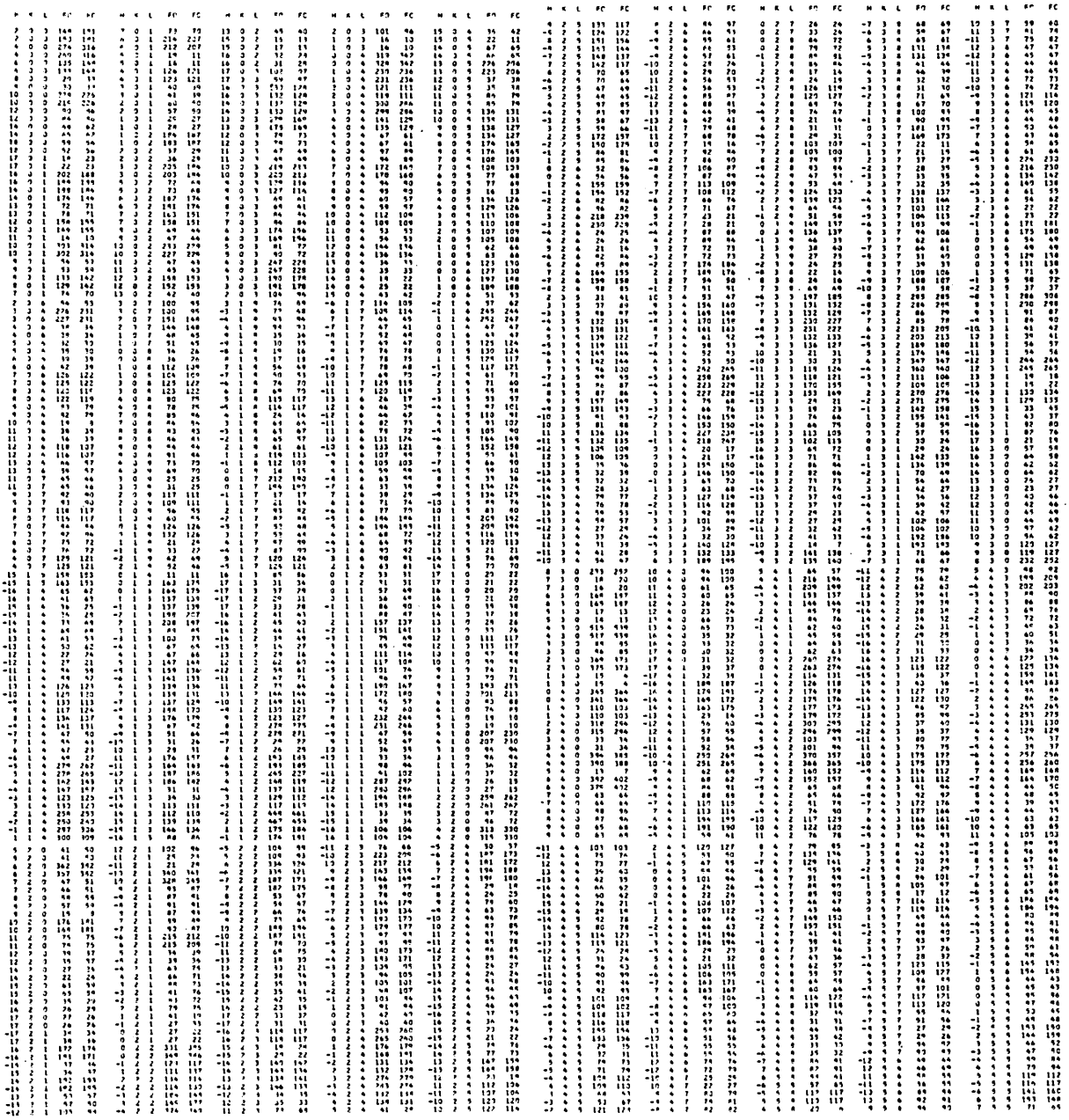

Table A3.9, continued

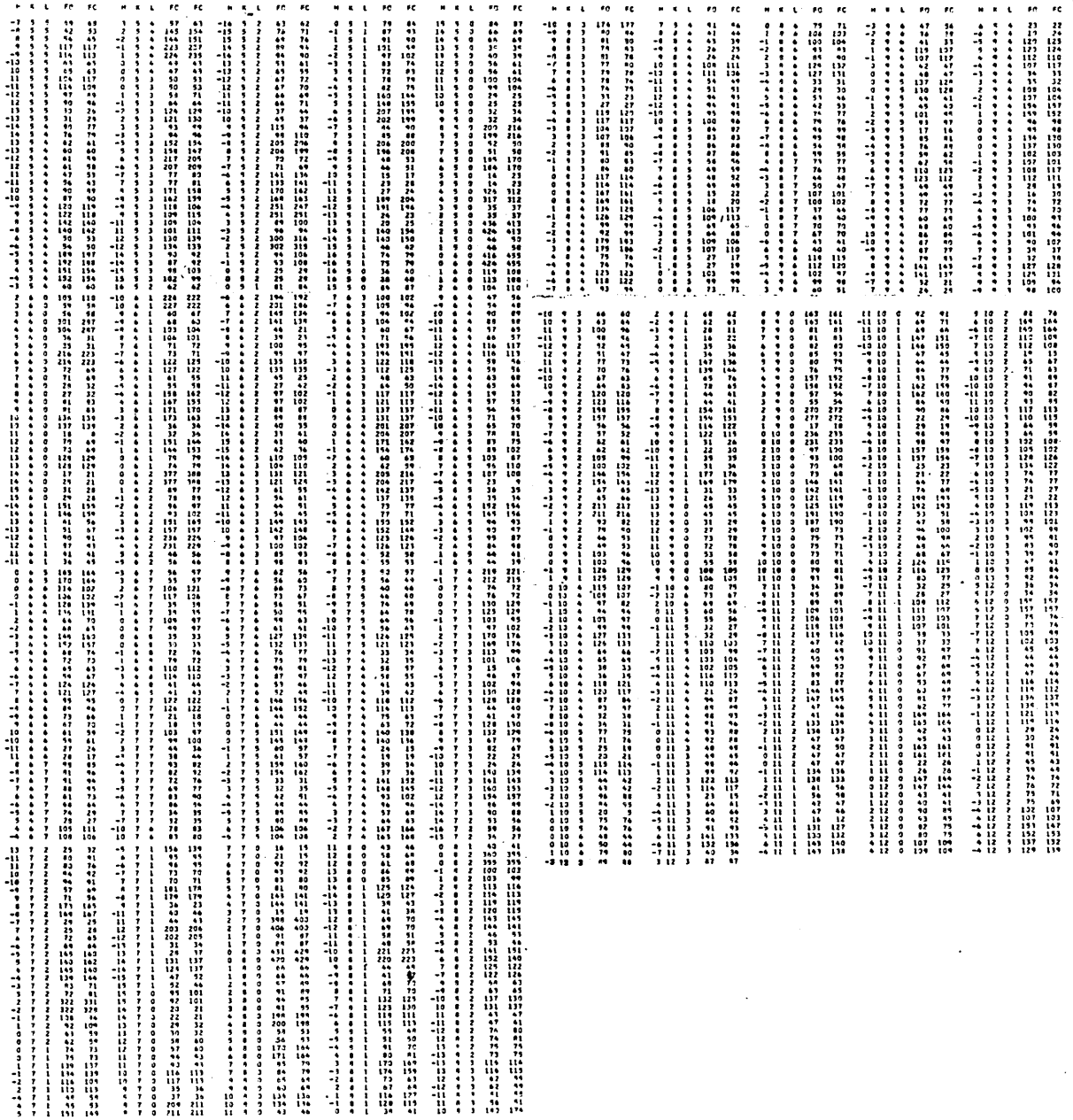

Appendix 4 : Point group, line group and factor group analyses

In this Appendix are contained the details of point, line and factor group analyses carried in this work. Section 1.2 dealt briefly with the applications of each method. The notation used here is essentially as denoted by Mitra and Gielisse.57

Definition of terms.

Reduction formula:

$$N_K = \frac{1}{N}\sum_j h_j \chi^{(R)}_j \chi^{(R)}_k$$

N_K = The number of times the k^{th} irreducible representation appears in the completely reduced reducible representation.

N = the order of the group (i.e. the total number of operations).

h_j = the number ofgroup operations contained in the j^{th} class

$\chi^{(R)}$ = the character in the k^{th} irreducible representation corresponding to operation R (from character tables)

$\chi^{(R)}$ = the character in the j^{th} reducible representation corresponding to operation R.

Group characters $C_J(R)$ for various representations.

Representation	Group character#
Total number of modes (3jn Cartesian coordinates)	= Wp(± l+2coscf)^)
Acoustic modes	X^"^) =±1 + 2cos<|>p
Translatory lattice modes	X^Tq) = [W^(s) - I] (± l+2cos<{>p)
Rotary lattice modes	$X^{\wedge}_J$-(R^ = (s—p)] x $_J$ p^

Wp - is the number of atoms invariant under the symmetry operation R

W^(s) - is the number of structural groups remaining invariant under symmetry operation R

$W_R(s-p)$ - is the number of polyatomic groups remaining invariant under an operation R (p is the number of monatomic groups)

ϕ_R - is the angle of rotation corresponding to the symmetry operation R (plus and minus signs stand, respectively, for proper and improper)

$\chi'_j(P)$ - is equal to $(1 \pm 2\cos\phi_R)$ for non-linear polyatomic groups, it is equal to $\pm 2\cos\phi_R$ for operations $C(\phi_R)$ and $S(\phi_R)$ in a linear polyatomic group, and it is equal to 0 for operations $C_2(\theta)$ and σ_v in a linear polyatomic group.

For the first analysis detailed workings are given of how T_A, T_o, R_o and n_{tot} are derived. For subsequent analyses only the results of T_A, T_o, etc. are tabulated. For each analysis internal displacement coordinates have been used to estimate the modes of vibration associated with specific bands; again only for the first analysis have detailed workings been given. In all analyses the organic ligands are taken as point masses.

Factor group analysis for (1,2,5-triphenylphosphole)HgX_2

These structures consist of discrete halogen-bridged dimers of C_i point symmetry which crystallizes in the triclinic space group $P\bar{1}$ (C_i^1, No. 2).[112] (1 dimer per unit cell).

C_i	E	i	n_{tot}	T_A	T_o	R_o	n_i
A_g	1	1	12	0	0	3	9
A_u	1	-1	12	3	0	0	9
ϕ_R	0	180					
$\pm 1+2\cos\phi_R$	3	-3					
W_R	8	0					
h_j	1	1					

Calculation of n_{tot} - using $N_k = \frac{1}{N} \sum_j h_j \chi_k(R) \chi'_j(n_{tot})$

$$N_{A_g} = \frac{1}{2}[24(1) + 0(1)] = 12$$

$$N_{A_u} = \frac{1}{2}[24(1) + 0(-1)] = 12$$

$$\Gamma_{tot} = 12A_g(R) + 12A_u(IR)$$

Calculation of T_A - using $N_k = \frac{1}{N} \sum_j h_j \chi_k(R) \chi'_j(T_A)$

	E	i
$\pm 1+2\cos\phi_R = \chi'_j(T_A)$ =	3	-3

$$N_{A_g} = \frac{1}{2}[3(1) + (-3)(1)] = 0$$

$$N_{A_u} = \frac{1}{2}[3(1) + (-3)(-1)] = 3$$

$$\Gamma_{T_A} = 3A_u(IR)$$

Calculation of T_o - using $N_k = \frac{1}{N} \sum_j h_j \chi_k(R) \chi'_j(T_o)$

	E	i
$\pm 1+2\cos\phi_R$ =	3	-3
$[W_R(s)-1]$ =	0	0

$$N_{A_g} = \frac{1}{2}[0(1) + 0(1)] = 0$$

$$N_{A_u} = \frac{1}{2}[0(1) + 0(-1)] = 0$$

$$\Gamma_{T_o} = 0$$

Calculation of R_o - using $\frac{1}{N}\sum_j h_j \chi_k(R)\chi'_j(R_o)$

	E	i
$W_r(s-p)$ =	1	1
$\chi'_j(p)$ =	3	3
$(=1\pm 2\cos\phi_R)$		

$$N_{A_g} = \frac{1}{2}[3(1) + 3(1)] = 3$$

$$N_{A_u} = \frac{1}{2}[3(1) + 3(-1)] = 0$$

$$\Gamma_{R_o} = 3A_g(R)$$

Using internal displacement coordinates one may predict the number and activity of modes due to $\nu(HgP)$, $\nu(HgX)_t$ and $\nu(HgX)_b$

The reduction formula used is :-

$$N_k = \frac{1}{N}\sum_j h_j S(j)\chi_k(R)$$

where $S(j)$ = the number of internal displacement coordinates unshifted by an operation in the j^{th} class

$\nu(HgP)$

C_i	E	i
h_j	1	1
$S(j)(HgP)$	2	0

$$N_{A_g} = \frac{1}{2}[2(1) + 0(1)] = 1$$

$$N_{A_u} = \frac{1}{2}[2(1) + 0(-1)] = 1$$

$$\Gamma\nu(HgP) = A_g(Ra) + A_u(IR)$$

$\underline{\nu(HgX)_t}$

C_i	E	i
h_j	1	1
$S(j)(HgX_t)$	2	0

$$N_{A_g} = \frac{1}{2}[2(1) + 0(1)] = 1$$

$$N_{A_u} = \frac{1}{2}[2(1) + 0(-1)] = 1$$

$$\Gamma\nu(HgX)_t = A_g(Ra) + A_u(IR)$$

$\underline{\nu(HgX)_b}$

C_i	E	i
h_j	1	1
$S(j)(HgX_b)$	4	0

$$N_{A_g} = \frac{1}{2}[4(1) + 0(1)] = 2$$

$$N_{A_u} = \frac{1}{2}[4(1) + 0(-1)] = 2$$

$$\Gamma\nu(HgX)_b = 2A_g(Ra) + 2A_u(IR)$$

Factor group analysis for $(PPh_3)HgX_2$

These structures consist of discrete halogen-bridged dimers of C_i point symmetry which crystallize in the monoclinic space group $P2_1/n$ ($\equiv P2_1/c$, C_{2h}^5 No. 14).[112] (2 dimers per unit cell).

C_{2h}^5	E	C_2	i	σ_h	n_{tot}	T_A	T_o	R_o	n_i
A_g	1	1	1	1	12	0	0	3	9
B_g	1	-1	1	-1	12	0	0	3	9
A_u	1	1	-1	-1	12	1	2	0	9
B_u	1	-1	-1	1	12	2	1	0	9
ϕ_R	0	180	180	0					
$\pm 1+2\cos\phi_R$	3	-1	-3	0					
W_R	16	0	0	0					
h_j	1	1	1	1					
$\chi_j'(n_{tot})$	48	0	0	0					
$\chi_j'(T_o)$	3	1	-3	-1					
$\chi_j'(R_o)$	6	0	6	0					
S(j)(Hg-P)	4	0	0	0					
S(j)(Hg-Cl_t)	4	0	0	0					
S(j)(Hg-Cl_b)	8	0	0	0					

$\Gamma_{Total} = 12A_g(Ra)+12B_g(Ra)+12A_u(IR)+12B_u(IR)$

$\Gamma_{int} = 9A_g(Ra)+ 9B_g(Ra)+ 9A_u(IR)+ 9B_u(IR)$

$\Gamma\nu(HgP) = A_g(Ra)+ B_g(Ra)+ A_u(IR)+ B_u(IR)$

$\Gamma\nu(HgX)_t = A_g(Ra)+ B_g(Ra)+ A_u(IR)+ B_u(IR)$

$\Gamma\nu(HgX)_b = 2A_g(Ra)+ 2B_g(Ra)+ 2A_u(IR)+ 2B_u(IR)$

Factor group analysis for $(PMe_3)HgX_2$

These structures consist of 'ionic' chains with $[Cl\text{-}Hg\text{-}PMe_3]^+$ cations and Cl^- anions. There is one chain per unit cell, consisting of two cations and two anions, which crystallizes in the triclinic space group $P\bar{1}$ (C_i^1, No. 2).[112]

This treatment has also been used for the $(C_4H_8S)HgX_2$ (X=Cl or Br), $(PPhMe_2)HgX_2$ (X=Cl or Br), α-$(PPh_2Me)HgCl_2$ and $(PPh_2Me)HgBr_2$ complexes.

C_i	E	i	n_{tot}	T_A	T_o	R_o	n_i
A_g	1	1	12	0	6	3	3
A_u	1	-1	12	3	3	3	3
ϕ_R	0	180					
$\pm 1+2\cos\phi_R$	3	-3					
W_R	8	0					
h_j	1	1					
$\chi_j'(n_{tot})$	24	0					
$\chi_j'(T_o)$	9	3					
$\chi_j'(R_o)$	6	0					
S(j)(HgP)	2	0					
$S(j)(HgX)_t$	2	0					

$\Gamma_{Total} = 12A_g(Ra) + 12A_u(IR)$

$\Gamma_{int\ (cation)} = 3A_g(Ra) + 3A_u(IR)$

$\Gamma\nu(HgP) = A_g(Ra) + A_u(IR)$

$\Gamma\nu(HgCl)_t = A_g(Ra) + A_u(IR)$

$\Gamma_{ion\ trans.} = 6A_g(Ra) + 3A_u(IR)$

Line group analysis for $(PEt_3)HgX_2$

(a)

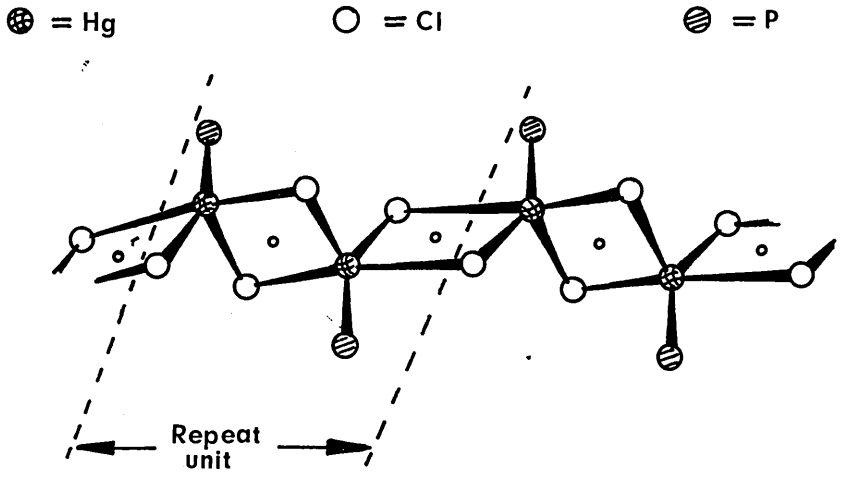

These structures consist of polymeric chains, as in (a) belonging to the C_i line group. This treatment has also been used for the (2,4,6-trimethylpyridine)HgX_2 complexes and α-$(PPh_2Me)HgCl_2$.

C_i	E	i	n_{tot}	R_o	T_A	n_{chain}
A_g	1	1	12	1	0	11
A_u	1	-1	12	0	3	9
ϕ_R	0	180				
$\pm 1+2\cos\phi_R$	3	-3				
W_R	8	0				
h_j	1	1				
$\chi_j(n_{tot})$	24	0				
S(j)(HgP)	2	0				
$S(j)(HgX)_b$	8	0				

$\Gamma_{Total} = 12A_g(Ra) + 12A_u(IR)$

$\Gamma_{chain} = 11A_g(Ra) + 9A_u(IR)$

$\Gamma\nu(HgP) = A_g(Ra) + A_u(IR)$

$\Gamma\nu(HgX)_b = 4A_g(Ra) + 4A_u(IR)$

Line group analysis for (2,4-dimethylpyridine)HgX_2

(a)

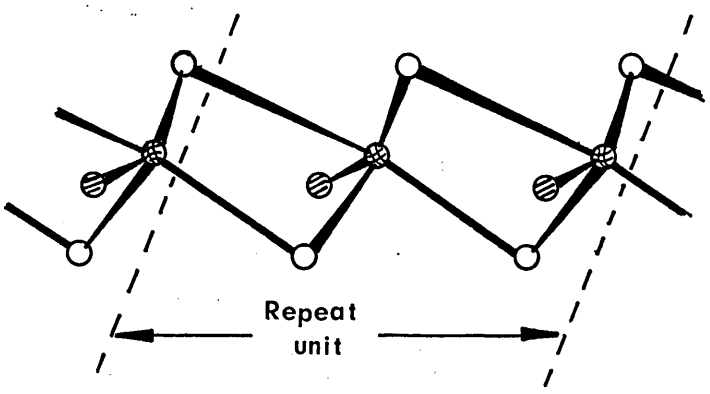

These structures are polymeric chains, as in (a) which belongs to the C_1 line group.

C_1	E	n_{tot}	R_o	T_A	n_{chain}
A	1	24	1	3	20
ϕ_R	0				
$\pm 1+2\cos\phi_R$	3	Γ_{Total} = 24A(IR,Ra)			
W_R	8				
h_j	1	Γ_{chain} = 20A(IR,Ra)			
$\chi'_j(n_{tot})$	24	$\Gamma\nu$(HgN) = 2A(IR,Ra)			
S(j)(HgN)	2	$\Gamma\nu(HgX)_b$ = 8A(IR,Ra)			
$S(j)(HgX_b)$	8				

T_A and R_o may be obtained directly from the C_1 character table.

Point group analysis for $(PBu^n_3)HgX_2$

These compounds exist as discrete tetrameric units of C_i point symmetry:-

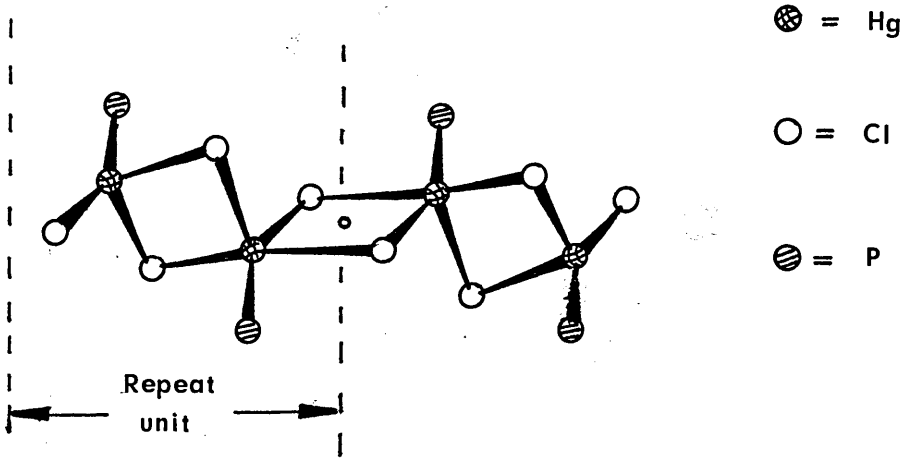

C_i	E	i	n_{tot}	R_o	T_A	n_i
A_g	1	1	24	3	0	21
A_u	1	-1	24	0	3	21
ϕ_R	0	180				
$\pm 1+2\cos\phi_R$	3	-3				
W_R	16	0				
h_j	1	1				
$\chi_j(n_{tot})$	48	0				
S(j)(HgP)	4	0				
$S(j)(HgCl_t)$	2	0				
$S(j)(HgCl_b)$	14	0				

$\Gamma_{Total} = 24A_g(Ra) + 24A_u(IR)$

$\Gamma n_i = 21A_g(Ra) + 21A_u(IR)$

$\Gamma\nu(HgP) = 2A_g(Ra) + 2A_u(IR)$

$\Gamma\nu(HgCl)_t = A_g(Ra) + A_u(IR)$

$\Gamma\nu(HgCl)_b = 7A_g(Ra) + 7A_u(IR)$

T_A and R_o may be obtained directly from the C_i character table.

Appendix 5 : Equations for predicting the positions of (HgX) modes in planar four-membered ring systems

(a) The equation of Baran[137] for predicting the relative positions of the two IR-active bridge stretching modes in a planar, symmetric four-membered ring.

The derivation starts from the simple idea viz. that the behaviour of a bridge X in a planar and symmetric four-membered ring within which it is simultaneously influenced by both central atoms M, can be described by the superposition of two linear harmonic oscillators, each representing an 'isolated' M-X bond. The bridge, then vibrates along R and (as in (i))

't v

'M

M

X

Ci)

The form of such a figure depends first of all upon the angle under which the central atoms influence the bridge. Using V to denote a vector of the ''isolated" linear movement in the M-X direction then equations la and lb describe the movement of the resulting components R^ and R^ in the

directions M-M and X-X respectively.

$$R_M^2 = 2V^2(1-\cos\phi) = 2V^2(1+\cos\varepsilon) \quad \text{..... Ia}$$

$$R_X^2 = 2V^2(1-\cos\varepsilon) = 2V^2(1+\cos\phi) \quad \text{..... Ib}$$

If one considers the two IR-active in-plane modes of vibration associated with the ring, as in (ii).

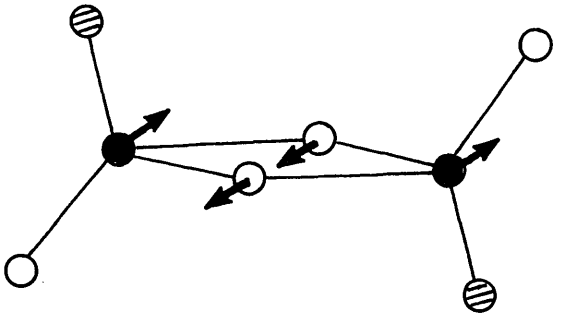

Corresponds to motion along R_X

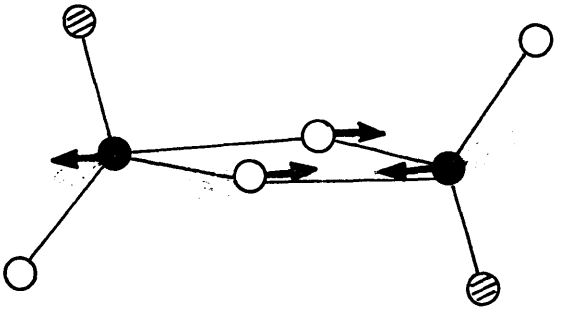

Corresponds to motion along R_M

(ii)

These forms of motion can be compared with the resultant vectors R_X and R_M.

For the sake of brevity Baran has called ring vibrations in the X-X and M-M directions ν_s and ν_a respectively. Rearrangement of equations Ia and Ib leads to two main relationships between $P = R_X/R_M = \nu_s/\nu_a$ of both components of the bridge vibrations and the angles of the bridged entity

$$\cos\varepsilon = \frac{1-P^2}{1+P^2} \qquad \text{and} \qquad \cos\phi = \frac{P^2-1}{P^2+1}$$

(b) <u>An extension of the formula of Baran[137] to include asymmetric ring systems</u>.

In the present case we need to introduce the two vectors W and V to denote 'isolated' linear movement along the two <u>different</u> bridges M-X. V^* represents the weaker of the two bridges.

* It should be emphasized that the vectors along M-X directions do not correspond to bond lengths but to 'bond energy terms' which are inversely proportional to bond lengths.

The derivation will be restricted to the simple case when the bridge angles are 90° i.e. only effect of extending the ring along one of its lengths will be discussed.

N.B. $\alpha + \beta = \varepsilon = \phi = 90^\circ$

in the present case.

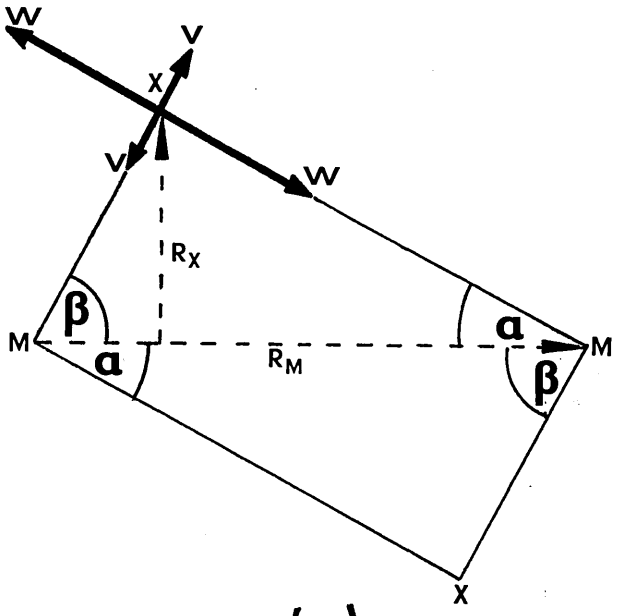

(iii)

In a similar way to Baran's derivation, equations 2a and 2b describe movement of the resulting components R_M and R_X in the directions M-M and also perpendicular to M-M (N.B. not along X-X).

$$R_X = W \sin\alpha + V \sin\beta \quad \ldots\ldots\ldots\ldots\ldots\ldots \quad 2a$$

$$R_M = W \cos\alpha + V \cos\beta \quad \ldots\ldots\ldots\ldots\ldots\ldots \quad 2b$$

The critical assumption is made that the IR-active modes of the asymmetric bridge will have the following forms of motion, as in (iv)

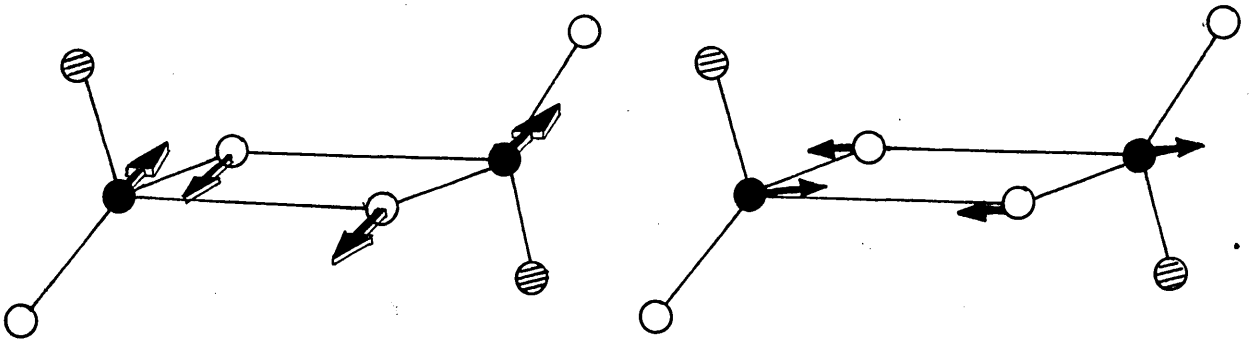

(iv)

i.e. vibration is along M-M and also 90° away from the M-M axis in the plane of the ring.

If this assumption is made again the following relationship will hold:-

$$P = R_X/R_M = \nu_s/\nu_a = \frac{W \sin\alpha + V \sin\beta}{W \cos\alpha + V \cos\beta}$$

Consider what happens, in qualitative terms, when the ring has been extended along one of its bonds as in (iii) (remember in the vector diagram, the vectors are inversely related to bond length). The vector V represents the vector along the extended bond length. Therefore in (iii) the M-X distance along V-V becomes smaller. This has the effect of decreasing α and increasing β.

The way in which changes in α and β affect R_X and R_M are described below.

The effect upon R_X:- (remember $\alpha + \beta = 90°$)

When α is 'small', $\sin\alpha$ is 'small', therefore the contribution of the stronger bond represented by vector W is also 'small'

When β is 'large', $\sin\beta$ is 'large' and therefore the contribution of the weaker bond represented by vector V is also 'large'

The overall effect is therefore that R_X is 'small'

The effect upon R_M:-

When α is 'small', $\cos\alpha$ is 'large', therefore the contribution of the stronger bond represented by vector W is also 'large.'

When β is 'large', $\cos\beta$ is 'small', and therefore the contribution of the weaker bond represented by vector V is also 'small.'

The overall effect is therefore that R_M is 'large.'

Consequently, changes in the asymmetry of the ring alters the ratio R_X/R_M. The ratio moves away from unity as the ring is extended along one of its bridges. Therefore one might expect from the relationship $R_X/R_M = \nu_s/\nu_a$ to observe a greater separation between the two IR-active $\nu(MX)_b$ modes with increasing asymmetry of the ring.

Appendix 6. Equations of least squares planes.

Equations of least square planes referred to orthogonal axes with distances (Å) of relevant atoms from the planes in square brackets.

$(PPh_3)HgCl_2$

Plane (a) i.e. ring A; C(11), C(12), C(13), C(14), C(15), C(16).

$$0.2433X + 0.1481Y - 0.9586Z + 0.3342 = 0$$

Plane (b) i.e. ring B; C(31), C(32), C(33), C(34), C(35), C(36).

$$.9061X - 0.2152Y - 0.3643Z + 3.0354 = 0$$

Plane (c) i.e. ring C; C(21), C(22), C(23), C(24), C(25), C(26).

$$-0.3279X + 0.9226Y - 0.2034Z - 1.3259 = 0$$

(N.B. Because the atoms of each ring have been refined to fit a regular hexagon, none of these atoms can possibly deviate from their mean planes.)

PPh_3 ligand[a]

Plane (a) i.e. ring A; C(11), C(12), C(13), C(14), C(15), C(16).

$$-0.6076X + 0.5671Y - 0.5561Z + 1.7832 = 0$$

[C(11) -0.001, C(12) 0.003, C(13) -0.007, C(14) 0.010, C(15) -0.009, C(16) 0.004]

Plane (b) i.e. ring B; C(21), C(22), C(23), C(24), C(25), C(26).

$$0.4762X - 0.1545Y - 0.8657Z - 0.1733 = 0$$

[C(21) 0.005, C(22) -0.009, C(23) 0.006, C(24) 0.002, C(25) -0.006, C(26) 0.003]

Plane (c) i.e. ring C; C(31), C(32), C(33), C(34), C(35), C(36).

$$0.5108X + 0.8527Y - 0.1095Z - 1.5162 = 0$$

[C(31) 0.005, C(32) -0.009, C(33) 0.006, C(34) 0.002, C(35) -0.006, C(36) 0.003]

$(TPP)HgCl_2$

Plane (a) i.e. ring A; C(17), C(18), C(19), C(20), C(21), C(22).

$$0.5073X + 0.3641Y - 0.7811Z + 1.3425 = 0$$

a - The mean planes have been determined in the present work using the atomic coordinates quoted in reference 111.

Plane (b) i.e. ring B; C(11), C(12), C(13), C(14), C(15), C(16).

$$0.6003X - 0.7531Y - 0.2694Z + 4.6047 = 0$$

Plane (c) i.e. ring C; C(5), C(6), C(7), C(8), C(9), C(10).

$$-0.5723X - 0.2966Y - 0.7645Z + 1.1630 = 0$$

(N.B. The atoms in the above phenyl rings have been refined as regular hexagons).

Plane (d) i.e. phosphole ring; P, C(1), C(2), C(3), C(4).

$$0.7648X + 0.0309Y - 0.6435Z + 3.0436 = 0$$

[P 0.037, C(1) -0.005, C(2) -0.034, C(3) 0.071, C(4) -0.069]

$(PEt_3)HgCl_2$

Plane (a) Hg, P, Cl(1), Cl(2).

$$-0.2701X + 0.9046Y - 0.3298Z - 0.9643 = 0$$

[Hg -0.578, P -1.051, Cl(1) 0.902, Cl(2) 0.726]

$(PMe_3)HgCl_2$

Plane (a) Hg, Cl(1), Hg', Cl(1'), Hg'', Cl(1'').

$$0.0004X + 1.0000Y - 0.0058Z - 0.0345 = 0$$

[Hg 0.070, Cl(1) 0.063, Hg' -0.139, Cl(1') -0.132, Hg'' 0.072, Cl(1'') 0.066]

α-$(PBu^n_3)HgCl_2$

Plane (a) Hg(2), Cl(2), Cl(4), P(2).

$$0.5670X + 0.4368Y - 0.6984Z - 1.3078 = 0$$

[Hg(2) 0.159, Cl(2) -0.027, Cl(4) -0.065, P(2) -0.067]

(2,4-dimethylpyridine)$HgBr_2$

Plane (a) Hg, Br(1), Br(2), N.

$$0.6377X - 0.0655Y - 0.7675Z + 1.7567 = 0$$

[Hg 0.155, Br(1) -0.043, Br(2) -0.056, N -0.056]

Plane (b) N, C(1), C(2), C(3), C(4), C(5).

$$0.3214X + 0.0827Y - 0.9433Z + 1.7724 = 0$$

[N 0.014, C(1) -0.032, C(2) 0.011, C(3) 0.024, C(4) -0.040, C(5) 0.024]

(2,4,6-trimethylpyridine)$HgCl_2$[a]

Plane (a) Hg, Cl(1), Cl(2), N

$$0.5444X - 0.3422Y - 0.7659 + 1.4693 = 0$$

[Hg -0.005, Cl(1) 0.002, Cl(2) 0.002, N 0.002]

Plane (b) N, C(1), C(2), C(3), C(4), C(5).

$$0.1930X - 0.0046Y - 0.9812Z + 1.4913 = 0$$

[N -0.009, C(1) 0.010, C(2) -0.001, C(3) -0.008, C(4) 0.009, C(5) 0.000]

a - The mean planes have been determined in the present work using the atomic coordinates quoted in reference 64.

Appendix 7 : The definition of cone angle (9)

The cone angle for a symmetric ligand PR^ (all three substituents being the same) is the apex angle of a cylindrical cone centred 2.28 Å from the centre of the P atom, which touches the van der Waals' radii of the outermost atoms, as in (a).

2.28A

2.28 A

02/2

(a)

(b)

For an unsymmetric ligand P R ^ R j as in (b), the cone angle may be given by:

$$= \sum_{i=1}^{2\ 3} ei/\text{«}\ ^{\wedge}$$

Less congestion around the bonding face of phosphorus, given by 0, was found*'5'5 to be conducive to greater *binding ability.

References

1. D.M. ADAMS, "Metal-ligand and Related Vibrations", Arnold, London, 1967.
2. I.S. AHUJA and P. RASTOGI, J. Chem. Soc. (A), 2161, 1970; I.S. AHUJA and R. SINGH, J. Inorg. Nuclear Chem., 36, 1505, 1974.
3. I.S. AHUJA and P. RASTOGI, J. Inorg. Nuclear Chem., 32, 2085, 1970.
4. H.SCHMIDBAUR and K.H. RATHLEIN, Chem. Ber., 106, 2491, 1973.
5. G.E. COATES and D. RIDLEY, J. Chem. Soc., 166, 1964.
6. F.G. MOERS and J.P. LANGHOUT, Rec. Trav. Chim., 92, 996, 1973.
7. G.B. DEACON, J.H.S. GREEN, and D.J. HARRISON, Spectrochim. Acta, 24A, 1921, 1968.
8. D.M. ADAMS, D.J. COOK, and R.D.W. KEMMITT, J. Chem. Soc. (A), 1067, 1968.
9. K. BRODERSON, R. PALMER, and D. BREITINGER, Chem. Ber., 104, 360, 1971.
10. M.A. BERNARD, F. BUSNOT, and J.F. LEQUERLER, Thermochimica Acta, 12, 387, 1975.
11. I.S. AHUJA, Inorg. Nuclear Chem. Lett., 6, 879, 1970.
12. A.J. PAPPAS, J.F. VILLA, and H.B. POWELL, Inorg. Chem., 8, 550, 1969.
13. G. SCHMAUSS and H. SPECKER, Z. Anorg. Chem., 363, 113, 1968.
14. J.E. FERGUSON and K.S. LOH, Austral. J. Chem., 26, 2615, 1973.
15. R.H. HANSON and E. MELOAN, Inorg. Nuclear Chem. Lett., 7, 461, 1971.
16. G. MARCOTRIGIANO and R. BATTISTUZZI, Inorg. Nuclear Chem. Lett., 8, 969, 1972;

    G. MARCOTRIGIANO, G. PEYRONEL, and R. BATTISTUZZI, J. Inorg. Nuclear Chem., 37, 1675, 1975;

    G. MARCOTRIGIANO, Z. Anorg. Chem., 417, 75, 1975; Ibid, 422, 80, 1976;

    G. MARCOTRIGIANO and R. BATTISTUZZI, J. Inorg. Nuclear Chem., 36, 3719, 1974.
17. G.B. AITKEN, J.L. DUNCAN, and G.P. McQUILLAN, J.C.S. Dalton, 2103, 1972.
18. R.J.H. CLARK and C.S. WILLIAMS, Inorg. Chem., 4, 350, 1965.
19. I.S. AHUJA and K.S. RAO, Indian J. Chem., 13, 413, 1975.

20. I.S. AHUJA and R. SINGH, J. Inorg. Nuclear Chem., 35, 302, 1973.

21. I.S. AHUJA and P. RASTOGI, J. Inorg. Nuclear Chem., 32, 2085, 1970.

22. A.C. HIREMATH and A.S.R. MURTHY, Indian J. Chem., 15A, 55, 1977.

23. F.A. DEVILLANOVA and G. VERANI, Transition Metal Chem., 2, 9, 1977.

24. G.B. AITKEN, J.L. DUNCAN, and G.P. McQUILLAN, J.C.S. Dalton, 2103, 1972.

25. A.C. HIREMATH and A.S.R. MURTHY, Curr. Sci., 45, 545, 1976.

26. F. CRISTIANI, F.A. DEVILLANOVA, and G. VERANI, Transition Metal Chem., 2, 50, 1977.

27. G.B. DEACON and J.H.S. GREEN, Spectrochim. Acta, 25A, 335, 1969.

28. I.S. AHUJA and A. GARG, Inorg. Chim. Acta, 6, 453, 1972.

29. D. DEFILIPPO, A. LAI, E.F. TROGU, G. VERANI, and C. PRETI, J. Inorg. Nuclear Chem., 36, 73, 1974.

30. M. MASSACESI, G. PONTICELLI, and C. PRETI, J. Inorg. Nuclear Chem., 38, 1556, 1976.

31. G.B. AITKEN and G.P. McQUILLAN, Inorg. Chim. Acta, 15, 221, 1975.

32. C. PRETI, G.TOSI, D. DEFILIPPO, and G. VERANI, J. Inorg. Nuclear Chem., 36, 3725, 1974.

33. G. DEVOTO, G. PONTICELLI, C. PRETI, and G. TOSI, J. Inorg. Nuclear Chem., 38, 1744, 1976.

34. M.A. HOOPER and D.W. JAMES, Austral. J. Chem., 24, 1331, 1971; Ibid., 24, 1345, 1971.

35. D. GRDENIC, Quart. Rev., 19, 1965.

36. G. DAVISON, "Introductory Group Theory for Chemists", Elsevier, London, 1971.

37. S.S. MITRA and P.J. GIELISSEIN, "Progress in Infrared Spectroscopy, Volume 2," (Editor, H.A. Szymanski), Plenum Press, New York, 47, 1964.

38. C.H. MACGILLAVRY, J.H. DEWILDE and J.M. BIJVOET, Z. Krist., 100A, 212, 1938; and
K. AURIVILLIUS and C. STALHANDSKE, Acta Chem. Scand. A30, 735, 1976.

39. A. WEISS and K. DAMM, Z. Naturforsch. (B), 9, 82, 1954.

40. K. SAGISAWA, K. KITAHAMA, H. KIRIYAMA, and R. KIRIYAMA, Acta Cryst. B30, 1603, 1974.

41. S.E. HARMSEN, Z. Krist., 100, 208, 1938.

42. J.T.R. DUNSMUIR and A.P. LANE, J. Inorg. Nuclear Chem., 33, 4361, 1971.

43. H.J. VERWEEL and J.M. BIJVOET, Z. Krist., 77, 122, 1931.

44. G.A. JEFFREY and M. VLASSE, Inorg. Chem., 6, 396, 1967.

45. P. BISCARINI, L. FUSINA, G. NIVELLINI, and G. PELIZZI, J.C.S. Dalton, 7, 664, 1977.

46. R.H. FENN, Acta Cryst., 20, 20, 1966.

47. M. SANDSTROM, Ph.D. Thesis, Royal Institute of Technology, Dept. of Inorganic Chemistry, Stockholm, 1978.

48. K. WEIDENHAMMER and M.L. ZIEGLER, Z. Anorg. Chem., 434, 152, 1977.

49. J.G. WHITE, Acta Cryst., 16, 397, 1963.

50. E.M. McPARTLIN, Personal Communication.

51. G.S. HARRISON, F. INGLIS, J. McKECHNIE, K.K. CHEUNG, and G. FERGUSON, Chem. Comm., 442, 1967.

52. S.M. NELSON and S.G. McFALL, Chem. Comm., 167, 1977.

53. P.T. BEURSKENS, W.P.J.H. BOSMAN, and J.A. CRAS, J. Cryst. Mol. Struct., 2, 183, 1972.

54. A.W. GAL, G. BEURSKENS, P.T. BEURSKENS, and J. WILLEMSE, Rec. Trav. Chim., **95**, 157, 1976.

55. R.H. FENN, Acta Cryst., 20, 24, 1966.

56. B. KAMENAR and A. NAGL, Acta Cryst., B32, 1414, 1976.

57. L.S. GLASSER, L. INGRAM, M.G. KING, and G.P. McQUILLAN, J. Chem. Soc. (A), 2501, 1967.

58. P.D. BROTHERTON, J.M. EPSTEIN, A.H. WHITE, and A.C. WILLIS, J.C.S. Dalton, 2341, 1974.

59. M. AUTHIER-MARTIN and A.L. BEAUCHAMP, Canad. J. Chem., 55, 1213, 1977.

60. N.L. HOLY, N.C. BAENZIGER, R.M. FLYNN, and D.C. SWENSON, J. Amer. Chem. Soc., 98, 7823, 1976.

61. R.C. EVANS, F.G. MANN, H.S. PEISER, and D. PURDIE, J. Chem. Soc., 1209, 1940.

62. S. KULPE, Z. Anorg. Chem., 349, 314, 1967.

63. M. AUTHIER-MARTIN, J. HUBERT, R. RIVEST, and A.L. BEAUCHAMP, Acta Cryst., B34, 273, 1978.

64. C.I. BRANDEN, Arkiv. Kemi., 22, 495, 1964.

65. J. KOZAREK and Q. FERNANDO, Inorg. Chem., 12, 2129, 1973.

66. C.I. BRANDEN, Arkiv. Kemi., 22, 485, 1964.

67. S. DAHL and P. GROTH, Acta Chem. Scand., 25, 1114, 1971.

68. G. SAWITSKI and H.G. SCHNERING, Chem. Ber., 107, 3266, 1974.

69. A.T. McPHAIL and G.A. SIM, Chem. Comm., 21, 1966.

70. M. FREY, Compt. Rend., 270, 1265, 1970.

71. Y.T. STRUCHKOV, A.I. KITAJGORODSKIJ, and T.L. KHOTSYANOVA, Doklady Akad. Nauk. SSSR., 93, 675, 1953.

72. P. BISCARINI, L. FUSINA, G.D. NIVELLINI, A. MANGIA, and G. PELIZZI, J.C.S. Dalton, 159, 1973.

73. F. GENET and J.C. LEGUEN, Acta Cryst., 25B, 2029, 1969.

74. L. FALTH, Chem. Scripta, 9, 71, 1976.

75. G. BANDOLI, D.A. CLEMENTE, L. SINDELLARI, and E. TONDELLO, J.C.S. Dalton, 451, 1975.

76. R.S. McEWEN and G.A. SIM, J. Chem. Soc. (A), 271, 1967.

77. C.I. BRANDEN, Chem. Scand., 17, 1363, 1963.

78. P. LAVERTUE, J. HUBERT, and A.L. BEAUCHAMP, Inorg. Chem., 15, 322, 1976.

79. A. KORCZYNSKI, Rocz. Chem., 42, 393, 1968.

80. A. KORCZYNSKI, Zesz. Navk. Politech. Lodz., Chem., 19, 85, 1967.

81. P.D. BROTHERTON, P.C. HEALY, C.L. RASTON, and A.H. WHITE, J.C.S. Dalton, 334, 1973.

82. A.J. CARTY and N.J. TAYLOR, J.C.S. Chem. Comm., 214, 1976.

83. C. CHIEH, Canad. J. Chem., 55, 1583, 1977.

84. D. GRDENIC and I. KRISTANOVIC, Arkiv. Kemi., 27, 143, 1955.

85. H. BRUSSET and F. MADAULE-AUBRY, Bull. Soc. Chim. France, 10, 3122, 1966.

86. R.S. McEWEN and G.A. SIM, J. Chem. Soc. (A), 1897, 1969.

87. R.S. McEWEN, G.A. SIM, and C.R. JOHNSON, J.C.S. Chem. Comm., 885, 1967.

88. L.E. ORGEL, J. Chem. Soc., 4186, 1958.

89. R.S. NYHOLM, Proc. Chem. Soc., 273, 1961.

90. K. KESSLER, Ph.D Thesis, University of Bristol, 1977.

91. R.M. BARR and M. GOLDSTEIN, J.C.S. Dalton, 1593, 1976.

92. Y. MIKAWA, R.J. JAKOBSEN, and J.W. BRASCH, J. Chem. Phys., 45, 4528, 1966.

93. R.P.J. COONEY, J.R. HALL, and M.A. HOOPER, Austral. J. Chem., 21, 2145, 1968.

94. Y. MARQUETON, F. ABBA, E.A. DECAMPS, and M.A. NUSIMOVICI, Compt. Rend., 272, 1014, 1971.

95. R.M. BARR and M. GOLDSTEIN, J.C.S. Dalton, 1180, 1974.

96. R.M. BARR, Ph.D Thesis, University of London, 1973.

97. E.C. ALYEA, D.A. SKELTON, R.G. GOEL, and W.G. OGINI, Canad. J. Chem., 55, 4227, 1977.

98. R.M. BARR, M. GOLDSTEIN, and W.D. UNSWORTH, J. Cryst. Mol. Struct., 4, 165, 1974.

99. D.M. ADAMS and J.B. CORNELL, J. Chem. Soc. (A), 884, 1967.

100. A.J. AARTS, H.O. DESSEYN, and M.A. HERMAN, Bull. Soc. Chim. Belg., 86, 345, 1977.

101. P. BISCARINI and L. FUSINA, J.C.S. Dalton, 1003, 1972.

102. T.B. BRILL and D.W. WERTZ, Inorg. Chem., 9, 2692, 1970.

103. P. BISCARINI and G.D. NIVELLINI, J. Chem. Soc. (A), 2206, 1969.

104. A.C. FABRETTI, G. PEYRONEL, and G.C. FRANCHINE, Spectrochim. Acta, 33A, 7, 1977.

105. S.C. JAIN and R. RIVEST, Inorg. Chim. Acta, 3, 1969.

106. P.L. GOGGIN, R.J. GOODFELLOW, S.R. HADDOCK, and J.G. EARY, J.C.S. Dalton, 647, 1972.

107. G.H. STOUT and L.H. JENSEN, "X-Ray Structure Determination: A Practical Guide," Collier-MacMillan, London, 1968.

108. B. MANN, Acta Cryst., A24. 321, 1968; p.A. DOYLE and P.S. TURNER, Ibid, A24, 390, 1968.

109. D.T. CROMER and D. LIBERMAN, J. Chem. Phys., J3, 1891, 1970.

NO. SHELX Computer Programs, G.M. Sheldrick , Cambridge University.

111. J.J. DALY, J. Chem. Soc., 1964, 3799.

112. "International Tables for X-Ray Crystallography" Vol. I, Kynoch Press, Birmingham, 1969.

113. W.P. 0ZBIRN, R.A. JACOBSON, and J.C. CLARDY, Chem. Comm., 1062, 1971.

114. G.W. BUSHNELL, Canad. J. Chem., J6, 1773, 1978.

115. G.G. MESSMER and E.L. AMMA, Inorg. Chem., **J,** 1775, 1966.

116. M.L. SCHNEIDER and H.M.M. SHEARER, J. Chem. Soc. Dalton, 354,1973.

117. D.W. ALLEN, I.W. NOWELL, A.C. OADES, and P.E. WALKER, J.C.S. Perkin(I), 98, 1978.

118. G.G. MESSMER, E.L. AMMA, and J.A. IBERS, Inorg. Chem., 725, 1967.

119. W. STAHLIN and H.R. OSWALD, Acta Cryst., B27. 1368, 1971.

120. D.M. ADAMS and D.C. NEWTON, "Tables for Factor Group and Point Group Analysis," Beckmann-RIIC Ltd., Croydon, 1970.

121. W.A. HENDERSON and C.A. STRULI, J. Amer. Chem.Soc., §g, 5791, I960.

122. C.A. TOLMAN, Chem. Rev., *11,* 313, 1977.

123. B.E. MANN, J.C.S. Perkin (II), 30, 1972.

124. M.J. GALLAGHER, D.P. GRADDON, and A.R. SHEIKH, Austral. J. Chem., *22,* 759, 1976.

125. S.O. GRIM, P.J. LUI, and R.L. KEITER, Inorg. Chem., 13, 342, 1974.

126. VON A. YAMASKI and E. FLUCK, **Z.** Anorg. Chem., 396. 297, 1973.

127. P. SHAH, Piss. Abstr. Int. B., 37, 2845, 1976.

128. R.C. CASS, G.E. COATES, and R.G. HAYTER, J. Chem. Soc., 4007, 1955.

129. R.G.PEARSON, J. Chem. Ed., 45, 581, 1968; Ibid., *45,* 643, 1968.

130. L.S. BARTELL and L.O. BROCKWAY, J. Chem. Phys., 32, 512, 1960.

131. S. AHRLAND, J. CHATT, and N.R. DAVIES, Quart. Rev., 12, 265, 1958.

132. Y. FARHANGI and D.P. GRADDON, Austral. J. Chem., 26, 983, 1973.

133. C.A. TOLMAN, J. Amer. Chem. Soc., 92, 2953, 1970.

134. K. NAKAMOTO, "Infrared Spectra of Inorganic and Coordination Compounds," 2nd. Edition, Wiley, New York, 1970.

135. T. ONISHI and T. SHIMANOUCHI, Spectrochim. Acta, 20, 325, 1964.

136. R. FORNERIS, J. HIRAISHI, and F.A. MILLER, Spectrochim. Acta, 26A, 581, 1970.

137. V. BARAN, J. Mol. Structure, 13, 1, 1972; Ibid., 13, 10, 1972.

138. P.L. GOGGIN, R.J. GOODFELLOW, and K. KESSLER, J.C.S. Dalton, 1914, 1977.

139. P.L. GOGGIN, J.C.S. Dalton, 1483, 1974.

140. I.R. BEATTIE, T.GILSON, and P. COCKING, J. Chem. Soc. A, 702, 1967.

141. E.A. ALLEN and W. WILKINSON, Spectrochim. Acta, 30A, 1219, 1974.

142. J.H.S. GREEN, Spectrochim. Acta, 24A, 137, 1968.

143. J.H.S. GREEN and D.J. HARRISON, Spectrochim. Acta, 29A, 293, 1973.

144. J.H.S. GREEN, D.J. HARRISON, W. KYNASTON, and H.M. PAISLEY, Spectrochim. Acta, 26A, 2139, 1970.

145. J.A.W. DALZIEL, A.F.C. HOLDING, and B.E. WATTS, J. Chem. Soc. A, 358, 1967.

146. F.A. COTTON and G. WILKINSON, "Advanced Inorganic Chemistry," 3rd. Ed., Interscience, London, 1972.

147. G.E. COATES and A. LAUDER, J.Chem. Soc., 1857, 1965.

148. A. LOEWENSCHUSS, A. ROW, and O. SCHNEPP, J. Chem. Phys., 50, 2502, 1969.

149. J.G. EVANS, P.L. GOGGIN, R.J. GOODFELLOW, and J.G. SMITH, J. Chem. Soc. A, 464, 1968.

150. R.J. BELL, "Introductory Fourier Transform Spectroscopy," Academic Press, New York, 1972.

151. M. GOLDSTEIN and H.A. WILLIS, Lab. Practice, 19, 1970.

152. N.W. ALCOCK, "The Analytical Method for Absorption Correction" in "Crystallographic Computing," Edited by F.R. AMMED, Munksgaard, Copenhagen, 1970.

Details of programme of postgraduate study.

The author has

a) Completed a series of postgraduate lectures at the University of Sheffield entitled 'Diffraction Studies';

b) attended a course of lectures on advanced aspects of vibrational spectroscopy, given by the Director of Studies;

c) completed a computing course at the Polytechnic dealing with the use of a printer plotter;

d) attended meetings of the Infrared and Raman Discussion Group at Southampton University and the Polytechnic of Wales;

e) participated in Departmental research colloquia, and presented a colloquium on his own work;

f) completed the following reading study programme:

(i) 'Introductory Group theory for Chemists', G. Davidson, Elsevier, 1971.

(ii) 'Vibrational spectroscopy of Solids', P.M.A. Sherwood, C.U.P., 1972.

(iii) 'Basic Raman Spectroscopy', J. Loader, Heyden Sadtler, 1970.

(iv) 'Chemical Infrared Fourier Transform Spectroscopy', P.R. Griffiths, Wiley, 1975.

(v) 'Tables for Factor-Group Analysis', D.M. Adams and D.C. Newton, Beckman, 1970.

(vi) 'Fortran Programming', J. Watters, Heinemann, 1969.

(vii) 'X-Ray structure Determination, a Practical Guide', G.H. Stout and L.H. Jenson, MacMillan, 1968.

(viii) 'Direct Methods in Crystallography', M.M. Woolfson, Oxford at the Clarendon Press, 1961.

(ix) 'Elements of X-ray Diffraction', B.D. Cullity, Addison-Wesley, Reading, Mass., (1956).

Crystal Structures of the 1:1 Complexes of Mercury(II) Chloride with Phosphines or Arsines: $R_3P,HgCl_2$ (R = Me, Et, or Ph) and $Ph_3As,HgCl_2$

By Norman A. Bell, Michael Goldstein,* Terry Jones, and Ian W. Nowell
(*Chemistry Department, Sheffield City Polytechnic, Pond Street, Sheffield* S1 1WB)

Reprinted from

Journal of The Chemical Society
Chemical Communications
1976

The Chemical Society, Burlington House, London W1V 0BN

Crystal Structures of the 1:1 Complexes of Mercury(II) Chloride with Phosphines or Arsines: $R_3P,HgCl_2$ (R = Me, Et, or Ph) and $Ph_3As,HgCl_2$

By NORMAN A. BELL, MICHAEL GOLDSTEIN,* TERRY JONES, and IAN W. NOWELL
(*Chemistry Department, Sheffield City Polytechnic, Pond Street, Sheffield* S1 1WB)

Summary The crystal structures of a series of mercury(II) chloride complexes $R_3M,HgCl_2$ have been found to range from discrete chlorine-bridged dimers (R = Ph, X = As or P) to chain-like arrangements made up of monomeric $Et_3P,HgCl_2$ units or $[Me_3P,HgCl]^+Cl^-$ ions.

MERCURY(II) CHLORIDE forms 1:1 complexes with a wide range of neutral unidentate ligands. The structures of many of these have been described as discrete chlorine-bridged dimers on the basis of Raman and/or far-i.r. spectroscopic work. The crystallographic and even the spectroscopic

evidence for this supposition is limited, yet it is frequently asserted[1] that such structures are prevalent. Hence we have determined the crystal structures of a series of these complexes, $Ph_3P,HgCl_2$ (I), $Me_3P,HgCl_2$ (II), and $Et_3P,HgCl_2$ (III).

We find that only (I) contains discrete chlorine-bridged dimers. The bridge is almost totally symmetrical with Hg–Cl(1) distances of 2·66 and 2·62(1) Å, which is in contrast to the less symmetrical arrangement found[2] in $Ph_3PSe,HgCl_2$ [2·60 and 2·78(1) Å]. Preliminary *X*-ray analysis of $Ph_3As,HgCl_2$ shows it to be isostructural with (I).

In (II) and (III) it is not possible to identify discrete dimeric units, and both contain chain-like arrangements in which mercury has an overall co-ordination number of five. Thus the structure of (II) is comparable to that found[3] in the tetrahydrothiophen complex $C_4H_8S,HgCl_2$, and may be interpreted as a zig-zag arrangement of $[Me_3P,HgCl]^+$ cations linked together by Cl^- anions. There is only one 'short' Hg–Cl bond, [Hg–Cl(2), 2·36(1) Å], while three further Cl^- anions lie at distances of 2·77, 2·94, and 3·49(1) Å from mercury.

Complex (III) is of yet different structure to the other two phosphine complexes (Figure). There are two short Hg–Cl bonds [Hg–Cl(1), 2·53; Hg–Cl(2), 2·40 Å], and (III) may be considered to contain monomeric $Et_3P,HgCl_2$ units linked together by relatively long intermolecular Hg–Cl interactions [Hg–Cl(1′), 3·03; Hg–Cl(2′), 3·20(1) Å]. The resulting chain-like arrangement is similar to that found[4] in the collidine complex $C_8H_{18}N,HgCl_2$, although the elongated trigonal bipyramidal geometry around mercury is more distorted in (III).

It is therefore clear that marked structural differences

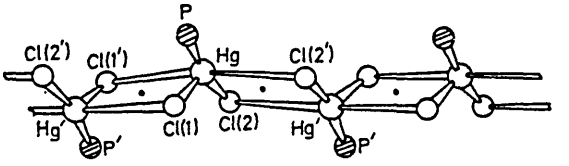

FIGURE. Molecular structure of $Et_3P,HgCl_2$ (III). *Crystal data*: Monoclinic, $a = 7{\cdot}44$, $b = 11{\cdot}54$, $c = 13{\cdot}44$ Å, $\beta = 105{\cdot}9°$; space group $P2_1/c$, $Z = 4$; $R = 0{\cdot}117$ for 1006 independent reflections. Important parameters: Hg–P, 2·36(1); Hg–Cl(2), 2·40(1); Hg–Cl(1), 2·54(1); Hg–Cl(1′), 3·03(1); and Hg–Cl(2′), 3·20(1) Å; and ∠P–Hg–Cl(2), 145·5(5); P–Hg–Cl(1), 115·3(5); Cl(1)–Hg–Cl(2), 99·1(5); and Cl(1′)–Hg–Cl(2′), 170·7(5)°.

exist between these 1 : 1 complexes, depending on the nature of the phosphine ligand. It is probably the larger size of the Ph_3P ligand relative to that of Et_3P or Me_3P which inhibits (I) from developing the extended structures found in (II) and (III), leading instead to the formation of discrete dimers. The structural trends are illustrated by comparison of the P–Hg–Cl(2) angles: 128·7(4)° for (I), 145·5(5)° for (II), and 161·8(3)° for (III).

All three phosphine complexes contain one short Hg–Cl bond, *ca.* 2·40 Å in length, and these values may be correlated with ν(Hg–Cl) frequencies that occur in the 280–300 cm^{-1} region of the i.r. spectrum. However, these same bands have often been used to indicate the presence of discrete chlorine-bridged dimers; such descriptions for (II) and (III) are incorrect and care is needed in spectra–structure correlations of this type.

We thank the S.R.C. for a Research Studentship (to T.J.).

(*Received, 8th September* 1976; *Com.* 1030.)

[1] G. B. Deacon and J. H. S. Green, *Spectrochim. Acta*, 1969, 25A, 355; G. E. Coates and D. Ridley, *J. Chem. Soc.*, 1964, 166; G. Marcotrigiano and R. Battistuzzi, *J. Inorg. Nuclear Chem.*, 1974, **36**, 3719; I. S. Ahujah and P. Rastogi, *ibid.*, 1970, **32**, 2085; F. G. Moers and J. P. Langhout, *Rec. Trav. chim.*, 1973, 92, 996; H. Schmidbaur and K. H. Rathlein, *Chem. Ber.*, 1973, **106**, 2491.
[2] L. S. D. Glasser, L. Ingram, M. G. King, and G. P. McQuillan, *J. Chem. Soc.* (*A*), 1969, 2501.
[3] C. I. Bränden, *Arkiv Kemi*, 1964, **22**, 495.
[4] S. Kulpe, *Z. anorg. Chem.*, 1967, **349**, 314.

Inorganica Chimica Acta, 28 (1978) L169–L170

Mixed Co-ordination in the Crystal Structures of Tertiary Phosphine Complexes of Mercury(II) Chloride: $(Me_2EtP)_3(HgCl_2)_2$ and $(Bu^n{}_3P)HgCl_2$

NORMAN A. BELL, MICHAEL GOLDSTEIN*, TERRY JONES and IAN W. NOWELL

Department of Chemistry, Sheffield City Polytechnic, Pond Street, Sheffield S1 1WB, U.K.

Received April 11, 1978

Tertiary phosphines are known [1] to form complexes with mercury(II) chloride having $R_3P:HgCl_2$ ratios of 2:1, 3:2, 1:1, 2:3, or 1:2, and many analogous compounds with other ligands have been described. However, crystallographic data are limited for all of these stoichiometries and the inherent dangers of the indiscriminate use of vibrational spectroscopy for structure elucidation of these systems have already been pointed out [2]. It is therefore to provide the first single crystal X-ray analysis of a 3:2 type complex and to extend the basis of vibrational spectra–structure correlations for such systems, that we report the crystal structures of $(Me_2EtP)_3(HgCl_2)_2$ (I) and $(Bu^n{}_3P)HgCl_2$ (II).

*Address correspondence to this author.

Results and Discussion

Crystals of (I) were selected from a sample thought to be $(Me_2EtP)_2HgCl_2$, but subsequent chemical and X-ray analyses showed that while the bulk of the sample had 2:1 stoichiometry, the larger crystals present had the composition of $(Me_2EtP)_3(HgCl_2)_2$. Complex (II) was obtained as the initial precipitate formed on adding an ethanolic solution of $Bu^n{}_3P$ to a solution of $HgCl_2$ in the same solvent, and was recrystallised from heptane/benzene.

Crystal Data

$C_{12}H_{33}P_3Hg_2Cl_4$ (I), orthorhombic, a = 18.755, b = 13.749, c = 9.740 Å. Space group $P2_12_12_1$, Z = 4, R = 0.055 for 2256 independent reflections.

$C_{12}H_{27}PHgCl_2$ (II), monoclinic, a = 13.698, b = 25.475, c = 10.621 Å, β = 100.78°. Space group $P2_1/n$, Z = 8, R = 0.089 for 1294 independent reflections.

Complex (I) is found to have an extended chain-like structure with the unusual feature of mercury atoms having alternating co-ordination numbers of four and five. The structure can be envisaged as consisting of $[(Me_2EtP)_2Hg]^+$ cations and $[(Me_2EtP)HgCl_3]^-$ anions linked together by chlorine bridges (Figure). Mercury has a distorted tetrahedral

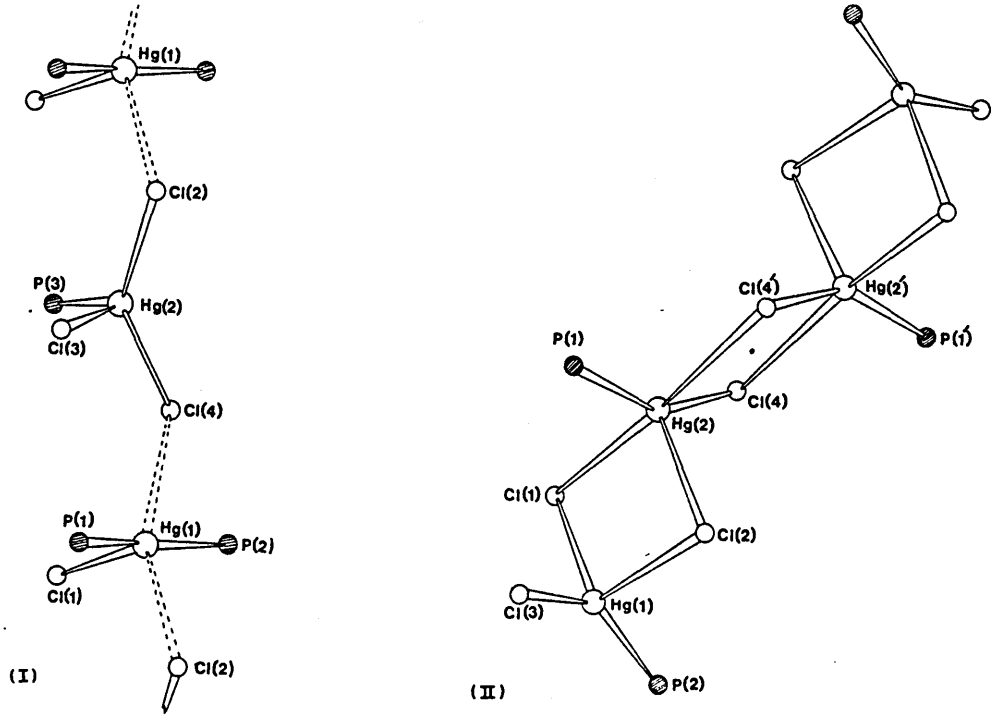

Figure. X-ray structures of $(Me_2EtP)_3(HgCl_2)_2$ (I) and $(Bu^n{}_3P)HgCl_2$ (II).

co-ordination within the anionic species with Hg–Cl distances varying from 2.46 to 2.64(1) Å and angles about mercury ranging from 98 to 133°. A 'T-shape' arrangement of one chlorine and two phosphorus atoms gives mercury a primary co-ordination of three within the $[(Me_2EtP)_2HgCl]^+$ cations, with the P–Hg–P bond angle being 172.2(3)°. The presence of two further chlorine atoms associated with the anions increases this coordination number to five, giving a distorted trigonal bipyramidal arrangement about mercury.

The novel feature of alternating four and five co-ordination about mercury is, surprisingly, also found in (II), which has a unique tetrameric structure. The terminal mercury atoms lie in distorted tetrahedral environments (angles at mercury vary from 92 to 148°), while the co-ordination polyhedra about the two central heavy atoms are best described as distorted trigonal bipyramids having a Cl(1)–Hg(2)–Cl(4′) bond angle of 177°. The presence in the tetrameric species of two short Hg–Cl bonds [Hg(1)–Cl(3), 2.29 Å; Hg(2)–Cl(4), 2.29 Å] along with two different asymmetric chlorine-bridged systems can, with hindsight, be correlated with ν(Hg–Cl) frequencies observed for the complex in the 100–300 cm^{-1} region of the i.r. spectrum. The latter consists of a complex pattern of bands, characteristically different from the spectra observed both for chlorine-bridged dimers as found [2] in $(Ph_3P)HgCl_2$, and for polymeric type structures as found [2] for example in $(Et_3P)HgCl_2$. It is therefore evident that the size of the ligand plays a particularly important role in determining the extent of association within such 1:1 phosphine complexes. Thus, while $(Ph_3P)HgCl_2$ is found to contain discrete chlorine-bridged dimers, the smaller Et_3P and Me_3P ligands allow closer approach, giving rise to polymeric structures. The formation of tetramers when $Bu^n{}_3P$ is the ligand in (II) thus represents an intermediate stage.

Acknowledgments

We thank the S.R.C. for a Research Studentship (to T. J.) and a grant, Dr. P. L. Goggin for the sample of (I), and Prof. M. R. Truter for data collection facilities for (I).

References

1 R. C. Evans, F. G. Mann, H. S. Peiser and D. Purdie, *J. Chem. Soc.*, 1209 (1940); H. Schmidbaur and K. H. Rathlein, *Chem. Ber., 106,* 2491 (1973); F. G. Moers and J. P. Langhout, *Rec. Trav. Chim., 92,* 996 (1973).
2 N. A. Bell, M. Goldstein, T. Jones and I. W. Nowell, *Chem. Comm., 1039* (1976).